Mass Production Cost Estimation of Direct H₂ PEM Fuel Cell Systems for Transportation Applications: 2015 Update

December 2015

Prepared By:

Brian D. James

Jennie M. Huya-Kouadio

Cassidy Houchins

Sponsorship and Acknowledgements

Disclaimer

Authors Contact Information

Strategic Analysis Inc. may be contacted at:

> Strategic Analysis Inc.
> 4075 Wilson Blvd, Suite 200
> Arlington VA 22203
> (703) 527-5410
> www.sainc.com

The authors may be contacted at:

> Brian D. James, BJames@sainc.com (703) 778-7114

Table of Abbreviations

ANL	Argonne National Laboratory
APTA	American Public Transportation Association
atm	atmospheres
BDI	Boothroyd Dewhurst Incorporated
BOL	beginning of life
BOM	bill of materials
BOP	balance of plant
C_{air}	Air Management System Cost (Simplified Cost Model)
C_{BOP}	Additional Balance of Plant Cost (Simplified Cost Model)
CC	capital costs
CCE	catalyst coated electrode
CCM	catalyst coated membrane
CEM	integrated compressor-expander-motor unit (used for air compression and exhaust gas expansion)
C_{Fuel}	Fuel Management System Cost (Simplified Cost Model)
C_{Humid}	Humidification Management System Cost (Simplified Cost Model)
CM	compressor motor
CNG	compressed natural gas
C_{stack}	Total Fuel Cell Stack Cost (Simplified Cost Model)
$C_{thermal}$	Thermal Management System Cost (Simplified Cost Model)
$DFMA^{TM}$	design for manufacture and assembly
DOE	Department of Energy
DOT	Department of Transportation
DSM^{TM}	dimensionally stable membrane (Giner membrane support)
DTI	Directed Technologies Incorporated
EEC	electronic engine controller
EERE	DOE Office of Energy Efficiency and Renewable Energy
EOL	end of life
ePTFE	expanded polytetrafluoroethylene
EW	equivalent weight
FCT	EERE Fuel Cell Technologies Program
FCTT	Fuel Cell Technical Team
FCV	fuel cell vehicle
Ford	Ford Motor Company Inc.
FTA	Federal Transit Administration
FUDS	Federal Urban Driving Schedule
G&A	general and administrative
GDE	gas diffusion electrode

GDL	gas diffusion layer
GM	General Motors Inc.
H_2	hydrogen
HFPO	hexafluoropropylene oxide
HDPE	high density polyethylene
ID	inner diameter
IR/DC	infra-red/direct-current
kN	kilo-Newtons
kW	kilowatts
kW_{e_net}	kilowatts of net electric power
LCA	life cycle analysis
LCCA	life cycle cost analysis
LT	low temperature
MBRC	miles between road calls
MEA	membrane electrode assembly
mgde	miles per gallon of diesel equivalent
mpgge	miles per gallon of gasoline equivalent
mph	miles per hour
NREL	National Renewable Energy Laboratory
NSTF	nano-structured thin-film (catalysts)
OD	outer diameter
ODS	optical detection system
OPCO	over-pressure, cut-off (valve)
PDF	probability distribution function
PEM	proton exchange membrane
PET	polyethylene terephthalate
Pt	platinum
PtCoMn	platinum-cobalt-manganese
QC	quality control
$Q/\Delta T$	heat duty divided by delta temperature
R&D	research and development
RFI	request for information
SA	Strategic Analysis, Inc.
TIM	traction inverter module
TVS	Twin Vortices Series (of Eaton Corp. compressors)
V	volt

Foreword

Energy security is fundamental to the mission of the U.S. Department of Energy (DOE) and hydrogen fuel cell vehicles have the potential to eliminate the need for oil in the transportation sector. Fuel cell vehicles[1] can operate on hydrogen, which can be produced domestically, emitting less greenhouse gasses and pollutants than conventional internal combustion engine (ICE), advanced ICE, hybrid, or plug-in hybrid vehicles that are tethered to petroleum fuels. Transitioning from standard ICE vehicles to hydrogen-fueled fuel cell vehicles (FCVs) could greatly reduce greenhouse gas emissions, air pollution emissions, and ambient air pollution, especially if the hydrogen fuel is derived from wind-powered electrolysis or steam reforming of natural gas.[2,3] A diverse portfolio of energy sources can be used to produce hydrogen, including nuclear, coal, natural gas, geothermal, wind, hydroelectric, solar, and biomass. Thus, fuel cell vehicles offer an environmentally clean and energy-secure pathway for transportation.

This research evaluates the cost of manufacturing transportation fuel cell systems (FCSs) based on low temperature (LT) proton exchange membrane (PEM) FCS technology. Fuel cell systems will have to be cost-competitive with conventional and advanced vehicle technologies to gain the market-share required to influence the environment and reduce petroleum use. Since the light duty vehicle sector consumes the most oil, primarily due to the vast number of vehicles it represents, the DOE has established detailed cost targets for automotive fuel cell systems and components. To help achieve these cost targets, the DOE has devoted research funding to analyze and track the cost of automotive fuel cell systems as progress is made in fuel cell technology. The purpose of these cost analyses is to identify significant cost drivers so that R&D resources can be most effectively allocated toward their reduction. The analyses are annually updated to track technical progress in terms of cost and to indicate how much a typical automotive fuel cell system would cost if produced in large quantities (up to 500,000 vehicles per year).

Bus applications represent another area where fuel cell systems have an opportunity to make a national impact on oil consumption and air quality. Consequently, beginning with year 2012, annually updated cost analyses have been conducted for PEM fuel cell passenger buses as well. Fuel cell systems for light duty automotive and buses share many similarities and indeed may even utilize identical stack hardware. Thus the analysis of bus fuel cell power plants is a logical extension of the light duty automotive power system analysis. Primary differences between the two applications include the installed power required (80 kilowatts of net electric power (kW_{e_net})[4] for automotive vs. ~160kW_{e_net} for

---

[1] Honda FCX Clarity fuel cell vehicle: http://automobiles.honda.com/fcx-clarity/; Toyota fuel cell hybrid vehicles: http://www.toyota.com/about/environment/innovation/advanced_vehicle_technology/FCHV.html

[2] Jacobson, M.Z., Colella, W.G., Golden, D.M. "Cleaning the Air and Improving Health with Hydrogen Fuel Cell Vehicles," *Science*, 308, 1901-05, June 2005.

[3] Colella, W.G., Jacobson, M.Z., Golden, D.M. "Switching to a U.S. Hydrogen Fuel Cell Vehicle Fleet: The Resultant Change in Energy Use, Emissions, and Global Warming Gases," *Journal of Power Sources*, 150, 150-181, Oct. 2005.

[4] Unless otherwise stated, all references to vehicle power and cost ($/kW) are in terms of kW net electrical (kW_{e_net}).

a 40 foot transit bus), desired power plant durability (nominally 5,000 hours lifetime for automotive vs. 25,000 hours lifetime for buses), and annual manufacturing rate (up to 500,000 systems/year for an individual top selling automobile model vs. ~4,000 systems/year for total transit bus sales in the US).[5]

The capacity to produce fuel cell systems at high manufacturing rates does not yet exist, and significant investments will have to be made in manufacturing development and facilities in order to enable it. Once the investment decisions are made, it will take several years to develop and fabricate the necessary manufacturing facilities. Furthermore, the supply chain will need to develop which requires negotiation between suppliers and system developers, with details rarely made public. For these reasons, the DOE has consciously decided not to analyze supply chain scenarios at this point, instead opting to concentrate its resources on solidifying the tangible core of the analysis, i.e. the manufacturing and materials costs.

The DOE uses these analyses as tools for R&D management and tracking technological progress in terms of cost. Consequently, non-technical variables are held constant to elucidate the effects of the technical variables. For example, the cost of platinum is typically held constant to insulate the study from unpredictable and erratic platinum price fluctuations. Sensitivity analyses are conducted to explore the effects of non-technical parameters.

To maximize the benefit of our work to the fuel cell community, Strategic Analysis Inc. (SA) strives to make each analysis as transparent as possible. The transparency of the assumptions and methodology serve to strengthen the validity of the analysis. We hope that these analyses have been and will continue to be valuable tools to the hydrogen and fuel cell R&D community.

---

[5] Total buses sold per year from American Public Transportation Association 2012 Public Transportation Fact Book, Appendix A Historical Tables, page 25, http://www.apta.com/resources/statistics/Documents/FactBook/2012-Fact-Book-Appendix-A.pdf. Note that this figure includes all types of transit buses: annual sales of 40' transit buses, as are of interest in this report, would be considerably lower.

Table of Contents

1 Overview

This 2015 report covers fuel cell cost analysis of both light duty vehicle (automotive) and transit bus applications for only the current year (i.e. 2015). This report is the ninth annual update of a comprehensive automotive fuel cell cost analysis[6] conducted by Strategic Analysis[7] (SA), under contract to the US Department of Energy (DOE). The first report (hereafter called the "2006 cost report") estimated fuel cell system cost for three different technology levels: a "current" system that reflected 2006 technology, a system based on projected 2010 technology, and another system based on projections for 2015. The 2007 update report incorporated technology advances made in 2007 and re-appraised the projections for 2010 and 2015. Based on the earlier report, it consequently repeated the structure and much of the approach and explanatory text. The 2008-2014, reports[8,9,10,11,12,13,14] followed suit, and this 2015 report[15] is another annual reappraisal of the state of technology and the corresponding costs. In the 2010 report, the "current" technology and the 2010 projected technology merged, leaving only two technology levels to be examined: the current status (then 2010) and the 2015 projection. In 2012, the 2015 system projection was dropped since the time frame between the current status and 2015 was so short. Also in 2012, analysis of a fuel cell powered 40 foot transit bus was added.

---

[6] "Mass Production Cost Estimation for Direct H_2 PEM Fuel Cell Systems for Automotive Applications," Brian D. James & Jeff Kalinoski, Directed Technologies, Inc., October 2007.

[7] This project was contracted with and initiated by Directed Technologies Inc. (DTI). In July 2011, DTI was purchased by Strategic Analysis Inc. (SA) and thus SA has taken over conduct of the project.

[8] James BD, Kalinoski JA, Baum KN. Mass production cost estimation for direct H2 PEM fuel cell systems for automotive applications: 2008 update. Arlington (VA): Directed Technologies, Inc. 2009 Mar. Contract No. GS-10F-0099J. Prepared for the US Department of Energy, Energy Efficiency and Renewably Energy Office, Hydrogen Fuel Cells & Infrastructure Technologies Program.

[9] James BD, Kalinoski JA, Baum KN. Mass production cost estimation for direct H2 PEM fuel cell systems for automotive applications: 2009 update. Arlington (VA): Directed Technologies, Inc. 2010 Jan. Contract No. GS-10F-0099J. Prepared for the US Department of Energy, Energy Efficiency and Renewably Energy Office, Hydrogen Fuel Cells & Infrastructure Technologies Program.

[10] "Mass Production Cost Estimation for Direct H_2 PEM Fuel Cell Systems for Automotive Applications: *2010 Update*," Brian D. James, Jeffrey A. Kalinoski & Kevin N. Baum, Directed Technologies, Inc., 30 September 2010.

[11] "Mass Production Cost Estimation for Direct H_2 PEM Fuel Cell Systems for Automotive Applications: 2011 Update," Brian D. James, Kevin N. Baum & Andrew B. Spisak, Strategic Analysis, Inc., 7 September 2012.

[12] "Mass Production Cost Estimation for Direct H_2 PEM Fuel Cell Systems for Automotive Applications: 2012 Update," Brian D. James, Andrew B. Spisak, Strategic Analysis, Inc., 18 October 2012.

[13] "Mass Production Cost Estimation of Direct H_2 PEM Fuel Cell Systems for Transportation Applications: 2013 Update" Brian D. James, Jennie M. Moton & Whitney G. Colella, Strategic Analysis, Inc., January 2014.

[14] "Mass Production Cost Estimation of Direct H_2 PEM Fuel Cell Systems for Transportation Applications: 2014 Update" Brian D. James, Jennie M. Moton & Whitney G. Colella, Strategic Analysis, Inc., January 2015.

[15] For previous analyses, SA was funded directly by the Department of Energy's Energy Efficiency and Renewable Energy Office. For the 2010 and 2011 Annual Update report, SA was funded by the National Renewable Energy Laboratory. For the 2012, 2013, 2014, and 2015 Annual update reports, SA is funded by Department of Energy's Energy Efficiency and Renewable Energy Office.

In this multi-year project, SA estimates the material and manufacturing costs of complete 80 kW$_{e\_net}$ direct-hydrogen Proton Exchange Membrane (PEM) fuel cell systems suitable for powering light-duty automobiles and 160 kWnet systems of the same type suitable for powering 40 foot transit buses. To assess the cost benefits of mass manufacturing, six annual production rates are examined for each automotive technology level: 1,000, 10,000, 30,000, 80,000, 100,000, and 500,000 systems per year. Since total U.S. 40 foot bus sales are currently ~4,000 vehicles per year, manufacturing rates of 200, 400, 800, and 1,000 systems per year are considered for the bus cost analysis.

A Design for Manufacturing and Assembly (DFMA^{TM}) methodology is used to prepare the cost estimates. However, departing from DFMA^{TM} standard practice, a markup rate for the final system assembler to account for the business expenses of general and administrative (G&A), R&D, scrap, and profit, is not currently included in the cost estimates. However, markup is added to components and subsystems produced by lower tier suppliers and sold to the final system assembler. For the automotive application, a high degree of vertical integration is assumed for fuel cell production. This assumption is consistent with the scenario of the final system assembler (e.g. a General Motors (GM) or a Ford Motor Company (Ford)) producing virtually all of the fuel cell power system in-house, and only purchasing select stack or balance of plant components from vendors). Under this scenario, markup is not applied to most components (since markup is not applied to the final system assembly). In contrast, the fuel cell bus application is assumed to have a very low level of vertical integration. This assumption is consistent with the scenario where the fuel cell bus company buys the fuel cell power system from a hybrid system integrator who assembles the power system (whose components, in turn, are manufactured by subsystem suppliers and lower tier vendors). Under this scenario, markup is applied to most system components. (Indeed, multiple layers of markup are applied to most components as the components pass through several corporate entities on their way to the bus manufacturer.)

In general, the system designs do not change with production rate, but material costs, manufacturing methods, and business-operational assumptions do vary. Cost estimation at very low manufacturing rates (below 1,000 systems per year) presents particular challenges. Traditional low-cost mass-manufacturing methods are not cost-effective at low manufacturing rates due to high per-unit setup and tooling costs, and lower manufacturing line utilizations. Instead, less defined and less automated operations are typically employed. For some repeat parts within the fuel cell stack (e.g. the membrane electrode assemblies (MEAs) and bipolar plates), such a large number of pieces are needed for each system that even at low system production rates (1,000/year), hundreds of thousands of individual parts are needed annually. Thus, for these parts, mass-manufacturing cost reductions are achieved even at low system production rates. However, other fuel cell stack components (e.g. end plates and current collectors) and all FCS-specific balance of plant (BOP) equipment manufactured in-house do not benefit from this manufacturing multiplier effect, because there are fewer of these components per stack (i.e. two endplates per stack, etc.).

The 2015 system reflects the authors' best estimate of current technology and, with only a few exceptions, is not based on proprietary information. Public presentations by fuel cell companies and other researchers along with an extensive review of the patent literature are used as a primary basis for modelling the design and fabrication of the technologies. Consequently, the presented information may lag behind what is being done "behind the curtain" in fuel cell companies. Nonetheless, the current-technology system provides a benchmark against which the impact of future technologies may be compared. Taken together, the analysis of this system provides a good sense of the likely range of costs for mass-produced automotive and bus fuel cell systems and of the dependence of cost on system performance, manufacturing, and business-operational assumptions.

2 Project Approach

The overall goal of this analysis is to transparently and comprehensively estimate the manufacturing and assembly cost of PEM fuel cell power systems for light duty vehicle (i.e. automotive) and transit bus applications. The analysis is to be sufficiently in-depth to allow identification of key cost drivers. Systems are to be assessed at a variety of annual manufacturing production rates.

To accomplish these goals, a three step system approach is employed:

1) System conceptual design wherein a functional system schematic of the fuel cell power system is defined.
2) System physical design wherein a bill of materials (BOM) is created for the system. The BOM is the backbone of the cost analysis accounting system and is a listing and definition of subsystems, components, materials, fabrication and assembly processes, dimensions, and other key information.
3) Cost modeling where Design for Manufacturing and Assembly (DFMA^{TM}) or other cost estimation techniques are employed to estimate the manufacturing and assembly cost of the fuel cell power system. Cost modeling is conducted at a variety of annual manufacturing rates.

Steps two and three are achieved through the use of an integrated performance and cost analysis model. The model is Excel spreadsheet-based although outside cost and performance analysis software is occasionally used as inputs. Argonne National Laboratory models of the electrochemical performance at the fuel cell stack level are used to assess stack polarization performance.

The systems examined within this report do not reflect the designs of any one manufacturer but are intended to be representative composites of the best elements from a number of designs. The automotive system is normalized to a system output power of 80 kW$_{e\_net}$ and the bus system to 160 kW kW$_{e\_net}$. System gross power is derived from the parasitic load of the BOP components.

The project is conducted in coordination with researchers at Argonne National Laboratory (ANL) who have independent configuration and performance models for similar fuel cell systems. Those models serve as quality assurance and validation of the project's cost inputs and results. Additionally, the project is conducted in coordination with researchers at the National Renewable Energy Laboratory (NREL) who are experts in manufacturing quality control, bus fuel cell power systems, and life-cycle cost modeling. Furthermore, the assumptions and results from the project are annually briefed to the US Car Fuel Cell Technology Team so as to receive suggestions and concurrence with assumptions. Finally, the basic approach of process based cost estimation is to model a complex system (eg. the fuel cell power system) as the summation of the individual manufacturing and assembly processes used to make each component of the system. Thus a complex system is defined as a series of small steps, each with a corresponding set of (small) assumptions. These individual small assumptions often have manufacturing existence proofs which can be verified by the manufacturing practitioners. Consequently, the cost analysis is further validated by documentation of all modeling assumptions and its source.

2.1 Integrated Performance and Cost Estimation

The fuel cell stack is the key component within the fuel cell system and its operating parameters effectively dictate all other system components. As stated, the systems are designed for a net system power. An integrated performance & cost assessment procedure is used to determine the configuration and operating parameters that lead to lowest system cost (on a $/kW basis). Figure 1 lists the basic steps in the system cost estimation and optimization process and contains two embedded iterative steps. The first iterative loop seeks to achieve computational closure of system performance[16] and the second iterative loop seeks to determine the combination of stack operational parameters that leads to lowest system cost.

1) Define system basic mechanical and operational configuration

2) Select target system net power production.

3) Select stack operating parameters (pressure, catalyst loading, cell voltage, air stoichiometry).

4) Estimate stack power density (W/cm^2 of cell active area) for those parameters.

5) Estimate system gross power (based on known net power target and estimation of parasitic electrical loads).

6) Compute required total active area to achieve gross power.

7) Compute cell active area (based on target system voltage).

8) Compute stack hydrogen and air flows based on stack and system efficiency estimates.

9) Compute size of stack and balance of plant components based on these flow rates, temperatures, pressures, voltages, and currents.

10) Compute actual gross power for above conditions.

11) Compare "estimated" gross power with computed actual gross power.

12) Adjust gross power and repeat steps 1-9.

13) Compute cost of power system.

14) Vary stack operating parameters and repeat steps 3-13.

Figure 1. Basic steps within the system cost estimation and optimization process

---

[16] The term "computational closure" is meant to denote the end condition of an iterative solution where all parameters are internally consistent with one another.

Stack efficiency[17,18] at rated power of the automotive systems was previously set at 55%, to match past DOE targets. However, in 2013, a radiator size constraint in the form of Q/ΔT was imposed (see Section 6.2.2), and stack efficiencies were allowed to fluctuate so as to achieve minimum system cost while also satisfying radiator constraints.

The main fuel cell subsystems included in this analysis are:
• 	Fuel cell stacks
• 	Air loop
• 	Humidifier and water recovery loop
• 	High-temperature coolant loop
• 	Low-temperature coolant loop
• 	Fuel loop (but not fuel storage)
• 	Fuel cell system controller
• 	Sensors

Some vehicle electrical system components explicitly excluded from the analysis include:

• 	Main vehicle battery or ultra-capacitor[19]
• 	Electric traction motor (that drives the vehicle wheels)
• 	Traction inverter module (TIM) (for control of the traction motor)
• 	Vehicle frame, body, interior, or comfort related features (e.g., driver's instruments, seats, and windows)

Many of the components not included in this study are significant contributors to the total fuel cell vehicle cost; however their design and cost are not necessarily dependent on the fuel cell configuration or stack operating conditions. Thus, it is our expectation that the fuel cell system defined in this report is applicable to a variety of vehicle body types and drive configurations.

2.2 Cost Analysis Methodology

As mentioned above, the costing methodology employed in this study is the Design for Manufacture and Assembly technique (DFMA[TM])[20]. Ford has formally adopted the DFMA[TM] process as a systematic means for the design and evaluation of cost optimized components and systems. These techniques are powerful and flexible enough to incorporate historical cost data and manufacturing acumen that have been accumulated by Ford since the earliest days of the company. Since fuel cell system production requires some manufacturing processes not normally found in automotive production, the formal DFMA[TM] process and SA's manufacturing database are buttressed with budgetary and price quotations

---

[17] Stack efficiency is defined as voltage efficiency X H2 utilization = Cell volts/1.253 X 100%.

[18] Multiplying this by the theoretical open circuit cell voltage (1.253 V) yields a cell voltage of 0.661 V at peak power.

[19] Fuel cell automobiles may be either "purebreds" or "hybrids" depending on whether they have battery (or ultracapacitor) electrical energy storage or not. This analysis only addresses the cost of an 80 kW fuel cell power system and does not include the cost of any peak-power augmentation or hybridizing battery.

[20] Boothroyd, G., P. Dewhurst, and W. Knight. "Product Design for Manufacture and Assembly, Second Edition," 2002.

from experts and vendors in other fields. It is possible to identify low cost manufacturing processes and component designs and to accurately estimate the cost of the resulting products by combining historical knowledge with the technical understanding of the functionality of the fuel cell system and its component parts. This DFMA^TM-style methodology helps to evaluate capital cost as a function of annual production rate. This section explains the DFMA^TM cost modelling methodology further and discusses FCS stack and balance of plant (BOP) designs and performance parameters where relevant.

The cost for any component analyzed via DFMA^TM techniques includes direct material cost, manufacturing cost, assembly costs, and markup. Direct material costs are determined from the exact type and mass of material employed in the component. This cost is usually based upon either historical volume prices for the material or vendor price quotations. In the case of materials or devices not widely used at present, the manufacturing process must be analyzed to determine the probable high-volume price for the material or device. The manufacturing cost is based upon the required features of the part and the time it takes to generate those features in a typical machine of the appropriate type. The cycle time can be combined with the "machine rate," the hourly cost of the machine based upon amortization of capital and operating costs, and the number of parts made per cycle to yield an accurate manufacturing cost per part. Operating costs include maintenance and spare parts, any miscellaneous expenses, and utility costs (typically electricity at $0.08/kWh).

The assembly costs are based upon the amount of time to complete the given operation and the cost of either manual labor or of the automatic assembly process train. The piece cost derived in this fashion is quite accurate as it is based upon an exact physical manifestation of the part and the technically feasible means of producing it as well as the historically proven cost of operating the appropriate equipment and amortizing its capital cost. Normally (though not in this report), a percentage markup is applied to the material, manufacturing, and assembly cost to account for profit, general and administrative (G&A) costs, research and development (R&D) costs, and scrap costs. This percentage typically varies with production rate to reflect the efficiencies of mass production. It also changes based on the business type, on the amount of value that the manufacturer or assembler adds to the product, and on market conditions.

Cost analyses were performed for mass-manufactured systems at six production rates for the automotive FC power systems (1,000, 10,000, 30,000, 80,000, 100,000, and 500,000 systems per year) and four production rates for the bus systems (200, 400, 800, and 1,000 systems per year). System designs did not change with production rate, but material costs, manufacturing methods, and business-operational assumptions (such as markup rates) often varied. Fuel cell stack component costs were derived by combining manufacturers' quotes for materials and manufacturing with detailed DFMA^TM-style analysis.

For some components (e.g. the bipolar plates and the coolant and end gaskets), multiple designs or manufacturing approaches were analyzed. The options were carefully compared and contrasted, and then examined within the context of the rest of the system. The best choice for each component was included in the 2015 baseline configuration. Because of the interdependency of the various components, the selection or configuration of one component sometimes affects the selection or

configuration of another. To handle these combinations, the DFMA^{TM} model was designed with switches for each option, and logic was built in that automatically adjusts variables as needed. As such, the reader should not assume that accurate system costs could be calculated by merely substituting the cost of one component for another, using only the data provided in this report. Instead, data provided on various component options should be used primarily to understand the decision process used to select the approach for the baseline configurations.

The DFMA^{TM}-style methodology proceeds through four iterative stages: (1) System Conceptual Design, (2) System Physical Design, (3) Cost Modeling, and (4) Continuous Improvement to Reduce Cost.

2.2.1   Stage 1: System Conceptual Design

In the system conceptual design stage, a main goal is to develop and verify a chemical engineering process plant model describing the FCS. The FCSs consume hydrogen gas from a compressed hydrogen storage system or other hydrogen storage media. This DFMA^{TM} modelling effort does not estimate the costs for either the hydrogen storage medium or the electric drive train. This stage delineates FCS performance criteria, including, for example, rated power, FCS volume, and FCS mass, and specifies a detailed drive train design. An Aspen HYSYS^{TM} chemical process plant model is developed to describe mass and energy flows, and key thermodynamic parameters of different streams. This stage specifies required system components and their physical constraints, such as operating pressure, heat exchanger area, etc. Key design assumptions are developed for the PEM fuel cell vehicle (FCV) system, in some cases, based on a local optimization of available experimental performance data.

2.2.2   Stage 2: System Physical Design

The physical design stage identifies bills of materials (BOMs) for the FCS at a system and subsystem level, and, in some cases, at a component level. A BOM describes the quantity of each part used in the stack, the primary materials from which the part is formed, the feedstock material basic form (i.e. roll, coil, powder, etc.), the finished product basic form, whether a decision was made to make the part internally or buy it from an external machine shop (i.e. make or buy decision), the part thickness, and the primary formation process for the part. The system physical design stage identifies material needs, device geometry, manufacturing procedures, and assembly methods.

2.2.3   Stage 3: Cost Modeling

The cost modelling approach applied depends on whether (1) the device is a standard product that can be purchased off-the-shelf, such as a valve or a heat exchanger, or whether (2) it is a non-standard technology not yet commercially available in high volumes, such as a fuel cell stack or a membrane humidifier. Two different approaches to cost modeling pervade: (1) For standard components, costs are derived from industry price quotes and reasonable projections of these to higher or lower manufacturing volumes. (2) For non-standard components, costs are based on a detailed DFMA^{TM} analysis, which quantifies materials, manufacturing, tooling, and assembly costs for the manufacturing process train.

2.2.3.1 Standardized Components: Projections from Industry Quotes

For standardized materials and devices, price quotations from industry as a function of annual order quantity form the basis of financial estimates. A learning curve formula is applied to the available data gathered from industry:

$$P_Q = P_I * F_{LC}^{\left(\frac{\ln\left(\frac{Q}{Q_I}\right)}{\ln 2}\right)} \tag{1}$$

where P_Q is the price at a desired annual production quantity [Q] given the initial quotation price [P_I] at an initial quantity Q_I and a learning curve reduction factor [F_{LC}]. F_{LC} can be derived from industry data if two sets of price quotes are provided at two different annual production quantities. When industry quotation is only available at one annual production rate, a standard value is applied to the variable F_{LC}.

2.2.3.2 Non-standard Components: DFMA™ Analysis

When non-standard materials and devices are needed, costs are estimated based on detailed DFMA™ style models developed for a specific, full physical, manufacturing process train. In this approach, the estimated capital cost [C_{Est}] of manufacturing a device is quantified as the sum of materials costs [C_{Mat}], the manufacturing costs [C_{Man}], the expendable tooling costs [C_{Tool}], and the assembly costs [C_{Assy}]:

$$C_{Est} = C_{Mat} + C_{Man} + C_{Tool} + C_{Assy} \tag{2}$$

The materials cost [C_{Mat}] is derived from the amount of raw materials needed to make each part, based on the system physical design (material, geometry, and manufacturing method). The manufacturing cost [C_{Man}] is derived from a specific design of a manufacturing process train necessary to make all parts. The manufacturing cost [C_{Man}] is the product of the machine rate [R_M] and the sum of the operating and setup time:

$$C_{Man} = R_M * (T_R + T_S) \tag{3}$$

where the machine rate [R_M] is the cost per unit time of operating the machinery to make a certain quantity of parts within a specific time period, T_R is the total annual runtime, and T_S is the total annual setup time. The cost of expendable tooling [C_{Tool}] is derived from the capital cost of the tool, divided by the number of parts that the tool produced over its life. The cost of assembly [C_{Assy}] includes the cost of assembling non-standard components (such as a membrane humidifier) and also the cost of assembling both standard and non-standard components into a single system. C_{Assy} is calculated according to

$$C_{Assy} = R_{Assy} * \sum T_{Assy} \tag{4}$$

where R_{Assy} is the machine rate for the assembly train, i.e. the cost per unit time of assembling components within a certain time period and T_{Assy} is the part assembly time.

2.2.4 Stage 4: Continuous Improvement to Reduce Cost

The fourth stage of continuous improvement to reduce cost iterates on the previous three stages. This stage weighs the advantages and disadvantages of alternative materials, technologies, system conceptual design, system physical design, manufacturing methods, and assembly methods, so as to iteratively move towards lower cost designs and production methods. Feedback from industry and research laboratories can be crucial at this stage. This stage aims to reduce estimated costs by continually improving on the three-stages above.

2.3 Vertical Integration and Markups

Vertical integration describes the extent to which a single company conducts many (or all) of the manufacturing/assembly steps from raw materials to finished product. High degrees of vertical integration can be cost efficient by decreasing transportation costs and turn-around times, and reducing nested layers of markup/profit. However, at low manufacturing rates, the advantages of vertical integration may be overcome by the negative impact of low machinery utilization or poor quality control due to inexperience/lack-of-expertise with a particular manufacturing step.

For the 2012 analysis, both the automotive and bus fuel cell power plants were cost modeled as if they were highly vertically integrated operations. However for the 2013 to the 2015 analysis, the automotive fuel cell system retains the assumption of high vertical integration but the bus system assumes a non-vertically integrated structure. This is consistent with the much lower production rates of the bus systems (200 to 1,000 systems per year) compared to the auto systems (1,000 to 500,000 systems per year). Figure 2 graphically contrasts these differing assumptions. Per long standing DOE directive, markup (i.e. business cost adders for overhead, general & administrative expenses, profit, research and development expenses, etc.) are not included in the power system cost estimates for the final system integrator but are included for lower tier suppliers. Consequently, very little markup is included in the automotive fuel cell system cost because the final integrator performs the vast majority of the manufacture and assemble (i.e. the enterprise is highly vertically integrated). In contrast, bus fuel cell systems are assumed to have low vertical integration and thus incur substantial markup expense. Indeed, there are two layers of markup on most components (one for the actual manufacturing vendor and another for the hybrid system integrator).

Standard DFMA^{TM} practice, calls for a markup to be applied to a base cost to account for general and administrative (G&A) expenses, research and development (R&D), scrap, and company profit. While markup is typically applied to the total component cost (i.e. the sum of materials, manufacturing, and assembly), it is sometimes applied at different levels to materials and processing costs. The markup rate is represented as a percentage value and can vary substantially depending on business circumstances, typically ranging from as low as 10% for pass-thru components, to 100% or higher for small businesses with low sales volume.

Within this analysis, a set of standard markup rates is adopted as a function of annual system volume and markup entity. Portraying the markup rates as a function of actual sales revenue would be a better correlating parameter as many expenses represented by the markup are fixed. However, that approach is more complex and thus a correlation with annual manufacturing rate is selected for simplicity. Generic markup rates are also differentiated by the entity applying the markup. Manufacturing markup represents expenses borne by the entity actually doing the manufacturing and/or assembly procedure. Manufacturing markup is assessed at two different rates: an "in-house" rate if the manufacture is done with machinery dedicated solely to production of that component and a "job-shop" rate if the work is sent to an outside vendor. The "in-house" rate varies with manufacturing rate because machine utilization varies directly (and dramatically) with manufacturing volume. The "job-shop" rate is held constant at 30% to represent the pooling of orders available to contract manufacturing businesses.[21] A pass-thru markup represents expenses borne by a company that buys a component from a sub-tier vendor and then passes it through to a higher tier vendor. Integrator's markup represents expenses borne by the hybrid systems integrator than sets engineering specifications, sources the components, and assembles them into a power system (but does not actually manufacture the components). More than one entity may be involved in supply of the finished product. Per DOE directive, no markup is applied for the final system assembler.

Assumptions Regarding Extent of Vertical Integration
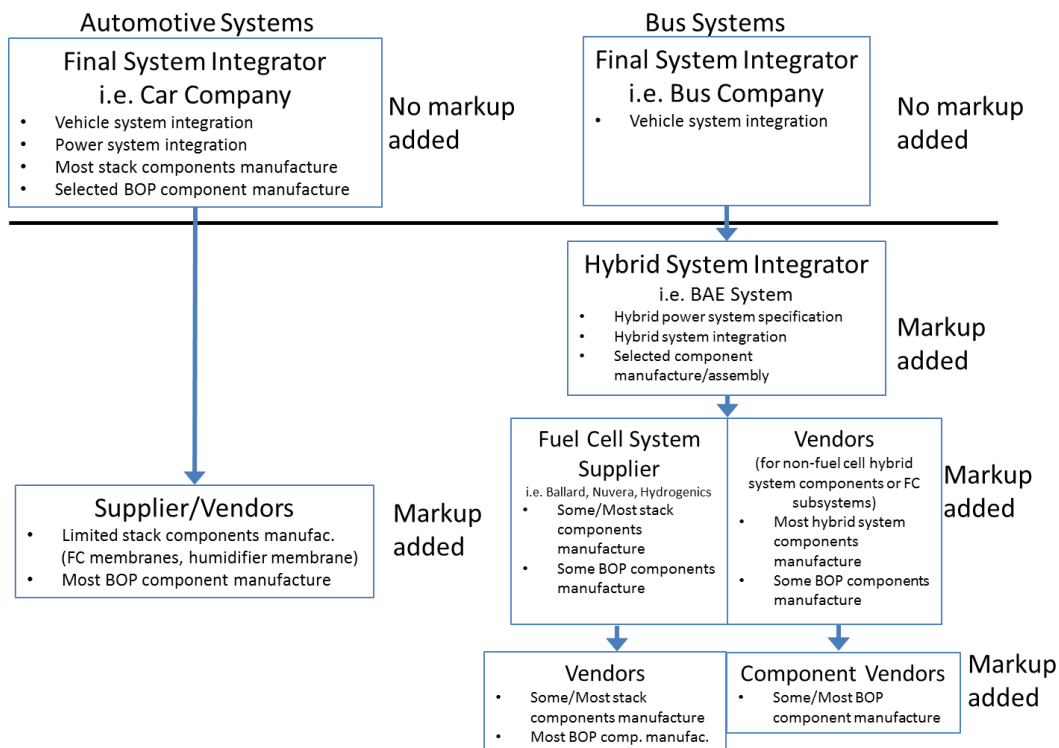
Figure 2: Comparison of bus and auto system vertical integration assumptions

---

[21] The job-shop markup is not really constant as large orders will result in appreciable increases in machine utilization and thus a (potential) lowering of markup rate. However, in practice, large orders are typically produced in-house to avoid the job-shop markup entirely and increase the in-house "value added". Thus in practice, job-shop markup is approximately constant.

Figure 3 lists the generic markup rates corresponding to each entity and production volume. When more than one markup is applied, the rates are additive. These rates are applied to each component of the automotive and bus systems as appropriate for that component's circumstances and generally apply to all components except the fuel cell membrane, humidifier, and air compressor subsystem. Markup rates for those components are discussed individually in the component cost results below.

Business Entity	Annual System Production Rate								
	200	400	800	1000	10k	30K	80k	100k	500k
Manufacturer (in-house)	58.8%	54.3%	50.1%	48.9%	37.5%	33.0%	29.5%	28.8%	23.9%
Manufacturer (job-shop)	30%	30%	30%	30%	30%	30%	30%	30%	30%
Pass-Thru	20.2%	19.6%	19.1%	19.0%	17.3%	16.6%	16.0%	15.8%	14.9%
Integrator	20.2%	19.6%	19.1%	19.0%	17.3%	16.6%	16.0%	15.8%	14.9%

Figure 3. Generic markup rates for auto and bus cost analysis

The numeric levels of markup rates can vary substantially between companies and products and is highly influenced by the competitiveness of the market and the manufacturing and product circumstances of the company. For instance, a large established company able to re-direct existing machinery for short production runs would be expected to have much lower markup rates than a small, one-product company. Consequently, the selection of the generic markup rates in Figure 3 is somewhat subjective. However, they reflect input from informal discussions with manufacturers and are derived by postulating a power curve fit to key anchor markup rates gleaned from manufacturer discussions. For instance, a ~23% manufactures markup at 500k systems per year and a 100% markup at a few systems/year are judged to be reasonable. A power curve fit fills in the intervening manufacturing rates. Likewise, a 30% job shop markup rate is deemed reasonable based on conversations and price quotes from manufacturing shops. The pass-thru and integrator markups are numerically identical and much less than the manufacture's rate as much less "value added" work is done. Figure 4 graphically displays the generic markup rates along with the curve fit models used in the analysis.

For the automotive systems, the application of markup rates is quite simple. The vast majority of components are modeled as manufactured by the final system integrator and thus no markup is applied to those components (by DOE directive, the final assembler applies no markup). The few automotive components produced by lower tier vendors (e.g. the CEM and the PEM membrane) receive a manufacturer's markup.

For the bus systems, the application of markup rate is more complex. System production volume is much lower than for automotive systems, and thus it is most economical to have the majority of components produced by lower-tier job-shops. Consequently, the straight job-shop 30% markup is applied for job-shop manufacturing expenses. Additionally, a pass-thru markup is added for expenses of the fuel-cell-supplier/subsystem-vendor, and an integrator markup is added for expenses of the hybrid integrator. These markups are additive. Like the auto systems, no markup is applied for the final system integrator.
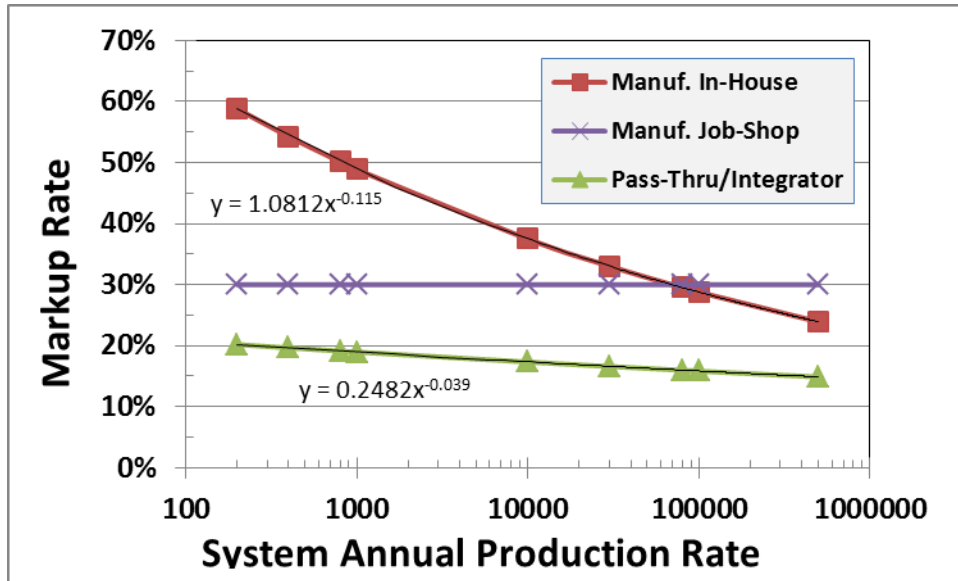
Figure 4. Graph of markup rates

Component level markup costs are reported in various sections of this report. Note that job-shop markup costs are included in the manufacturing cost line element, whereas all other markup costs (pass-thru and integrator) are included in the markup cost line element.

3 Overview of the Bus System

Fuel cell transit buses represent a growing market segment and a logical application of fuel cell technology. Fuel cell transit buses enjoy several advantages over fuel cell automobiles, particularly in the early stages of fuel cell vehicle integration, due to the availability of centralized refueling, higher bus power levels (which generally are more economical on a $/kW basis), dedicated maintenance and repair teams, high vehicle utilization, (relatively) less cost sensitivity, and purchasing decision makers that are typically local governments or quasi-government agencies who are often early adopters of environmentally clean technologies.

Transit bus fuel cell power systems are examined in this report. The transit bus market generally consists of 40' buses (the common "Metro" bus variety) and 30' buses (typically used for Suburban/Commuter[22] to rail station routes). While the 30' buses can be simply truncated versions of 40' buses, they more commonly are based on a lighter and smaller chassis (often school bus frames) than their 40' counterparts. Whereas 40' buses typically have an expected lifetime of 500k to 1M miles, 30' buses generally have a lower expected lifetime, nominally 200k miles.

There are generally three classes of fuel cell bus architecture[23]:
- hybrid electric: which typically utilize full size fuel cells for motive power and batteries for power augmentation;
- battery dominant: which use the battery as the main power source and typically use a relatively small fuel cell system to "trickle charge" the battery and thereby extend battery range;
- plug-in: which operate primarily on the battery while there is charge, and use the fuel cell as a backup power supply or range extender.

In May 2011, the US Department of Energy issued a Request for Information (RFI) seeking input[24] from industry stakeholders and researchers on performance, durability, and cost targets for fuel cell transit buses and their fuel cell power systems. A joint DOE-Department of Transportation (DOT)/Federal Transit Administration (FTA) workshop was held to discuss the responses, and led to DOE publishing fuel cell bus targets for performance and cost as shown in Figure 5. While not explicitly used in this cost analysis, these proposed targets are used as a guideline for defining the bus fuel cell power plant analyzed in the cost study. In addition to the 2016 and ultimate DOE targets, the 2014 status of fuel cell bus technology is added for comparison. Values from the 2014 status are from an annual report written by NREL and the Federal Transit Administration in 2014.[25]

The cost analysis in this report is based on the assumption of a 40' transit bus. Power levels for this class of bus vary widely based primarily on terrain/route and environmental loads. Estimates of fuel cell power plant required[26] net power can be as low as 75 kW for a flat route in a mild climate to 180+kW for

---

[22] Commuter buses are typically shorter in overall length (and wheel base) to provide ease of transit through neighborhoods, a tighter turning radius, and more appropriate seating for a lower customer user base.
[23] Personal communication with Leslie Eudy, National Renewable Energy Laboratory, 25 October 2012.
[24] "Fuel Cell Transit Buses", R. Ahluwalia, , X. Wang, R. Kumar, Argonne National Laboratory, 31 January 2012.
[25] "Fuel Cell Buses in U.S. Transit Fleets: Current Status 2014", L. Eudy and M. Post, National Renewable Energy Laboratory, and C. Gikakis, Federal Transit Administration, December, 2014.
[26] Personal communication with Larry Long, Ballard Power Systems, September 2012.

a hillier urban route in a hot climate. Accessory loads on buses are much higher than on light duty passenger cars. Electric power is needed for climate control (i.e. cabin air conditioning and heating), opening and closing the doors (which also impacts climate control), and lighting loads. In a hot climate, such as Dallas Texas, accessory loads can reach 30-60 kW, although 30-40 kW is more typical[27]. Industry experts[28] note that the trend may be toward slightly lower fuel cell power levels as future buses become more heavily hybridized and make use of high-power-density batteries (particularly lithium chemistries).

Parameter	Units	2014 Status[a]	2016 Target	Ultimate Target
Bus Lifetime	years/miles	5/151,000[b]	12/500,000	12/500,000
Power Plant Lifetime[cd]	hours	17,211[ef]	18,000	25,000
Bus Availability	%	72	85	90
Fuel Fills[g]	per day	1	1 (<10 min)	1 (<10 min)
Bus Cost[h]	$	2,000,000	1,000,000	600,000
Power Plant Cost[c, h]	$	N/A[i]	450,000	200,000
Road Call Frequency (Bus/Fuel-Cell System)	miles between road calls (MBRC)	1,408-6,363/ 10,406-37,471	3,500/15,000	4,000/20,000
Operating Time	hours per day/days per week	19/7	20/7	20/7
Scheduled and Unscheduled Maintenance Cost[j]	$/mile	N/A	0.75	0.40
Range	miles	294[k]	300	300
Fuel Economy	mgde[l]	7.26	8	8

a The summary of results for 2014 status represents a snapshot from NREL fuel cell bus evaluation data: data generally from August 2013–July 2014 with the exception of BC Transit, which covers April 2013 through March 2014.

b Status represents. Accumulated totals for existing fleet through July 2014; these buses have not reached end of life.

c The power plant is defined as the fuel cell system and the battery system. The fuel cell system includes supporting subsystems such as the air, fuel, coolant, and control subsystems. Power electronics, electric drive, and hydrogen storage tanks are excluded.

d According to an appropriate duty cycle.

e The status for power plant hours is for the fuel cell system only; battery lifetime hours were not available.

f The highest-hour power plant was transferred from an older-generation bus that had accumulated more than 6,000 hours prior to transfer.

g Multiple sequential fuel fills should be possible without increase in fill time.

h Cost projected to a production volume of 400 systems per year. This production volume is assumed for analysis purposes only, and does not represent an anticipated level of sales.

i Capital costs for subsystems are not currently reported by the manufacturers.

j Excludes mid-life overhaul of power plant.

k Based on fuel economy and 95% tank capacity.

l Miles per gallon diesel equivalent (mgde).

Figure 5. Proposed DOE targets (From US DOE[29]) and 2014 status (From NREL and FTA[25]) for fuel cell-powered transit buses.

---

[27] Personal communication with Larry Long, Ballard Power Systems, September 2012.

[28] Personal communication with Peter Bach, Ballard Power Systems, October 2012.

[29] "Fuel Cell Bus Targets", US Department of Energy Fuel Cell Technologies Program Record, Record # 12012, March 2, 2012. http://www.hydrogen.energy.gov/pdfs/12012_fuel_cell_bus_targets.pdf

The cost analysis in this report is based on a 160 kW$_{net}$ fuel cell bus power plant. This power level is within the approximate range of existing fuel cell bus demonstration projects[30] as exemplified by the 150 kW Ballard fuel cell buses[31] used in Whistler, Canada for the 2010 winter Olympics, and the 120kW UTC power PureMotion fuel cell bus fleets in California[32] and Connecticut. Selection of a 160 kW$_{net}$ power level is also convenient because it is twice the power of the nominal 80kW$_{net}$ systems used for the light duty automotive analysis, thereby easily facilitating comparisons to the use of two auto power plants.

The transit bus driving schedule is expected to consist of much more frequent starts and stops, low fractional time at idle power (due to high and continuous climate control loads), and low fractional time at full power compared to light-duty automotive drive cycles.[33] While average bus speeds depend on many factors, representative average bus speeds[34] are 11-12 miles per hour (mph), with the extremes being a New York City type route (~6 mph average) and a commuter style bus route (~23 mph average). No allowance has been made in the cost analysis to reflect the impact of a particular bus driving schedule.

There are approximately 4,000 forty-foot transit buses sold each year in the United States[35]. However, each transit agency typically orders its own line of customized buses. Thus while orders of identical buses may reach 500 vehicles at the high end, sales are typically much lower. Smaller transit agencies sometimes pool their orders to achieve more favorable pricing. Of all bus types[36] in 2011, diesel engine power plants are the most common (63.5%), followed by CNG/LNG/Blends (at 18.6%), and hybrids (electrics or other) (at only 8.8%). Of hybrid electric 40' transit bus power plants, BAE Systems and Alison are the dominant power plant manufacturers. These factors combine to make quite small the expected annual manufacturing output for a particular manufacturer of bus fuel cell power plants. Consequently, 200, 400, 800, and 1,000 buses per year are selected as the annual manufacturing rates to be examined in the cost study. This is considered a representative estimates for near-term fuel cell bus sales, perhaps skewed towards the upper end of production rates to facilitate the general DFMA™ cost methodology employed in the analysis. However, these production rates could alternately be viewed as a low annual production estimate if foreign fuel cell bus sales are considered.

---

[30] "Fuel Cell Transit Buses", R. Ahluwalia, X. Wang, R. Kumar, Argonne National Laboratory, 31 January 2012.

[31] The Ballard bus power systems are typically referred to by their gross power rating (150kW). They deliver approximately 140kW net.

[32] "SunLine Unveils Hydrogen-Electric Fuel Cell Bus: Partner in Project with AC Transit", article at American Public Transportation Association website, 12 December 2005, http://www.apta.com/passengertransport/Documents/archive_2251.htm

[33] Such as the Federal Urban Drive Schedule (FUDS), Federal Highway Drive Schedule (FHDS), Combined Urban/Highway Drive Cycle, LA92, or US06.

[34] Personal communication with Leslie Eudy, National Renewable Energy Laboratory, 25 October 2012.

[35] Personal communication with Leslie Eudy, National Renewable Energy Laboratory, 25 October 2012.

[36] 2012 Public Transportation Fact Book, American Public Transportation Association (APTA), 63rd Edition September 2012. Accessed February 2013 at http://www.apta.com/resources/statistics/Documents/FactBook/APTA_2012_Fact%20Book.pdf

4 System Schematics and Bills of Materials

System schematics are a useful method of identifying the main components within a system and how they interact. System flow schematics for each of the systems in the current report are shown below. Note that for clarity, only the main system components are identified in the flow schematics. As the analysis has evolved throughout the course of the annual updates, there has been a general trend toward system simplification. This reflects improvements in technology to reduce the number of parasitic supporting systems and thereby reduce system cost. The path to system simplification is likely to continue, and, in the authors' opinion, remains necessary to achieve or surpass cost parity with internal combustion engines.

The authors have conducted annually updated DFMA^{TM} analysis of automotive fuel cell systems since 2006. Side by side comparison of annually updated system diagrams is a convenient way to assess important changes/advances. However, no configuration changes were made between the 2014 and 2015 auto and bus system diagrams. The 2014/2015 diagrams for the automotive and bus systems are shown below.

4.1 2014/2015 Automotive System Schematic

The system schematic for the 2014/2015 light duty vehicle (auto) fuel cell power system appears in **Figure 6**.
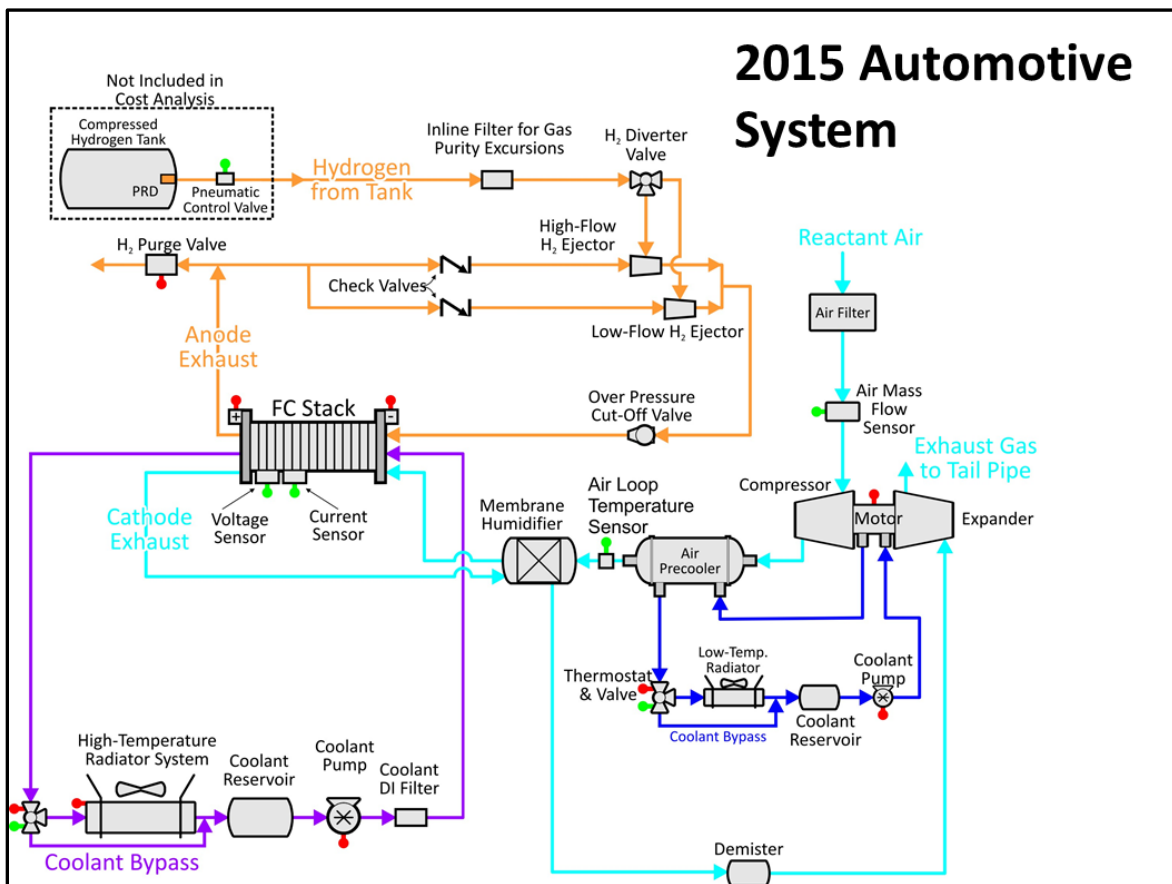
Figure 6. Flow schematic for the 2014/2015 automotive fuel cell system

4.2 2014/2015 Bus System Schematic

The system schematic for the 2014/2015 bus fuel cell power system appears in Figure 7. Power system hardware and layout are directly analogous to the 2014/2015 auto system with the exception of two key differences. 1) The automotive system contains one 80kW fuel cell stack as opposed to the bus system which contains two 80kW stacks, and 2) the automotive system operates at a higher pressure than the bus system, leading to the automotive system's air supply subsystem employing a compressor, motor, and expander (CEM) unit while the bus system uses only a compressor and motor unit.
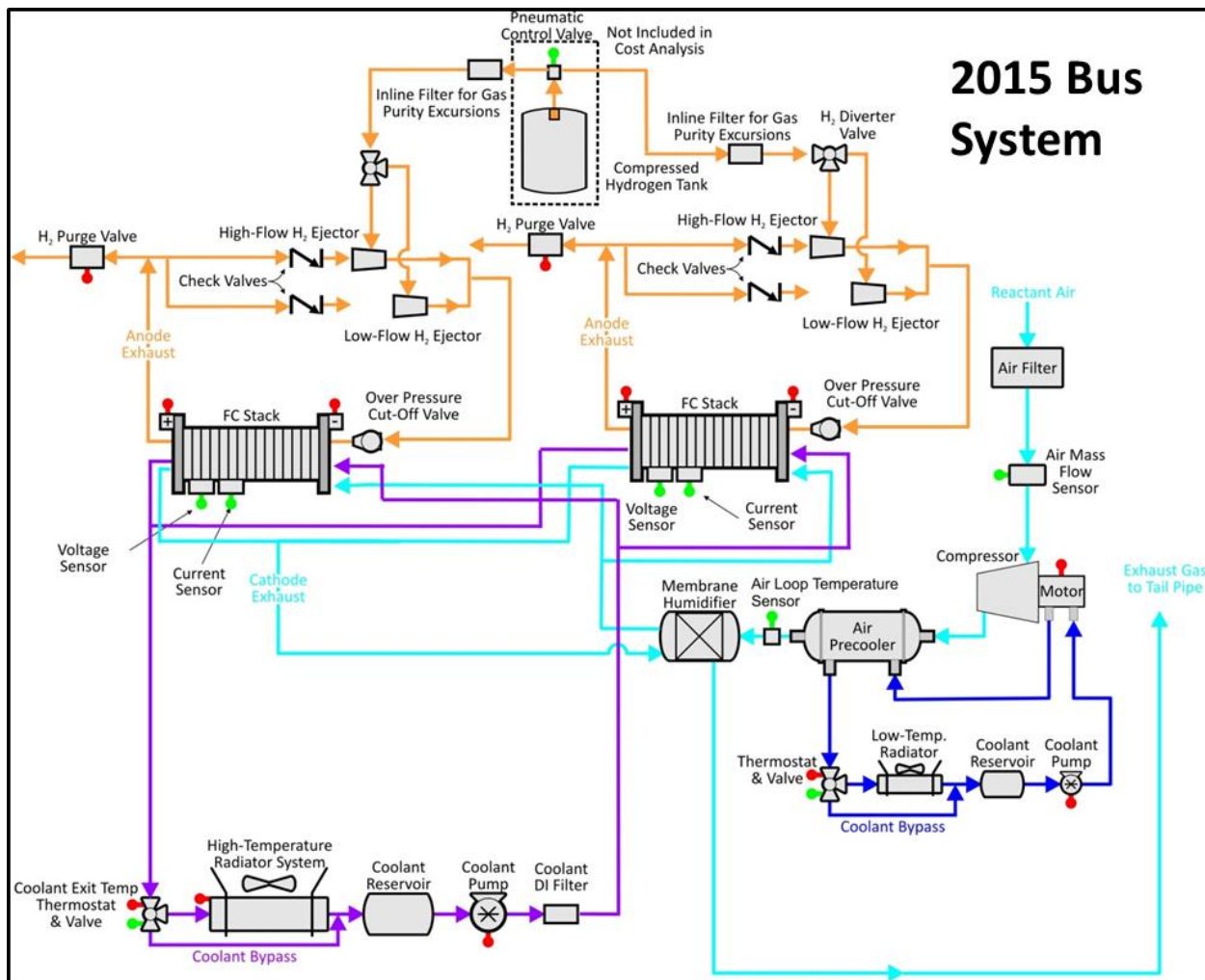
Figure 7. Flow schematic for the 2014/2015 bus fuel cell system

5 System Cost Summaries

Complete fuel cell power systems are configured to allow assembly of comprehensive system Bills of Materials, which in turn allow comprehensive assessments of system cost. Key parameters for the 2014 and 2015 automotive and bus fuel cell power systems are shown in Figure 8 below, with cost result summaries detailed in subsequent report sections.

The bus stack design differs from the automotive stack design in that (1) bus stacks are assumed to operate at a lower pressure and thereby have a lower stack power density; and (2) bus stacks are assumed to operate with a higher Pt catalyst loading so as to meet the greater longevity requirements for buses compared with cars. With a general correlation between Pt loading and stack durability, the bus system, in comparison with the automotive system, has a much higher platinum (Pt) loading due to an assumed longer lifetime. Also, the coolant stack exit temperature is much lower for the bus than for the automotive system primarily due to the typically very low part power operation of the bus stacks. In other words, the bus stacks are typically operating a greater percentage of the time at a lower percentage of their maximum power, compared with passenger cars. As a result, the bus exhaust temperature is lower. A bus is assumed to have a greater surface area available for radiator cooling and therefore is not subject to a Q/ΔT constraint. A more detailed discussion of the key differences between the automotive and bus systems appears in Section 9.1.

5.1 Cost Summary of the 2015 Automotive System

Results of the cost analysis for the 2015 automotive technology system at each of the six annual production rates are shown below. Figure 9 details the cost of the stacks, Figure 10 details the cost of the balance of plant components, and Figure 11 details the cost summation for the system. Figure 12 shows a graph of the stack and total system cost at all manufacturing rates including error bars based on Monte Carlo sensitivity analysis. Assumptions pertaining to the Monte Carlo analysis are detailed in section 13.2.

While the cost results, particularly the $/kW results, are presented to the penny level, this should not be construed to indicate that level of accuracy in all cases. Rather, results are presented to a high level of monetary discretization to allow discernment of the direction and approximate magnitude of cost changes. Those impacts might otherwise be lost to the reader due to rounding and rigid adherence to rules for significant digits, and might be misconstrued as an error or as having no impact.

	2014 Auto Technology System	2015 Auto Technology System	2014 Bus Technology System	2015 Bus Technology System
Power Density (mW/cm^2)	834	746	601	739
Total Pt loading (mgPt/cm^2)	0.153	0.142	0.4	0.5
Total Pt Loading (kW$_{gross}$/g)	5.29	4.91	1.45	1.39
Net Power (kW$_{net}$)	80	80	160	160
Gross Power (kW$_{gross}$)	92.75	88.22	187.6	194.7
Cell Voltage (V)	0.672	0.661	0.676	0.659
Operating Pressure (atm)	2.5	2.5	1.8	1.9
Stack Temp. (Coolant Exit Temp) (°C)	95	94	74	72
Air Stoichiometry	2	1.5	2.1	1.8
Q/ΔT (kW$_{th}$/°C)	1.45	1.45	4.66	5.4
Active Cells	372	378	740	758
Membrane Material	Nafion on 25-micron ePTFE	No change from 2014	Nafion on 25-micron ePTFE	No change from 2014
Radiator/ Cooling System	Aluminum Radiator, Water/Glycol Coolant, DI Filter, Air Precooler	No change from 2014	Aluminum Radiator, Water/Glycol Coolant, DI Filter, Air Precooler	No change from 2014
Bipolar Plates	Stamped SS 316L with TreadStone Coating	No change from 2014	Stamped SS 316L with TreadStone Litecell™ Coating	No change from 2014
Air Compression	Centrifugal Compressor, Radial-Inflow Expander	No change from 2014	Eaton-Style Multi- Lobe Compressor, Without Expander	No change from 2014
Gas Diffusion Layers	Carbon Paper Macroporous Layer with Microporous Layer (Ballard Cost)	No change from 2014	Carbon Paper Macroporous Layer with Microporous Layer (Ballard Cost)	No change from 2014
Catalyst & Application	3M Nanostructured Thin Film (NSTF™) Pt/Co/Mn: Cath: 0.103mgPt/cm^2 Anode: 0.05mgPt/cm^2	Slot Die Coating of: Cath.: Dispersed 0.092 mgPt/cm^2 d-PtNi on C Anode: Dispersed 0.05mgPt/cm^2 Pt on C	3M Nanostructured Thin Film (NSTF™) of Pt/Co/Mn: Cath: 0.35mgPt/cm^2 Anode: 0.05mgPt/cm^2	Slot Die Coating of: Cath.: Dispersed 0.5 mgPt/cm^2 Pt on C Anode: Dispersed 0.1mgPt/cm^2 Pt on C
Air Humidification	Plate Frame Membrane Humidifier	No change from 2014	Plate Frame Membrane Humidifier	No change from 2014
Hydrogen Humidification	None	None	None	None
Exhaust Water Recovery	None	None	None	None
MEA Containment	Screen Printed Seal on MEA Sub-gaskets, GDL crimped to CCM	Screen Printed Seal on MEA Sub-gaskets, GDL hot pressed to CCM	Screen Printed Seal on MEA Sub-gaskets, GDL crimped to CCM	Screen Printed Seal on MEA Sub-gaskets, GDL hot pressed to CCM
Coolant & End Gaskets	Laser Welded(Cooling)/ Screen-Printed Adhesive Resin (End)	No change from 2014	Laser Welded (Cooling), Screen-Printed Adhesive Resin (End)	No change from 2014
Freeze Protection	Drain Water at Shutdown	No change from 2014	Drain Water at Shutdown	No change from 2014
Hydrogen Sensors	2 for FC System[37]	No change from 2014	3 for FC System[38]	No change from 2014
End Plates/ Compression System	Composite Molded End Plates with Compression Bands	No change from 2014	Composite Molded End Plates with Compression Bands	No change from 2014
Stack Conditioning (hrs)	5	2	5	2

Figure 8. Summary chart of the 2014 and 2015 fuel cell systems

---

[37] There are a total of 4 hydrogen sensors on-board the FC vehicle: 2 under the hood in the power system (within cost estimate), 1 in the passenger cabin (not in cost estimate), and 1 in the fuel system (not in cost estimate).
[38] Additional sensor added to bus system due to the larger fuel cell compartment.

Annual Production Rate	Sys/yr	2015 Automotive System					
		1,000	10,000	30,000	80,000	100,000	500,000
System Net Electric Power (Output)	kWnet	80	80	80	80	80	80
System Gross Electric Power (Output)	kWgross	88.22	88.22	88.22	88.22	88.22	88.22
Stack Components							
Bipolar Plates (Stamped)	$/stack	$1,607	$632	$593	$571	$565	$558
MEAs							
Membranes	$/stack	$3,213	$994	$615	$410	$374	$206
d-PtNi Catalyst Ink & Application (Dispersion)	$/stack	$2,527	$1,129	$980	$952	$940	$913
GDLs	$/stack	$2,509	$750	$422	$252	$224	$96
M & E Cutting & Slitting	$/stack	$0	$22	$10	$5	$4	$3
MEA Sub-Gaskets	$/stack	$917	$274	$153	$126	$124	$116
Coolant Gaskets (Laser Welding)	$/stack	$219	$43	$43	$33	$31	$30
End Gaskets (Screen Printing)	$/stack	$1	$1	$1	$1	$1	$0
End Plates	$/stack	$100	$81	$71	$65	$64	$56
Current Collectors	$/stack	$8	$7	$7	$7	$7	$6
Compression Bands	$/stack	$10	$9	$8	$6	$6	$5
Stack Housing	$/stack	$64	$12	$8	$7	$7	$6
Stack Assembly	$/stack	$80	$61	$42	$36	$35	$34
Stack Conditioning	$/stack	$60	$18	$18	$16	$17	$13
Total Stack Cost	**$/stack**	$11,360	$4,049	$2,985	$2,496	$2,407	$2,052
Total Stacks Cost (Net)	**$/kWnet**	$142.00	$50.62	$37.32	$31.20	$30.09	$25.64
Total Stacks Cost (Gross)	**$/kWgross**	$128.77	$45.90	$33.84	$28.29	$27.28	$23.25

Figure 9. Detailed stack cost for the 2015 automotive technology system

Annual Production Rate	Sys/yr	2015 Automotive System					
		1,000	10,000	30,000	80,000	100,000	500,000
System Net Electric Power (Output)	kWnet	80	80	80	80	80	80
System Gross Electric Power (Output)	kWgross	88.22	88.22	88.22	88.22	88.22	88.22
BOP Components							
Air Loop	$/system	$1,850	$1,438	$1,143	$998	$966	$936
Humidifier & Water Recovery Loop	$/system	$1,209	$298	$181	$147	$137	$107
High-Temperature Coolant Loop	$/system	$476	$443	$414	$366	$349	$327
Low-Temperature Coolant Loop	$/system	$76	$72	$70	$66	$63	$60
Fuel Loop	$/system	$346	$306	$291	$261	$251	$238
System Controller	$/system	$171	$151	$137	$103	$96	$82
Sensors	$/system	$437	$331	$291	$260	$253	$212
Miscellaneous	$/system	$263	$165	$136	$123	$119	$115
Total BOP Cost	**$/system**	$4,828	$3,204	$2,662	$2,323	$2,234	$2,075
Total BOP Cost	**$/kW (Net)**	$60.35	$40.05	$33.28	$29.04	$27.92	$25.94
Total BOP Cost	**$/kW (Gross)**	$54.73	$36.32	$30.18	$26.33	$25.32	$23.52

Figure 10. Detailed balance of plant cost for the 2015 automotive technology system

		2015 Automotive System					
Annual Production Rate	Sys/yr	1,000	10,000	30,000	80,000	100,000	500,000
System Net Electric Power (Output)	kWnet	80	80	80	80	80	80
System Gross Electric Power (Output)	kWgross	88.22	88.22	88.22	88.22	88.22	88.22
Component Costs/System							
Fuel Cell Stack (High Value)	$/system	$12,597	$4,870	$3,742	$3,231	$3,140	$2,757
Fuel Cell Stack (Nominal Value)	$/system	$11,360	$4,049	$2,985	$2,496	$2,407	$2,052
Fuel Cell Stack (Low Value)	$/system	$10,174	$3,498	$2,497	$2,072	$1,995	$1,663
Balance of Plant (High Value)	$/system	$5,341	$3,650	$2,908	$2,545	$2,447	$2,278
Balance of Plant (Nominal Value)	$/system	$4,828	$3,204	$2,662	$2,323	$2,234	$2,075
Balance of Plant (Low Value)	$/system	$4,474	$2,740	$2,468	$2,155	$2,071	$1,835
System Assembly & Testing	$/system	$148	$103	$101	$101	$101	$101
Cost/System (High Value)	$/system	$17,750	$8,297	$6,570	$5,714	$5,529	$4,982
Cost/System (Nominal Value)	$/system	$16,336	$7,357	$5,749	$4,920	$4,742	$4,228
Cost/System (Low Value)	$/system	$15,149	$6,644	$5,242	$4,486	$4,321	$3,825
Total System Cost	$/kWnet	$204.20	$91.96	$71.86	$61.50	$59.27	$52.84
Cost/kWgross	$/kWgross	$185.18	$83.39	$65.16	$55.77	$53.75	$47.92

Figure 11. Detailed system cost for the 2015 automotive technology system

Figure 12. Automotive Stack and Total System Cost at all manufacturing rates. Error bars are based on Monte Carlo sensitivity analysis and denote the middle 90% confidence range of results.

5.2 Cost Summary of the 2015 Bus System

Results of the cost analysis of the 2015 bus technology system at 200, 400, 800, and 1,000 systems per year production rates are shown below. Figure 13 details the cost of the stacks, Figure 14 details the cost of the balance of plant components, and Figure 15 details the cost summation for the system. Figure 16 shows a graph of projected stack and total system cost at all manufacturing rates including error bars based on Monte Carlo sensitivity analysis. Assumptions pertaining to the Monte Carlo analysis are detailed in sections 13.2.

		2015 Bus System			
Annual Production Rate	**Sys/yr**	200	400	800	1,000
System Net Electric Power (Output)	**kWnet**	160	160	160	160
System Gross Electric Power (Output)	**kWgross**	194.71	194.71	194.71	194.71
Stack Components					
Bipolar Plates (Stamped)	**$/stack**	$1,222	$1,180	$1,104	$1,072
MEAs					
Membranes	**$/stack**	$8,807	$5,942	$4,519	$4,029
Catalyst Ink & Application (dispersed I	**$/stack**	$9,708	$7,535	$5,340	$5,283
GDLs	**$/stack**	$7,646	$5,166	$3,495	$3,082
M & E Cutting & Slitting	**$/stack**	$24	$23	$13	$13
MEA Gaskets (Frame or Sub-Gasket)	**$/stack**	$645	$524	$481	$432
Coolant Gaskets (Laser Welding)	**$/stack**	$197	$168	$131	$193
End Gaskets (Screen Printing)	**$/stack**	$2	$1	$1	$1
End Plates	**$/stack**	$168	$156	$146	$143
Current Collectors	**$/stack**	$13	$13	$12	$12
Compression Bands	**$/stack**	$17	$16	$15	$14
Stack Insulation Housing	**$/stack**	$276	$148	$84	$71
Stack Assembly	**$/stack**	$158	$142	$132	$130
Stack Conditioning	**$/stack**	$290	$151	$146	$120
Total Stack Cost	**$/stack**	**$29,532**	**$21,351**	**$15,717**	**$14,677**
Total Cost for all 2 Stacks	**$/2 stacks**	**$59,064**	**$42,702**	**$31,435**	**$29,354**
Total Stacks Cost (Net)	**$/kWnet**	**$369.15**	**$266.88**	**$196.47**	**$183.46**
Total Stacks Cost (Gross)	**$/kWgross**	**$303.34**	**$219.31**	**$161.44**	**$150.75**

Figure 13. Detailed stack cost for the 2015 bus technology system

		2015 Bus System			
Annual Production Rate	**Sys/yr**	200	400	800	1,000
System Net Electric Power (Output)	**kWnet**	160	160	160	160
System Gross Electric Power (Output)	**kWgross**	194.71	194.71	194.71	194.71
BOP Components					
Air Loop	**$/system**	$8,863	$7,421	$6,445	$6,193
Humidifier & Water Recovery Loop	**$/system**	$1,278	$1,043	$896	$859
High-Temperature Coolant Loop	**$/system**	$1,935	$1,873	$1,813	$1,794
Low-Temperature Coolant Loop	**$/system**	$222	$216	$209	$207
Fuel Loop	**$/system**	$997	$950	$905	$891
System Controller	**$/system**	$584	$533	$488	$474
Sensors	**$/system**	$1,121	$1,119	$1,116	$1,115
Miscellaneous	**$/system**	$1,118	$909	$792	$766
Total BOP Cost	**$/system**	**$16,119**	**$14,064**	**$12,664**	**$12,299**
Total BOP Cost	**$/kW (Net)**	**$100.74**	**$87.90**	**$79.15**	**$76.87**
Total BOP Cost	**$/kW (Gross)**	**$82.78**	**$72.23**	**$65.04**	**$63.17**

Figure 14. Detailed balance of plant cost for the 2015 bus technology system

		2015 Bus System			
Annual Production Rate	**Sys/yr**	**200**	**400**	**800**	**1,000**
System Net Electric Power (Output)	kWnet	160	160	160	160
System Gross Electric Power (Output)	kWgross	194.71	194.71	194.71	194.71
Component Costs/System					
Fuel Cell Stacks (High Value)	$/system	$80,433	$62,651	$42,291	$39,875
Fuel Cell Stacks (Nominal Value)	$/system	$59,064	$42,702	$31,435	$29,354
Fuel Cell Stacks (Low Value)	$/system	$50,925	$39,706	$26,005	$24,215
Balance of Plant (High Value)	$/system	$17,564	$15,302	$13,768	$13,368
Balance of Plant (Nominal Value)	$/system	$16,119	$14,064	$12,664	$12,299
Balance of Plant (Low Value)	$/system	$14,582	$12,743	$11,506	$11,185
System Assembly & Testing	$/system	$464	$339	$275	$262
Cost/System	$/system	$97,034	$77,117	$55,289	$52,505
Cost/System	$/system	$75,647	$57,104	$44,374	$41,915
Cost/System	$/system	$67,305	$53,907	$38,771	$36,614
Total System Cost	$/kWnet	$472.79	$356.90	$277.34	$261.97
Cost/kWgross	$/kWgross	$388.51	$293.28	$227.90	$215.27

Figure 15. Detailed system cost for the 2015 bus technology system

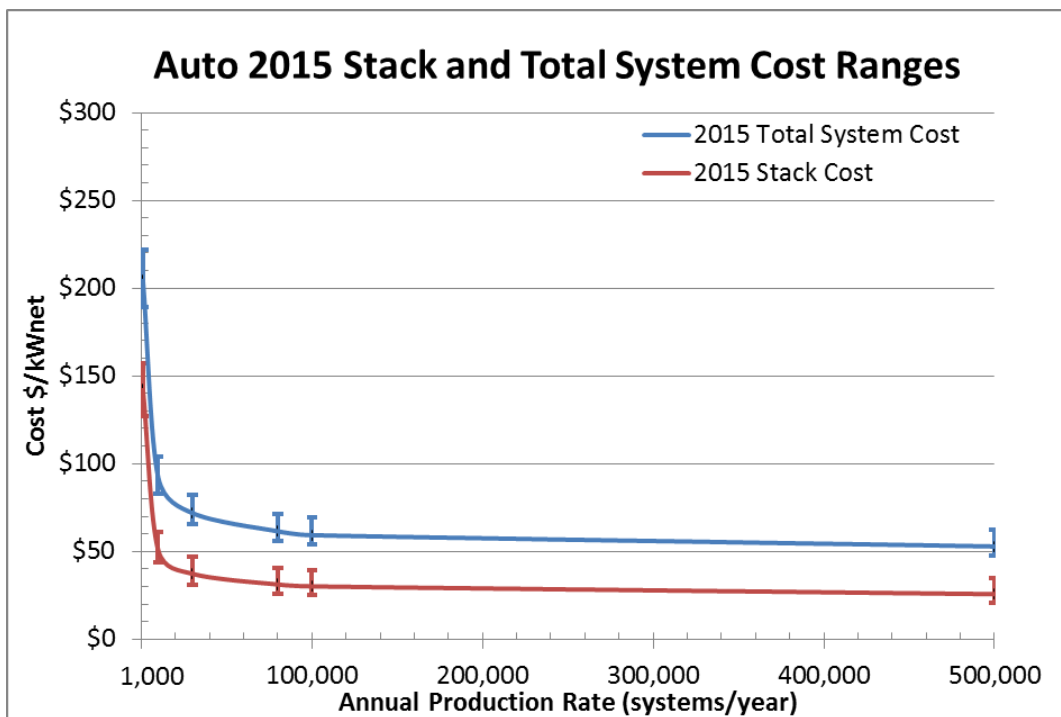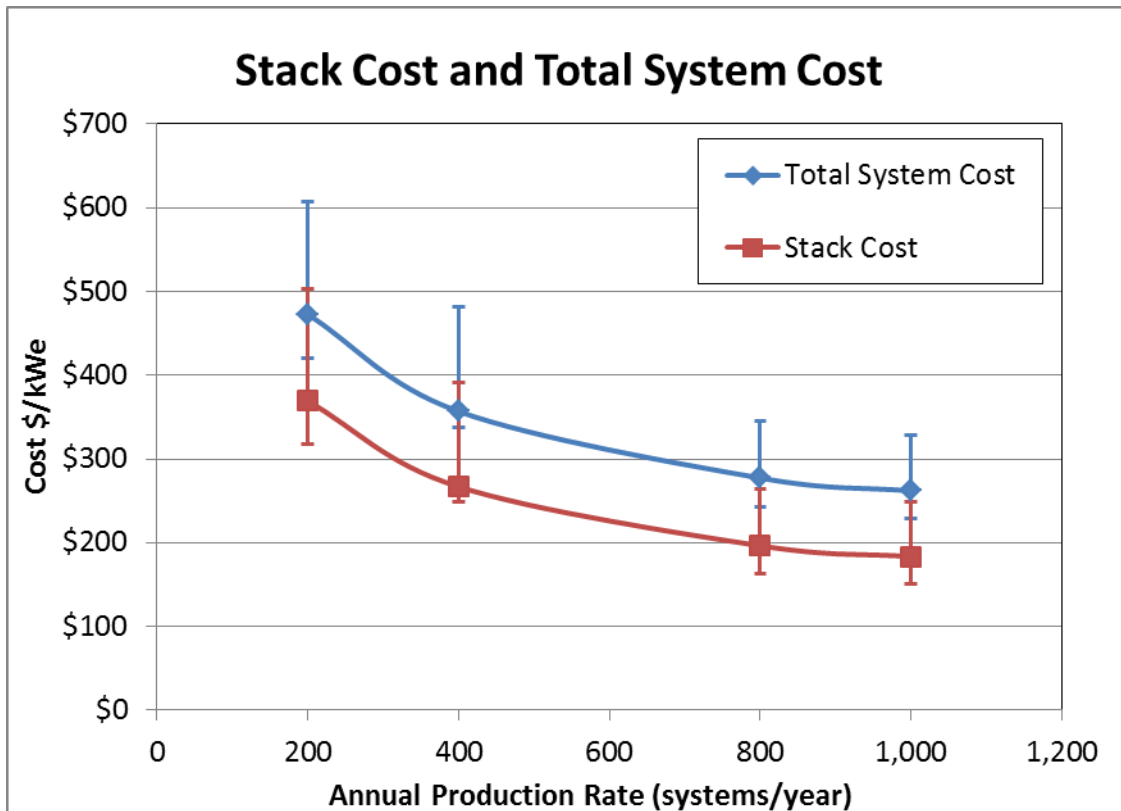**Figure 16. Bus Stack and Total System Cost at all manufacturing rates. Error bars are based on Monte Carlo sensitivity analysis and denote the middle 90% confidence range of results.**

6 Automotive Power System Changes and Analysis since the 2014 Report

This report represents the ninth annual update to the 2006 SA fuel cell cost estimate report[39]. Like the other eight updates before it, this annual report contains updates to the analysis based on advances made over the course of the previous year (i.e. 2015) and reflects new technologies, improvements, and corrections made in the cost analysis. The 2015 analysis closely matches the methodology and results formatting of the 2014 analysis.[40]

The major changes in 2015 result from switching from NSTF to a dispersed dealloyed PtNi catalyst. While the dealloyed PtNi catalyst has lower power density, the overall Pt loading was reduced and the air stoichiometry was lowered, leading to a lower system cost. In previous years, Argonne National Laboratory (ANL) provided stack polarization modeling results of 3M nanostructured thin film (NSTF) catalyst membrane electrode assemblies (MEA's). For 2014, SA performed an independent analysis of the 3M NSTF data on which to base the 2014 stack operating point. In 2015, SA collaborated with ANL to identify and incorporate into the cost analysis an optimized operating point for the new catalyst, dealloyed PtNi on carbon. Additional changes to the stack and BOP components involve updating the design and manufacturing methods to involve a handful of new technologies and the most up-to-date feedback from industry. These changes include updates to parasitic load calculations, MEA and bipolar plate geometry adjustments, sub-gasket processing assumptions, hydrogen sensor costs, and projected manufacturing methods at low volume (1,000 to 30,000 systems per year). Other changes include updated membrane humidifier area calculations and stack conditioning assumptions.

Noteworthy changes since the 2014 update report and their corresponding effects on system cost at 500,000 systems per year are listed in Figure 17 below.

---

[39] "Mass Production Cost Estimation for Direct H_2 PEM Fuel Cell Systems for Automotive Applications", Brian D. James, Jeff Kalinoski, Directed Technologies Inc., October 2007.
[40] "Mass Production Cost Estimation of Direct H_2 PEM Fuel Cell Systems for Transportation Applications: 2014 Update," Brian D. James, Jennie M. Moton & Whitney G. Colella, Strategic Analysis, Inc., January 2015.

Change	Reason	Change from previous value ($/kW)	Cost ($/kW) (@ 500k sys/yr)
2014 Final Cost Estimate		**NA**	**$54.84**
Polarization and Catalyst System	Reduction in power density from 834 to 746mW/cm^2 in switching from ternary PtCoMn NSTF catalyst to JM dealloyed PtNi dispersed catalyst on cathode, reduction of O$_2$ stoich from 2 to 1.5, and lower Pt loading (0.153 to 0.142mgPt/cm^2).	**($1.04)**	**$53.80**
Parasitic Load	Re-evaluated air pressure drop within system components. Reduced coolant pump and cooling fan power to align with ANL's modeling assumptions.	**($0.92)**	**$52.88**
Geometry Changes	Modification to catalyzed area of membrane and reduced the active to total area ratio from 0.8 to 0.625, and reduction of total catalyzed area to align with the thickness the subgasket is covering.	**$0.87**	**$53.75**
Subgaskets	Updated assumptions for subgasket equipment configuration.	**($0.46)**	**$53.29**
H2 Sensors	Updated price quote for H2 sensors.	**($0.23)**	**$53.06**
Minor Changes	Changed humidifier membrane area calaculation from scaling to using inlet and outlet air flow conditions. Updated stack conditioning assumptions.	**($0.21)**	**$52.84**
2015 Value		**($1.99)**	**$52.84**

Figure 17. Changes in automotive power system costs at 500,000 systems per year since 2014 update

In addition to the changes specified in the above table, considerable changes were made to the low volume (1,000 to 30,000 systems per year) automotive system cost estimates. To illustrate the significance of the low volume cost changes, Figure 18 provides a description and the resulting cost impact at 1,000 systems per year. Further low volume change details are provided in Section 6.7.

Change	Reason	Change from previous value	Cost ($/kW) (@ 1k sys/yr)
2014 Final Cost Estimate		NA	$273.03
Polarization and Catalyst System	Reduction in power density from 834 to 746mW/cm^2 in switching from ternary PtCoMn NSTF catalyst to JM dealloyed PtNi dispersed catalyst on cathode, reduction of O$_2$ stoich from 2 to 1.5, and lower Pt loading (0.153 to 0.142mgPt/cm^2).	($0.89)	$272.14
Parasitic Load	Re-evaluated air pressure drop within system components. Reduced coolant pump and cooling fan power to align with ANL's modeling assumptions.	($1.56)	$270.58
Geometry Changes	Modification to catalyzed area of membrane and reduced the active to total area ratio from 0.8 to 0.625.	$0.88	$271.47
H2 Sensors	Updated price quote for H2 sensors.	($16.45)	$255.01
Low Volume Changes	Resizing of machinery to obtain higher utilization and lower capital cost of equipment (PVD for Treadstone coating), replacing robots with manual labor for BPPs, re-evaluation of vertical integration for humidifier membrane material, and alternative roll cut approach for subgasket processing.	($44.06)	$210.95
QC Changes	Change to QC systems include membrane, catlayst application, bipolar plates, cutting/slitting, and membrane humidifier.	($6.42)	$204.54
Minor Changes	Changed humidifier membrane area calaculation from scaling to using inlet and outlet air flow conditions, revised stack conditioning times, humidifier coating equipement parameters. Updated stack conditioning assumptions.	($0.34)	$204.20
2015 Value		($68.83)	$204.20

Figure 18. Changes in automotive power system costs at 1,000 systems per year since 2014 update

While the above changes were made to the baseline system and thus impacted the baseline cost projections, numerous side analyses were also completed during 2015. These side studies investigated the following topics:

- DFMA^{TM} cost analysis of the Giner Electrochemical Systems dimensionally stable membrane (DSM^{TM}) fabrication method as an alternative to ePTFE membrane support
- DFMA^{TM} cost analysis of binary dealloyed PtNi NSTF catalyst application (including application of an interlayer) as an alternative to PtCoMn NSTF
- DFMA^{TM} cost analysis of polyaniline (PANI)-Fe-C catalyst synthesis as an alternative to Pt-based catalysts

6.1 Dealloyed Binary Catalyst Selection Process

From 2010 to 2014, NSTF ternary-based catalyst (PtCoMn) was used for the baseline automotive system. Recent progress has led to improved performance of dealloyed binary catalysts of dispersed platinum/nickel on a carbon support (PtNi/C or PtNi on C). Consequently, the 2015 baseline catalyst was switched to the binary dealloyed PtNi/C catalyst per DOE direction and Fuel Cell Technical Team (FCTT) recommendation. Full DFMA^{TM} analyses of both dispersed and NSTF dealloyed binary catalyst synthesis and their applications were completed in 2015 for the automotive system to allow direct comparison between the two catalysts.

Two catalyst systems were cost modeled by SA in support of the catalyst selection process:

1) 3M binary (d-PtNi) NSTF catalyst and

2) Johnson Matthey (JM) dispersed d-PtNi (applied via slot die coating)

To determine the lowest cost catalyst system, cost models of each catalyst system must be paired with their respective polarization curves (either from experimental data or modeling projections). Experimental single-cell data of the d-PtNi NSTF catalyst was provided by 3M. The data covered a range of operating conditions but not a sufficiently wide range to allow a full computational sweep of all relevant parameters to find the optimized lowest system cost. Instead, SA examined the experimental data and selected a data set that was similar to (but not exactly duplicating) conditions expected to be cost optimal. From this data set (90˚C, 2.5 atm, air stoichiometry 2.5), SA applied a voltage reduction of 8 mΩ·cm^{-2} (10 mV at 1.24 A/cm^{-2}) to adjust for stack bipolar plate losses not reflected in the single-cell testing data. SA also applied a relative performance decrease to account for operation at a reduced air stoichiometry of 2. The adjustment for lower air stoichiometry was based on the difference between NSTF data measured at 2 and 2.5 air stoichiometries provided by 3M (with all other conditions held constant between the two data sets). Finally, no adjustment was made to the performance to account for different operating temperatures. Based on SA's 2014 analysis and confirmed by 3M, it was assumed that increasing the temperature from 90˚C to 95˚C would have very little impact on performance. In this manner, experimentally-derived performance was used to predict the stack performance for the d-PtNi NSTF catalyst; a full optimization study to determine operating conditions that would provide the lowest cost while maintaining the Q/ΔT constraint was not conducted. SA intended to use this same approach for the JM binary catalyst; however, the experimental data available was very limited and did not include results at operating conditions suitably close to the expected optimal conditions to enable a fair comparison.

To predict stack performance of JM d-PtNi catalyst based cells, ANL developed a first-principles performance model using experimental data supplied by Johnson Matthey. The ANL model was used in combination with simplified system cost modeling correlations supplied by SA to allow optimization of the stack operating conditions for lowest system cost. Those optimized operating conditions were presented by ANL at the 2015 Annual Merit Review[41].

A comparison between the cost and performance of the 3M d-PtNi NSTF and JM d-PtNi catalysts is shown in Figure 19. The resulting fuel cell system cost is similar for the two catalysts, $51kW$_{net}$ and $54/kW$_{net}$ for 3M d-PtNi NSTF and $53/kW$_{net}$ for JM d-PtNi. The lower stack cost for the NSTF system ($21/kW$_{net}$ vs. $26/kW$_{net}$ for JM dispersed catalyst) is due largely to the lower total Pt loading of 0.133mg/cm^2 for NSTF. The NSTF catalyst system is shown at two operating conditions (one at air stoichiometry of 2 and one at 2.5) in the bottom two rows of Figure 19. The NSTF's higher air stoichiometry increases the sizing of the BOP components (i.e. air compressor and humidifier), making

---

[41] R. K. Ahluwalia, X. Wang, and J-K Peng, "Fuel Cell Systems Analysis", Presented at the 2015 DOE Hydrogen and Fuel Cells Program Review, Washington, D.C., June 8-12, 2015.

the BOP cost more expensive than the optimized JM dispersed catalyst system at air stoichiometry of 1.5.

As discussed previously, the performance comparison is not one-to-one. The ANL performance for the JM d-PtNi catalyst is based on an optimization model derived from experimental cell data while the 3M d-PtNi NSTF performance is not optimized and derived only from experimental cell data (data at 1.5 air stoichiometry has yet to be provided from 3M for this catalyst). 3M data at air stoichiometry 2 is extrapolated from the air stoichiometry 2.5 data, so there is no detailed performance model that verifies the performance to be 957mW/cm^2 at air stoichiometry of 2. Therefore, SA proposed using ANL's catalyst performance model for the JM d-PtNi catalyst combined with SA's JM d-PtNi cost model for the 2015 baseline system. SA plans to compare the cost and performance of both catalyst systems when an optimized model for the 3M binary NSTF catalyst is available.

Catalyst System	Pressure (atm)	O_2 Stoich	Temp (°C)	Pt loading (mgPt/cm^2)	Voltage (mV)	Power Density (mW/cm^2)	SA Stack Cost at 500k sys/yr ($/kWnet)	SA System Cost at 500k sys/yr ($/kWnet)	Notes
JM Dispersed D-PtNi (cathode) **JM Dispersed Pt/C (anode)** (ANL optimized oper. cond., presented at 2015 AMR)	2.5	1.5	94.1	0.05(a) 0.092(c) Total: 0.142	661	746	$26	$53	Used for 2015 Baseline
3M D-PtNi NSTF (cathode) **3M Dispersed Pt/C (interlayer)** **3M PtCoMn NSTF (anode)** (3M exp. data adj. by SA-stoich 2)	2.5	2	95	0.015(a) 0.103(c) 0.015(int) Total: 0.133	672	957	$21	$51	-SA adjusted exp. results for O_2 stoich and stack losses -assumed same performance at 90°C and 95°C.
3M D-PtNi NSTF (cathode) **3M Dispersed Pt/C (interlayer)** **3M PtCoMn NSTF (anode)** (3M exp. data adj. by SA-stoich 2.5)	2.5	2.5	95	0.015(a) 0.103(c) 0.015(int) Total: 0.133	684	973	$21	$54	-SA adjusted exp. results only for stack losses -assumed same performance at 90°C and 95°C.
*All systems are assuming an active to total area ratio of 0.625 and Q/ΔT of 1.45									

Figure 19. Comparison of JM dispersed d-PtNi and 3M d-PtNi NSTF catalyst system results.

The d-PtNi NSTF application DFMA^{TM} analysis assumptions are detailed in Section 7.2, while the dispersed JM d-PtNi catalyst synthesis and application DFMA^{TM} are described in Section 8.1.3.

6.2   2015 Polarization Model
Each analysis year, stack performance is re-examined to incorporate any performance improvements or analysis refinements over the previous year. For 2015, SA collaborated with ANL to define an optimized stack polarization for dispersed dealloyed PtNi catalyst.

6.2.1   2015 Polarization Model and Resulting Polarization Curves
Historically, ANL supplied SA with a simplified polarization model: a numerical model allowing average stack cell voltage to be projected based on five variables (current density, cathode catalyst loading, air stoichiometry, stack pressure, and coolant temperature at the stack outlet). This simplified model was

generated from regression analysis of data generated by ANL's Neural Net first-principals computer model. SA then used Monte Carlo analysis to determine the combination of stack parameters which led to lowest system cost. In 2014, ANL developed an alternative stack polarization model to the Neural Net model used in all previous analysis. This "non-Neural Net" model was specifically developed to better model water balance within the cell and allow optimization of cell inlet humidity levels for optimal performance. In 2015, ANL conducted an internal optimization to determine the optimal stack operating conditions using this non-Neural Net model. Unlike previous years, only the optimized stack conditions, rather than a simplified polarization model, were transmitted to SA.

Operating Parameter	2014 Conditions	2015 Optimized Conditions
Cell Voltage	0.672 volts/cell	0.661 volts/cell
Current Density	1,241 mA/cm^2	1,129 mA/cm^2
Power Density	834 mW/cm^2	746 mW/cm^2
Peak Stack Pressure	2.5 atm	2.5 atm
Total Catalyst Loading	0.153 mgPt/cm^2	0.142 mgPt/cm^2
Peak Cell Temperature[42]	100°C	100°C
Air Stoichiometric Ratio	2	1.5
Q/ΔT	1.45	1.45

Figure 20. Table of 2015 auto fuel cell system operating conditions compared to 2014 values.

While the cell voltage did not change significantly compared to 2014 conditions, power density decreased significantly, in part due to a lower Pt loading and lower air stoichiometric flow rate. The air stoichiometric ratio was reduced from 2 to 1.5, leading to a substantial reduction in the stack gross power and compressor/expander/motor cost. Figure 21 graphically compares the 2014 and 2015 polarization curves and design operating points.

---

[42] Peak cell temperature is assumed to be 5 degrees higher than the fuel cell coolant exit temp (same as the single cell testing temperature).
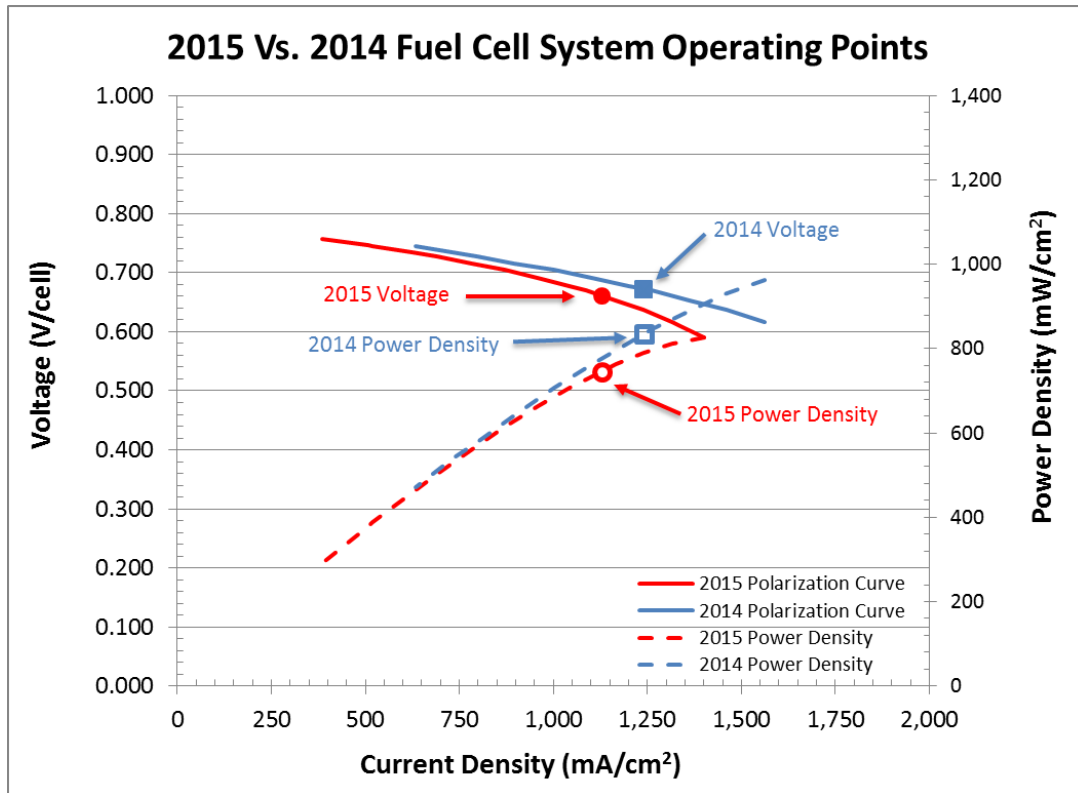
Figure 21. 2015 vs. 2014 polarization modeling results.
(2014 System Operating Point: 0.672V at 1,241 mA/cm^2 with 298.9cm^2/cell active area,
2015 System Operating Point: 0.661V at 1,129 mA/cm^2 with 312.8cm^2/cell active area)

6.2.2   Q/ΔT Constraint

As directed by DOE and consistent with DOE's 2012 MYRD&D plan, a radiator Q/ΔT constraint was placed on the system beginning in 2013. Q/ΔT is a measure of radiator size, where Q is the fuel cell radiator's heat rejection duty. Q is a function of the temperatures and mass flows of the stack inlet and outlet streams, stack efficiency (i.e. how much heat is generated within the stack), and the extent of liquid product water produced (i.e. how much energy goes into changing the product water from liquid to vapor). ΔT is the difference between the stack coolant exit temperature (typically 80-94°C) and the worst case ambient air temperature (assumed to be 40°C). Radiator size scales with Q/ΔT, thus a large Q/ΔT indicates that the stack needs a large radiator to reject waste heat. The DOE 2017 target for Q/ΔT is <1.45 kW$_{th}$/°C and consequently this limit is imposed on the 2013, 2014, and 2015 automotive analysis. All analyses prior to 2013 did not impose a Q/ΔT limit and the 2012 value was ~1.7 kW$_{th}$/°C implying a larger radiator than the automotive community (and DOE) feels is reasonable to incorporate into a light duty automobile.

While the computation of Q/ΔT appears simple (as it is merely the ratio of two easily understood parameters), it is more complex in practice. Q/ΔT is quite sensitive to both Q and ΔT and Q varies considerably depending on the extent of water condensation at the cathode. Water condensation is a function of temperature and gas flows within the cell and is more accurately analyzed by the ANL full polarization model than by the SA cost model. However, the Q/ΔT <=1.45 constraint recommended by

the FCTT was based on a simplified, short-hand computation method that assumes all product water remains in the vapor phase: Q/ΔT = 1.450. Thus for 2015, per DOE directive, the optimization constraint is also assessed by this definition.

$$\frac{Q}{\Delta T} = \frac{P_{gross}\,(1.25 - V_{cell})}{V_{cell}\,(T_{coolant} - T_{ambient})}$$

Where P_{gross} is the gross power of fuel cell stack, V_{cell} is cell voltage at rated power, 1.25 represents the open circuit cell voltage at representative operating conditions, and $T_{coolant}$ and $T_{ambient}$ are the coolant temperature out of the fuel cell stack and ambient temperature (40˚C), respectively.

6.3   Re-evaluation of Parasitic Loads and Gross Power

To better align with ANL's optimized thermodynamic model, SA re-evaluated parameters in the cost model that directly affect the parasitic load and the volume of the fuel cell system. The changes to parasitic loads and pressure drop within the system result in a cost reduction of $0.92/kWnet at 500,000 systems per year since 2014 and are summarized in Figure 22.

The pressure at the inlet and outlet of each component must be specified in order to accurately size the compressor and the expander, and to calculate the resulting parasitic power losses for the system. The air compressor outlet pressure is determined by the desired stack inlet pressure (2.5atm) plus any pressure drop within the BOP components upstream of the stack. The air pressure drops through the pre-cooler and the membrane humidifier were adjusted to ANL model values, ~0.03atm for each. The same pressure drop was applied to the humidifier after the stack and through the demister, overall reducing the pressure drop after the stack. Although the pressure into the expander, 2.23 atm, is higher in 2015 than in 2014 (2.14 atm vs. 2.23 atm), the total power out of the expander is lower in 2015 (4.67kW vs. 5.78kW) due to the lower air flow rate stoichiometry (1.5 vs. 2.0).

The high temperature loop coolant pump and radiator fan power were previously constant values for the 2014 analysis. The coolant pump power was changed to a calculation based on the heat rejection required by the stack and the coolant flow rate. The coolant fan power is now based on a 133W fan with fan efficiency 45%, fan motor efficiency 90%, and DC-DC converter efficiency 95%.

Air Pressure (atm)	2014 Value	2015 Value
Air Compressor Outlet	2.65	2.57
Air Precooler Outlet	2.64	2.54
Membrane Humidifier Outlet (into stack)	2.50	2.50
Stack Outlet	2.30	2.30
Membrane Humidifier Outlet (out of stack)	2.15	2.26
Air Demister Outlet	2.14	2.23
Parasitic Load (kW)		
Air Compressor Shaft Power	14.16	10.42
Expander Power Out	5.78	4.67
Air Compressor (net of expander)	10.47	7.20
High-Temperature Coolant Loop Pump	1.1	0.52
High-Temperature Coolant Loop Radiator Fan	0.9	0.35
Low-Temperature Coolant Loop Pump	0.18	0.06
Other (Controller, Instruments, etc.)	0.1	0.1
Total Parasitic Loads	**12.75**	**8.22**

Figure 22. Table comparing pressure drop and parasitic loads from 2014 to 2015 values.

6.4 Re-evaluation of Cell Geometry

In 2015, the ratio of active to total area (active area of MEA to total cell area) was reduced from 0.8 to 0.625 based on patent drawings,[43] photos, and discussions with industry researchers. The previously assumed ratio of 0.8 was based on informal conversations with members of the fuel cell community. The recent release of patents from Toyota prompted SA to reevaluate this ratio. This smaller active to total area is assumed to be much more representative of current cell design than the previously assumed ratio of 0.8. Moreover, this reduction in ratio is broadly consistent with increased power density which requires a greater manifold area per active area. A range of values, from as low as 0.6 and as high as 0.65, were identified during this reevaluation. as representative of modern automotive cells. A middle value of 0.625 was selected for the 2015 baseline system active to total ratio, while the range of 0.55 to 0.8 was used in the sensitivity analysis to capture the full range of ratios used historically or optimistically. This modification raised the baseline cost $1.12/kWnet at 500k systems per year due to increased total bipolar plate area (for the same active area). Simultaneously, the catalyzed border around the active area was reduced from 5mm to 3.2mm based on a re-evaluation of cell geometry, resulting in a reduction of $0.25/kWnet. Thus the total combined cost increase resulting from these two changes was $0.87/kWnet ($1.12-$0.25=$0.87/kWnet).

---

[43] US Patent 6,833,213 B2 to Toyota.

6.5 MEA Sub-Gasket Processing Assumption Change

The capital cost for the sub-gasket application process train is based on a one meter web width. Previously, the processing calculation had restricted the sub-gasket process to a single cell width (~20cm) resulting in an internal inconsistency in the processing time between the modeled 20 cm cell width and capital cost of a 1m wide web machine. The single cell width was also not consistent with the processing width for catalyst application and cutting and slitting operations. Consequently, the DFMA^{TM} model was updated to accommodate a common web width between the sub-gasket and catalyst application operations. The capital cost remains constant (as appropriate for 1m web widths) but the times associated with running the equipment went down due to the increased number of cells processed across the web width. At approximately one meter wide, 5 cells can fit across the processing width. This resulted in a reduction of $0.46/kWnet at 500k systems per year compared to 2014 estimates.

Processing multiple ~20 cm cells across the 1 m web width is technically challenging, particularly in context of the already complex sub-gasket machinery. Upon scrutiny by NREL team members, it was noted that the available processing equipment is not a barrier, but that aligning the individually cut parts with the individual apertures in the destination web across the web width could prove challenging. SA made the assumption that although the process may not have been demonstrated at multiple cells across the width of the web in current processes, it may be possible in the near future.

6.6 Updated Hydrogen Sensor Prices

The same hydrogen sensor costs have been used in the DFMA^{TM} model since 2008: $850/sensor at 1k systems per year down to $100/sensor at 500k systems per year based on price quotation from Makel Engineering. Quotes from NTM Sensors were obtained in 2015 at 1k ($199/sensor) and 1M ($75/sensor) sensors per year. The baseline system design calls for 2 sensors, thus requiring 1M sensors per year at the highest volume. NTM emphasized that they are not currently making 1M sensors per year, and the quote given at that quantity is a projected cost target. A curve fit was used to establish sensor cost projections at production volume between the two quotes provided. The sensor quote is combined with a ~$20 connector cost as recommended by NTM. The sensors do not come with individual control boards, unlike the sensors from Makel Engineering that do, however the sensors are assumed to be controlled by the fuel cell power system controller. Thus only minimal cost is incurred for an extra signal line. NTM currently supplies to fuel cell system integrators for fuel cell buses, but not currently to car companies.

6.7 Low Production Volume Changes

As part of 2015 activities, SA was tasked by DOE to investigate differences between low volume (1,000-30,000 systems per year) and high volume (>30,000- 500,000 systems per year) manufacturing processes. Understanding the crossover point from a low volume to a high volume process can be helpful to DOE and fuel cell companies when charting the transition to greater production volumes or

for planning capital expenditures for a projected market size. Consequently, one goal of this analysis is to attain greater understanding of the most cost effective low volume manufacturing processes and their corresponding "break-points" i.e. the system production rates that correspond to both low capital expenditure and high equipment utilization.

SA first investigated alternative low production volume manufacturing approaches for stack components. Low volume production methods from the 2014 baseline system were re-examined and improvements were made to equipment capital cost to achieve more appropriately sized machines and/or simplified processes (to reduce capital cost or increase the machine utilization). For example, the Treadstone bipolar plate coating requires a physical vapor deposition (PVD) machine and the 2014 analysis postulated, at all production rates, a high capital cost conveyance plate-feeder system for transferring plates in and out of the PVD chamber. Upon re-examination, manual labor was selected for the 2015 analysis as this was judged to be both more likely to be used at low volume and has a much lower capital expenditure. The tradeoff of labor cost versus capital cost is important to recognize and define for low volumes. Additionally, smaller, lower capital cost PVD machines (having a smaller work area inside the PVD chamber) were considered.

Other processes, such as NSTF catalyst coating have significant capital costs due to numerous and expensive processing steps. The tables in Figure 23 shows the comparison of the equipment capital cost required for NSTF application compared to a slot die coating process for applying the catalyst to the membrane (at 1,000 systems per year sizing). Although the different processes may result in different performance of the fuel cell stack, a fuel cell company may choose to produce a lower (power density) performing stack if the capital cost is too expensive. A more detailed analysis of the comparison between slot die coating and NSTF coating application is explained in Section 6.7.1.

The approach SA used to change a process is based on the following considerations:

If the cost of the fuel cell component is significantly higher at low manufacturing rates than at high rates, the high cost may be due to:
- Improperly-sized machine (resulting in high capital cost with low utilization)
- Unnecessarily complicated (and expensive) process

Possible solutions to lower the cost include:
- Selection of a smaller or more appropriately sized machine
- Use of alternative (but proven) processing method
- Consideration of component fabrication by a third-party (Job Shopped)

NSTF Equipment	Capital Cost
Evacuation Ch. #1	$81,143
Evacuation Ch. #2	$152,144
PR-149 Sublimation Unit	$104,167
PVD Catalyst Cylindrical Magnetron Sputtering Unit	$220,383
Annealing Oven	$446,426
Re-Press. Ch. #1	$131,858
Re-Press. Ch. #2	$81,143
Unwind/Rewind	$56,062
Catalyst Decal Appli. Sys.	$104,167
IR/DC QC System	$210,000
Total	$1,587,496

Slot Die Coating Equipment	Capital Cost
Ultrasonic Mixer	$27,169
Slot Die Coating Machine	$362,102
IR/DC QC System	$210,000
Total	$572,102

Figure 23. Catalyst application capital costs: NSTF equipment listing (left) and slot die coating equipment (right). Both tables are representative of equipment for 1,000 systems per year.

A summary of the changes made to all stack components at low production volumes are outlined in the table in Figure 24. More detailed analyses of specific components described in this section of the report include:

1. Catalyst Coating (NSTF vs. Slot Die Coating)
2. Sub-gasket Process Design
3. Removal of Cutting/Slitting
4. Job Shop Components (non-repeat components, i.e. end gaskets, end plates, and current collectors)
5. Air Humidifier Membrane Production Process Assumption

Additional analyses that did not affect the baseline cost of the system at low volume include the following (found in Section 7.4):

1. Bipolar Plate Material and Coating (Titanium base material with gold coating vs. Stainless Steel base material with Treadstone Coating)
2. Bipolar Plate Forming (Hydroforming vs. Stamping)

Component	Modeled High Volume Manufacturing Method	Modeled Low volume Manufacturing Method	Job Shop	Cost Impact at 1k systems per year ($/kWnet)
BPP forming	Stamping (robotic stacking)	Stamping (manual stacking)	No, cost reduction is very small	Manual Stacking (-$0.27) QC Change (-$0.15)
BBP Coating	SS base with Treadstone coating	Same	No- specialty vendor component	Lower Cost PVD Machine (-$4.83)
Membrane	Ionomer coated ePTFE	Same	No- specialty vendor component	QC Change (-$10.71)
Catalyst Coating	Slot Die Coating	Same	No- proprietary process retained in-house	QC Change (amount proprietary)
Sub-gasket	Roll-to-Roll process	Manual/robotic assembly	No – proprietary process retained in-house	Roll Cut Process (-$7.31) QC Changes (-$0.16)
Cutting/Slitting		Same	NA	Removed (-$6.16)
End Gaskets	Screen Printed (in-house)	Screen Printed (job shop)	Yes - greatly reduces cost/ not considered proprietary	Job Shop (-$1.90)
End Plates	Compression Molding (in-house)	Compression Molding (job shop)	Yes - greatly reduces cost/ not considered proprietary	Job Shop (-$1.10)
Current Collectors	Stamping (in-house) (robotic stacking)	Stamping (job-shop) (manual stacking)	Yes - greatly reduces cost/ not considered proprietary	Job Shop (-$0.59)
Air Humidifier Membrane	Ionomer coated ePTFE laminated to PET GDL	Same (increase to 5x production needed at 1k sys/yr only)	No- specialty vendor component	High Vol & smaller equip. (-$20.58) QC Change (-$0.04)

Figure 24. Table of component changes for low volume production

6.7.1 Alternative Methods for Catalyst Coating (Other than NSTF)

As mentioned previously, NSTF can have a relatively high capital cost due to the highly complex process of growing nanostructures in a vacuum. As an alternative method for coating catalyst onto membrane material, slot die coating was considered as a high throughput process with a relatively lower capital cost. Multiple companies provided capital cost pricing and basic operating parameters for slot die coating catalyst on to membranes. Three of the four companies who provided information have sold or quoted pilot coating machines for PEM fuel cell companies. Little information could be provided about the specific systems (due to proprietary content), but most of the companies provided generic coating machine information based on the catalyst material content and preferred coating speeds (or area of catalyst coated membrane output).

In comparison to NSTF, slot die coating is the least expensive manufacturing process (per active area of MEA) at less than 40,000m^2 per year (~30,000 FCS per year) as seen in Figure 25. It should be noted that Figure 25 shows processing costs only. With NSTF, there is no catalyst synthesis prior to coating. For slot die coating there is a catalyst synthesis to make the powder that goes into the slurry (not included in the costs here). Additionally, the cost comparison shown is based on $/m^2 to remove the difference in performance between the two types of coating methods. To make a fair comparison, similar performance data is needed to determine the amount of material required for the 80kWnet stack. This type of comparison is heavily dependent on the platinum loading and operating conditions that affect the gross power and ultimately active area required. Full system comparisons are ideal, as seen in Section 6.1.
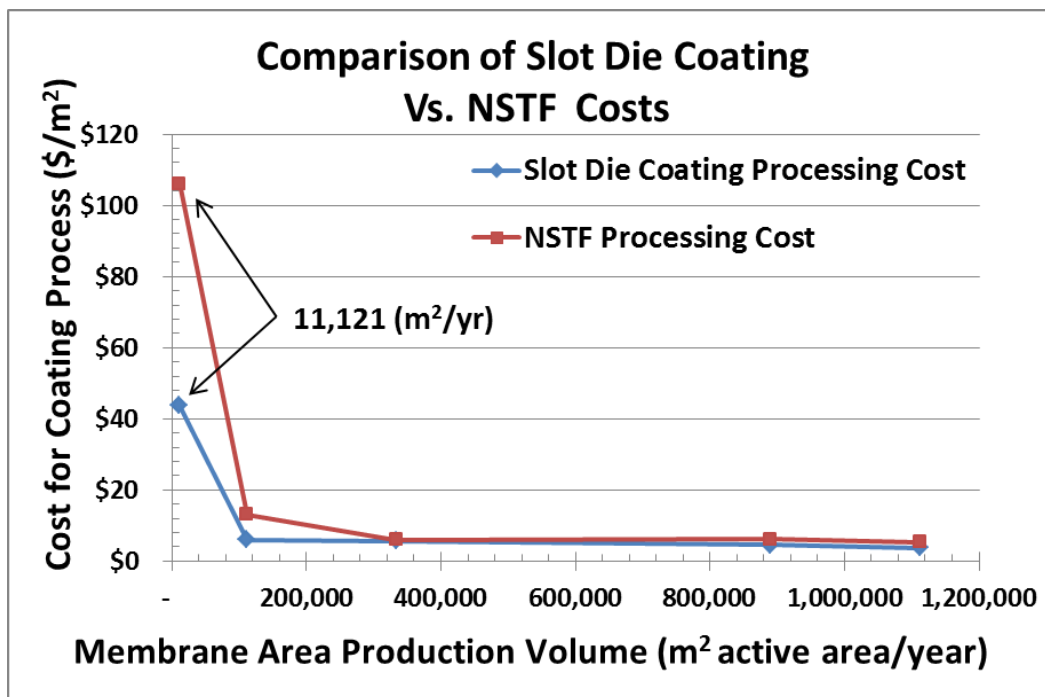
Figure 25. Comparison of slot die coating with NSTF coating production cost ($/m^2 active area) at multiple production volumes.

6.7.2   Sub-gasket Process Design

In 2012, SA examined a sub-gasket as an alternative sealing approach to insertion molded frame gaskets. The sub-gasket consists of thin layers of PET material cut into window-frame shapes and laminated to themselves and to the periphery of the MEA to form a contiguous and flat sealing surface against the bipolar plate. A thin bead of adhesive sealing material is screen-printed onto the bipolar plates to form a gas- and liquid-tight seal between the bipolar plate and the sub-gasket material. The sub-gasket layers are bonded to the MEA in a roll-to-roll process based upon a 3M patent application.[44] While the construction is relatively simple in concept, fairly complex machinery is required to handle, place and align the thin sub-gasket and MEA layers. Section 8.1.6 references the complete sub-gasket process steps.

At 1,000 systems per year, the high-throughput roll-to-roll 3M sub-gasket process is only utilized 2.5% of the time and has high capital cost (~$3M). SA contemplated whether this process would be job-shopped (sent to a third party for fabrication). When applying the sub-gasket (with the GDL) the cell is practically in its complete form and expected to be proprietary to the fuel cell integrator. An alternative solution was investigated to see if lower cost machinery to apply the sub-gasket in discrete parts (not roll-to-roll) could reduce the cost. The PET, membrane, and GDL would be stamped into rectangular cells and assembled with robots and laborers (robotic stacking), one at a time. This approach was selected for low-volume production due to its lower cost. Figure 26 shows the step-by-step process (view of through-cell cross-sections) for the low volume sub-gasket technique.

In switching to a discretized operation of robotic stacking, the capital cost reduces to $814k with an 88.5% utilization of equipment at 1,000 systems per year. This results in a $7.31/kWnet cost reduction, not including the removal of the cutting/slitting cost ($6.16/kWnet) which is unnecessary since the MEAs are already in discrete cells. The manufacturing cross-over point for this process (point at which the high throughput roll-to-roll process becomes less expensive than robotic stacking) is at approximately 2,000 systems per year (25k m^2 MEA area per year), as shown in Figure 27. At such a low cross-over point, a vehicle OEM may be willing to accept the sub-optimal high cost roll-to-roll process at 1,000 systems per year, confident that cost savings are in the near future.

---

[44] "Fuel Cell Subassemblies Incorporating Sub-gasketed Thrifted Membranes," US2011/0151350A1
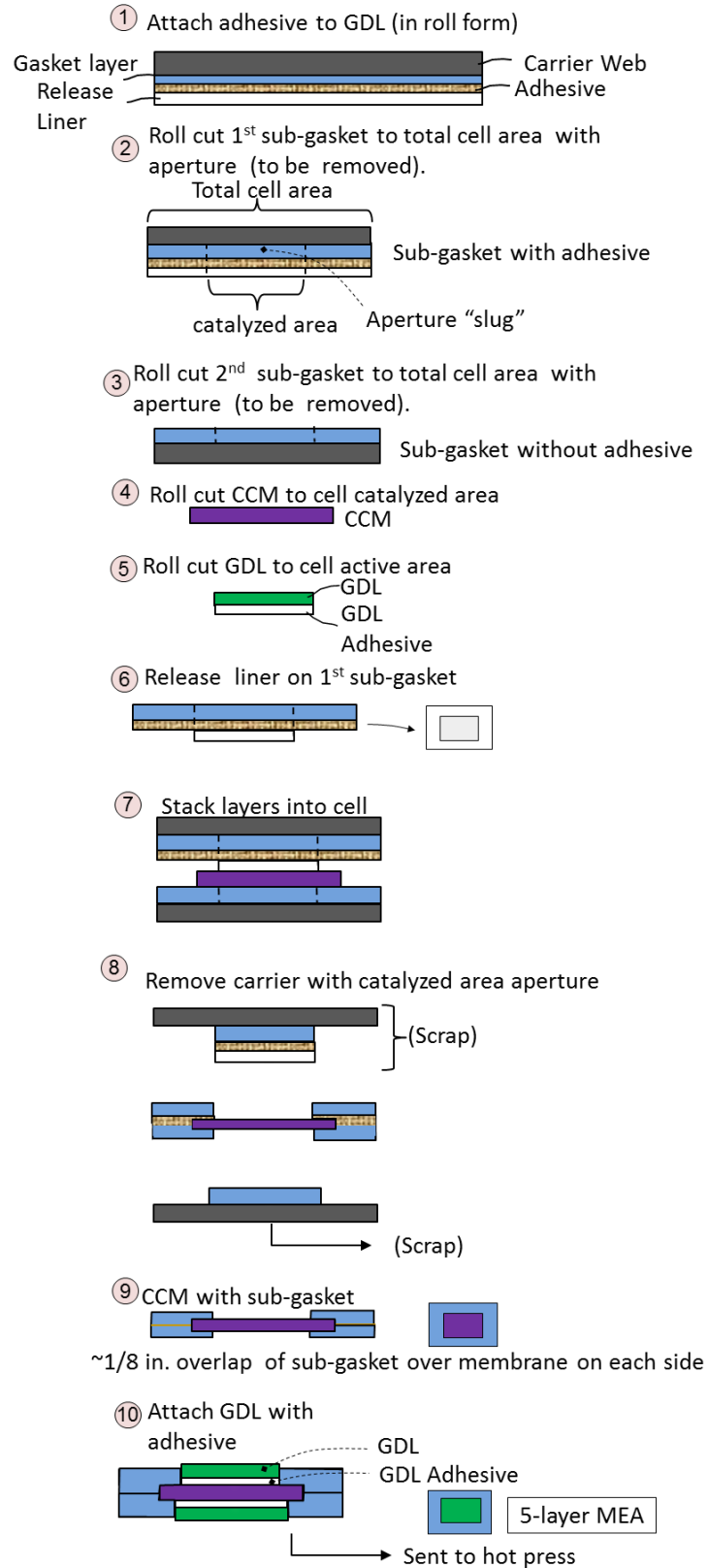
Figure 26. Labeled processing steps for sub-gasket manufacturing at low volumes
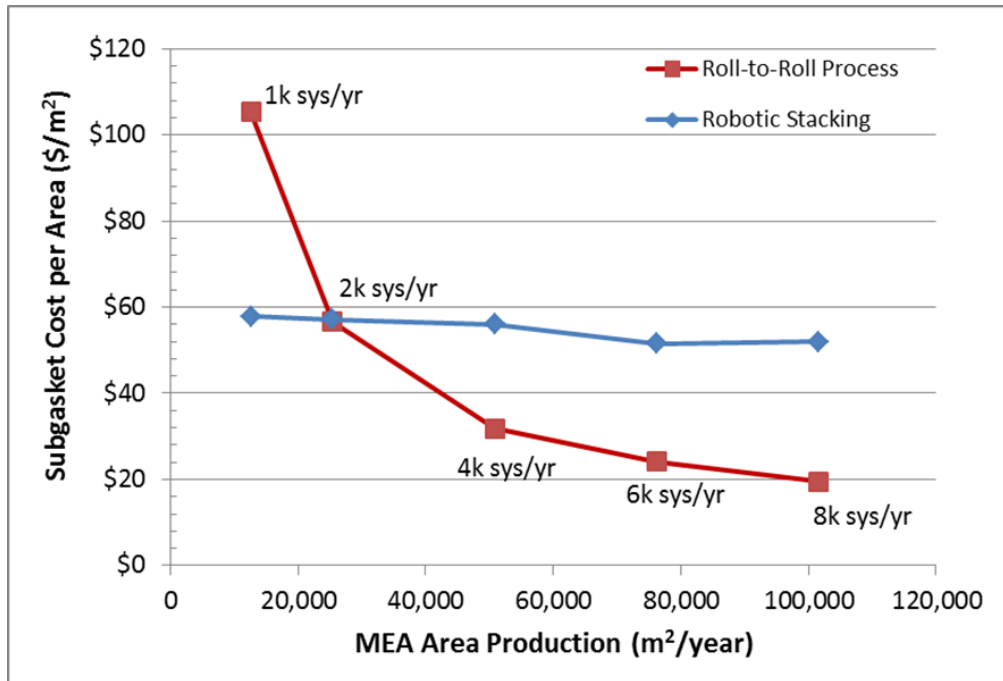
Figure 27. Graph showing cost cross-over for low volume to high volume sub-gasket process

6.7.3 Job Shop of Screen Printing End Gaskets

Due to the small number of end gaskets required in a stack (2) and resulting low machine utilization, the cost per screen printed part at low volumes is quite high ($76.63/part at 1,000 systems per year). Even when a smaller screen printing unit is used, the cost does not go below $52/part at 1,000 systems per year (2,000 parts per year). The table in Figure 28 shows how the cost could be significantly reduced if the part was outsourced to a third party vendor or "Job-Shop". Note that although both the in-house and job-shop costs are labeled as "costs", the job-shop "cost" contains job-shop markup and thus represents their selling price.

Job shopping two other non-repeat components of the stack, the end plates and current collectors, provides the OEM a cost benefit due to the same low utilization and high capital cost of machinery experienced by the end gasket.

Machine	"Small" Machine (Keywell KY-912GL)	"Production" Machine (DEK Horizon)
Projected In-House (1k sys/yr) Cost, $/part	$52.23/part (0.05% util.)	$76.63 (0.16% util.)
Projected Job-Shop (1k sys/yr) Cost, $/part	$0.11/part (37% util.)	$0.50/part (37% util.)

Figure 28. Table showing two types of screen printing machines for "In-House" and "Job-Shop" and the associated cost per part of the end gasket with corresponding machine utilization.

6.7.4 Air Humidifier Membrane Production Process Assumption

The plate-frame air humidifier membrane production process utilizes slot die coating (modeled after a Gore-style manufacturing process) to apply ionomer to expanded polytetrafluoroethylene (ePTFE). The membrane production for 1,000 air humidifiers is roughly 1,200m^2. At such a low volume of membrane production, the slot die coating process is heavily underutilized. However, SA postulates that the humidifier manufacturer would most likely have multiple products and customers with similar membrane requirements. Therefore, the cost of membrane per m^2 is based on aggregate process line production rather than on the production from only one product. To model this aggregate production, a 5x multiplier is placed on the membrane fabrication at the 1,000 systems/year level for purposes of computing membrane cost per square meter. This reduces the cost of membrane for the humidifier from $860 to $237 per system, a cost reduction of approximately $8/kWnet.

6.8   Summary of Quality Control Procedures

The quality control (QC) systems were updated for the 2015 DFMA^{TM} analysis and reflect further review and analysis by QC expert Mike Ulsh of NREL. Overall, a more rigorous definition of the quality control systems was established. The general approach for defining the new QC systems was to:

1. Postulate the required resolution for defect identification.
2. Specify equipment needed to achieve desired resolution at specified line speed.
3. Incorporate automatic adjustment (within the model) for web width processing that vary with production volume.
4. Identify and define QC equipment changes for low volume production processes.

When low volume processing assumptions changed, SA requested the expertise of NREL to identify changes required for the updated process. While under review, NREL suggested additional changes for high volume processes as well. A detailed table of changes between 2014 and 2015 and low volume (1,000 systems per year) and high volume (500k systems per year) is shown in Figure 29.

Membrane: An Optical Detection System (ODS) was added to replace X-Ray Fluorescence (XRF). ODS is more appropriate for detecting membrane defects such as pinholes, folds, bends, scratches, and thickness non-uniformity in the ionomer. The capital cost is lower for ODS than for XRF (details of the cost reduction cannot be shared due to proprietary capital cost values). The entire membrane fabrication process is assumed to be completed at 1 m web width and requires 13 cameras to cover the entire web width at the targeted detection resolution. A higher web processing speed is accommodated by a camera with a high refresh rate (125 kHz).

Dispersed (slot die coating) CCM: XRF was added to the infrared/direct-current (IR/DC) QC system at all production rates. IR/DC is able to detect cracks and delamination, and XRF can determine the Pt loading and composition of the CCM. NREL suggested having both as that is what is currently used by most fuel cell manufacturers. Additionally, the IR/DC cost is now calculated based on web width and the number of cameras needed (2 at 1,000 systems per year and 7 at 500,000 systems per year).

Sub-gasket: The ODS QC system did not change, but capital cost was adjusted at each manufacturing rate to account for changes in web width (cell material across width), and whether a conveyor system is required. At low volume (only 1,000 systems per year) the assumption is that the ODS system would be vertically mounted above the stacked MEA with sub-gaskets due to the assembly process being discrete, not continuous. Therefore, the conveyor system for the QC of sub-gaskets was removed when there was no need for a continuous process.

Bipolar Plate: At high volumes, an optical system is used to check for any large placement anomalies during robotic stacking. At low volumes, the bipolar plates are stacked manually. Therefore the optical system is removed from the QC at low volume as the worker is manually stacking plates and can observe any placement anomalies. This reduced the QC system to only the laser triangulation probe capital cost ($70k). The optical system was estimated at $30k and kept only for the high production volumes.

MEA (after cutting/slitting): At high volume, the system was changed from XRF to ODS. At low volume, the QC does not apply because cutting and slitting is a part of the sub-gasket process when cells are discretized: thus there is no MEA QC. The capital cost of the ODS (only at high volume) is now based on the web width and the number of cameras required (7 at 500,000 systems per year).

Membrane Air Humidifier: The second station of the Gore humidifier membrane processing QC changed to apply a larger detection resolution than previously mandated (from 20 microns to 100 microns). This is a reasonable pinhole size threshold as there is little adverse effect if small amounts of air cross over from one side of the humidifier membrane to the other. The previously used 20 microns was based on the fuel cell membrane processing QC that cannot permit larger deformations. The upper limit crack size that still results in low impact on the system is not well defined. SA judges 100 microns to be a reasonable detection resolution, but will continue to investigate a proper value through discussions with ANL and Gore. This change reduces the capital cost by $355k (from $392k down to $36.5k) at 1,000 systems per year and $300k (from $392k to $92k) at 500,000 systems per year. The capital cost is also derived from the number of cameras required over the width of the web at the requisite detection size.

Part Tested	2013 /2014 Diagnostic System	2015 Diagnostic System (Low Volume)	2015 Diagnostic System (High Volume)	Comment on Change from 2014 to 2015	Detection Resolution	Total QC Cost	Fault/Parameters Tested
Membrane	XRF OR Optical Diagnostic System - QC - PROPRIETARY	Optical Detection System (ODS)	Optical Detection System (ODS)	Changed from XRF to ODS System at low and high volume	20 micron	$205k (per line 1k and 500k sys/yr)	Visual inspection to locate pinholes in ionomer, discolorations that would indicate thickness variation
Dispersed (slot die coating) Catalyst	IR/DC QC System ($210k)	IR/DC QC System + XRF QC System	IR/DC QC System + XRF QC System	While IRDC gives full width uniformity, added XRF QC System can detect loading/thickness of electrode layers. XRF is most widely used today.	2,000 microns	1k sys/yr: = $1.028M 500k sys/yr: = $1.123M	IRDC gives full width uniformity, XRF loading/thickness rastoring across web width.
Gasketed MEA (Subgasket)	Optical Detection System (ODS) (commercial system from Keyence)	Optical Detection System (ODS) (commercial system from Keyence) mounted above single stacked cell or on arm of robot.	Optical Detection System (ODS) (commercial system from Keyence)	At 1k sys/yr, ODS is mounted above the single stacked sub-gasketed cell or on the arm of the robot. Any conveyor system was removed. At high volume, adjusted cost increased number of cells across the width of web.	0.6mm	(1k sys/yr) $50k (no conveyor system required) (500k sys/yr): $210k	Misalignment of subgasket and membrane. Folds, bends, tears, scratches in subgasket or membrane.
Bipolar Plate	NIST Non-Contact Laser Triangulation Probe, Optical Detection System (commercial system from Keyence)	NIST Non-Contact Laser Triangulation Probe ($70.6k)	NIST Non-Contact Laser Triangulation Probe, Optical Detection System (commercial system from Keyence) ($100.6k)	No change at high volume. At low volume, update to not include ODS system. BPP stacking by worker can simultaneously inspect part so no ODS system needed.	~30 micron over 3 scan lines (one side of plate, 3 probes, single pass), 0.6 mm for Optical Camera (entire plate, one side)	(1k sys/yr): $70.6k (no optical system) (500k sys/yr): $100k	Triangulation: flow field depth, plate flatness. Optical System: general dimensions, completeness of manifold apertures.
MEA (after cutting/slitting)	XRF (point measurement only)	NA	Optical Detection System (ODS) (commercial system from Keyence)	Previously used XRF does not detect cracks and delamination, however ODS is able to detect this.	0.6mm	(1k sys/yr): NA (500k sys/yr): $210k	Thickness, cracks, delamination, misalignment of cutting/slitting.
Air Humidifier Membrane Station B (inspection of ePTFE web)	Optical Detection System	Optical Detection System	Optical Detection System	Set of line cameras to optically detect pinholes or other anomolies of top surface of ePTFE/ionmer membrane. Higher anomally detection size and also adapt calculation to account for various web widths.	100 micron	(1k sys/yr): $36.5k (30cm web width - 1 line camera) (500k sys/yr): $92k (1 m web width - 4 line cameras)	Visual inspection to locate pinholes in ionomer, discolorations that would indicate thickness variation or other problems.

Figure 29. Summary of changes for quality control systems used in stack and membrane humidifier manufacture.

7 Automotive Power System Side Analyses

This section contains analyses completed during 2015 that either may have helped determine a certain pathway for the baseline system, or may apply to components that will be in a future baseline system when performance has been demonstrated to meet or exceed the performance of current baseline system components.

7.1 DFMA™ of Giner Dimensionally Stable Membrane (DSM™) Fabrication
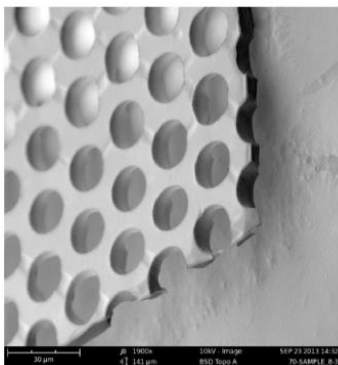
Figure 30. Giner's dimensionally stable membrane (DSM[TM]**) support layer made of polysulfone (PSU) (Image from Giner 2014 AMR Presentation,**[45]** slide 19)**

In exploring ways to reduce the cost of membrane materials, DOE has supported research in alternative methods for production of porous substrate materials for PEM membranes and/or humidifier membranes. Conventional systems currently use expanded polytetrafluroethylene (ePTFE) as the substrate material but ePTFE of the quality required for fuel cell membrane application is quite expensive ($1.80 to $10/m^2 as described in SA's 2014 analysis (Section 8.1.2.2)).

Giner Electrochemical Systems, LLC (now merged with Giner, Inc.) has explored multiple pathways for processing low cost materials to make perforated structural supports to contain the ionomer.[46] From those pathways, Giner has down-selected to a roll-to-roll process of pressing a micromold into a softened bilayer of PFSA ionomer and polysulfone (PSU) to form a dimensionally stable membrane (DSM[TM]) structure as seen in Figure 30.[47] A follow-on process for filling the pores with the desired ionomer solution makes the complete fuel cell membrane. Giner's inert thin film support can be used as a low cost alternative to ePTFE as the main substrate raw material (PSU) cost is low (~$14.33/kg). A comparison of the dimensions and porosity of the baseline ePTFE support and Giner's DSM[TM] substrate appears in Figure 31.

---

[45] Mittelsteadt, C., Argun, A., Lacier, C., Willey, J., "Dimensionally Stable High Performance Membranes", Giner, Inc. presentation at the 2014 US DOE Fuel Cell Program Annual Merit Review and Peer Evaluation Meeting, Arlington, VA, June 18,2015. (slide 19)

[46] Mittelsteadt, C., Argun, A., Lacier, C., "Dimensionally Stable High Performance Membrane", Giner, Inc. 2014 Annual Progress Report, 2014.

[47] Mittelsteadt C. K.; Argun, A. A**.;** Lacier, C.; Willey, J. "*Micromold Methods for Fabricating Perforated Substrates and for Preparing Solid Polymer Electrolyte Composite Membranes*" U.S. Patent Application Publication No. 2014/0342271 A1 (Nov. 20, 2014), **2014.**

	SA Baseline Membrane Substrate	SA Estimate of Giner DSM™ Substrate
Support Material	ePTFE	PSU/PFSA
Pore Size (µm)	Range (0.02 to 40 µm)[48]	20 (7 µm spacing)
Substrate Thickness (µm)	25	10
Porosity Vol%	95%	50%
Substrate Vol%	5%	50%

Figure 31. Comparison table of ePTFE and Giner DSM™ dimensions and porosity.

SA conducted a DFMA™ cost analysis of the Giner DSM™ (support only) based on the processing steps illustrated in Figure 32. A PFSA/PSU bi-layer film is coated onto a backer sheet and goes through a rotary micromold to form holes. The perforated substrate is then rolled-up on a re-wind stand. In this manner, a 10 µm thick, perforated bi-layer sheet is formed on a backer film. The backer film (carrier) is not punctured by the micromold and can be reused.

Although not included in the cost analysis of the substrate, the remaining steps to produce a PEM membrane from the DSM™ substrate are next described for completeness. The continuous web of substrate is run through an ionomer coating station to fill the holes with ionomer and coat the top of the bi-layer (the PSU side). After drying, the fuel cell membrane is then complete and can be removed from the backer film for use. Conceptually, the resulting membrane (DSM™) is a perforated PSU substrate fully encapsulated and occluded by PFSA on both sides with sufficient and pre-defined PSU layer porosity (50%) to allow good fuel cell performance.

Two QC optical detection systems measure the thickness of the substrate before and after the holes are made. In Giner's DSM design, there is no drying step required because the material is sufficiently dried at room temperature for 1 minute (at 3 m/min line speed) before being rolled up. However, SA feels that at high volume, an optional heating section could be inserted after the micromold to speed up drying time and therefore increase the overall rate of membrane production. (At low production rates, line speed may be reduced to a rate which allows the membrane to dry between stations without a dedicated dryer, as in Giner's demonstrated processes.) The capital cost for the machinery used in this process is estimated at between $1.3M (1k systems per year) and $2M (500k systems per year) based on the summation of individual processing equipment.

The DFMA™ analysis of Giner's porous substrate was completed in 2015 as a side study. Cost results are shown in Figure 33 and a comparison to Giner cost estimates for their roll-to-roll DSM™ and their current method of DSM™ fabrication appears in Figure 34. Even though the Giner-style substrate is

---

[48] "Expanded Polytetrafluoroethylene Membranes and Their Applications"
https://www.gore.com/MungoBlobs/827/932/ExpandedPTFEandTheirMembranes_Gore_Chapter23_Feb2008.pdf

predicted to be lower cost than the ePTFE substrate, it was not used for the baseline auto fuel cell system due to unknown performance in a complete MEA.
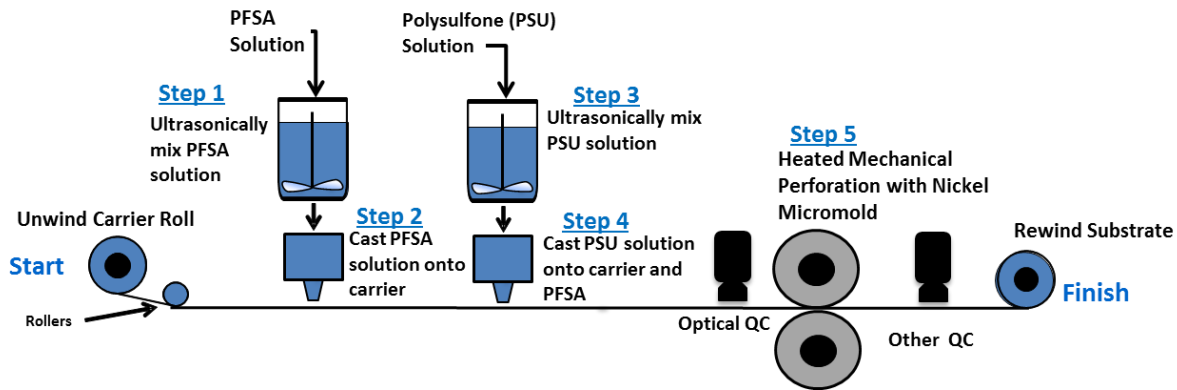
Figure 32. Diagram of SA's Interpretation of the manufacturing process for Giner's DSM^TM support. Process modeled using acetone as the solvent (in PFSA and PSU solutions) and polyimide for carrier, however other combinations of solvent and backer can be used and are not restricted to the modeled materials.

Annual Production Volume	systems/year	1,000	10,000	30,000	80,000	100,000	500,000
Annual Membrane Production (Net)	m2/year	11,464	114,635	343,003	914,676	1,143,345	5,716,724
Substrate Cost	$/m2	$85.96	$10.36	$5.28	$5.36	$4.50	$3.85

Figure 33. Cost results of Giner substrate over all the automotive production volumes (3m/min).
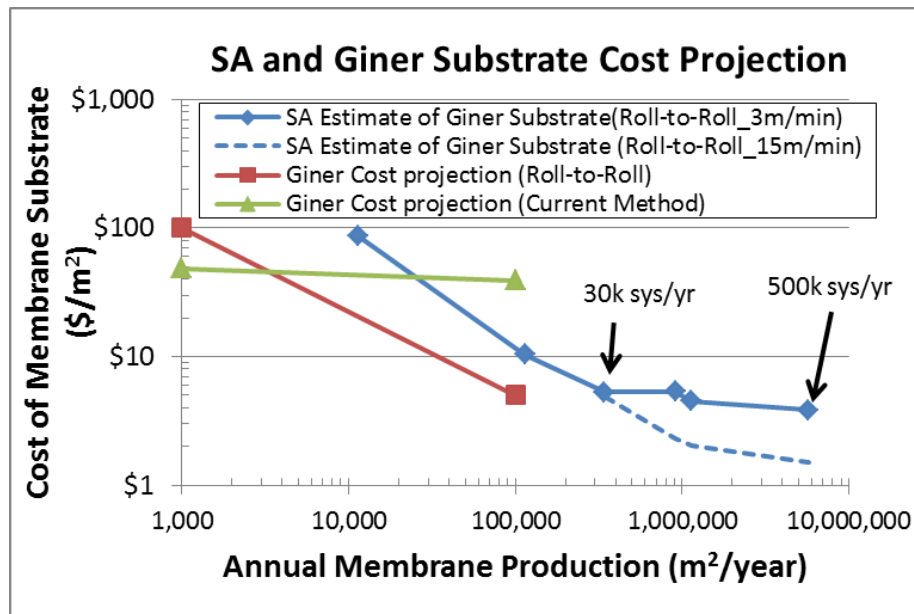
Figure 34. Comparison of SA estimate for Giner DSM^TM (at 3m/min and 15 m/min line rates) and Giner's estimate for their DSM^TM and their current method.
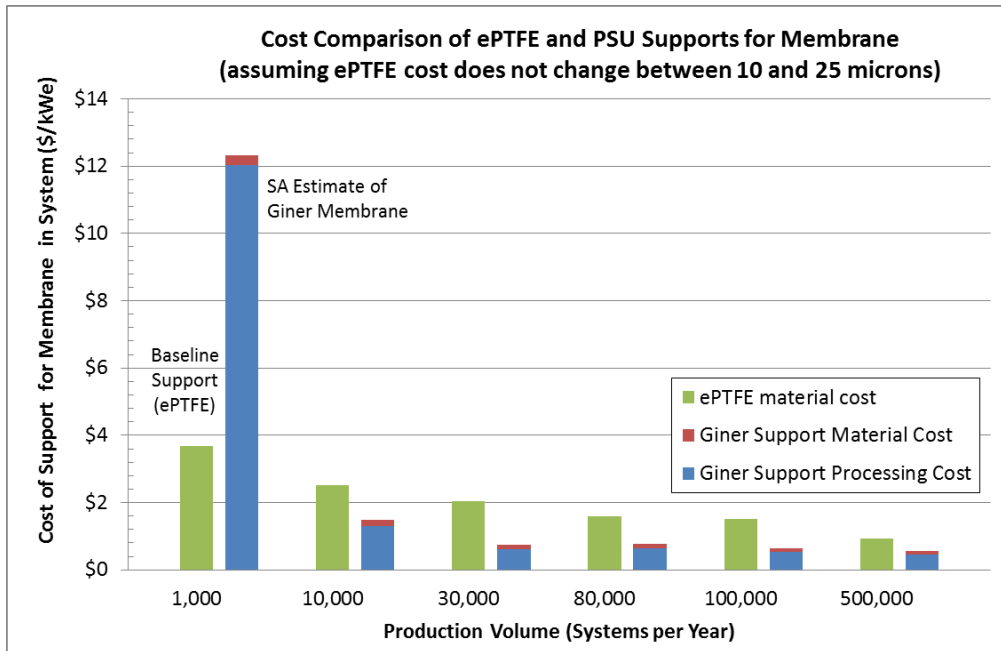
Figure 35. Cost results and comparison of SA's estimate for Giner DSM^{TM} (3m/min) to baseline membrane support material ePTFE.
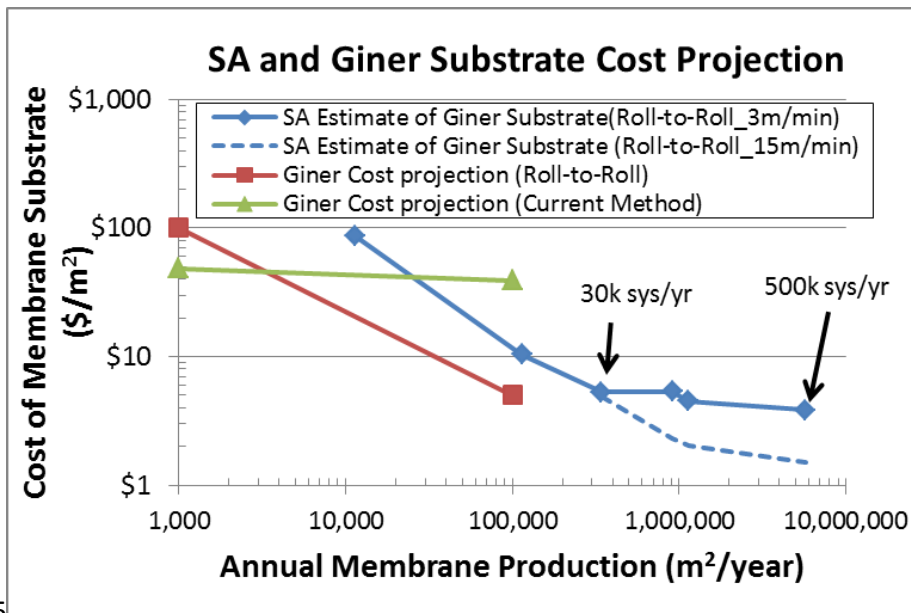
Figure 35

Figure 34 graphically compares the SA and Giner substrate cost projected and shows that SA's estimate is approximately double the Giner estimate ($10/m^2 compared to $5/m^2) at 100k m^2/year. However there are assumption differences between the two analyses that may explain this disparity. The SA analysis assumes Nafion PFSA as the material for both the substrate PFSA and ionomer coating ($103/kg at 98,000 kg/year to $338/kg at 233 kg/year) while Giner uses a proprietary non-Nafion low equivalent

weight[49] (EW) PFSA for the DSM^{TM} supported membrane. SA's cost estimate includes a 25% material markup and 54% processing markup (at ~ 100k m^2/year) while Giner's markup assumptions are unknown. Even though SA projects a higher cost, SA's estimate shows that the Giner substrate cost is still less than projected ePTFE cost at all but the lowest production volume (1,000 systems per year) yielding potential savings of ~$0.38/kWnet at 500k systems per year assuming the same performance and durability (Figure 35). The low volume cost results reflect the high capital cost of equipment and low utilization**.** The cost to fill the pores with Nafion is expected to be the same for an ePTFE substrate as for the Giner's DSM^{TM}. As an example, at 500,000 systems per year, the cost of the Giner DSM^{TM} support is $3.85/m^2 ($0.55/kWnet) while the ePTFE substrate is estimated to be closer to $6.50/m^2 ($0.93/kWnet).

The Giner DSM^{TM} fabrication process is demonstrated at 3m/min, however at larger volumes, the speed of the line could be increased as along as the process has the ability to form holes without deformation of the adjacent holes. If the line speed were to increase to 15m/min, the resulting membrane cost would decrease to $1.52/m^2 ($0.22/kWnet). This cost reduction is based only on an increase in line rate and does not account for larger tooling that maybe required.

7.2   DFMA™ of Binary Dealloyed PtNi Catalyst Application using NSTF

As described in Section 6.1, attention has shifted toward binary dealloyed PtNi catalysts. To compare dispersed and NSTF dealloyed PtNi catalyst, a side study was conducted of the NSTF dealloyed PtNi catalyst in 2015.

3M provided single cell polarization data for d-PtNi NSTF catalyst MEAs (inclusive of a catalyst interlayer coated on the cathode GDL). A cross-section of the MEA (not to scale) is shown in Figure 36. The single cell test data is for an MEA with a dealloyed PtNi NSTF cathode with a Pt/C interlayer on the GDL and a ternary PtCoMn NSTF anode. The NSTF application cost model is the same for both the PtCoMn and the d-PtNi with the exception of an additional dealloying step for d-PtNi. The block diagram for the NSTF catalyst application process is shown in Figure 37 (top) with the dealloying step highlighted in blue. In the dealloying step, the web is submerged in a ferric acid bath for 2.5 minutes (0.8 m/min web speed), rinsed, dried, and re-wound onto a roll. Calendaring of the NSTF electrodes onto the membrane is not shown in the diagram, but is assumed to follow the same methods used for ternary PtCoMn NSTF catalyst application (described in SA's 2014 Update report).[50] The process used to apply an interlayer of catalyst onto the GDL of the cathode using slot die coating is shown at the bottom of Figure 37.

---

[49] Equivalent weight is defined as grams of dry polymer per mole of acid groups.
[50] "Mass Production Cost Estimation of Direct H$_2$ PEM Fuel Cell Systems for Transportation Applications: 2014 Update" Brian D. James, Jennie M. Moton & Whitney G. Colella, Strategic Analysis, Inc., January 2015.
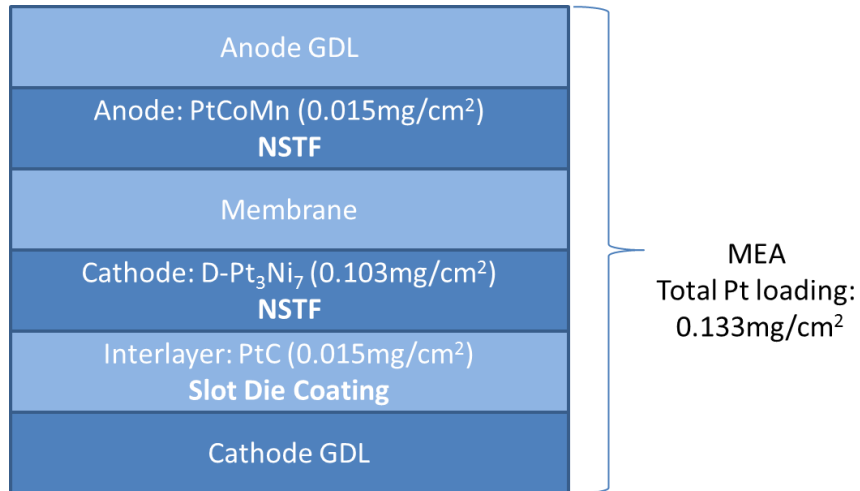
Figure 36. Pt Loading for each layer of the 3M test cell

DFMA Process Diagram: Dealloyed PtNi Catalyst Processing Using NSTF (Cathode only)
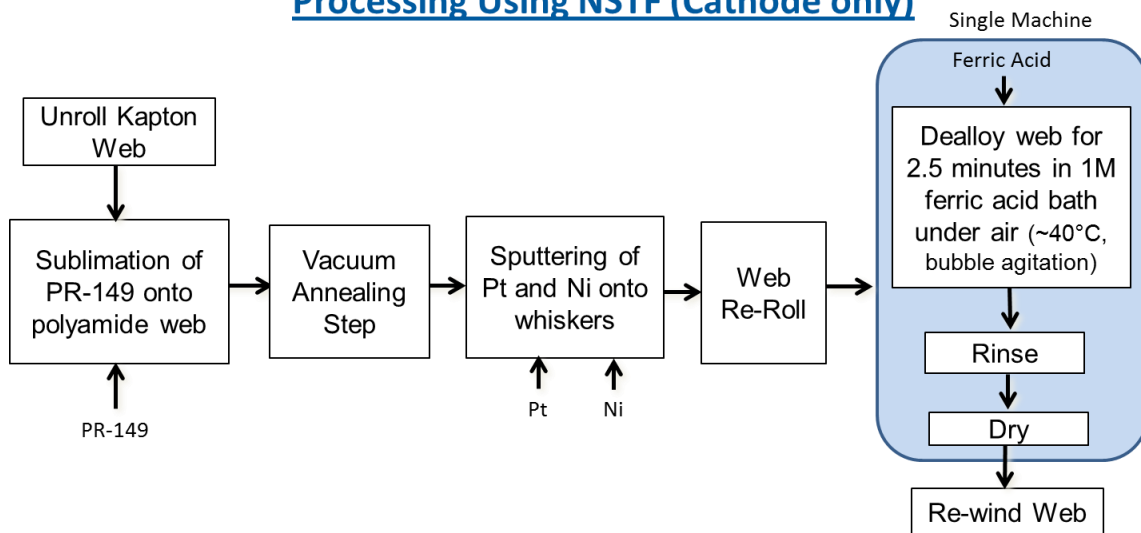
DFMA Process Diagram: Interlayer Coat onto Cathode GDL
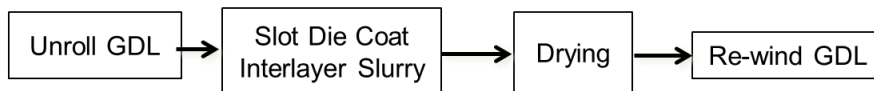
Figure 37. Process diagram for dealloyed PtNi catalyst processing using NSTF (top) and process for interlayer coating (bottom)

Cost results are shown in Figure 38 for d-PtNi NSTF catalyst synthesis and application. The results illustrate that the processing costs dominate at low volume and material costs dominate at high volume. The two material costs appear to remain constant over all production volumes due to the constant cost of platinum ($1,500/tr.oz.) making up the majority of the material cost. The cost results are expressed in $/kWnet based on calculated material required from the operating conditions and performance derived from the single cell test data. The data from 3M was adapted by SA to include voltage losses for conversion from single cell performance to stack performance and to a lower air stoichiometry. The cost of d-PtNi is lower than ternary PtCoMn NSTF at high volumes as seen in Figure 39 due to the lower Pt loading and higher power density. At 1,000 systems per year, the processing cost dominates because of the extra dealloying and interlayer of the d-PtNi catalyst. However at higher volumes, the processing cost becomes insignificant compared to the cost of platinum. The development of higher performing catalysts with reduced platinum content (from either the unique and complex application techniques or creative catalyst structures) outweighs the impact of any sort of custom application process when it comes to lowering the cost of catalyst systems.
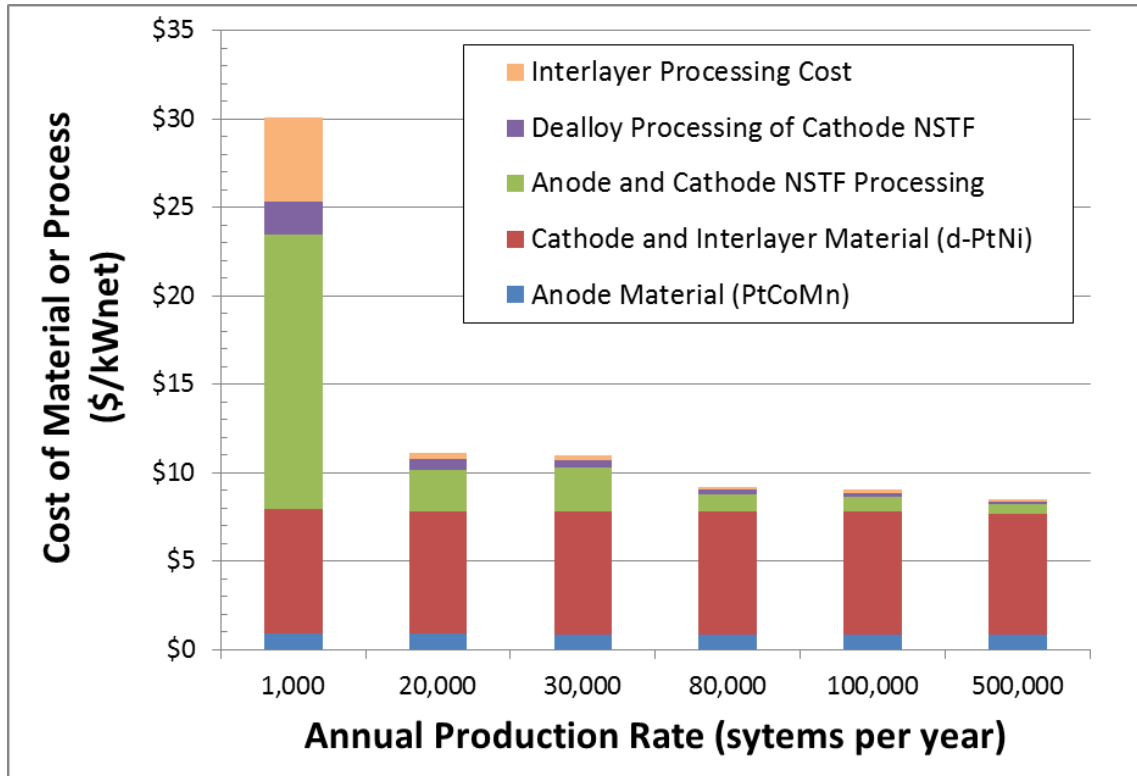
Figure 38. Breakdown in binary d-PtNi NSTF catalyst and application at all production rates
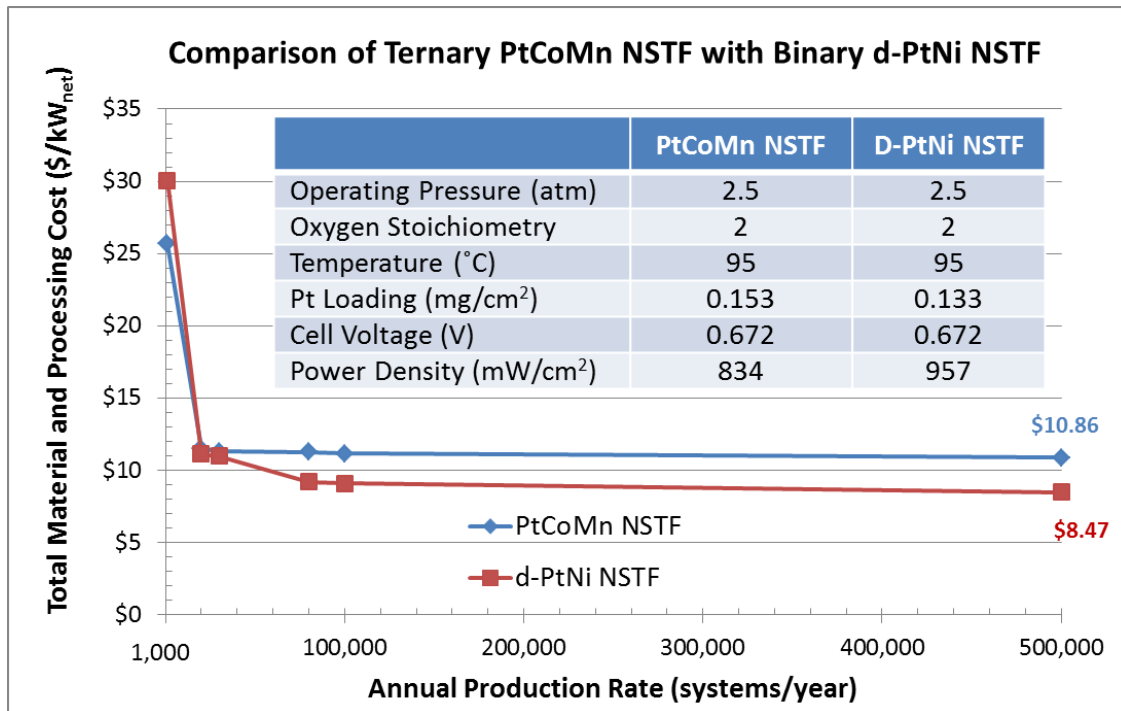
Figure 39. Comparison (graphically and parametrically) for ternary PtCoMn and binary d-PtNi catalysts

7.3 DFMA™ of Non-Pt Polyaniline (PANI)-Fe-C Catalyst Synthesis

Dr. Piotr Zelenay at Los Alamos National Lab (LANL) has demonstrated power density of 330mW/cm^2 on H$_2$ and air for polyaniline-Iron-Carbon (PANI-Fe-C) catalyst (95 wt% Carbon, >2% Fe). A full DFMA^{TM} analysis of PANI-Fe-C catalyst synthesis based on scale-up of the LANL procedures was completed during 2015. Figure 40 shows the processing system diagram for the catalyst synthesis.

Steps in cost modeling of the PANI catalyst synthesis include:

1) Carbon activation (oxidation of carbon in nitric acid),
2) Catalyst reaction: first polymerization of hydrogen chloride, aniline, and iron chloride, second polymerization by adding ammonia persulfate to make PANI, and combining carbon to PANI,
3) Drying in air at 200˚C on a belt dryer,
4) Grinding of the resulting powder (10 micron particle size),
5) Rotary kiln pyrolysis: calcined at 900˚C for 1 hour in an inert environment, then
6) An acid leach for 8 hours in hydrogen sulfate, wash and filtration, and
7) Pyrolysis at 900˚C for 1 hour in an inert environment.

PANI-Fe-C Catalyst Process Model

Step 1a:
1. Carbon
2. 70% HNO$_3$
Mix for 5 hours at 90°C/Reflux
Step 1b:
1. Water Wash
2. Hot dry
2 hours until pH 5-7

Step 2a: Mix Reagents
1. 1.0M HCl
2. Aniline
3. FeCl$_3$

Step 2b: 1st Polymerization
Stir 30 minutes

Step 2c: 2nd Polymerization
7. (NH$_4$)$_2$S$_2$O$_8$
Stir 5 hours at ~23°C

Reaction Vessel:
Oxidation of Carbon

Carbon Storage

Step 2d: Add Carbon to PANI
Mix for 48 hours at ~23°C

Reaction Vessel

Step 3:
Combustion Air at 200°C

Belt Dryer

Step 4: Grinding
(to 10 μm)

Step 5: Rotary Calciner
1 hour hold at 900°C,
30°C/min ramp rate

N$_2$ Sweep Gas

Step 6:
Acid Leach
0.5M H2SO4
Treat for 8 hours at 90°C
DI Water Wash

H$_2$SO$_4$

Filtration

Step 7: Pyrolysis Oven
1 hour hold at 900°C,
30°C/min ramp rate

Solid Catalyst Product

N$_2$ Sweep Gas

Figure 40. Process diagram of the PANI-Fe-C catalyst synthesis.

From this process, the catalyst powder cost is estimated to be of $91.30/kg at 500,000 systems per year (at 970g system), compared to a d-PtNi catalyst cost of ~ $20,000/kg (~20g/system). The breakdowns in PANI-Fe-C catalyst materials and processing cost are shown in Figure 41 at 1,000 and 500,000 systems per year.

In comparison to the 2015 baseline catalyst (d-PtNiC) using slot die coating application, the PANI catalyst (also with slot die coating application) is still more expensive due to a very low power density (330mW/cm^2). The cell size and/or number of stacks would increase due to this lower power density, resulting in a more expensive stack, as shown in Figure 42 (middle columns). However, the extra costs for membrane/GDL/plates/etc. necessitated by the lower power density are partially offset by the greatly reduced material cost of the PANI catalyst compared to d-PtNiC. Overall, stack cost is about 33% greater with PANI ($34.09/kWnet for PANI and $25.64/kWnet for d-PtNiC) at 500,000 systems per year. If the PANI catalyst were to increase its power density from 330mW/cm^2 to 746mW/cm^2, the stack cost would reduce to $15.29/kWnet (as seen in Figure 42 left columns). Thus, assuming equivalent performance (which has not yet been achieved), the projected value of a non-Pt catalyst is ~ $10/kWnet

less expensive (i.e. the difference between $15.29/kWnet and $25.64.kWnet).

Material and Manufacturing Cost Breakdowns at 1k and 500k systems per year
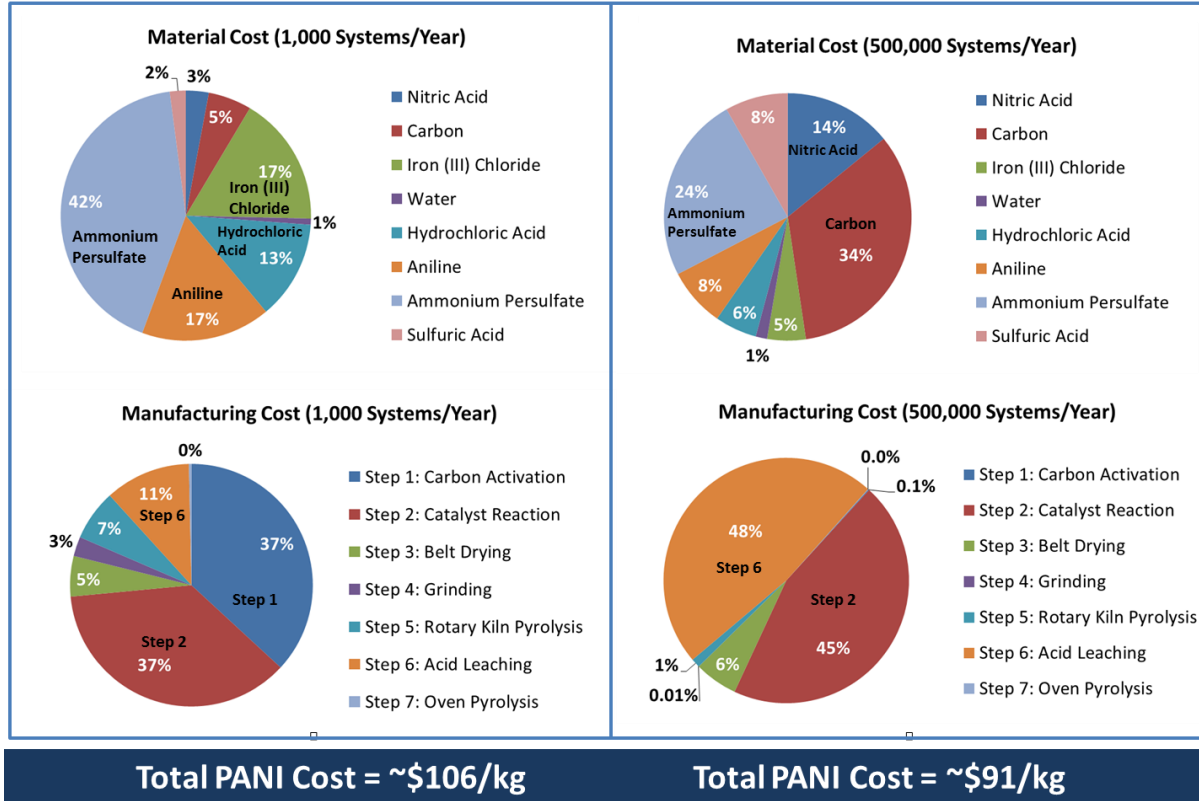
Figure 41. Pie charts showing the breakdown of the materials and manufacturing cost for the PANI-Fe-C catalyst synthesis process at both 1,000 and 500,000 systems per year.

At 330 mW/cm^2 PANI catalyst requires two stacks

		PANI Power Density (746 mW/cm^2)		PANI Power Density (330 mW/cm^2)		d-PtNiC Power Density (746 mW/cm^2)	
Annual Production Rate	systems/year	1,000	500,000	1,000	500,000	1,000	500,000
System Net Electric Power (Output)	kWnet	80	80	80	80	80	80
System Gross Electric Power (Output)	kWgross	88.22	88.22	88.22	88.22	88.22	88.22
Stacks per System	stacks/system	1	1	2	2	1	1
Component Costs per Stack							
Bipolar Plates (Stamped)	$/stack	$1,608	$558	$1,122	$607	$1,607	$558
MEAs		**$7,597**	**$515**	**$6,181**	**$601**	**$9,210**	**$1,343**
Membranes	$/stack	*$3,214*	*$206*	*$2,381*	*$199*	*$3,213*	*$206*
Catalyst and Application	$/stack	$914	$84	$1,072	$193	$2,527	$913
GDLs	$/stack	*$2,510*	*$96*	*$1,849*	*$71*	*$2,509*	*$96*
M & E Hot Pressing	$/stack	*$43*	*$9*	*$30*	*$9*	*$43*	*$9*
M & E Cutting & Slitting	$/stack	*$0*	*$3*	*$0*	*$3*	*$0*	*$3*
MEA Frame/Gaskets	$/stack	*$917*	*$116*	*$849*	*$125*	*$917*	*$116*
Coolant Gaskets (Laser Welding)	$/stack	$219	$30	$115	$32	$219	$30
End Gaskets (Screen Printing)	$/stack	$1	$0.47	$1	$0.48	$1	$0.47
End Plates	$/stack	*$100*	*$56*	*$105*	*$59*	*$100*	*$56*
Current Collectors	$/stack	*$8*	*$6*	*$9*	*$7*	*$8*	*$6*
Compression Bands	$/stack	*$10*	*$5*	*$10*	*$5*	*$10*	*$5*
Stack Insulation Housing	$/stack	*$64*	*$6*	*$35*	*$6*	*$64*	*$6*
Stack Assembly	$/stack	*$80*	*$34*	*$77*	*$34*	*$80*	*$34*
Stack Conditioning	$/stack	*$60*	*$13*	*$60*	*$13*	*$60*	*$13*
Total Stack Cost	**$/stack**	$9,748	$1,223	$7,716	$1,364	$11,360	$2,052
Total Cost for all Stacks	**$/stacks**	$9,748	$1,223	$15,432	$2,727	$11,360	$2,052
Total Stacks Cost (Net)	**$/kWnet**	$121.85	$15.29	$192.90	$34.09	$142.00	$25.64
Total Stacks Cost (Gross)	**$/kWgross**	$110.49	$13.86	$174.92	$30.92	$128.77	$23.25
Total Catalyst Cost	**$/kg**	$122.18	$75.05	$106.02	$91.30	$24,208	$19,756

In the same range of cost per kWnet

Figure 42. Table with comparison of PANI (at 746 and 330mW/cm^2) versus d-PtNiC (at 746mW/cm^2) catalyst stack costs.

7.4 Low Production Volume Detailed Side Analyses

7.4.1 Bipolar Plate Material and Coating

Inspired by the new Toyota Mirai fuel cell vehicle,[51] titanium (Ti) bipolar plates (instead of 316 stainless steel (SS) plates) were investigated for potential cost benefit at lower production volumes. Since Ti is much more expensive per kg than stainless steel, a cost advantage seems unlikely unless the cost for coating a stainless steel plate (to reduce corrosion and increase conductivity) more than offsets the difference in material cost. Ti pricing was based on commercially pure (CP) Grade 2 Ti sheet metal at 0.003 inches thickness, $157/kg material cost (based on a price quote from ATI Metals at 9 metric tons order size for uncoated coil), with a low contact resistance gold coating. Stainless steel pricing is based on SS 316 sheet metal at 0.003 inches thickness, $11/kg material cost (based on price quote for uncoated coil), with a Treadstone anti-corrosion and low contact-resistance coating. At the

---

[51] http://www.kobelco.co.jp/english/releases/2015/1190697_14516.html

manufacturing rates established for the baseline system, Ti plates are assessed to be always more expensive than the baseline SS bipolar plates. Quotations for thicker Ti sheets were obtained (0.021 inches thick) since milling costs to achieve thin sheets are a substantial cost contributor. Figure 43 shows that even at $27/kg, Ti plates would still be more expensive than SS plates (due to the greater mass per area of bipolar plate). A cross-over point may occur below 1,000 systems per year if the Treadstone coating costs become so much more expensive than gold coating that they offsets the high cost of Ti. However, this possibility was not fully explored since the production volume would be well below the area of interest.
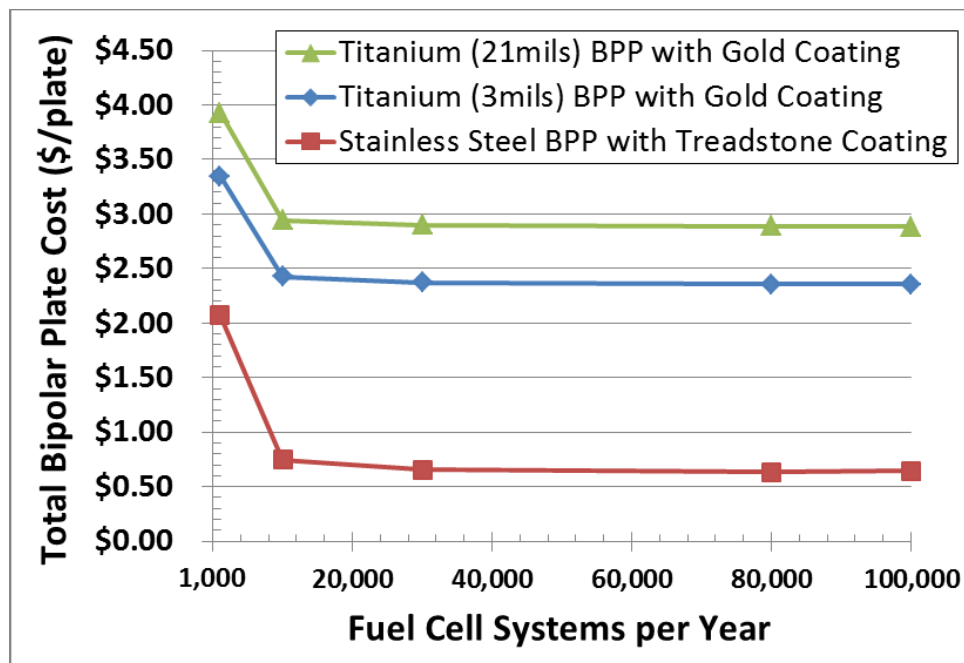
Figure 43. Graph showing cost of stainless steel bipolar plates (single plates) with Treadstone coating compared to a thin (0.003 inch) and thick (0.021 inch) titanium bipolar plate with gold coating.

7.4.2 Bipolar Plate Forming

The baseline DFMA[TM] model uses progressive stamping to form the stainless steel bipolar plates. However, sequential stamping and hydroforming are also viable alternatives to form very thin metal plates. Stamping and hydroforming companies were contacted to gather information on the cost and limits of the machinery. Hydroforming and stamping (both sequential and progressive) have several significant differences:

> 1) Typical hydroforming cycle times are ~15-20 seconds while stamping usually only takes ~1 second

2) Stamping dies (tooling) are more expensive (~$40k) than hydroforming dies (~$10-15k) because they are typically manufactured from harder materials to withstand greater impact and abrasion forces, making them more difficult/time-consuming to machine.

In conversations with hydroforming and stamping vendors, hydroforming is expected to be less expensive than stamping at lower volumes (<50,000 parts per year or about 60 systems year) because of the lower die costs.

Multiple hydroforming service providers contacted could not hydroform stainless steel in sheet thicknesses less than 0.018 inches thick due to rupture concerns from the material elongation during the hydroforming process. The stamped plates for the baseline system are 0.003 inches thick to minimize overall weight and material cost within the stack (and also to minimize voltage drop and laser welding time). However, a hydroforming machine manufacturer, Triform, carries a hydroforming machine that can hydroform SS down to 0.002 inches thickness. The capital cost and operating parameters for the Triform 16-5BD machine are used for hydroforming projections.

Note that the hydroforming operation is well suited to form the flow field and gasket groove patterns of the plate but is not suited to piercing, lancing, or cutting operations. Thus a separate cutting operation is needed to trim around the perimeter of each cell and to cut any manifold or tie-rod holes. These cutting operations are based on a 35 ton stamping press.

Borit is a Belgium based hydroforming company well experienced in bipolar plate fabrication. Their technology couples hydroforming with sheet metal unwinding units to provide a more rapid load and unload compared to traditional operations. Input from Borit was not received in time for publication but will be incorporated in future updates of this report.

Stamping may be sequential or progressive. Since four stages of stamping (and thus four stamping dies) are required to provide all bipolar plate features, a sequential stamping concept would entail each bipolar plate undergoing four separate and sequential stamping operations either on four separate machines or on the same machine with four die change outs. The capital cost and operating parameters for a small machine, Komatsu OBS 60 ton, are used for sequential stamping projections.

Progressive stamping uses a single machine to stamp all features progressively i.e. all four dies are actuated simultaneously in the press with the part indexed from die to die. The capital cost and operating parameters are based on a 130 ton progressing stamping machine (see Section 8.1.1.1 for more details).

Die (tooling) cost and lifetime are also important assumptions for accurate cost predictions (see Figure 44). Dies can be refurbished to extend their service life. Such die refurbishment is appropriate at high volumes but may not be appropriate under low production rate operation where the die may not reach its initial lifetime limit before the die-design is desired to be updated. Consequently, die refurbishments are typically associated with progressive dies since they typically are used in high volume production operations.

Parameter	Hydroforming	Sequential Stamping	Progressive Stamping
Base Machine Cost	$190k (total sys = $352k)	$75k (total sys = $175k)	$177k (total sys = $450k)
Die Cost ($/die)	$12k (hydroform) $26k (cutting) Total = $38k	$39k Complete tooling set (4 dies)	($39k x3)+($50k 2x) Complex Die Refurbishment = $217k
Lifetime (cycles)	~1,200k	600k	600k x3 =1,800k (two refurbishments)

Figure 44. Tables showing the machine and die cost assumptions for all three forming processes.

Consideration is also given to whether the parts are made in-house or by a third party (job-shop). When making this decision, there are additional variables to consider such as the base machine utilization of the third party vendor and the vendor markup that would be applied. Vendor base utilization refers to the base workload of the machine prior to the vendor accepting the plate order: the higher the vendor's machine utilization, the lower his costs to produce the plates (savings which ideally would be passed along to the customer). Vendor markup refers to the profit, overhead, and general and administrative costs charged to the customer.

Figure 45 compares job-shop and in-house manufacturing costs for hydroforming, sequential stamping, and progressive stamping. The manufacturing rate cross-over point at which progressive stamping becomes less expensive than sequential stamping or hydroforming is below the region of interest (100,000 plates per year or 130 systems per year). Progressive stamping is always less expensive than sequential stamping or hydroforming above 1,000 systems per year. Similar results are seen in a hydroforming/stamping comparison from MIT.[52] Fluctuations/discontinuities in the cost curves are a result of either an increase in the number of tooling sets needed per machine lifetime or an increase in the number of simultaneous lines needed to meet the capacity.

[52] Matwick, S. E., "An Economic Evaluation of Sheet Hydroforming and Low Volume Stamping and the Effects of Manufacturing Systems Analysis", Master's Thesis for Master of Science in Material Science and Engineering at MIT, pg40, February, 2003. http://msl.mit.edu/theses/Matwick_S-thesis.pdf
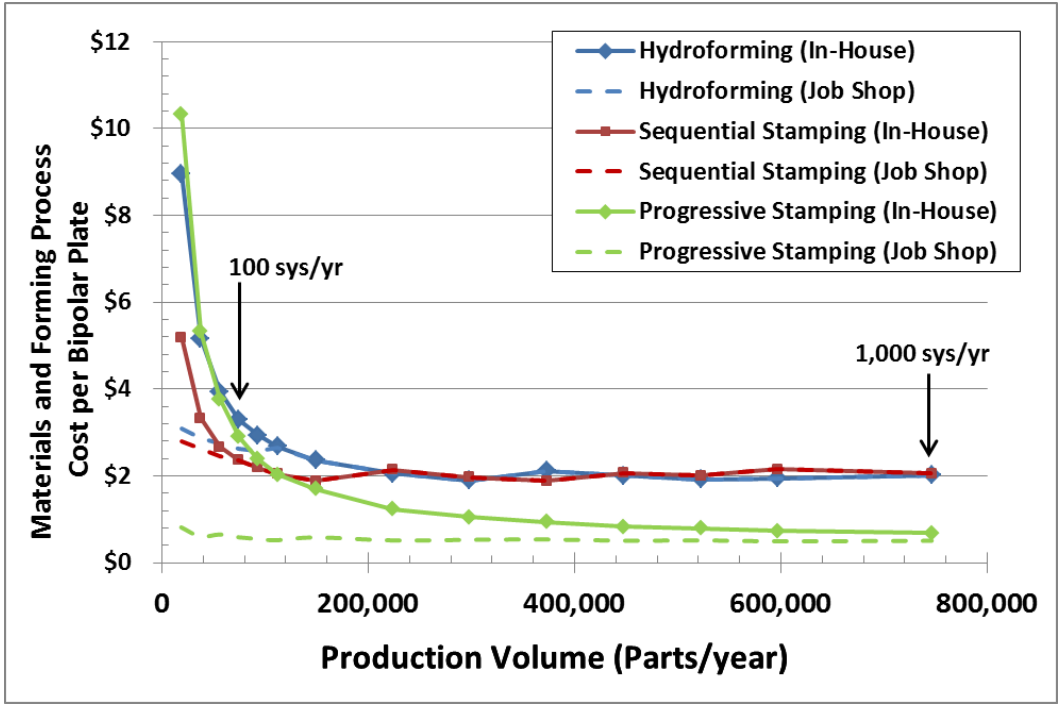
Figure 45. Comparison of single bipolar plate material and processing costs for hydroforming, sequential stamping, and progressive stamping with both in-house and job-shopped projections up to 746,000 parts per year (1,000 FCS per year).

8 Description of 2014 Automotive Fuel Cell System Manufacturing Assumptions and Cost Results

8.1 Fuel Cell Stack Materials, Manufacturing, and Assembly

8.1.1 Bipolar Plates

Each stack in the system consists of hundreds of active cells, each of which contains two bipolar plates. A one-to-one (1:1) ratio of active cells to cooling cells is assumed, to facilitate better temperature uniformity throughout the stack. Consequently, one side of the bipolar plate is a cooling cell flow field and the other side is an active cell flow field. In previous estimates, the cathode and anode flow field sides of the bipolar plates were envisioned as having identical flow patterns and being symmetrical. Consequently, only one bipolar plate design was needed and the cells could be flipped 180 degrees to alternate between cathode flow fields and anode flow fields. However, based on feedback from Ballard Power Systems Inc., different designs were assumed for the anode plates compared with the cathode plates. At the very end of each stack on either side, an extra bipolar plate sits and is not part of the repeating cell unit. This extra bipolar plate is only half-used, as it does only cooling. Specially-designed end gaskets are used to block off the flow into the gas channel side of those plates. Because each system contains hundreds of bipolar plates, hundreds of thousands of plates are needed even at the lowest production rate. This high level of production of a repeating component even at low system production levels means that bipolar plate mass-manufacturing techniques are applicable across a wide range of system production rates.

The stamped metal plates were selected because of consistent industry feedback suggesting that this material and manufacturing method is the most common approach currently implemented with success.

8.1.1.1 Progressive Die Stamping of the Bipolar Plates

Sheet metal stamping is selected for production of the bipolar plates and is inferred to be employed by GM for their fuel cell stacks.[53] Since ~700 plates are needed per system and multiple features are required on each plate (flow fields, manifolds, etc.), progressive die stamping is a logical choice for manufacturing method. In progressive die stamping, coils of sheet metal are fed into stamping presses having a series of die stations, each one sequentially imparting one or more features into the part as the coil advances. The parts move through the stationary die stations by indexing and a fully formed part emerges from the last station. As shown in Figure 46, the four main sequential die stations envisioned are (1) shearing of the intake manifolds, (2) shearing of the exhaust manifolds, (3) shallow forming of the flow field paths, and (4) shearing off of the part.

---

[53] The composition and manufacturing method for production of GM bipolar plates is a trade secret and is not known to the authors. However, a review of GM issued patents reveals that they are actively engaged in metallic plate research.
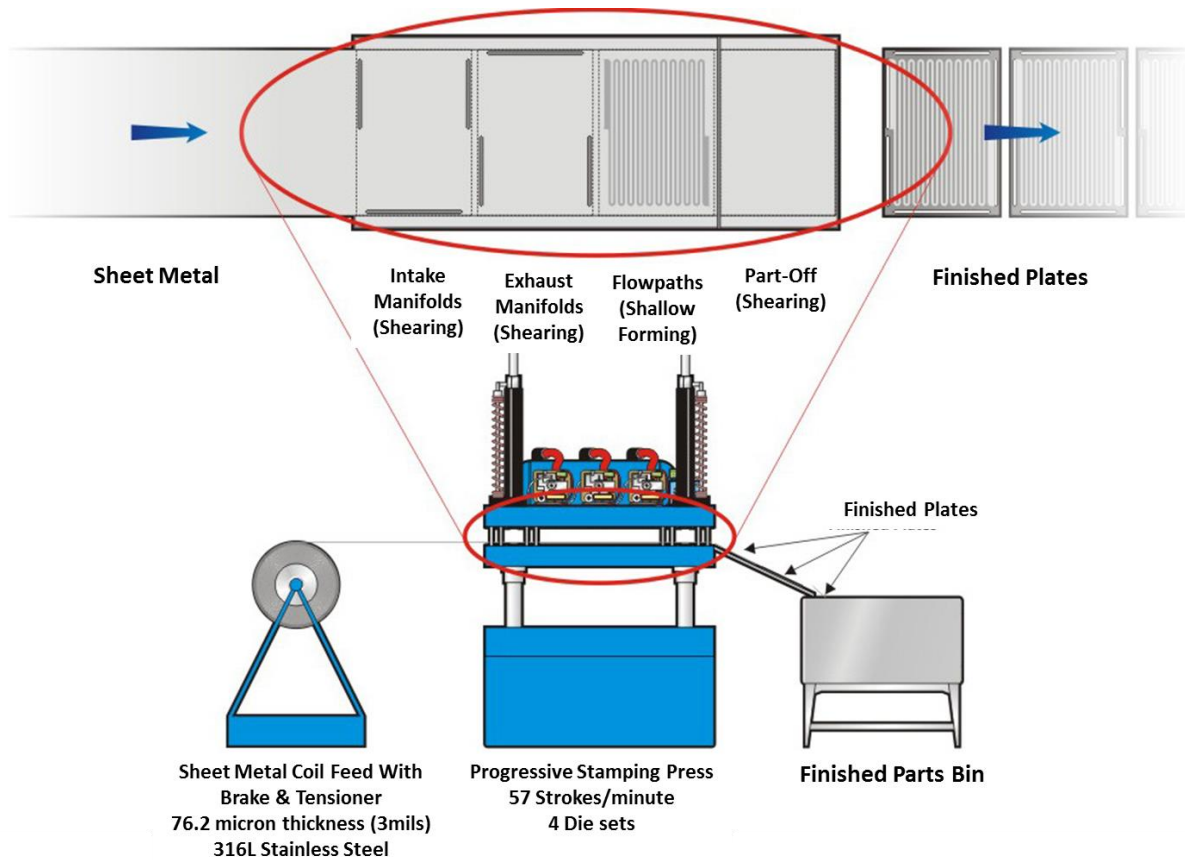
Figure 46. Bipolar plate stamping process diagram

Costs for bipolar plate progressive die stamping were obtained following the standard SA methodology described above. In summary, capital costs, maintenance costs, and electric power requirements were derived from manufacturer price quotes and also survey data supplied within Boothroyd Dewhurst Inc. (BDI) proprietary software. These data were then used to estimate true annual operating costs when the manufacturing line is operated at less than full capacity and 100% utilization. The cost estimation process and assumptions are described more fully below.

Capital Cost and Press Tonnage: Press clamping force is the primary factor influencing both the size and cost of a metal forming press. Price quotes and performance data for AIRAM Press Co. Ltd pneumatic presses ranging from 50 tons to 210 tons of clamping force were analyzed to develop a function describing the approximate purchase cost as a function of clamping force. The cost of supporting equipment required for press operation was then added to the base press cost. Some of the supporting equipment has a fixed cost regardless of press size, while other supporting equipment costs scale with press size. A sheet metal coil feeder was judged necessary and its cost was found to be largely independent of press size. To ensure part accuracy, a sheet metal straightener was added, although it may prove to be ultimately unnecessary due to the thin material used (76.2 microns, or 3 mils).

Press force needed in the progressive die is a function of the material thickness, the material tensile strength, the perimeter of cutting, and the perimeter and depth of bending or other forming. In early

modeling efforts, the press force was computed based on the assumption that the channels in the plate active area were merely formed by bending. Thus, in the 2006 report[54], it was estimated that a 65-ton press was necessary to produce the bipolar plates. However, it was noted that there was disagreement in the bipolar plate stamping community regarding the necessary press tonnage to form the plates, for example, with one practitioner stating that a 1,000-ton press was needed. This particularly high press tonnage being quoted may be due to the metal in the flow field channels being swaged[55] rather than bent in this particular manufacturer's case. Subsequent review by Ballard suggested that the previous 2006 SA estimate for total stamping system capital cost was substantially too low either due to a discrepancy with the required press tonnage or with the supporting equipment, or both. Consequently, in this revised analysis, the estimated capital cost is increased five-fold to better reflect industry feedback and to better approximate the higher cost of a larger tonnage press.

Press Speed: The speed of the press (in strokes per minute) varies with press size (kilo-Newtons (kN)): a small press is capable of higher sustained operating speeds than a large press. Press speed is a function of press size, and this relationship is shown in Figure 47.

Curve Fit:
Strokes/min = $574.39 \cdot \text{Force(kN)}^{-0.3267}$
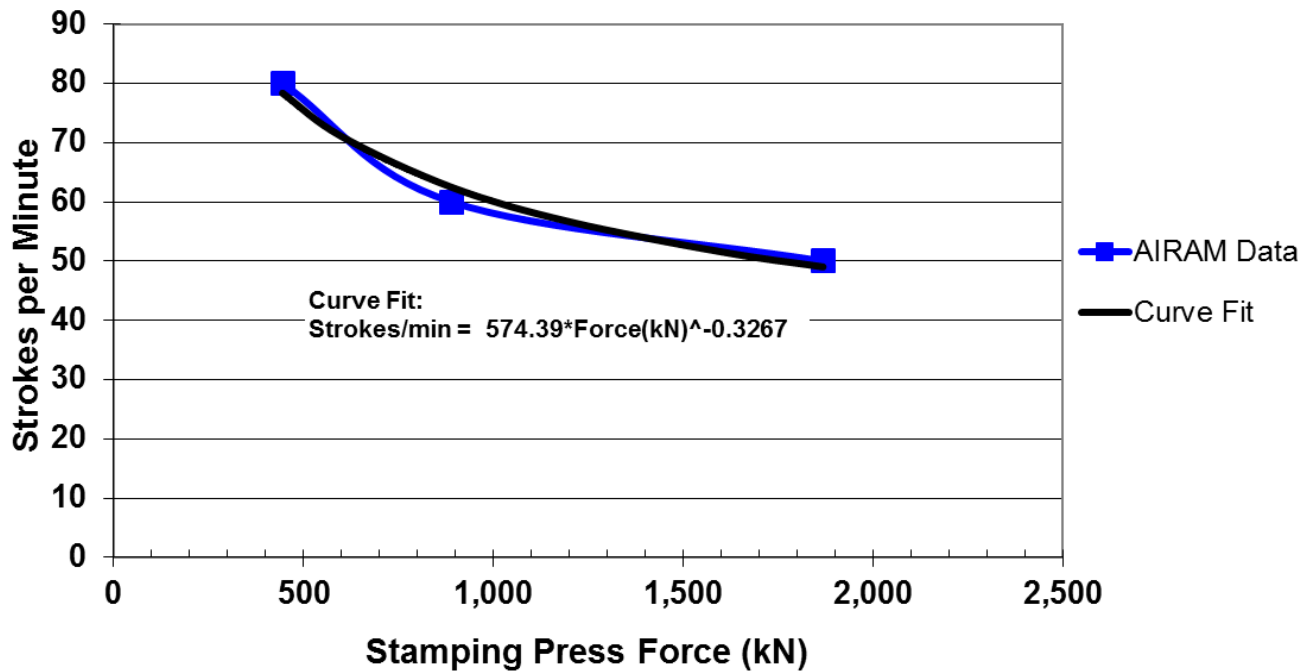
Figure 47. Press speed vs. press force

Quality Control System: A non-contact laser triangulation probe developed by NIST provides detailed information concerning flow field depth, plate size, thickness and defects for the stamped bipolar plate. As shown in Figure 48, the sensor must be able to scan three plates at a time in order to match the speed of the stamping press, which is producing nearly three plates every two seconds. The

---

[54] "Mass Production Cost Estimation for Direct H_2 PEM Fuel Cell Systems for Automotive Applications," Brian D. James & Jeff Kalinoski, Directed Technologies, Inc., October 2007.
[55] Use of the word "swaged" is meant to denote a more substantial lateral movement of metal during the process than is typically observed within bending or stamping operations.

measurement area for each sensor is 600 mm by 300 mm, significantly larger than the size of a single plate. The line speed has been proven at roughly 300 mm/second but further R&D could increase the effective speed to an estimated maximum of 2 m/sec. Since the probes are inexpensive, they add little additional capital cost; consequently, three sensors are envisioned for the system to ensure adequate measurement overlap for each plate and to match the stamping speed.

Part Collection Robot
(3 plates simultaneously)

NIST Non-Contact Laser Triangulation Probe
Optical Detection System
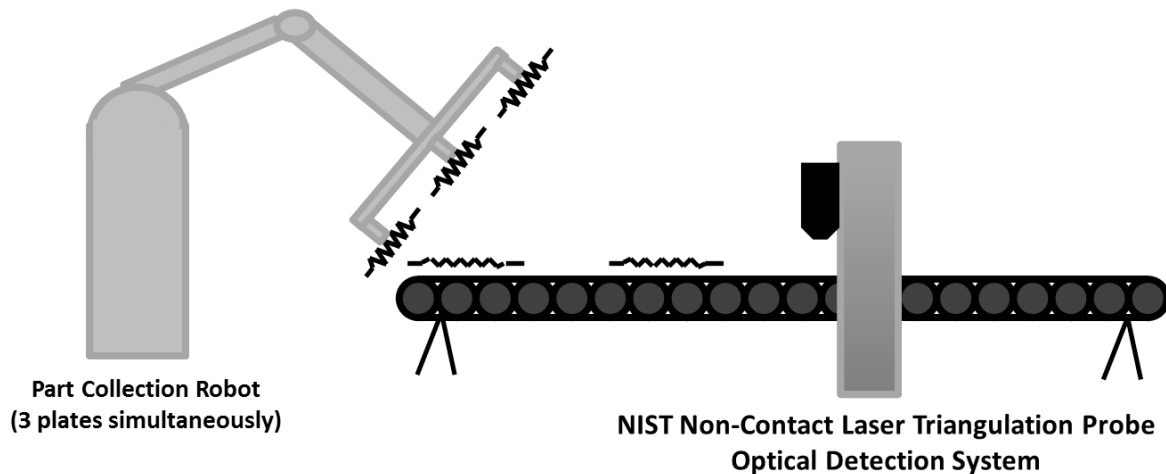
Figure 48. Bipolar plate part collection and quality control: NIST Non-Contact Laser Triangulation Probe, Optical Detection System

<u>**Maintenance:**</u> The same press operated at higher speeds tends to require maintenance more frequently. Based on discussion with industry vendors, the minimum life of a set of these stamping machine wear parts was estimated to be 10 million cycles, with a total replacement cost estimated to be 20 to 25% of complete press initial capital cost depending on machine size. Since the above cycle life is the minimum number of cycles, but could be substantially more, an approximation is applied to this latest modelling iteration such that the maintenance cost of the press is estimated to be 15% of initial press capital cost every 10 million cycles. This approach deviates from SA's historically-implemented methodology, which estimates maintenance costs as a percentage of initial capital costs per year rather than per cycle. Applying a similar cycle-based lifetime criterion, feeder equipment maintenance is estimated to be 5% of initial feeder capital cost every 10 million cycles.

<u>**Utilities:**</u> The principal sources of demand for electricity in the progressive die process train are the air compressor for the pneumatic press and the electric motor for turning the coil feeder. Compressor power is a function of the volumetric airflow requirement of each press size and was estimated to vary between 19 kW at the low end (50-ton press) and 30 kW at the high end (210-ton press).[56] Based on available data, a mathematical relationship was developed to describe electric power consumption as a function of press size.

---

[56] Information provided through conversations with AIRAM (http://www.airam.com/)

Machine Rate: Using the above information for total line capital, maintenance, and utilities costs, mathematical expressions can be generated that relate machine rates with various size presses at varying utilization. Basic input parameters are summarized in Figure 50 and Figure 51.

Die Cost: Die costing is estimated according to the equations outlined in the Boothroyd and Dewhurst section on sheet metal stamping. As expected, complex stamping operations require more intricate, and therefore more expensive, dies. The first two, and final, press steps are simple punching and sheering operations and therefore do not require expensive dies. The flowpath-forming step involves forming a complex serpentine shape, which requires a highly complex die that is significantly more expensive than the dies for other steps in the process. This step also requires the majority of press force. The die cost figures are listed below in Figure 49 (under "Tooling"). Note that "secondary operations" refers to the coating process that will be further discussed in Section 8.1.1.2.

Annual Production Rate	1,000	10,000	30,000	80,000	100,000	500,000
Materials ($/stack)	$276	$271	$270	$270	$270	$270
Manufacturing ($/stack)	$183	$47	$33	$32	$31	$30
Tooling ($/stack)	$104	$95	$95	$95	$94	$95
Secondary Operations: Coating ($/stack)	$1,045	$218	$195	$175	$170	$164
Total Cost ($/stack)	$1,607	$632	$593	$571	$565	$558
Total Cost ($/kWnet)	$20.09	$7.90	$7.41	$7.13	$7.06	$6.98

Figure 49. Cost breakdown for stamped bipolar plates

Die Lifetime: Over time, the repetitive use of the dies to form the metallic bipolar plates will cause these tools to wear and lose form. Consequently, the dies require periodic refurbishing or replacement depending on the severity of the wear. Based on communication with 3-Dimensional Services, Inc., dies for progressive bipolar plate stampings are estimated to last between 400,000 and 600,000 cycles before refurbishment, and may be refurbished 2 to 3 times before replacement. Thus, a die (tooling) lifetime of 1.8 million cycles (3 x 600,000) is specified, with a die cost of $228,154 ($100,000 of which is from the two refurbishments, at $50,000 each).

Annual Production Rate	1,000	10,000	30,000	80,000	100,000	500,000
Equipment Lifetime (years)	15	15	15	15	15	15
Interest Rate	10%	10%	10%	10%	10%	10%
Corporate Income Tax Rate	40%	40%	40%	40%	40%	40%
Capital Recovery Factor	0.175	0.175	0.175	0.175	0.175	0.175
Equipment Installation Factor	1.4	1.4	1.4	1.4	1.4	1.4
Maintenance/Spare Parts (% of CC)	13%	13%	13%	13%	13%	13%
Miscellanous Expenses (% of CC)	2%	2%	2%	2%	2%	2%
Power Consumption (kW)	25	33	33	33	33	33

Figure 50. Machine rate parameters for bipolar plate stamping process

Annual Production Rate	1,000	10,000	30,000	80,000	100,000	500,000
Capital Cost ($/line)	$403,724	$530,446	$530,446	$530,446	$530,446	$530,446
Costs per Tooling Set ($)	$222,603	$222,603	$222,603	$222,603	$222,603	$222,603
Tooling Lifetime (cycles)	1,800,000	1,800,000	1,800,000	1,800,000	1,800,000	1,800,000
Simultaneous Lines	1	2	4	10	12	59
Laborers per Line	1.25	0.25	0.25	0.25	0.25	0.25
Line Utilization	11.7%	58.6%	87.8%	93.6%	97.5%	99.2%
Cycle Time (s)	1.01	1.01	1.01	1.01	1.01	1.01
Effective Total Machine Rate ($/hr)	$463.48	$120.33	$84.90	$80.50	$77.84	$76.79
Stainless Steel Cost ($/kg)	$11.37	$11.18	$11.10	$11.10	$11.10	$11.10

Figure 51. Bipolar plate stamping process parameters

8.1.1.2 Alloy Selection and Corrosion Concerns

One of the challenges presented by using metallic plates is that they are more susceptible to corrosion than carbon-based plates. For this reason, alloy selection is very important. There is much uncertainty in the fuel cell community as to which alloy and surface treatments are needed to provide adequate corrosion resistance. Although some believe that suitable stainless steel alloys exist that adequately address this problem, others insist that protective coatings are necessary. If the right coating method were selected, it may be possible to use a cheaper and/or lighter (but less corrosion-resistant) material for the plates, which could help offset the cost of coating. In determining the coating method and/or plate material, consideration must be given to the different corrosion environments each plate will encounter: hydrogen and coolant for the anode plates, and oxygen and coolant for the cathode plates.

Literature and patent reviews and conversations with researchers indicate that coatings/surface treatments may not be needed and that 316L stainless steel (or another commercial alloy of similar cost) is appropriate. However, further input from the USCAR Fuel Cell Technical Team suggested that coatings *are* necessary. At the direction of the Fuel Cell Tech Team, coatings were included in the system cost and are based on a 76.2-micron (3-mil) stainless steel 316L alloy metallic bipolar plates coated using a proprietary process from TreadStone Technologies, Inc.

An anti-corrosion coating is applied to both sides of the bipolar plates based on TreadStone's proprietary LiteCell™ process. A DFMA™ analysis was conducted based on information from TreadStone's patent US 7,309,540, as well as information transferred under a non-disclosure agreement, with close collaboration with C.H. Wang and Gerry DeCuollo of TreadStone Technologies, Inc.

According to the patent, the coating consists of "one or more resistant layers, comprising conductive vias through the resistant layer(s)" (see Figure 52). The resistant layer provides excellent corrosion protection, while the vias provide sufficient electrical conduction to improve overall conductivity through the plate.
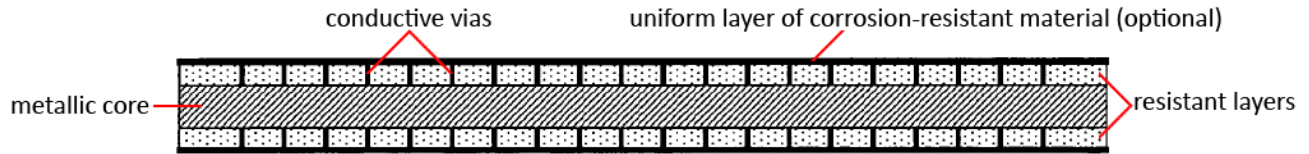
Figure 52. Conductive vias shown in US patent 7,309,540 for TreadStone Technologies, Inc. anti-corrosion coating

The resistant layer is applied via a physical vapor deposition process. Details of the manufacturing process are considered proprietary, so only limited explanation is provided here.

The postulated coating application follows a three-step process. The major step is the deposition of a non-continuous layer of gold dots (~1% surface coverage) via a patented low-cost process designed to impart low contact resistance. The plate coating is applied after bipolar plate stamping. The gold layer is only applied to one side of the plates because only one side requires low contact resistance.

The cost breakdown for the TreadStone process is shown in Figure 53. The coating cost is observed to be primarily a function of annual production rate, with cost spiking at low quantities of only 1,000 systems per year. This is a reflection of low utilization of the coating system, and the application cost could perhaps be reduced with an alternate application technique.

Annual Production Rate	1,000	10,000	30,000	80,000	100,000	500,000
Materials ($/stack)	$72	$72	$72	$72	$72	$72
Manufacturing ($/stack)	$973	$147	$123	$103	$98	$92
Total Cost ($/stack)	$1,045	$218	$195	$175	$170	$164
Total Cost ($/kWnet)	$13.06	$2.73	$2.44	$2.18	$2.13	$2.05

Figure 53. Cost breakdown for TreadStone LiteCell™ bipolar plate coating process

8.1.2 Membrane

The total cost of the fuel cell membrane (uncatalyzed) is estimated as the summation of three components:

1. ionomer (input material cost)
2. ePTFE substrate (input material cost)
3. manufacturing cost of casting into membrane form

Each component is described in detail below.

8.1.2.1 Ionomer Cost

Ionomer cost is based upon a 2010 Dow Chemical reference report[57] on high-volume manufacture of Nafion-like long side chain perfluorosulfonic acid proton exchange membranes from hexafluoropropylene oxide (HFPO) raw material. In this report, ionomer material and manufacturing

---

[57] "High Volume Cost Analysis of Perfluorinated Sulfonic Acid Proton Exchange Membranes," Tao Xie, Mark F. Mathias, and Susan L. Bell, GM, Inc., May 2010.

costs are analyzed at extremely high volumes: as high as 6,000 MT/year (although only ~400MT/year of material is suitable for 500k vehicles/year). The combination of extremely high production volume and simpler manufacturing process—the industry report models membrane casting rather than application to an ePTFE substrate—results in reported finished membrane cost much lower than calculated by the SA model. Rather than using the direct results of the Dow cost report, the 2012 Fuel Cell Tech Team recommended that the membrane continue to be modeled as an ePTFE-supported membrane and that we adapt the Dow ionomer price to plant sizes more in line with expected annual demand. Consequently for the 2012- 2015 analyses, a production-volume-dependent scaling relationship was derived from the Dow report data and used to estimate ionomer price at various fuel cell system annual production rates. This ionomer price curve is shown in Figure 54. Data points on the graph correspond to the six annual system manufacturing rates analyzed in the study.
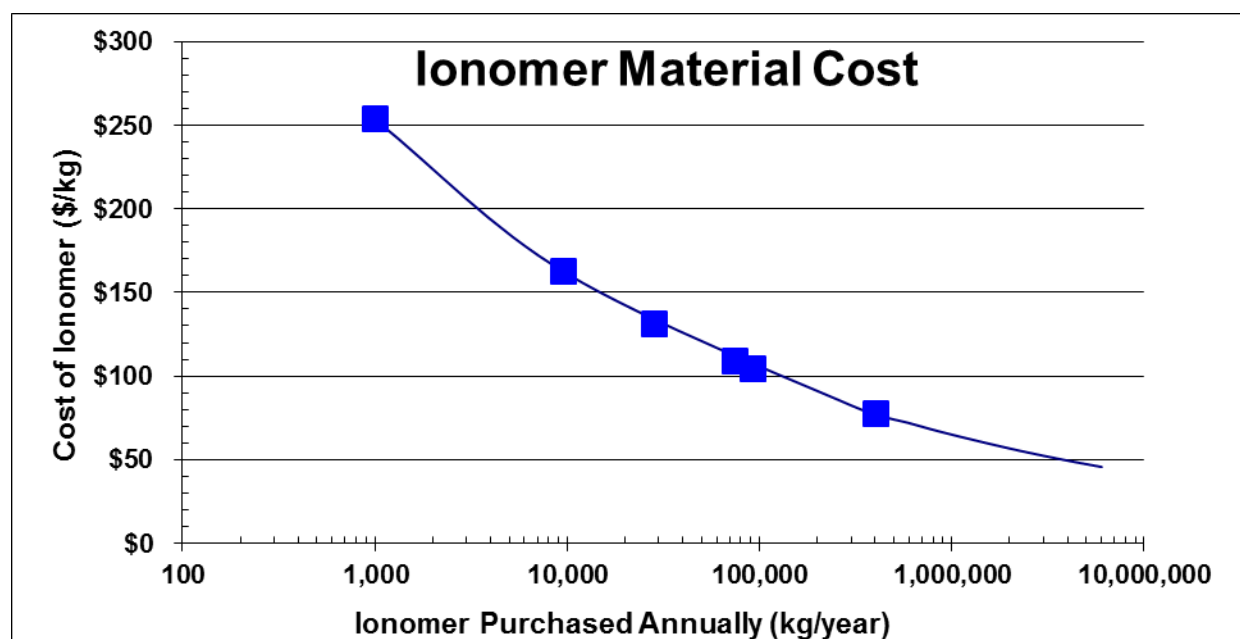
Figure 54. Ionomer material cost curve

8.1.2.2 ePTFE Cost

An expanded polytetrafluoroethylene (ePTFE) porous layer is modeled as a mechanical substrate for the ionomer membrane. Use of an ePTFE supported fuel cell membrane is well documented in the literature and is a continuation of past SA cost analysis practice. A ground-up DFMA^{TM} cost analysis of ePTFE was initiated but it soon became evident that such an analysis was impractical as the specific (and crucial) processing steps[58] were closely guarded industry secrets unavailable as inputs into the cost analysis. While ePTFE is manufactured in high production volume for the textiles industry (eg. Gore-Tex), there are different qualities available and also potentially different processing steps for fuel cell applications. For this reason, a quote base cost estimated is used within the 2015 report.

---

[58] ePTFE uses a particular grade of non-expanded PTFE as a precursor material and then applies a multi-stage, presumably bi-axially, mechanical stretching regiment to attain an optimized node and fibril end structure of the 95+% porous ePTFE. Exact parameters of those stretching steps, along with proprietary heat treatments or other non-disclosed steps, are highly confidential to W.L. Gore and other fuel cell ePTFE manufacturers.

Quotes from multiple ePTFE manufacturers were obtained, all on the basis of confidentially. These cost quotes (without attribution to their source) are shown in Figure 55. W.L. Gore & Associates, Inc., the predominant supplier of ePTFE to the fuel cell industry did not provide a cost quotation, although they did review this cost analysis.

A wide range of prices is observed in Figure 55 due to both differences between manufacturers and uncertainty in projection to high manufacturing volumes. ePTFE prices are affected by the quality and cost of the starting PTFE material and one manufacturer suggested that only the better quality "fuel cell grade" of PTFE was suitable for fuel cell applications. The lower red curve in Figure 55 represents an ePTFE price quote from a Chinese supplier of textile grade ePTFE which probably isn't well suited to fuel cell applications but is included in the graph to illustrate the ePTFE price floor. The other price quotations are from US suppliers. Price quotes were obtained for both 10 micron and 25 micron ePTFE thickness but prices did not vary appreciably, indicating that the majority of cost was in the processing steps. A mid-range price of ePTFE is used in the cost analysis, with the upper and lower bound price quotes used as limits in the sensitivity analysis.
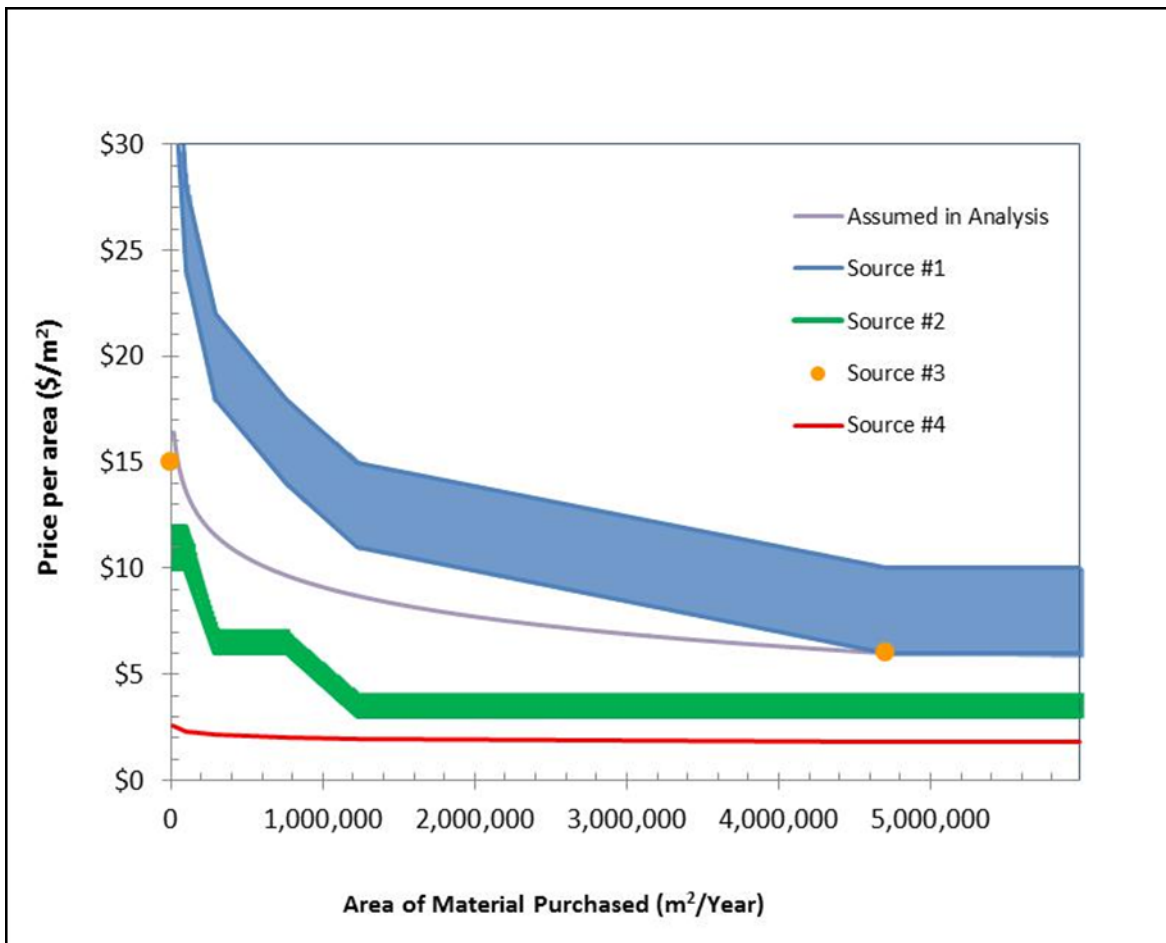
Figure 55. ePTFE price quotations and data selected for use in SA DFMA^{TM} models

8.1.2.3 Membrane Manufacturing Cost

The membrane manufacturing method for 2015 is modeled as factory-based roll-to-roll processing, unchanged from previous SA analyses. The analysis is not based on a detailed enumeration of capital costs but rather uses industry supplied approximate plant cost estimates combined with estimated yield rates, labor requirements, line speeds, and markup rates to derive a simplified cost curve representing manufacturing cost as a function of membrane annual production rate.

As schematically detailed in Figure 56, the membrane fabrication process consists of eight main steps:

Unwinding: An unwind stand with tensioners is used to feed the previously procured ePTFE substrate into the process line. A web width of ~ 1m is deemed feasible for both the membrane fabrication line and the subsequent catalyzation.

First Ionomer Bath: The ePTFE substrate is dipped into an ionomer/solvent bath to partially occlude the pores.

First Infrared Oven Drying: The web dries via infrared ovens. A drying time of 30 seconds is postulated. Since the web is traveling quickly, considerable run length is required. The ovens may be linear or contain multiple back-and-forth passes to achieve the total required dwell time.

Second Ionomer Bath: The ionomer bath dipping process is repeated to achieve full occlusion of the ePTFE pores and an even thickness, pinhole-free membrane.

Second Infrared Oven Drying: The web is dried with a second bank of infra-red ovens after the second ionomer bath.

Boiling Water Hydration: The web is held in boiling water for 5 minutes to fully hydrate the ionomer. Optimal selection of the ionomer may reduce or eliminate this boiling step.

Air Dryer: High velocity air is used to dry the web after the hydration step.

Rewind: The finished membrane is wound onto a spool for transport to the catalyzation process line.
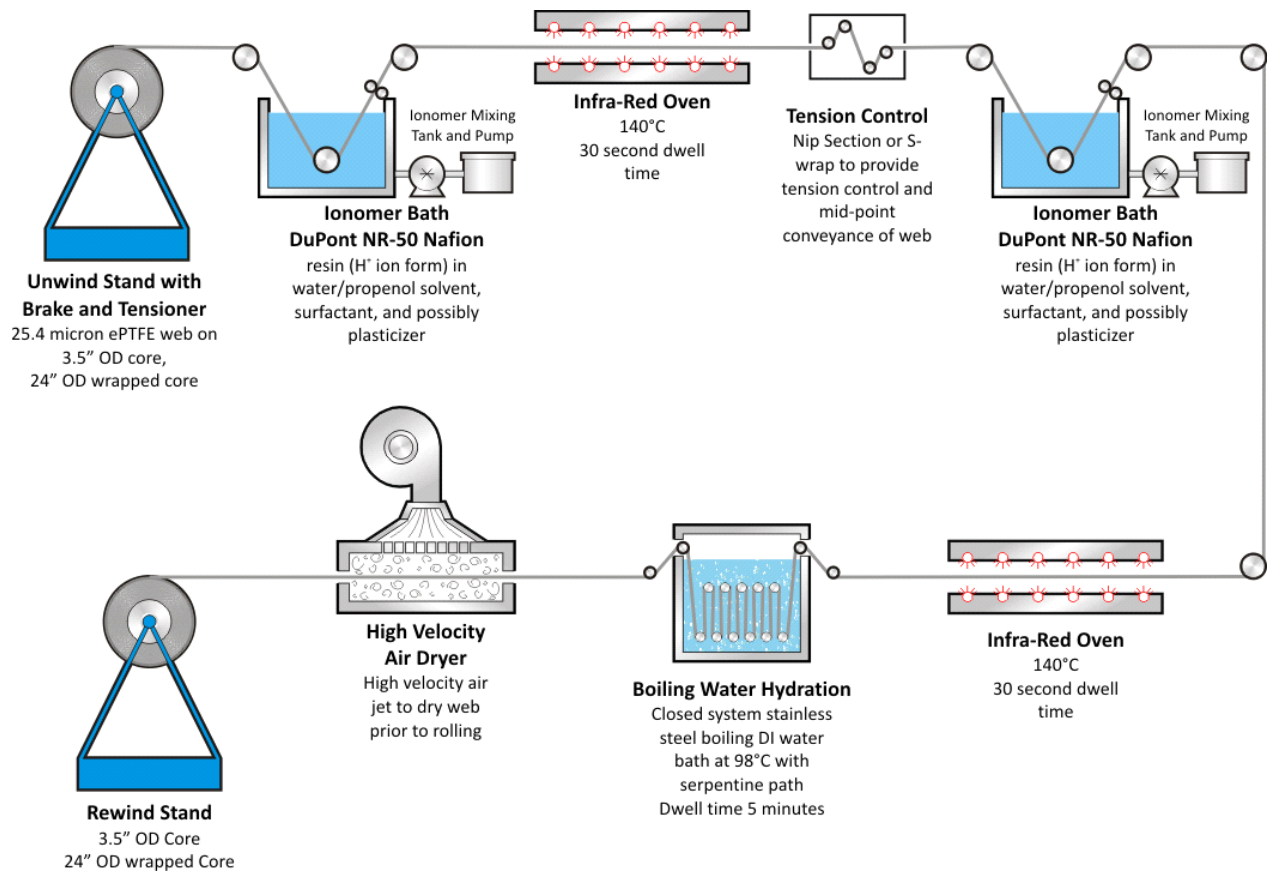
Figure 56. Membrane fabrication process diagram

Details of the simplified membrane fabrication cost analysis are shown in Figure 57. Two roll-to-roll plants are postulated: a "low-speed plant" (5 m/min) and a "high-speed" plant (35 m/min). Run at part load, they cover the full span of membrane production requirements (1,000 to 500,000 vehicles/year).

Key assumptions are noted below.

Capital Cost: Capital costs are coarsely estimated based on industry input and are significantly greater than previous element-by-element summations based on component price quotes.

Web speed: Even the "high-speed" web (35 m/min) is very slow by converting machinery standards where speeds of 100 m/min are often achieved. This is a nod toward cost conservativeness and a reflection that the upper bound of membrane web speed is not known at this time.

Discount Rate: The discount rate is increased to 20% to reflect the increased business risk of a membrane production line.[59]

---

[59] While all fuel cell system manufactured components share similar market risk in that the demand for fuel cell vehicles is uncertain, some components (e.g. the membrane manufacturing line) utilize specialized equipment that can't be resold or repurposed for other markets. Furthermore, the membrane manufacturing line is one of the largest capital investments thereby amplifying the consequences of missing production projections.

Production for Simultaneous Product Lines: In virtually all other components of the automotive fuel cell stack, it is assumed that there is vertical integration and dedicated component production for a single vehicle product. For the membrane however, it is likely that a separate company would fabricate the membrane for multiple car companies or, at least, that the membrane plant would produce membrane for more than one line of vehicles. Consequently, a multiplier on the yearly membrane demand is included to reflect supply to multiple vehicle product lines. This multiplier is not constant as production rate increases since the plant is at some point limited by capacity. The non-constant nature of the multiplier leads to unevenness in the resulting $/m^2 cost projections.

Peak Equipment Utilization: Input from a membrane supplier raised the point that average plant utilization would be significantly affected under scenarios of rapid demand growth. Consequently, utilization (at most manufacturing rates) is limited to 67% to reflect the five-year average utilization assuming 25% per year demand growth. For the 500,000 vehicles per year case, plant utilization is allowed to increase to 80% to reflect a more stable production scenario.

Production/Cutting Yield: There are appreciable cutting losses associated with the roll-to-roll manufacturing process, which directly affect the membrane material costs. ePTFE yield was assessed at 77% to 98%. It is assumed that a portion of ionomer in the scrap membrane is able to be recycled. Consequently, it is assumed for costing purposes that the ionomer material wastage rate is half that of the overall membrane areal scrap rate (making the ionomer yield 89% to 99%). Manufacturing yield is assessed at the same yield as ePTFE.

Workdays and Hours: The maximum plant operating hours are assumed to be 20 hours per day, 240 days per year. Actual hours vary based on actual plant utilization.

Cost Markup: The standard methodology throughout the analysis has been not to apply manufacturer markups, in keeping with the vertically integrated manufacturing assumption, and the directives of the DOE on this costing project. However, since it is likely that the membrane producer will not be vertically integrated, a markup is included in our membrane cost estimate. Furthermore, because the membrane is a critical component of the stack, significantly higher margins are allocated than are typical to the automotive industry where there is a large supplier base with virtually interchangeable products competing solely on price. Markup on the manufacturing process varies from 40% to 70%. A constant 25% markup rate is applied to the materials (ePTFE and ionomer) in keeping with auto industry practice of the auto company supplying high cost materials to the vendor rather than paying a full markup for the vendor to procure the materials.

Revenue: Annual membrane fabricator revenue is not an input in the analysis. Rather it is an output. However, it is worth noting that even at high membrane production rates, company revenues are still only about $35M per year. This is a modest company size and supports the notion of allowing higher-than-average markups as a means to entice people into the business.

Simplified Computation of Membrane Manufacturing Cost							
Annual Veh. Prod. (1 product line)	vehicle/year	1,000	10,000	30,000	80,000	130,000	500,000
Capital Amortization							
Capital Cost (Membrane Fabrication)	$	$15,000,000	$15,000,000	$15,000,000	$35,000,000	$35,000,000	$35,000,000
Machine Lifetime	years	10	10	10	10	10	10
Discount Rate	%	20%	20%	20%	20%	20%	20%
Corporate Income Tax Rate	%	40%	40%	40%	40%	40%	40%
Capital Recovery Factor (CRF)		0.331	0.331	0.331	0.331	0.331	0.331
Labor Costs							
Min. Mfg. Labor Staff (Simul. on 1 Shift)	FTE	5	25	25	50	50	50
Labor Rate	$/min	1	1	1	1	1	1
Machine Costs							
Maintenance/Spare Parts (% of installed C.C./year)	%	5%	5%	5%	5%	5%	5%
Miscellaneous Expenses	%	5%	5%	5%	5%	5%	5%
Total Power Consumption	kW	200	200	250	350	350	350
Electrical Utility Cost	$/kWh	0.07	0.07	0.07	0.07	0.07	0.07
Membrane Production Parameters							
Simul. Product Lines to Which Memb. is Supplied		5	3.25	2.2	2	1.75	1.5
Vehicle Annual Production	veh/year	5,000	32,500	66,000	160,000	227,500	750,000
m^2 per Vehicle	m^2/vehicle	13.00	13.00	13.00	13.00	13.00	13.00
Peak Equipment Utilization Due to Growth	%	67%	67%	67%	67%	67%	100%
Production/Cutting Yield	%	77%	84%	88%	91%	93%	97.956%
Gross Production @ 100% Utilization (plant)	m^2/year	1,440,000	1,440,000	1,440,000	10,080,000	10,080,000	10,080,000
Gross Production (plant)	m^2/year	83,927	500,053	974,185	2,275,706	3,176,927	9,953,438
Net Production (plant)	m^2/year	65,000	422,500	858,000	2,080,000	2,957,500	9,750,000
Net Production of 1 Line	m^2/year	13,000	130,000	390,000	1,040,000	1,690,000	6,500,000
Design Web Speed	m/min	5	5	5	35	35	35
Web Width	m	1	1	1	1	1	1
Work Days per Year	days/year	240	240	240	240	240	240
Plant Utilization	% of 20hr days	5.8%	34.7%	67.7%	22.6%	31.5%	98.7%
Hours per Year of Production	hrs/year	280	1,667	3,247	1,084	1,513	4,740
Hours per Day of Production	hrs/day	1.17	6.95	13.53	4.52	6.30	19.75
Annual Cost Summation							
Capital Recovery Cost	$/year	$4,963,069	$4,963,069	$4,963,069	$11,580,494	$11,580,494	$11,580,494
Labor Cost	$/year	$576,000	$2,880,000	$4,870,927	$5,760,000	$5,760,000	$14,219,197
Maintenance/Spares Cost	$/year	$750,000	$750,000	$750,000	$1,750,000	$1,750,000	$1,750,000
Miscellaneous Expenses	$/year	$750,000	$750,000	$750,000	$1,750,000	$1,750,000	$1,750,000
Utility Cost	$/year	$3,917	$23,336	$56,827	$26,550	$37,064	$116,123
Effective Machine Rate	$/min	$420	$94	$58	$321	$230	$103
Total Manufacturing Cost ($/net m2, pre-markup)							
From computations	$/m²	$108.35	$22.17	$13.28	$10.03	$7.06	$3.02
From simplified curve fit	$/m²	$ 93.83	$ 25.84	$ 13.97	$ 8.06	$ 6.15	$ 2.89
Manufacturing Cost Markup %	%	70%	59%	54%	49%	47%	40%
Gross Margin	%	41%	37%	35%	33%	32%	29%
Annual Revenue (on manufacturing only)	$/year	$10,368,358	$17,348,407	$18,407,310	$24,970,418	$26,626,707	$39,451,822
Total Manufacturing Cost ($/net m2, post-markup)							
From computations	$/m²	$184.21	$35.22	$20.39	$14.93	$10.34	$4.22
From simplified curve fit	$/m²	$ 159.51	$ 41.06	$ 21.45	$ 12.01	$ 9.00	$ 4.05

Figure 57. Simplified membrane manufacturing cost analysis assumptions

Membrane manufacturing cost is plotted against membrane annual volume in Figure 58 below. Note that membrane material costs (ionomer and ePTFE) are not included. Membrane manufacturing costs are computed using the multiple production line assumption. To aid in numerical calculation, a power curve was curve-fit to the cost computations.

The chart contains the following annotations:

> Manufacturing cost alone: no materials included.
> Assumes multiple product lines are pooled together to raise membrane plant volume.
> m² refers to the approximate square meters of active area needed per year for a single order.

$$y = 18{,}886x^{-0.56}$$

Axis labels: Y-axis "Membrane Manufacturing Cost, \$/m² (Pre-marukup)"; X-axis "Net Membrane Volume, m²/year"

Figure 58. Membrane manufacturing cost vs. annual membrane manufacturing volume

8.1.2.4 Total Membrane Cost

Figure 59 summarized cost results for the un-catalyzed ePTFE supported membrane.

Annual Production Rate	1,000	10,000	30,000	80,000	100,000	500,000
Materials (\$/m²)	\$47	\$30	\$24	\$19	\$18	\$12
Manufacturing (\$/m²)	\$206	\$48	\$24	\$13	\$11	\$4
Total Cost (\$/m2 (total) total)	\$253	\$78	\$48	\$32	\$29	\$16
Total Cost (\$/stack)	\$3,213	\$994	\$615	\$410	\$374	\$206
Total Cost (\$/kWnet)	\$40.17	\$12.43	\$7.69	\$5.12	\$4.67	\$2.57

Figure 59. Cost breakdown for the membrane (un-catalyzed)

8.1.3 Catalyst Cost

As described previously in Section 6.1, a dispersed binary d-PtNi catalyst is used for the baseline catalyst system and is applied in catalyst ink form via a slot die coating deposition method. The synthesis of the dry powder d-PtNi catalyst (before being made into a catalyst ink) is described within this section and maybe summarized as a wet chemistry based mixture of platinum and nickel with carbon. The cost of platinum, one of the greatest influencers on stack cost, is assumed to be \$1,500/troy ounce for the baseline system.

8.1.3.1 Platinum Cost

The raw material cost of platinum is the major cost element of the catalyst ink. At the direction of the DOE, a platinum cost of $1,500 per troy ounce is selected (and represents a price increase from the $1,100/troy ounce used in in 2013 and prior SA analyses). As shown in Figure 60, the $1,500/troy ounce Pt price reflects the average and likeliest value of Pt within the last eight year span. Interestingly, as shown in Figure 61, Pt is currently at a multi-year price low ($855/tr.oz. in December 2015).
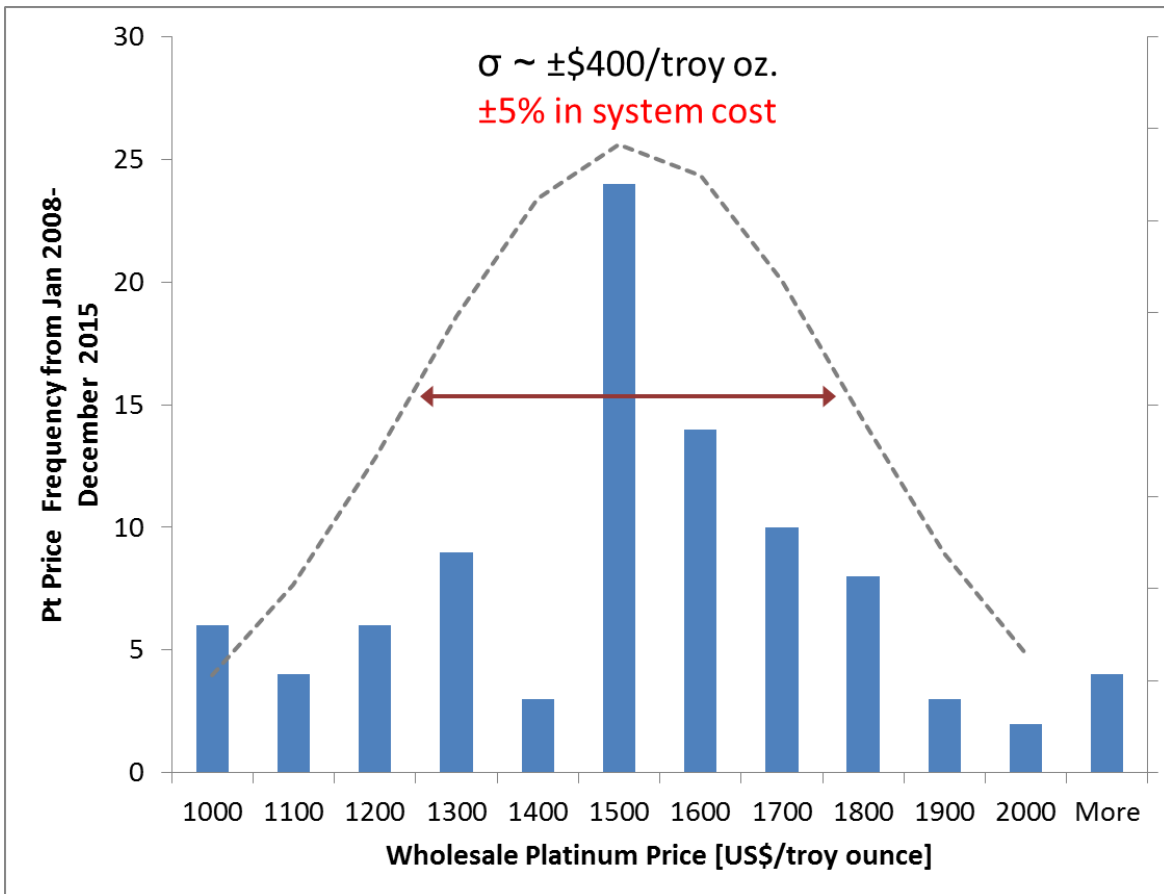
Figure 60. Pt price distribution over eight years (2008-2016)
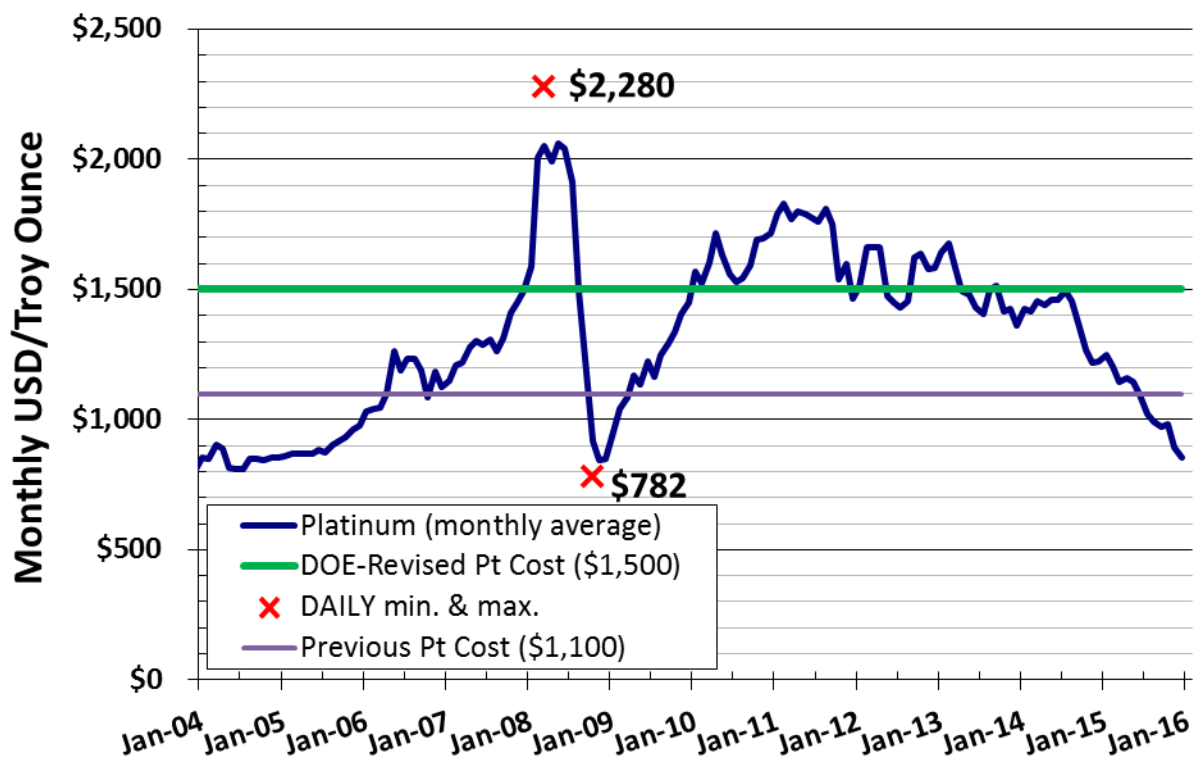
Figure 61. Twelve-year graph of monthly Pt prices

8.1.3.2 Catalyst Powder Synthesis

The PtNiC analysis draws from open literature sources for definition of representative processing steps. While inspired by the dealloyed binary catalysts of Johnson Matthey (JM), the analysis does not purport to model the JM catalyst synthesis exactly and may differ from JM catalysts in important and unknown ways. The dealloyed PtNiC catalyst analysis results are incorporated into the 2015 baseline system.

The binary catalyst powder synthesis processing steps are outlined in Figure 62. A variety of Pt donor compounds are available as inputs to catalyst synthesis. Chloroplatinic acid (CPA) is selected as a representative reactant as its production method is described in the literature, but many other reactants may viably be used. The Pt compound preferred by JM is not discernable from the patent literature.

Preparing the CPA involves dissolving platinum sponge into a 4:1 mix of hydrochloric and nitric acids, called "aqua regia," via the reaction:

$$\text{Pt} + 4\ \text{HNO}_3 + 6\ \text{HCl} \rightarrow \text{H}_2\text{PtCl}_6 + 4\ \text{NO}_2 + 4\ \text{H}_2\text{O}$$

The CPA (H_2PtCl_6) is brownish-red in color, and is isolated by evaporating the solution to a thick syrup, which becomes solid at room temperature. Cost of the CPA was obtained by combining Pt material cost with CPA preparation cost, derived from a DFMA^{TM} analysis. Further costs associated with precipitating the CPA onto the platinum were also obtained using DFMA^{TM}.

The CPA is next reacted with nickel chloride and Ketjen carbon within a precipitation reactor to form the PtNiC precursor. The precipitate precursor slurry (solid precursor in excess acid liquids) is run through a press filter and washed with water, then dried and crushed, resulting in a precursor powder. Based on literature[60] parameters, the precursor powder is annealed at 1,000˚C to improve the activity and stability of the catalyst powder. The dealloying step uses nitric acid to etch away nickel over 24 hours. Filter, wash, dry, and catalyst crush steps are needed to form the final catalyst PtNi on C powder used in the catalyst electrode inks.

Dealloyed PtNiC Catalyst Processing Steps
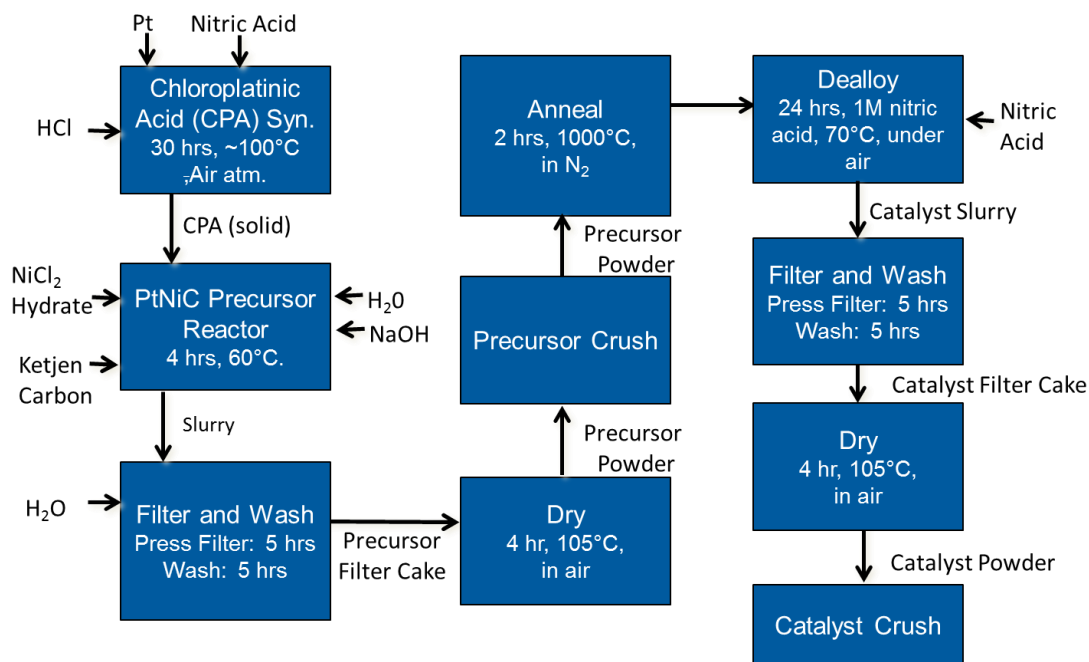
Figure 62. Processing steps for dealloyed binary PtNiC catalyst powder synthesis

Final cost results of the dealloyed catalyst powder synthesis process are shown in Figure 63 where the table shows the cost of each processing step at all manufacturing rates. Figure 64 shows a further breakdown of materials, manufacturing, markup, and total cost for each processing step at both 1,000 and 500,000 systems per year manufacturing rates. Highlighted in Figure 64 are the dominant cost of Pt (circled in red), other material costs (circled in blue), and the most expensive processing step (circled in green).

---

[60] Wang, C., et al., "Design and synthesis of bimetallic electrocatalyst with multilayered Pt-skin surfaces", Journal of the American Chemical Society, 2011. 133(36): p. 14396-14403.

Catalyst Powder Synthesis		Annual System Prodution Rate					
Component Costs per 80kWnet Fuel Cell System		1,000	10,000	30,000	80,000	100,000	500,000
Step 1: Catalyst PtNiC Precursor	$/system	$1,166.25	$936.79	$909.87	$898.47	$895.89	$883.46
Step 2: Precursor Filtration	$/system	$29.90	$8.79	$3.20	$1.74	$1.38	$0.27
Step 3: Precusor Wash	$/system	$11.83	$1.11	$0.37	$0.14	$0.12	$0.03
Step 4: Precursor Drying	$/system	$79.96	$7.61	$2.55	$1.02	$0.84	$0.27
Step 5: Precursor Crushing	$/system	$42.16	$3.98	$1.49	$0.57	$0.47	$0.13
Step 6: Precursor Annealing	$/system	$150.67	$14.42	$6.83	$2.60	$2.10	$0.54
Step 7: Catalyst Dealloying	$/system	$93.41	$19.88	$6.98	$3.06	$2.60	$1.44
Step 8: Catalyst Filtration	$/system	$29.97	$8.27	$2.91	$1.52	$1.20	$0.22
Step 9: Catalyst Wash	$/system	$11.84	$1.11	$0.37	$0.14	$0.11	$0.03
Step 10: Catalyst Dry	$/system	$79.96	$7.59	$2.52	$0.98	$0.80	$0.22
Step 11: Catalyst Crushing	$/system	$42.16	$3.97	$1.48	$0.56	$0.45	$0.11
Total Catalyst Process Cost	$/system	$1,738.10	$1,013.53	$938.59	$910.81	$905.96	$886.73

Figure 63. Cost of each processing step for the dealloyed catalyst at production rates between 1,000 and 500,000 systems/year.

		All at 1k systems per year				All at 500k systems per year			
Component Costs per 80kWnet Fuel Cell System		Materials	Manuf.	Markup	Total	Materials	Manuf.	Markup	Total
Platinum Cost		$911.28	$0.00	$0.00	$911.28	$876.24	$0.00	$0.00	$876.24
Step 1: Catalyst PtNiC Precursor	$/system	$88.96	$61.02	$104.99	$254.97	$3.01	$2.15	$2.06	$7.22
Step 2: Precursor Filtration	$/system	$0.00	$17.59	$12.31	$29.90	$0.00	$0.19	$0.08	$0.27
Step 3: Precursor Wash	$/system	$0.00	$6.96	$4.87	$11.83	$0.00	$0.02	$0.01	$0.03
Step 4: Precursor Drying	$/system	$0.00	$47.03	$32.93	$79.96	$0.00	$0.19	$0.08	$0.27
Step 5: Precursor Crushing	$/system	$0.00	$24.80	$17.36	$42.16	$0.00	$0.09	$0.04	$0.13
Step 6: Precursor Annealing	$/system	$0.00	$88.63	$62.05	$150.67	$0.00	$0.39	$0.15	$0.54
Step 7: Catalyst Dealloying	$/system	$0.46	$54.48	$38.46	$93.41	$0.47	$0.56	$0.41	$1.44
Step 8: Catalyst Filtration	$/system	$0.00	$17.63	$12.34	$29.97	$0.00	$0.16	$0.06	$0.22
Step 9: Catalyst Wash	$/system	$0.00	$6.96	$4.87	$11.84	$0.00	$0.02	$0.01	$0.03
Step 10: Catalyst Dry	$/system	$0.00	$47.03	$32.93	$79.96	$0.00	$0.16	$0.06	$0.22
Step 11: Catalyst Crushing	$/system	$0.00	$24.80	$17.36	$42.16	$0.00	$0.08	$0.03	$0.11
Total Cost		$1,000.71	$396.92	$340.47	$1,738.10	$879.72	$4.01	$3.00	$886.73

Figure 64. Detailed cost breakdown for each dealloyed catalyst processing step at 1,000 and 500,000 systems per year.

8.1.3.3 Total Catalyst Synthesis and Material Cost

Figure 65 summarized cost results for the catalyst synthesis process and materials.

Annual Production Rate	1,000	10,000	30,000	80,000	100,000	500,000
Material ($/stack)	$1,001	$910	$898	$890	$888	$880
Manufacturing ($/stack)	$397	$60	$24	$12	$10	$4
Markup ($/stack)	$340	$43	$17	$8	$7	$3
Total Cost ($/stack)	$1,738	$1,014	$939	$911	$906	$887
Total Cost ($/kWnet)	$21.73	$12.67	$11.73	$11.39	$11.32	$11.08

Figure 65. Cost summary for catalyst synthesis and materials

8.1.4 Dispersed Catalyst Ink and Application to Membrane

There are numerous methods to apply the catalyst ink into the membrane electrode assembly. Some systems apply the catalyst ink (either directly or via decal transfer) onto the membrane to form a catalyst coated membrane (CCM). Others apply the catalyst ink directly onto the gas diffusion layer (GDL) to form a gas diffusion electrode (GDE).

SA analysis from 2006 to 2010 was based on the CCM-based inking application (specifically slot die coating of the catalyst ink directly onto a moving membrane web via a Coatema VertiCoater system). Such an approach had the advantage of being one of the least costly application techniques judged adequate for high production rates and reasonably high MEA performance. In 2011, SA switched to a new method of catalyst deposition that had shown significant improvements in power density and reported durability at low Pt loadings. Developed at 3M, the Nanostructured Thin Film Catalyst (NSTF) deposition process begins with vapor sublimation of a layer of crystalline finger-like projections, or "whiskers", to create a high surface area substrate on which the active catalysts may be deposited. Vapor deposition methods are utilized to deposit a very thin layer of platinum and other metals (cobalt and manganese) onto the whiskers in a very precise and uniform manner. The resulting catalyst coated whiskers can then be pressed into the fuel cell membrane to form a porous mat electrode intimately bonded to the membrane. This NSTF catalyst application method was used in SA analyses from 2011 to 2014. In 2015, the baseline reverted back to a slot die coating method for applying the dealloyed binary catalyst to the membrane.

In 2014/2015, SA examined two types of slot die coating methods: 1) dual-sided simultaneous slot die coating of anode and cathode onto the membrane, and 2) single-sided sequential (anode then cathode) slot die coating. Feedback from industry indicated differing opinions as to the best method of applying the catalyst ink. The simultaneous coating process would seem to be the obviously lower cost pathway given its 2x processing time advantage. However, at low production rates, the higher capital cost of the simultaneous coating system more than offsets its speed advantage and makes it more expensive than sequential coating. It is estimated that the two application methods would yield similar performance and are compared to each other in that respect. Both methods were examined for each volume of the baseline system and results show that sequential single-sided coating is lower cost only at 1,000 systems per year.

Multiple slot die coating companies provided information on dual-sided simultaneous and single-sided sequential coating techniques and input parameters. The results of the analysis reflect a combination of different machines with respective capital costs and operating conditions. Due to the proprietary nature of the detailed cost breakdown, SA is unable to provide this information. However, top level operating parameters are shown in Figure 66 and specify coating web width and web speeds of both dual-sided and single-sided coating machines. In all cases, the process starts with ultrasonic mixing of the dry catalyst powder (15 wt% PtNiC) with methanol (40.7 wt%), water (40.7 wt%), and ionomer (3.6 wt% Nafion) to form catalyst ink slurry.[61]

In some dual-sided coating cases the membrane is carried vertically through a set of rollers after coating so as to avoid web sag and eliminate/minimize roller contact with the wet slurry. Other machines execute dual sided horizontal coating (within one meter distance between anode and cathode coatings). In both cases, the catalyst coated membrane is dried under multiple sets of heaters before being rewound onto a take-up spool. The membrane that is coated vertically allows the CCM a long unsupported span during which the coating can dry before touching a roller. The horizontal coating

---

[61] Umicore Patent #US 7,141,270

includes flotation drying, eliminating any smearing or damage to the CCM before it is dried. The vertical and horizontal dual-sided simultaneous slot die coating methods are described in Figure 67 and Figure 68, respectively. The capital cost of equipment for all methods includes an ultrasonic mixer, web handling equipment (unwind, tension control, and rewind), coating machine (frame, backing roll, slot die, and fluid delivery), and drying system (supply and exhaust fans).

Parameter	Sequential Slot Die Coating Machine	Dual-Sided Vertical Coating Machine	Dual-Sided Horizontal Coating Machine
Power Consumption	80kW	60kW	500kW[62]
Line Speed	12m/min	13m/min	25m/min
Web Roll Length	1,500m	1,500m	1,500m
Web Width	30cm	50cm	90cm
Number of Laborers	1	1	3

Figure 66. Table of Slot Die Coating parameters comparing three different machines
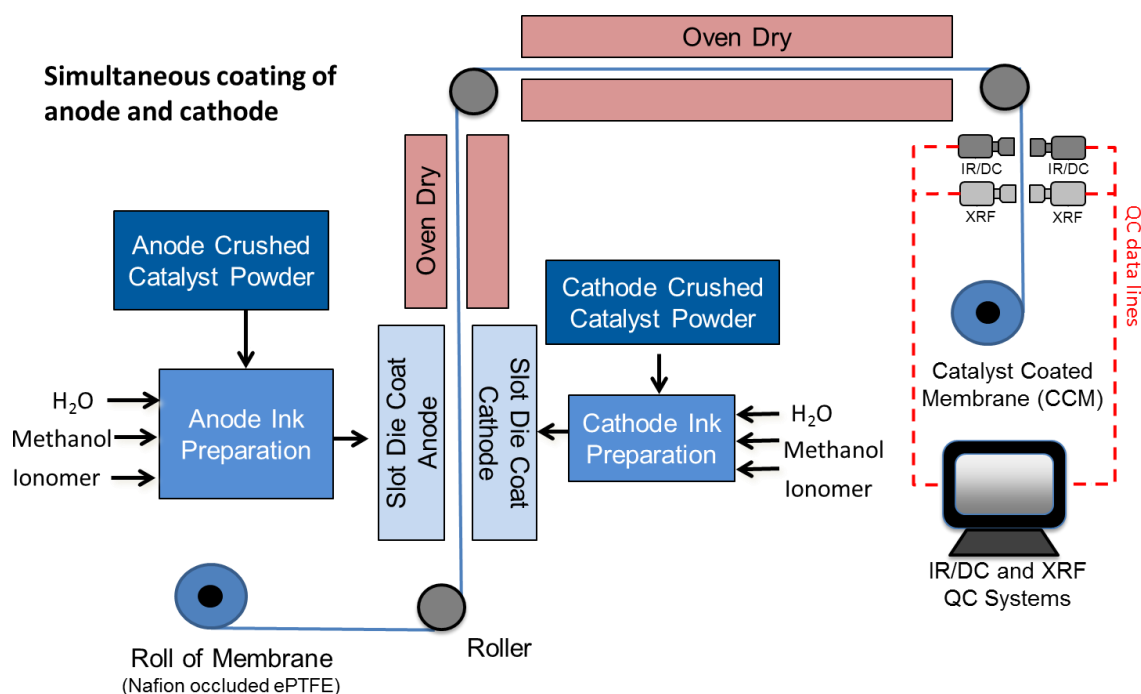
Figure 67. Vertical dual-sided simultaneous slot die coating of dealloyed PtNiC catalyst process flow diagram

---

[62] Electrical power used for heating the air for drying is 455kW or 91% of the total 500kW. All other components in process require the remaining 45kW or 9% of the total 500kW.

Dual-Sided Simultaneous Slot Die Coating (Horizontal)
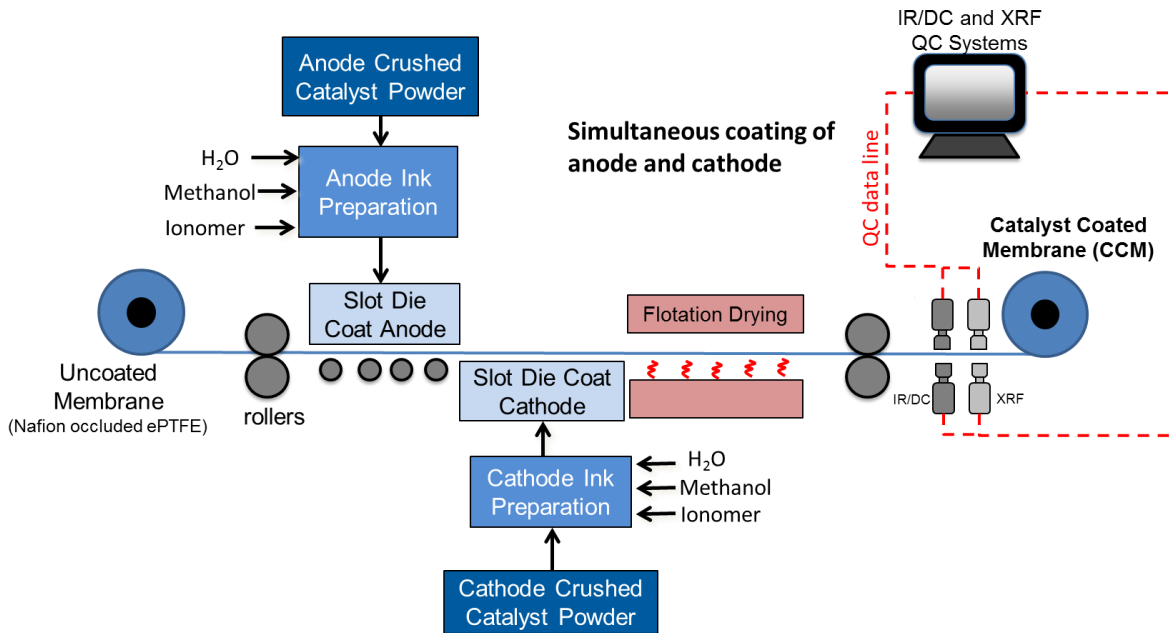
Figure 68. Horizontal dual-sided simultaneous slot die coating of dealloyed PtNi catalyst process flow diagram

The second slot die coating method (sequential or single-sided coating) is illustrated in Figure 69. In the first step, the anode ink is prepared within an ultrasonic mixer by mixing dry anode catalyst powder with water, methanol, and ionomer. In the second step, the membrane is unrolled while the anode ink is slot die coated onto the continuously moving membrane. This single layer is dried under heaters and rolled onto a take-up spool. The coating operation is then repeated in a second slot die coater to apply the cathode ink to the opposite face of the membrane. It is possible to use one coating line to alternately apply anode and cathode layers. Therefore, the cost analysis is based on use of one coater for both lines (anode and cathode). For the sequential process, extra time is required to coat two sides (compared to simultaneous coating), and longer roll change-out times are needed (due to sequential operation). Additionally, there may be difficulties with registering the web, particularly after it goes through the drying oven a single time.

Sequential Slot Die Coating Catalyst
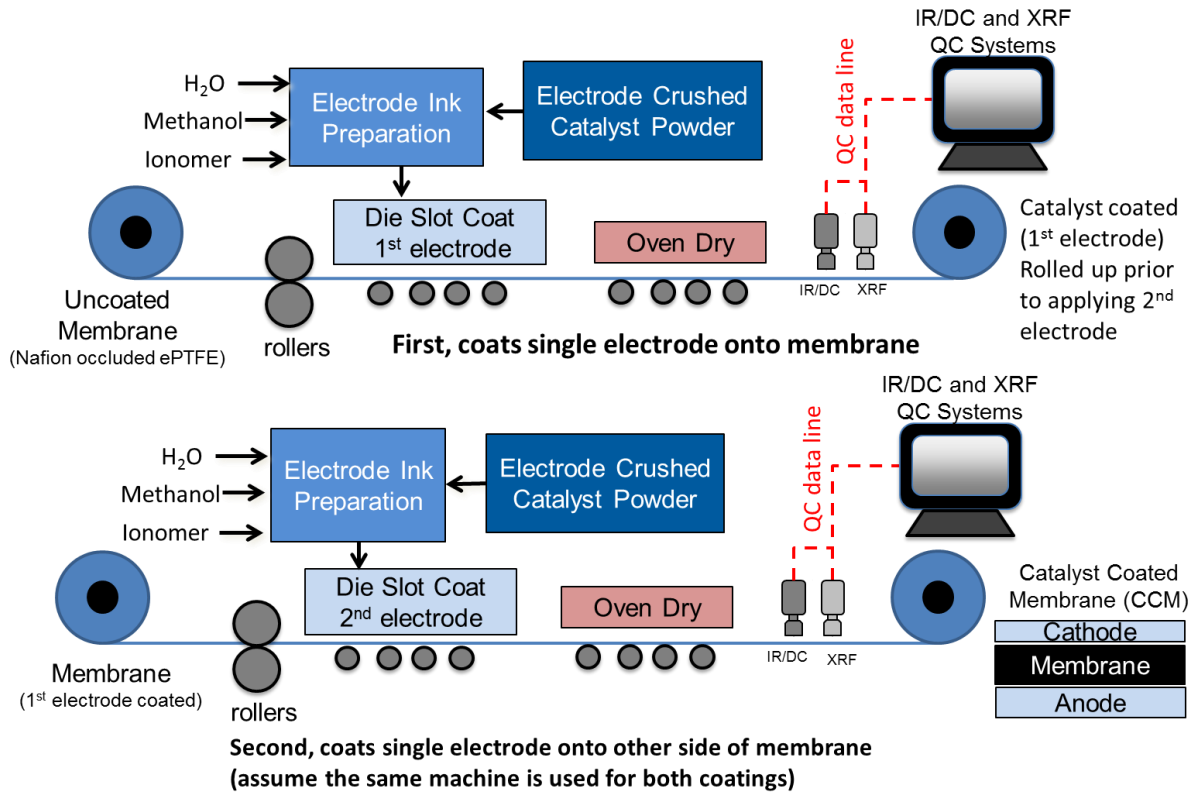
Figure 69. Flow Diagram of Sequential Slot Die Coating of Electrodes

Patch, island coating, window coating, "window frame", or interrupted coating all describe coating techniques to pattern the ink onto the web rather than provide a 100% fully coated coverage. Such non 100% coverage coating is not assumed in this analysis. Patch coating is generally desirable in that it reduces catalyst coating on areas of the membrane that will not be active within the fuel cell, thereby reducing catalyst cost. Within the DFMA^{TM} model, SA does not include this capability for two reasons 1) the sub-gasket process assumes a continuous coating of the membrane that is cut into separate parts and realigned with appropriate spacing between active areas, 2) when presented to the Fuel Cell Technical Team, it is assumed to be a future capability of slot die coating that has not been demonstrated successfully at high volumes while maintaining polarization performance.

The quality control equipment associated with the slot die coating process incudes IR/DC and XRF. An IR/DC system is used to assess the uniformity of the electrode layers at a single location within the slot die coating production sequence. The IR/DC system[63] operates by placing two conductive rollers across the width of the web a short distance from one another. An electric current is fed to one of the roller,

---

[63] Niccolo V. Aieta, Prodip K. Das, Andrew Perdue, Guido Bender, Andrew M. Herring, Adam Z. Weber, Michael J. Ulsh, "Applying infrared thermography as a quality-control tool for the rapid detection of polymer-electrolyte-membrane-fuel-cell catalyst-layer-thickness variations", Journal of Power Sources, Volume 211, 1 August 2012, Pages 4-11.

and then down the length of the electrode layer (anode and cathode) to be collected by the other roller. An IR camera mounted above the electrode and peering down onto the moving web is used to visually assess the temperature signature of the electrode and detect anomalies that would be indicative of electrode thickness variation, improper catalyst loading, improper particle size, non-uniform platinum distribution, or other general defects.[64] Due to the simplicity of the signal processing required, IR camera systems can easily match the line speed of the catalyst deposition (25 m/min). To achieve appropriate resolution (at 500k systems/year), six IR cameras are needed at each analysis site to achieve a 1m total field of view (the web width) at a 25 m/min web speed. Two systems are needed per line for all production volumes using dual-sided coating method corresponding to viewing of 1) the anode after drying, and 2) the cathode after drying. Only one system is needed for sequential single-sided coating at 1k systems per year as it is assumed that the IR/DC equipment is viewing one catalyst layer at a time after coating. X-Ray Fluorescence (XRF) is included as an additional QC feature for the catalyst coating processing that was not originally included in the 2014 NSTF catalyst application. It was recommended by NREL to be included for the baseline as it is currently used in addition to IR/DC QC by many CCM suppliers. XRF is appropriate for determination of material composition (i.e. Pt loading and content of material) and electrode thickness that can directly affect performance.

8.1.4.1 Total Catalyst Ink and Application Cost

Machine rate and process parameters are show in Figure 70 and Figure 71 . The overall cost breakdown at various production rates is summarized in Figure 71Figure 72.

Annual Production Rate	1,000	10,000	30,000	80,000	100,000	500,000
Equipment Lifetime (years)	14	14	14	13	13	13
Interest Rate	10%	10%	10%	10%	10%	10%
Corporate Income Tax Rate	40%	40%	40%	40%	40%	40%
Capital Recovery Factor	0.177	0.180	0.180	0.186	0.186	0.186
Equipment Installation Factor	1.40	1.40	1.40	1.40	1.40	1.40
Maintenance/Spare Parts (% of CC)	5%	5%	5%	5%	5%	5%
Miscellanous Expenses (% of CC)	1%	1%	1%	1%	1%	1%
Power Consumption (kW)	83	58	58	753	753	753

Figure 70. Slot die coating application process parameters

Annual Production Rate	1,000	10,000	30,000	80,000	100,000	500,000
Capital Cost ($/Line)	Proprietary					
Coating Web Width (cm)	30	50	50	91	91	91
Simultaneous Lines	1	1	1	1	1	4
Laborers per Line	1.00	1.00	1.00	3.00	3.00	3.00
Line Utilization	9.5%	18.3%	52.3%	58.5%	72.6%	85.4%
Effective Total Machine Rate ($/hr)	$1,428.92	$1,140.89	$430.52	$1,027.20	$866.45	$766.11
Line Speed (m/s)	0.2	0.2	0.2	0.4	0.4	0.4

Figure 71. Machine rate parameters for slot die coating process

---

[64] Private conversation with Michael Ulsh, NREL.

Annual Production Rate	1,000	10,000	30,000	80,000	100,000	500,000
Material ($/stack)	$7	$4	$3	$2	$2	$1
Manufacturing ($/stack)	$782	$112	$39	$38	$32	$25
Total Cost ($/stack)	$789	$116	$42	$41	$34	$26
Total Cost ($/kWnet)	$9.86	$1.45	$0.52	$0.51	$0.43	$0.33

Figure 72. Cost summary for slot die coating process

8.1.5 Gas Diffusion Layer

The gas diffusion layer (GDL) costs for 2011 and previous analyses were based upon a price quote for a vendor macroporous layer combined with a DFMA^{TM} analysis of a microporous layer addition. This resulted in a GDL cost of ~$11/m^2 at 500k systems/year ($2.54/kWnet).

The 2014 GDL cost estimates are based on recent DOE-funded research by Ballard Power Systems for cost reduction of a teflonated ready-to-assemble GDL consisting of a non-woven carbon base layer with two microporous layers.[65] The Ballard analysis[66] estimates a cost of ~$4.45/m^2 at 10M m^2/year (approximately equivalent to 500k systems/year) and a cost of $56/m^2 at less than 100k m^2/year (approximately equivalent to 5k systems/year). Based upon these data points, a learning curve exponent of 0.6952 was derived and used to estimate the GDL cost at intermediate production rates. Figure 73 graphically portrays GDL cost used in the analysis as a function of annual GDL production.
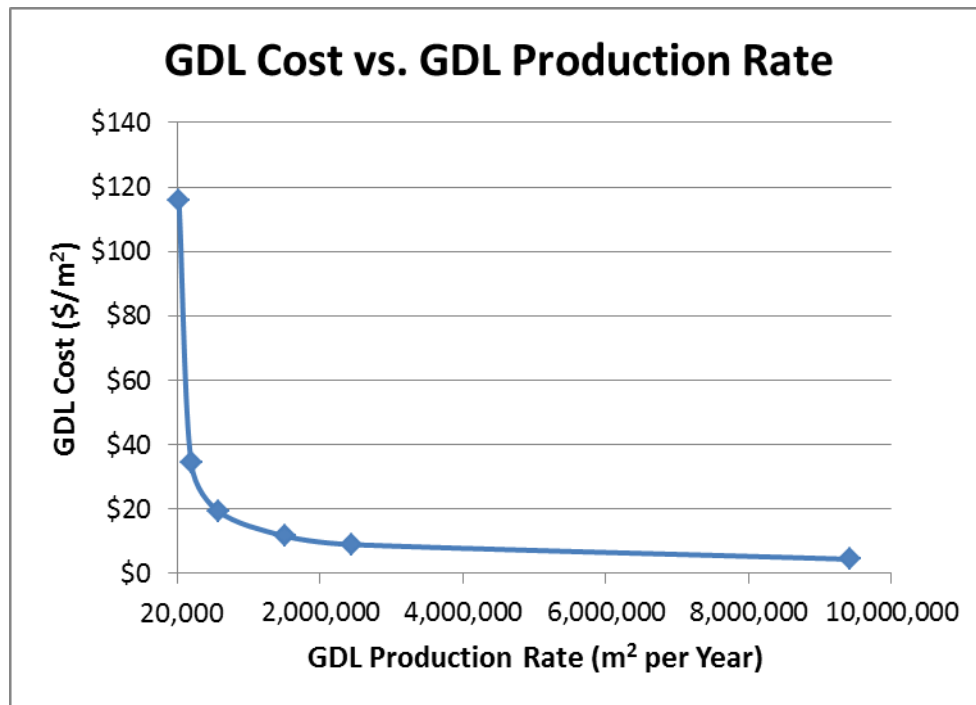
Figure 73. GDL cost as a function of production rate

---

[65] "Reduction in Fabrication Costs of Gas Diffusion Layers," Jason Morgan, Ballard Power Systems, DOE Annual Merit Review, May 2011.
[66] Personal communication with Jason Morgan of Ballard Power Systems, 24 July 2012.

The overall cost breakdown at various system values and technology levels is shown in Figure 74.

Annual Production Rate	1,000	10,000	30,000	80,000	100,000	500,000
GDL Cost ($/stack)	$2,509	$750	$422	$252	$224	$96
Total Cost ($/stack)	$2,509	$750	$422	$252	$224	$96
Total Cost ($/kWnet)	$31.37	$9.38	$5.27	$3.15	$2.80	$1.20

Figure 74. Cost breakdown for GDL

8.1.6 MEA Sub-Gaskets

Prior to 2012, the fuel cell systems analyzed by SA were assumed to use MEA frame gaskets for gas and liquid sealing between the membrane and the bipolar plate.[67] The frame gaskets were insertion-molded around the periphery of the MEA and added substantial cost due to high cycle time and the relatively high cost of custom injection-moldable sealant. Consequently, during the 2012 analysis, an examination was conducted of fuel cell manufacturer processes and patents to identify an alternative lower cost sealing approach. The use of sub-gaskets was identified as a promising alternative and was selected for the 2012 to 2015 fuel cell systems.

The sub-gasket sealing approach consists of thin layers of PET gasketing material, judiciously cut into window-frame shapes and laminated to themselves and the periphery of the MEA to form a contiguous and flat sealing surface against the bipolar plate. A thin bead of adhesive sealing material is screen-printed onto the bipolar plates to form a gas- and liquid-tight seal between the bipolar plate and the sub-gasket material. The bipolar plate design has been changed to incorporate a raised surface at the gasket bead location to minimize the use of the gasket material. Screen printing of the gasket bead onto the bipolar plates is a well-understood and demonstrated process. The sub-gasket layers are bonded to the MEA in a roll-to-roll process, shown in Figure 75, based upon a 3M patent application.[68] While the construction is relatively simple in concept, fairly complex machinery is required to handle and attain proper placement and alignment of the thin sub-gasket and MEA layers. This sub-gasket process has four main steps:

1. Formation of a catalyst coated membrane (CCM) web
2. Attachment of membranes to the first half of the sub-gasket ladder web
3. Attachment of the second half of the sub-gasket ladder web to the half sub-gasketed membrane
4. Attach GDLs to sub-gasketed membrane to form five-layer MEAs (in roll form)

---

[67] "Mass Production Cost Estimation for Direct H2 PEM Fuel Cell Systems for Automotive Applications: 2010 Update," Brian D. James, Jeffrey A. Kalinoski & Kevin N. Baum, Directed Technologies, Inc., 30 September 2010.
[68] "Fuel Cell Subassemblies Incorporating Sub-gasketed Thrifted Membranes," US2011/0151350A1
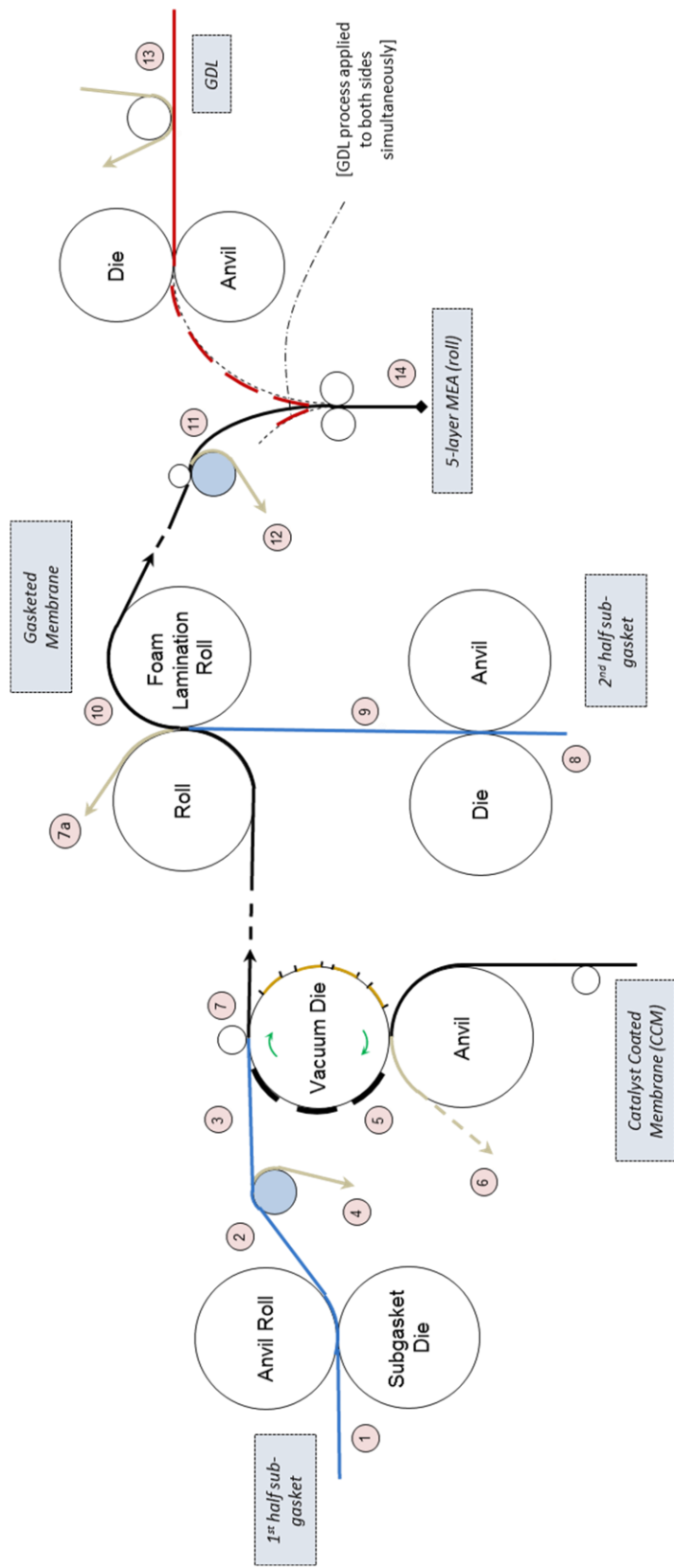
Figure 75. Roll-to-roll sub-gasket application process

Labels in figure:
- GDL (13)
- [GDL process applied to both sides simultaneously]
- Die
- Anvil
- 5-layer MEA (roll) (14)
- 11
- 12
- Gasketed Membrane
- Foam Lamination Roll (10)
- Anvil
- 2nd half sub-gasket
- Roll (7a)
- Die (8)
- 9
- Vacuum Die (7)
- Anvil
- Catalyst Coated Membrane (CCM)
- 3, 4, 5, 6
- 2
- Anvil Roll
- Subgasket Die
- 1st half sub-gasket
- 1

95
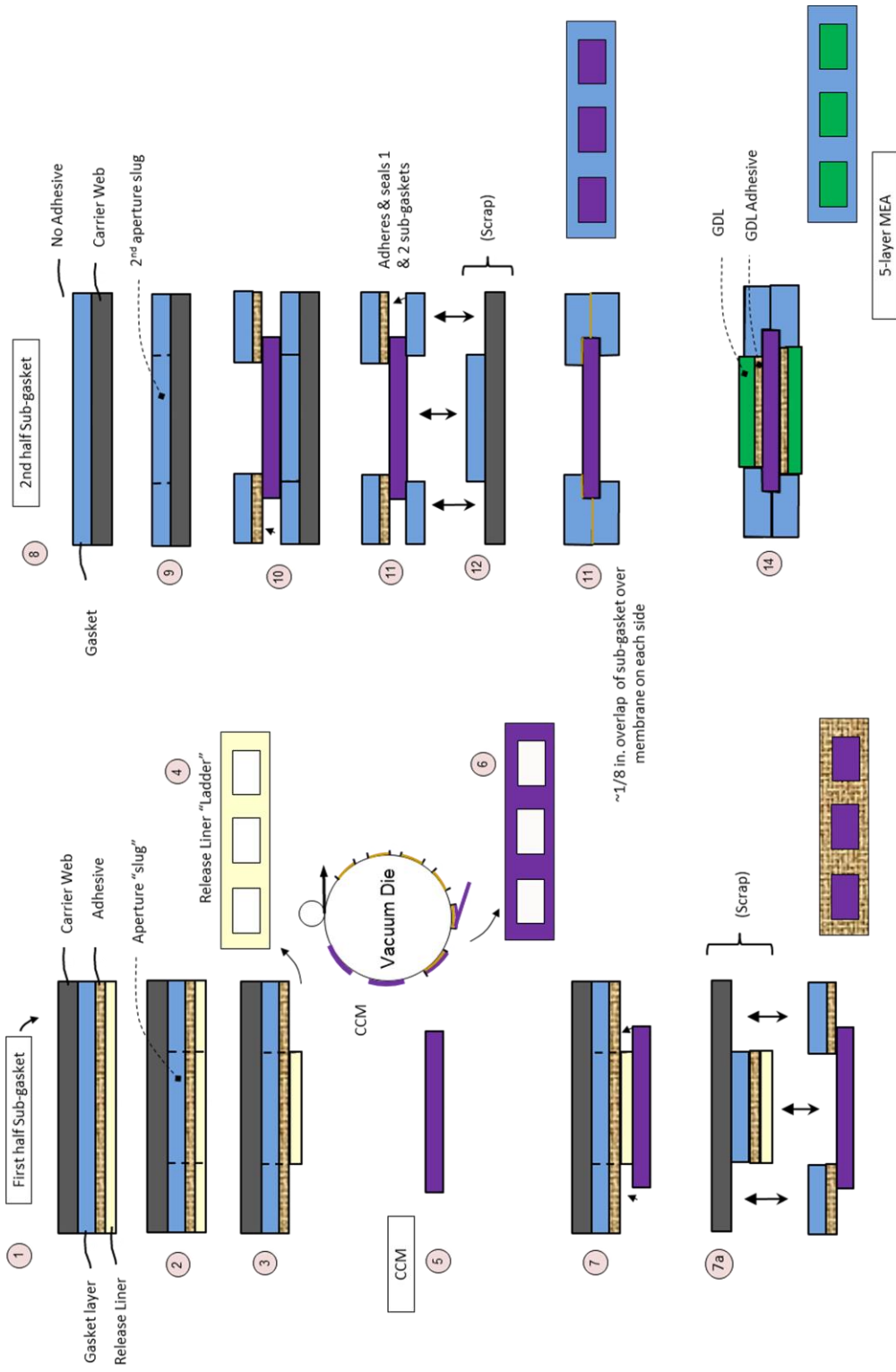
Figure 75. (continued)

The process uses a proprietary 3M "pressure sensitive adhesive," which is modeled at a notional $20/kg based on high end generic adhesive surrogates. The sub-gasket layer consists of two layers of 0.1mm PET film at $1.67/m^2 based on a high-volume internet price quote. These materials experience significant waste using this process, as the center section of both the sub-gasket layers (corresponding to the fuel cell active area) and the adhesive liner is scrapped. The process capital equipment is based on component analogy to membrane web processing units and is assumed to operate at a line speed of 30m/min with five line workers.

While the process train illustrated in Figure 75 is based on a 3M patent, the implementation of it for cost modeling purposes differs in two important respects. First, the process shows a "ladder" of scrap CCM being left over (component 6) after the vacuum die cutter separates the CCM active area (component 5) from the CCM roll. This amount of CCM wastage would normally be approximately equal to the difference between the bipolar plate total area and the membrane active area: a substantial scrap fraction.[69] Consequently, to minimize this CCM wastage, additional machinery is postulated for cost modeling purposes to allow the active area CCM pieces to be cut from the CCM roll contiguously (i.e. with no scrap between pieces) and then placed appropriately to fit into the picture portion of the picture-frame sub-gaskets. This may be accomplished by rotary, indexed, or robotic pick-and-place machinery. While this approach adds mechanical complexity and capital cost, it avoids the high CCM scrap rates that otherwise would occur. Second and as previously discussed in Section 6.5, the 3M patent is silent on the issue of how many cells are processed simultaneously in the web width direction. While 1 cell wide is inferred, multiple cells across the width is a reasonable engineering extrapolation. Cost computations are based on a nominal 1 meter web width that can process 5 cells simultaneously. This adds mechanical complexity and capital cost but overall leads to reduced part cost due to an increased processing rate.

At 1,000 systems per year production, an alternative processing method was investigated and used for the sub-gasket. As described in Section 6.7.2, the sub-gasket process has quite high capital cost with very high throughput resulting in very low utilization at low volumes. Instead, a robotic stacking approach was used where the material for each of the sub-gasket components is cut to the cell size and stacked with a robot. This change in process affects the processing methods of the hot pressing and cutting and slitting. More on these changes are described in their respective sections.

A thin bead of sealing material is screen printed onto the bipolar plates to form a gas and liquid tight seal between the bipolar plate and the sub-gasket material. This process is directly analogous to the screen-printed coolant gaskets analyzed in past cost analyses.[70] The cost of this screen printing step is combined with that of the sub-gasket procedure described above, and presented as a single cost result in Figure 9.

---

[69] For an active to total area ratio of 0.625, scrap as a percentage of active area would be 0.375/0.625 = 60%.
[70] The reader is directed to section 4.4.9.3 of the 2010 update of the auto fuel cell cost analysis for a more detailed discussion. "Mass Production Cost Estimation for Direct H$_2$ PEM Fuel Cell Systems for Automotive Applications: *2010 Update*," Brian D. James, Jeffrey A. Kalinoski & Kevin N. Baum, Directed Technologies, Inc., 30 September 2010.

8.1.7 Sub-gasket Formation

Details of the MEA sub-gasket formation process appear in Figure 76 and Figure 77 with cost results shown in Figure 78.

Annual Production Rate	1,000	10,000	30,000	80,000	100,000	500,000
Equipment Lifetime (years)	15	13	13	13	13	13
Interest Rate	10%	10%	10%	10%	10%	10%
Corporate Income Tax Rate	40%	40%	40%	40%	40%	40%
Capital Recovery Factor	0.175	0.186	0.186	0.186	0.186	0.186
Equipment Installation Factor	1.4	1.4	1.4	1.4	1.4	1.4
Maintenance/Spare Parts (% of CC)	10%	10%	10%	10%	10%	10%
Miscellanous Expenses (% of CC)	7%	7%	7%	7%	7%	7%
Power Consumption (kW)	101	101	101	101	101	101

Figure 76. MEA Sub-gasket process parameters

Annual Production Rate	1,000	10,000	30,000	80,000	100,000	500,000
Capital Cost ($/Line)	$864,129	$2,908,600	$2,908,600	$2,958,600	$2,958,600	$2,958,600
Simultaneous Lines	1	1	1	1	1	3
Laborers per Line	2	5	5	5	5	5
Line Utilization	88.8%	8.4%	24.2%	37.4%	46.3%	72.6%
Effective Total Machine Rate ($/hr)	$219.32	$4,660.05	$1,773.84	$1,250.47	$1,054.62	$758.04
Line Speed (m/s)	0.3	0.5	0.5	0.5	0.5	0.5
Kapton Tooling Cost ($/m2)	$6.47	$3.56	$3.34	$3.28	$3.27	$3.24
Subgasket Material Cost ($/m2)	$1.67	$1.67	$1.67	$1.67	$1.67	$1.67

Figure 77. MEA Sub-gasket machine parameters

Annual Production Rate	1,000	10,000	30,000	80,000	100,000	500,000
Material ($/stack)	$63	$63	$63	$63	$63	$63
Manufacturing ($/stack)	$654	$132	$48	$20	$16	$11
Tooling (Kapton Web) ($/stack)	$18	$10	$9	$9	$9	$8
Total Cost ($/stack)	$735	$205	$120	$91	$88	$83
Total Cost ($/kWnet)	$9.19	$2.56	$1.50	$1.14	$1.10	$1.03

Figure 78. Cost breakdown for MEA Sub-gasket

8.1.7.1 Screenprinted Sub-gasket Seal

Details of the screenprinted sub-gasket seal application step appear in Figure 79 and Figure 80 with cost results shown in Figure 81.

Annual Production Rate	1,000	10,000	30,000	80,000	100,000	500,000
Screen Printing Machine Type	DEK Horizon	DEK PV 1200	DEK PV 1200	DEK PV 1200	DEK PV 1200	DEK PV 1200
Equipment Lifetime (years)	15	15	15	15	15	15
Interest Rate	10%	10%	10%	10%	10%	10%
Corporate Income Tax Rate	40%	40%	40%	40%	40%	40%
Capital Recovery Factor	0.175	0.175	0.175	0.175	0.175	0.175
Equipment Installation Factor	1.4	1.4	1.4	1.4	1.4	1.4
Maintenance/Spare Parts (% of CC)	3%	1%	1%	1%	1%	1%
Miscellanous Expenses (% of CC)	12%	12%	12%	12%	12%	12%
Power Consumption (kW)	61	166	166	166	166	166

Figure 79. Screenprinted Sub-gasket process parameters

Annual Production Rate	1,000	10,000	30,000	80,000	100,000	500,000
Screen Printing Machine Type	DEK Horizon	DEK PV 1200	DEK PV 1200	DEK PV 1200	DEK PV 1200	DEK PV 1200
Capital Cost ($/Line)	$392,735	$1,458,755	$1,458,755	$1,458,755	$1,458,755	$1,458,755
Simultaneous Lines	1	1	1	3	4	17
Laborers per Line	0.25	0.25	0.25	0.25	0.25	0.25
Line Utilization	30.6%	32.5%	97.4%	86.6%	81.2%	95.5%
Effective Total Machine Rate ($/hr)	$165.16	$521.11	$189.98	$210.68	$223.09	$193.29
Line Speed (m/s)	1.00	1.00	1.00	1.00	1.00	1.00
Index Time (s)	$9.62	$4.00	$4.00	$4.00	$4.00	$4.00
Resin Cost ($/kg)	$15.19	$15.19	$15.19	$15.19	$15.19	$15.19

Figure 80. Screenprinted sub-gasket machine parameters

Annual Production Rate	1,000	10,000	30,000	80,000	100,000	500,000
Material ($/stack)	$12	$12	$12	$12	$12	$12
Manufacturing ($/stack)	$170	$57	$21	$23	$24	$21
Total Cost ($/stack)	$182	$69	$33	$35	$36	$33
Total Cost ($/kWnet)	$2.27	$0.86	$0.41	$0.44	$0.45	$0.41

Figure 81. Cost breakdown for screenprinted sub-gasket

8.1.7.2 Total MEA Sub-gasket & Seal Cost'

The total cost of the sub-gasket (sub-gasket formation plus screenprinted seal) appears in Figure 82.

Annual Production Rate	1,000	10,000	30,000	80,000	100,000	500,000
Material ($/stack)	$75	$75	$75	$75	$75	$75
Manufacturing ($/stack)	$824	$189	$69	$43	$41	$32
Tooling (Kapton Web) ($/stack)	$18	$10	$9	$9	$9	$8
Total Cost ($/stack)	$917	$274	$153	$126	$124	$116
Total Cost ($/kWnet)	$11.46	$3.42	$1.91	$1.58	$1.56	$1.45

Figure 82. Cost breakdown for total MEA sub-gasket

8.1.8 Hot Pressing CCM and GDLs

Bonding of the three layers of the MEA (the catalyst-coated membrane plus GDL on either side) is desirable for intimate electronic/ionic contact, proper alignment of the parts, and ease of subsequent MEA handling. In switching from a NSTF-based catalyst coating process to a slot die coating process, an

alternative method was needed to bond the GDLs to the CCM. Industry feedback[71] confirmed that the procedure of hot pressing the membrane and GDL to bond the parts was incompatible with the NSTF catalyst layer.[72] Consequently for the 2014 cost analysis (NSTF-based), the layers of the MEA were crimped together periodically along the edges after the MEA gasketing process and before the cutting and slitting process, to an extent sufficient to hold the assembly together. For NSTF, hot pressing is incompatible because there is no ionomer material in the catalyst to melt to the GDL. The 2015 baseline system (catalyst ink based) added hot pressing to bond the ionomer in the catalyst ink to the GDL layers.

As described in Figure 83, the hot-pressing process in starts with the roll that comes off the sub-gasket line; the gasketed catalyzed membrane sandwiched between two GDLs. Each of the two wind stands (wind and unwind) is equipped with a brake and a tensioner. The sandwiched MEA travels through the hot press and then is rewound back into a roll. The press is heated to 160°C, and is indexed with a press time of 90 seconds. It takes 3 seconds to open the press, advance the roll to the next section, and re-close the press, making the cycle time 93 seconds. The section advance time could be quicker, but because of the limited tensile strength of the materials, 3 seconds is appropriate. Furthermore, 3 seconds is only 1/30th of the press time, and for an already-inexpensive process, the savings in speeding up the section advance would be minimal. The press is 100 cm wide by 150 cm in length, so approximately 18 to 22 cells get hot-pressed at a time, depending on the cell geometry. The idea of hot pressing the MEA with the sub-gasket is a potential problem. This assumption was not based on what is currently done in practice and has not been demonstrated in industry. However the PET film melting point is 250˚C while the hot pressing is only at 160˚C and the press die is portioned to only press the GDL and not the gaskets.

At 1,000 systems per year, the cells are prematurely cut into single cell units, requiring an alternative delivery method to the hot pressing machine. Normally an automated process would only require a worker ¼ of their time, but for the 1,000 system per year production rate, SA assumed a full time worker that manually inserts the MEA into the press and then visually inspects them afterward for holes, delamination, etc. As is described in the cutting and slitting section, no additional cutting or slitting is required for the MEA at 1k systems per year because the cells are already in final form. The inspection of the cell after the hot pressing is important because it takes the place of the Optical Detection System (ODS) QC inspection after the cutting and slitting process.

---

[71] Personal communication with Mark Debe of 3M, November 2011.
[72] Previous cost analysis postulated bonding of the GDL and catalyst coated membrane through a hot pressing procedure since the ionomer within the catalyst ink composition could serve as a bonding agent for the GDL. However, there is no ionomer in the NSTF catalyst layer and thus hot pressing would not be effective for NSTF MEA's.

CCM with GDL
Unwind Stand with Brake & Tensioner 0.6m ID spool, 1 m width

Hot-Pressing Station
Large, flat surface, 1m wide, 1.5m length, 160˚C, 90 second clamp time.

Hot-Pressed M&E
Rewind Stand with Tensioner 0.6m ID spool, 1m width
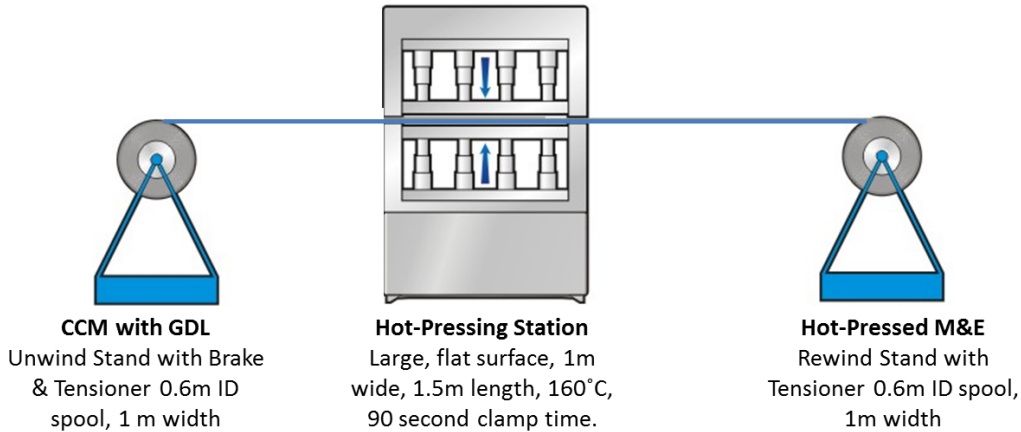
Figure 83. Hot-pressing process diagram for pressing two GDL layers and the CCM.

8.1.8.1 *Hot Pressing CCM and GDLs Cost Breakdown*

Machine rate and process parameters are show in Figure 84 and Figure 85. The overall cost breakdown at various production rates is summarized in Figure 86.

Annual Production Rate	1,000	10,000	30,000	80,000	100,000	500,000
Equipment Lifetime (years)	15	15	15	15	15	15
Interest Rate	10%	10%	10%	10%	10%	10%
Corporate Income Tax Rate	40%	40%	40%	40%	40%	40%
Capital Recovery Factor	0.175	0.175	0.175	0.175	0.175	0.175
Equipment Installation Factor	1	1	1	1	1	1
Maintenance/Spare Parts (% of CC)	5%	5%	5%	5%	5%	5%
Miscellanous Expenses (% of CC)	7%	7%	7%	7%	7%	7%
Power Consumption (kW)	15	16	16	16	16	16

Figure 84. Hot-pressing process parameters

Annual Production Rate	1,000	10,000	30,000	80,000	100,000	500,000
Capital Cost ($/Line)	$56,062	$126,795	$126,795	$126,795	$126,795	$126,795
Simultaneous Lines	$1	$2	$5	$8	$10	$50
Laborers per Line	1	0	0	0	0	0
Line Utilization	14%	82%	99%	99%	99%	99%
Effective Total Machine Rate ($/hr)	$90.61	$29.39	$26.60	$26.60	$26.60	$26.60
Total Cycle Time (seconds)	105	93	93	93	93	93

Figure 85. Machine rate parameters for hot-pressing process

Annual Production Rate	1,000	10,000	30,000	80,000	100,000	500,000
Manufacturing ($/stack)	$42	$16	$15	$9	$9	$9
Tooling ($/stack)	$1	$0	$0	$0	$0	$0
Total Cost ($/stack)	$43	$17	$15	$9	$9	$9
Total Cost ($/kWnet)	$0.54	$0.21	$0.19	$0.11	$0.11	$0.11

Figure 86. Cost summary for hot-pressing process

8.1.9 MEA Cutting, and Slitting

As shown in Figure 87, the rolls of hot-pressed MEA are fed through cutters and slitters to trim to the desired dimensions for insertion into the stack. The 100-cm-wide input roll (width at 500k systems per year) is slit into ribbon streams of the appropriate width (again, depending on cell geometry). The streams continue through to the cutters, which turn the continuous material into individual rectangles. These rectangles are then sorted into magazine racks.
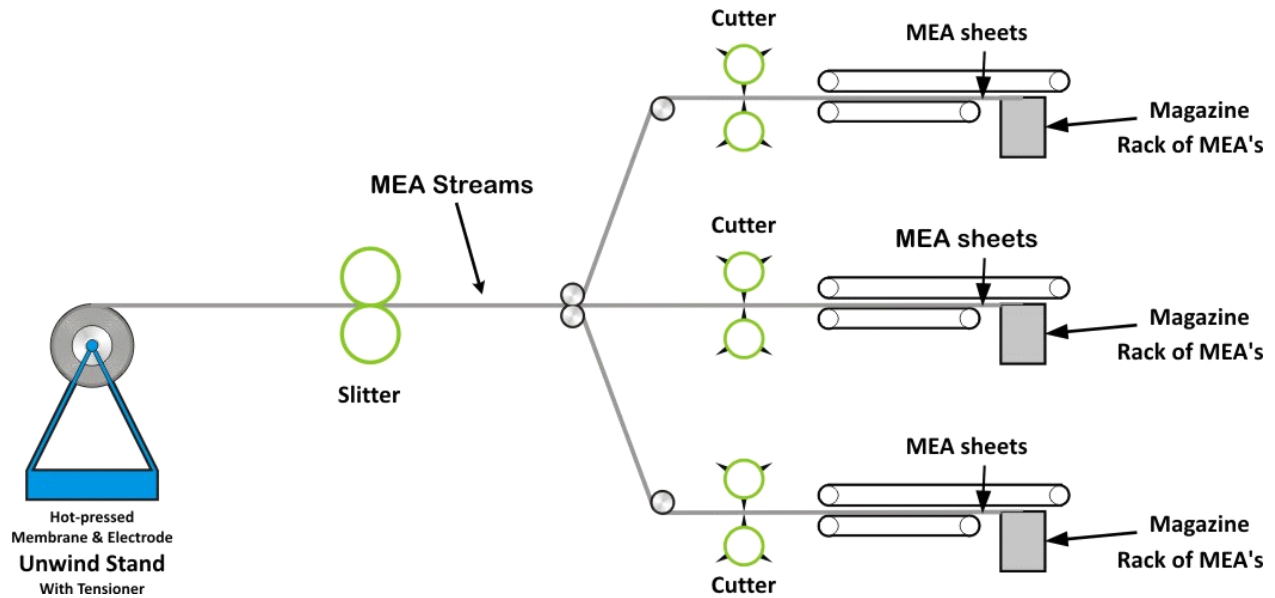
Figure 87. Cutting & slitting process diagram

Figure 88 and Figure 89 further detail the process parameters. This process is not used at all production rates. At 1,000 systems per year, there is no cutting and slitting due to the fact that the cells are already discretized for the sub-gasket process. Figure 90 summarizes the overall cost of the cutting and slitting operation.

Annual Production Rate	1,000	10,000	30,000	80,000	100,000	500,000
Equipment Lifetime (years)	0	14	14	14	14	14
Interest Rate	0	10%	10%	10%	10%	10%
Corporate Income Tax Rate	0	40%	40%	40%	40%	40%
Capital Recovery Factor	0	0.180	0.180	0.180	0.180	0.180
Equipment Installation Factor	0	1.4	1.4	1.4	1.4	1.4
Maintenance/Spare Parts (% of CC)	0	10%	10%	10%	10%	10%
Miscellanous Expenses (% of CC)	0	7%	7%	7%	7%	7%
Power Consumption (kW)	0	18	18	18	18	18

Figure 88. Cutting & Slitting process parameters

Annual Production Rate	1,000	10,000	30,000	80,000	100,000	500,000
Capital Cost ($/line)	0	$419,136	$419,136	$469,136	$469,136	$469,136
Costs per Tooling Set ($)	0	$5,606	$5,606	$5,606	$5,606	$5,606
Tooling Lifetime (cycles)	0	200,000	200,000	200,000	200,000	200,000
Simultaneous Lines	0	1	1	1	1	2
Laborers per Line	0	0.25	0.25	0.25	0.25	0.25
Line Utilization	0	4.7%	13.8%	21.8%	27.2%	68.0%
Effective Total Machine Rate ($/hr)	0	$1,129.91	$395.01	$283.27	$229.19	$99.38
Line Speed (m/s)	0	1.2	1.3	1.3	1.3	1.3

Figure 89. Machine rate parameters for Cutting & Slitting process

Annual Production Rate	1,000	10,000	30,000	80,000	100,000	500,000
Manufacturing ($/stack)	$0	$18	$6	$3	$2	$1
Tooling ($/stack)	$0	$4	$4	$2	$2	$2
Total Cost ($/stack)	$0	$22	$10	$5	$4	$3
Total Cost ($/kWnet)	$0.00	$0.27	$0.12	$0.06	$0.06	$0.04

Figure 90. Cost breakdown for Cutting & Slitting process

8.1.10 End Plates

In a typical PEM fuel cell stack, the purposes of an end plate are threefold:

- Evenly distribute compressive loads across the stack

- Cap off and protect the stack

- Interface with the current collector

Typically there is also a separate insulator plate at each end to electrically insulate the stack from the rest of the vehicle. However the SA end plate design, based on a UTC patent (see Figure 91), eliminates the need for separate insulators. Thus, the SA modeled end plates also serve a fourth function: electrical insulation of the ends of the stack.

The end plate is made from a compression-molded composite (LYTEX 9063), is mechanically strong (455 MPa) to withstand the compressive loading, and is sufficiently electrically non-conductive ($3x10^{14}$ ohm-cm volume resistivity). Use of this material allows for an end plate with lower cost and lower thermal capacity than the typical metal end plates, with the additional benefit of having very low corrosion susceptibility. The benefits of lower cost and corrosion resistance are obvious, and the low thermal capacity limits the thermal energy absorbed during a cold start, effectively accelerating the startup period.
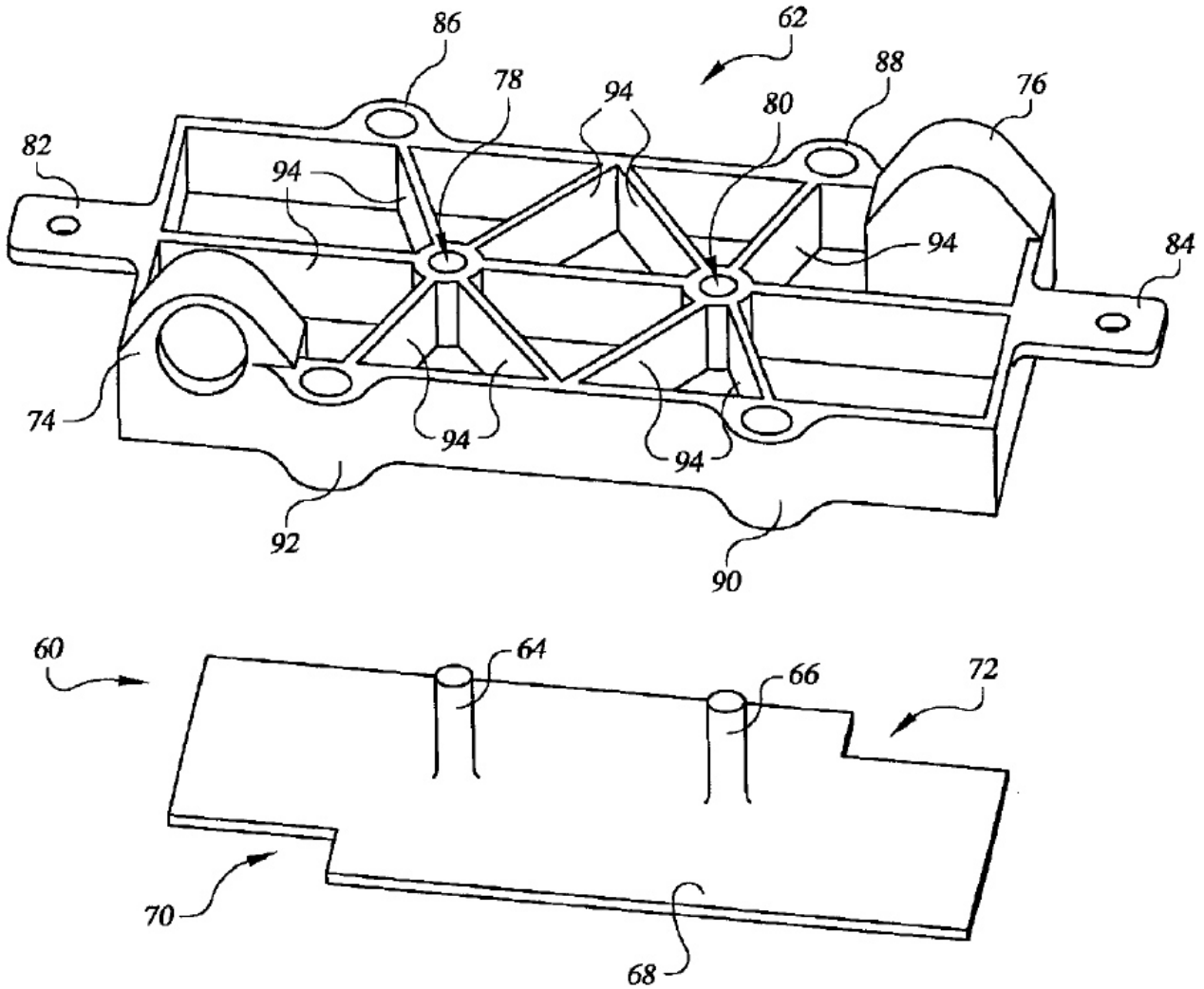
Figure 91. End plate concept (Figure courtesy of US patent 6,764,786)

LYTEX 9063 is a high performance engineered structural composite (ESC) molding compound consisting of epoxy and glass fiber reinforcement. It is designed for military and aerospace structural applications requiring excellent mechanical properties, retention of properties at elevated temperatures, good chemical resistance and excellent electrical properties. For all of these reasons, it is ideally suited for this application.

The end plates are manufactured via compression molding. A summary of the procedure is as follows:[73]

- Remove enough LYTEX from cold storage for one day's usage. Allow it to warm to room temperature.

- Clean mold thoroughly. Apply a uniform thin coating of a mold release. (Note: Once the mold is conditioned for LYTEX, only periodic reapplications are required.)

---

[73] Based on Quantum Composites recommended procedures for LYTEX molding.

- Adjust mold temperature to 300°F (148°C).

- Adjust molding pressure on the material to 1,500 psi (105 kg/cm).

- Remove protective film completely from both sides of the LYTEX.

- Cut mold charge so the LYTEX covers approximately 80% of the mold area and is about 105% of the calculated part weight.

- Dielectrically preheat the LYTEX quickly to 175°F (80°C).

- Load material into mold and close the mold.

- Cure for 3 minutes

- Remove part from mold. Because of low shrinkage and high strength, the part may fit snugly in the mold.

- Clean up mold and begin again.

- Re-wrap unused LYTEX and return to cold storage.

In 2015, alternative low production volume techniques were investigated including job shop of non-repeat stack components. End plates were found to be an excellent candidate for job shop due to the low volume of parts and status as a low proprietary level component. Details of the end plate processing parameters are shown in Figure 92 and Figure 93.

Annual Production Rate	1,000	10,000	30,000	80,000	100,000	500,000
Equipment Lifetime (years)	15	15	15	15	15	15
Interest Rate	10%	10%	10%	10%	10%	10%
Corporate Income Tax Rate	40%	40%	40%	40%	40%	40%
Capital Recovery Factor	0.175	0.175	0.175	0.175	0.175	0.175
Equipment Installation Factor	1.4	1.4	1.4	1.4	1.4	1.4
Maintenance/Spare Parts (% of CC)	10%	10%	10%	10%	10%	10%
Miscellanous Expenses (% of CC)	12%	12%	12%	12%	12%	12%
Power Consumption (kW)	29	29	60	63	63	68

Figure 92. End plate compression molding process parameters

As seen in Figure 94, the material represents the majority of the end plate costs, ranging from 86% to 96%, depending on the production rate.

Annual Production Rate	1,000	10,000	30,000	80,000	100,000	500,000
Capital Cost ($/line)	$230,074	$230,074	$447,958	$479,084	$479,084	$541,337
Costs per Tooling Set ($)	$25,802	$25,802	$73,942	$79,602	$79,602	$90,438
Tooling Lifetime (cycles)	300,000	300,000	300,000	300,000	300,000	300,000
Simultaneous Lines	1	1	1	1	1	3
Laborers per Line	0.5	0.5	0.5	0.5	0.5	0.5
Cycle Time (s)	310.16	310.16	345.72	350.80	350.80	360.96
Cavities/Platen	2	2	9	10	10	12
Effective Total Machine Rate ($/hr)	$1,253.29	$149.07	$352.55	$170.50	$141.96	$118.45
LYTEX Cost ($/kg)	$30.89	$25.87	$23.77	$22.04	$21.67	$19.14
Job Shop or Manufactured	Job Shop	Job Shop	Job Shop	Manufactured	Manufactured	Manufactured
Job Shop Line Utilization (%)	39.6%	62.7%	56.1%	46.4%	58.0%	82.9%
Job Shop Machine Rate ($/min)	$2.29	$1.64	$2.99	$3.69	$3.08	$2.57
Manufactured Line Utilization (%)	2.6%	25.7%	19.1%	46.4%	58.0%	82.9%
Manufactured Machine Rate ($/min)	$20.89	$2.48	$5.88	$2.84	$2.37	$1.97
Line Utilization Used (%)	39.6%	62.7%	56.1%	46.4%	58.0%	82.9%
Manufacturing Rate Used ($/min)	$2.29	$1.64	$2.99	$2.84	$2.37	$1.97

Figure 93. Machine rate parameters for compression molding process

Annual Production Rate	1,000	10,000	30,000	80,000	100,000	500,000
Material ($/stack)	$7.36	$6.59	$6.52	$6.46	$6.44	$5.83
Manufacturing ($/stack)	$0.15	$0.17	$0.04	$0.04	$0.04	$0.04
Tooling ($/stack)	$0.13	$0.01	$0.01	$0.01	$0.01	$0.01
Secondary Operations ($/stack)	$0.53	$0.53	$0.53	$0.53	$0.53	$0.53
Total Cost ($/stack)	$8	$7	$7	$7	$7	$6
Total Cost ($/kWnet)	$0.10	$0.09	$0.09	$0.09	$0.09	$0.08

Figure 94. Cost breakdown for end plates

8.1.11 Current Collectors

The function of the current collectors is to channel the electrical current that is distributed across the active area of the stack down to the positive and negative terminals. In the SA modeled design, based on the UTC patent (Figure 91) and shown in Figure 95 , two copper current studs protrude through the end plates to connect to a copper sheet in contact with the last bipolar plate.
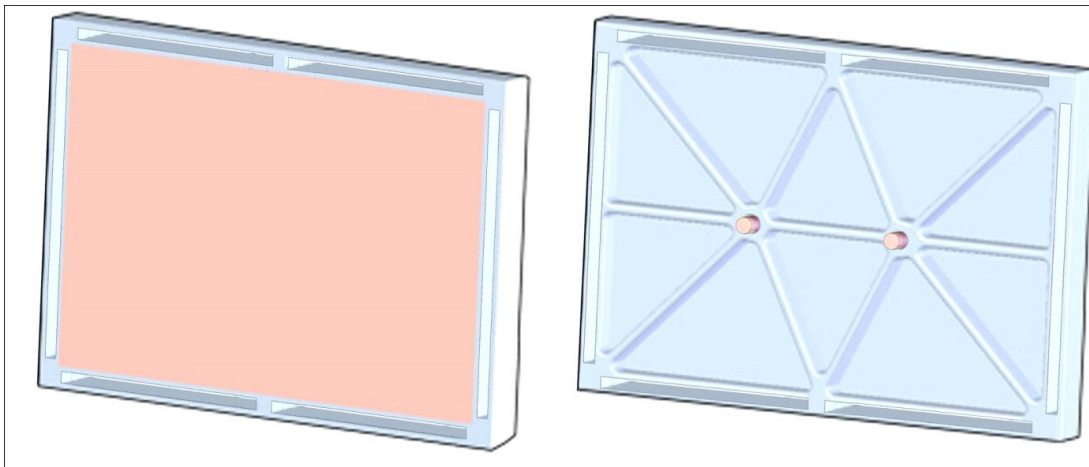
Figure 95. End plate and current collector[74]

---

[74] Some details of the port connections are not shown in the illustration.

The current collectors were designed to fit snugly within the end plate. A shallow (0.3 mm) cavity in the end plate provides room for the 1 mm thick copper sheet, sized to the active area of the cells. The remaining 0.7 mm of the sheet thickness protrudes from the end plate, and the end plate gasket seals around the edges.

The face of the current collector is pressed against the coolant side of the last bipolar plate in the stack. With the compression of the stack, it makes solid electrical contact with the bipolar plate, and thus can collect the current generated by the stack.

The other side of the current collector is flush against the inner face of the end plate. Two copper studs protrude through their corresponding holes in the end plate, where they are brazed to the current collector sheet. On the outside of the end plate, these studs serve as electrical terminals to which power cables may be attached.

Manufacturing the current collectors is a fairly simple process. A roll of 1 mm thick copper sheeting is stamped to size, and 8 mm diameter copper rod is cut to 2.43 cm lengths. The ends of the rods are then brazed to one face of the sheet. At low production (1,000 systems per year), a manual cutting process is used. All other manufacturing rates use an automated process that cuts parts from a roll of copper sheet stock.

Similar to the end plates, current collector cost estimates are based on job shopping to attain a lower cost. Details of current collector processing parameters are shown in Figure 96 and Figure 97. Cost results are shown in Figure 98.

Annual Production Rate	1,000	10,000	30,000	80,000	100,000	500,000
Equipment Lifetime (years)	10	10	15	15	15	15
Interest Rate	10%	10%	10%	10%	10%	10%
Corporate Income Tax Rate	40%	40%	40%	40%	40%	40%
Capital Recovery Factor	0.205	0.205	0.175	0.175	0.175	0.175
Equipment Installation Factor	1.4	1.4	1.4	1.4	1.4	1.4
Maintenance/Spare Parts (% of CC)	13%	13%	13%	13%	13%	13%
Miscellanous Expenses (% of CC)	2%	2%	2%	2%	2%	2%
Power Consumption (kW)	17	17	23	23	23	23

Figure 96. Current collector manufacturing process parameters

Annual Production Rate	1,000	10,000	30,000	80,000	100,000	500,000
Costs per Tooling Set ($)	$1,889	$1,889	$1,889	$1,889	$1,889	$1,889
Tooling Lifetime (cycles)	400,000	400,000	400,000	400,000	400,000	400,000
Capital Cost ($/line)	$35,595	$70,160	$166,573	$166,573	$166,573	$166,573
Simultaneous Lines	1	1	1	1	1	1
Laborers per Line	1.00	1.00	0.25	0.25	0.25	0.25
Line Utilization	0.1%	0.6%	0.4%	1.1%	1.4%	7.1%
Effective Total Machine Rate ($/hr)	$8,111.11	$1,685.56	$4,567.63	$1,728.70	$1,382.03	$287.83
Index Time (s)	3.00	3.00	0.54	0.54	0.54	0.54
Copper Cost ($/kg)	$15.78	$12.92	$11.50	$10.23	$9.94	$7.86
Job Shop or Manufactured	Job Shop	Job Shop	Job Shop	Job Shop	Job Shop	Job Shop
Job Shop Line Utilization (%)	37.1%	37.6%	37.4%	38.1%	38.4%	44.1%
Job Shop Machine Rate ($/min)	$1.29	$1.54	$1.42	$1.40	$1.39	$1.25
Manufactured Line Utilization (%)	0.1%	0.6%	0.4%	1.1%	1.4%	7.1%
Manufactured Machine Rate ($/min)	$135.19	$28.09	$76.13	$28.81	$23.03	$4.80
Line Utilization Used (%)	37.1%	37.6%	37.4%	38.1%	38.4%	44.1%
Manufacturing Rate Used ($/min)	$1.29	$1.54	$1.42	$1.40	$1.39	$1.25

Figure 97. Machine rate parameters for current collector manufacturing process

Annual Production Rate	1,000	10,000	30,000	80,000	100,000	500,000
Material ($/stack)	$7.36	$6.59	$6.52	$6.46	$6.44	$5.83
Manufacturing ($/stack)	$0.15	$0.17	$0.04	$0.04	$0.04	$0.04
Tooling ($/stack)	$0.13	$0.01	$0.01	$0.01	$0.01	$0.01
Secondary Operations ($/stack)	$0.53	$0.53	$0.53	$0.53	$0.53	$0.53
Total Cost ($/stack)	$8	$7	$7	$7	$7	$6
Total Cost ($/kWnet)	$0.10	$0.09	$0.09	$0.09	$0.09	$0.08

Figure 98. Cost breakdown for current collector manufacturing process

8.1.12 Coolant Gaskets/Laser-welding

Coolant gaskets seal between the facing coolant-flow sides of the bipolar plates, around the perimeter of the flow fields, and thus prevent coolant from leaking into the air or hydrogen manifolds. There is a coolant gasket in every repeat unit, plus an extra at the end of the stack. Thus each stack has hundreds of coolant gaskets.

Three methods coolant gaskets methods have been previously analyzed:

- insertion molding to apply the coolant gasket

- screen printing of the coolant gasket

- laser welding

Laser welding of the bipolar plate edges (to eliminate the need of a separate coolant) has been selected for every system analyzed since 2008 and is also selected for the 2015 design.

Laser welding is an option that only applies to use with metallic bipolar plates. The idea of welding two plates together to form a seal is a popular approach in the fuel cell industry, an alternative to injection-molding with potential for increased production rates. Conversations with Richard Trillwood of Electron Beam Engineering of Anaheim, California indicate that grade 316L stainless steel is exceptionally well-

suited to laser welding. Additionally, the thinness of the plates allows welding from the plate face, which is significantly quicker and thus less expensive than edge welding around the perimeter. Figure 99 details key process parameters.

Annual Production Rate	1,000	10,000	30,000	80,000	100,000	500,000
Equipment Lifetime (years)	15	15	15	15	15	15
Interest Rate	10%	10%	10%	10%	10%	10%
Corporate Income Tax Rate	40%	40%	40%	40%	40%	40%
Capital Recovery Factor	0.175	0.175	0.175	0.175	0.175	0.175
Equipment Installation Factor	1.4	1.4	1.4	1.4	1.4	1.4
Maintenance/Spare Parts (% of CC)	10%	10%	10%	10%	10%	10%
Miscellanous Expenses (% of CC)	12%	12%	12%	12%	12%	12%
Power Consumption (kW)	35	35	35	35	35	35

Figure 99. Coolant gasket laser welding process parameters

Laser welding provides a number of distinct advantages compared to traditional gasketing methods. The welds are extremely consistent and repeatable, and do not degrade over time as some gaskets do. It also has extremely low power requirements, and very low maintenance and material costs. Consumables include argon gas, compressed air and a cold water supply. Maintenance involves lamp replacement every three months, lens cleaning, and general machine repair. Trillwood suggests that the welding speed is limited to a range of 60 to 100 inches per minute, with a maximum of three parts being welded simultaneously. However, according to *Manufacturing Engineering & Technology*,[75] laser welding speeds range from 2.5m/min to as high as 80 m/min. A welding speed of 15 m/min (0.25m/s) is selected as a conservative middle value.

Figure 100 shows the machine rate parameters, and Figure 101 shows the cost breakdown.

Annual Production Rate	1,000	10,000	30,000	80,000	100,000	500,000
Capital Cost ($/line)	$450,717	$856,433	$856,433	$856,433	$856,433	$856,433
Gaskets Welded Simultaneously	1	3	3	3	3	3
Runtime per Gasket (sec/gasket)	6.5	2.2	2.2	2.2	2.2	2.2
Simultaneous Lines	1	1	3	6	7	34
Laborers per Line	0.25	0.25	0.25	0.25	0.25	0.25
Line Utilization	20%	68%	68%	90%	97%	99%
Effective Total Machine Rate ($/hr)	$321.55	$189.37	$189.37	$145.56	$136.80	$133.29
Material Cost ($/kg)	$0.00	$0.00	$0.00	$0.00	$0.00	$0.00

Figure 100. Machine rate parameters for gasket laser-welding process

Annual Production Rate	1,000	10,000	30,000	80,000	100,000	500,000
Material ($/stack)	$0	$0	$0	$0	$0	$0
Manufacturing ($/stack)	$219	$43	$43	$33	$31	$30
Tooling ($/stack)	$0	$0	$0	$0	$0	$0
Total Cost ($/stack)	$219	$43	$43	$33	$31	$30
Total Cost ($/kWnet)	$2.74	$0.54	$0.54	$0.41	$0.39	$0.38

Figure 101. Cost breakdown for coolant gasket laser welding

---

[75] *Manufacturing Engineering & Technology*, by Kalpakjian & Schmid (5th edition), p. 957.

8.1.13 End Gaskets

The end gaskets are very similar to the coolant gaskets but are sandwiched between the last bipolar plate and the end plate, rather than between two bipolar plates. This means that welding is not an option, as the end plates are non-metallic. They also have a slightly different geometry than the coolant gaskets, due to their function as a seal against reactant gasses rather than the coolant. Like the coolant gaskets, they were initially modeled using insertion molding, but were switched to a screen printing approach beginning in 2008. The largest difference between coolant gaskets and end gaskets is simply the quantity needed; with only two end gaskets per stack, there are far fewer end gaskets than coolant gaskets. Screen printing of the end gaskets is selected for the 2014 design.

Conversations with DEK International confirmed initial SA assumptions and various screen printers were examined for their efficacy at five production levels. To screen print a seal onto a bipolar plate, a single plate, or a pallet holding several plates, is first fed into the machine by conveyor. Once in the screen printer, it is locked into place and cameras utilize fiducial markers on either the plate itself or the pallet for appropriate alignment. A precision emulsion screen is placed over the plates, allowing a wiper to apply the sealing resin. After application, the resin must be UV cured to ensure adequate sealing.

Two different scenarios were examined in the screen printing process. In the first, one plate would be printed at a time, reducing costs by halving the need for handling robots to align plates. It would also avoid the necessity of a pallet to align multiple plates in the screen printer. The second scenario requires two handling robots to place four plates onto prefabricated self-aligning grooves in a pallet, ensuring proper alignment in the screen printer. The advantage of this technique is reduced cycle time per plate. However, it would result in increased capital costs due to more expensive screen printers, increased necessity for handling robots and precise mass-manufacture of pallets. Small variations in the grooves of pallets would lead to failure of the screen printer to align properly or apply the resin appropriately.

Printers: Three different screen printer models were examined as recommended by representatives from the DEK Corporation. The Horizon 01i machine was suggested for one-plate printing. The Europa VI and the PV-1200 were both evaluated for four plate printing. Comparison of the screen printers can be seen in Figure 102. After cost-analysis, it was determined that, despite the reduced cycle time (12.26 second to 4 seconds), the PV-1200 and Europa VI machines were more expensive, even at higher volumes. The Horizon was cheapest at all production levels.

		Screen Printers (DEK)		
Machine		Horizon	Europa VI	PV-1200
Cycle Time	s	9.63	12.26	4
Cost	$	$150,000	$200,000	$1,000,000
Power Consumption	kW	3.5	3.5	0.7
Print Area	in^2	400	841	841

Figure 102. Screen printer comparison

Resin: The selected resin formula is based upon information gleaned from the Dana Corporation US patent 6,824,874. The patent outlines several resins that would be suitable to provide an effective seal

between bipolar plates and resin "A" was selected for its formulaic simplicity. However, any of the other recommended resins could be substituted with negligible changes in cost and performances.

UV Curing: Following printing, a short conveyor is needed to transfer the printed plate to a UV curing system. Consultation with representatives from UV Fusion Systems Inc. of Gaithersburg, Maryland, along with information from the Dana Corporation resin patent indicated that the VPS 1250 lamp carrying 350 watt type D and type H+ bulbs[76] would be adequate to cure the resin. If it is only necessary to cure a single plate, then one seven inch type D, and one seven inch type H+ bulb should be used. In order to ensure full UV coverage, for a 24 inch pallet holding four plates, three side-by-side ten inch bulbs of both types would be employed.

Patent research indicates that roughly two seconds of exposure for each type of lamp is sufficient for curing. When using the PV-1200 screen printer the curing time for both lamps matches the cycle time for the screen printer. If using the Horizon printer, the cure time is less than half the cycle time for the printer, yet in both situations the plates could be indexed to match the screen printer cycle time. A shutter would be built into the lamp to block each bulb for half of the time the plate is within the system to ensure adequate exposure of both light types. Rapidly turning the bulbs on and off is more destructive to the bulb life than continuous operation, making a shutter the preferred method of alternating light sources.

Cost estimation for UV curing system includes cost of lamps, bulbs, power supply rack, light shield to protect operators, and blowers for both lamp operation and heat reduction.

Maintenance: Communication with DEK has indicated that, if properly cared for, the screen printers have a lifetime of twenty years, but on average are replaced after only eight years due to poor maintenance practices. The modeled lifetime is specified as ten years. Regular maintenance, including machine repair, cleaning, and replacement of screens every 10,000 cycles costs an estimated $10,000 per year.

Utilities: Relatively little power is used by the printers. A belt-drive system that collects and releases parts is the primary power consumer of the screen printers. Additional consumption comes from the alignment system, the wiper blade and the screen controls. Depending on the specifications of the individual printer, power consumption varies from 0.7 to 3.5 kW. On the other hand, the UV curing system has higher power demand. The total power usage, ranging from 61 to 166 kW, is primarily consumed by the lamps, but also by the exhaust blowers and the modular blowers for the lamps.

Figure 103 shows the key process parameters, as selected for the model. The capital cost includes the cost of the screen printer, plus a UV curing system, plate handling robots, and a conveyor belt. Figure 104 shows the assumed machine rate parameters and Figure 105 the cost breakdown. Being a non-repeat component, the end gasket benefits from lower cost when job shopped, like the end plate and current collector. The machine rate table compares the effective machine rates for in-house

---

[76] Type D and Type H+ bulbs refer to the specific light wavelength emitted. Both wavelengths are needed for curing.

manufacture versus job shopping and shows the job shop option to always be less expensive except at 500,000 systems/year.

Annual Production Rate	1,000	10,000	30,000	80,000	100,000	500,000
Equipment Lifetime (years)	15	15	15	15	15	15
Interest Rate	10%	10%	10%	10%	10%	10%
Corporate Income Tax Rate	40%	40%	40%	40%	40%	40%
Capital Recovery Factor	0.175	0.175	0.175	0.175	0.175	0.175
Equipment Installation Factor	1.4	1.4	1.4	1.4	1.4	1.4
Maintenance/Spare Parts (% of CC)	3%	3%	3%	3%	3%	3%
Miscellanous Expenses (% of CC)	12%	12%	12%	12%	12%	12%
Power Consumption (kW)	61	61	61	61	61	61

Figure 103. End gasket screen printing process parameters

Annual Production Rate	1,000	10,000	30,000	80,000	100,000	500,000
Screen Printing Machine Type	DEK Horizon	DEK Horizon	DEK Horizon	DEK Horizon	DEK Horizon	DEK Horizon
Capital Cost ($/line)	$392,735	$392,735	$392,735	$392,735	$392,735	$392,735
Gaskets Printed Simultaneously	1	1	1	1	1	1
Runtime per Gasket (s)	9.62	9.62	9.62	9.62	9.62	9.62
Simultaneous Lines	1	1	1	1	1	1
Laborers per Line	0.25	0.25	0.25	0.25	0.25	0.25
Line Utilization	0.2%	1.6%	4.8%	12.9%	16.2%	80.8%
Effective Total Machine Rate ($/hr)	$28,098	$2,836	$957	$369	$298	$73
Material Cost ($/kg)	$15.19	$15.19	$15.19	$15.19	$15.19	$15.19
Job Shop or Manufactured	Job Shop	Job Shop	Job Shop	Job Shop	Job Shop	Manufactured
Job Shop Line Utilization (%)	37.2%	38.6%	41.8%	49.9%	53.2%	80.8%
Job Shop Machine Rate ($/min)	$3.01	$2.91	$2.71	$2.33	$2.21	$1.57
Manufactured Line Utilization (%)	0.2%	1.6%	4.8%	12.9%	16.2%	80.8%
Manufactured Machine Rate ($/min)	$468.30	$47.26	$15.95	$6.15	$4.97	$1.21
Line Utilization Used (%)	37.2%	38.6%	41.8%	49.9%	53.2%	80.8%
Manufacturing Rate Used ($/min)	$3.01	$2.91	$2.71	$2.33	$2.21	$1.21

Figure 104. Machine rate parameters for end gasket screen printing process

Annual Production Rate	1,000	10,000	30,000	80,000	100,000	500,000
Material ($/stack)	$0.08	$0.08	$0.08	$0.08	$0.08	$0.08
Manufacturing ($/stack)	$0.98	$0.95	$0.88	$0.76	$0.72	$0.39
Tooling ($/stack)	$0.00	$0.00	$0.00	$0.00	$0.00	$0.00
Total Cost ($/stack)	$1.06	$1.02	$0.96	$0.83	$0.80	$0.47
Total Cost ($/kWnet)	$0.01	$0.01	$0.01	$0.01	$0.01	$0.01

Figure 105. Cost breakdown for end gasket screen printing

8.1.14 Stack Compression

Traditional PEM fuel cells use tie-rods, nuts and Belleville washers to supply axial compressive force to ensure fluid sealing and adequate electrical connectivity. However, the use of metallic compression bands is assumed, as used by Ballard Power Systems and described in US Patent 5,993,987 (Figure 106). Two stainless steel bands of 2 cm width are wrapped axially around the stack and tightened to a pre-determined stack compressive loading, and then the ends of the bands are tack welded to each other. The end plates' low conductivity allows them to act as insulators, to prevent shorting of the stack. Custom recesses in the end plates are used to provide a convenient access to the lower surface of the bands to enable welding. The edges of the bipolar plates do not contact the compressive bands. The costs are reported as part of the stack assembly section, as shown in Figure 110.
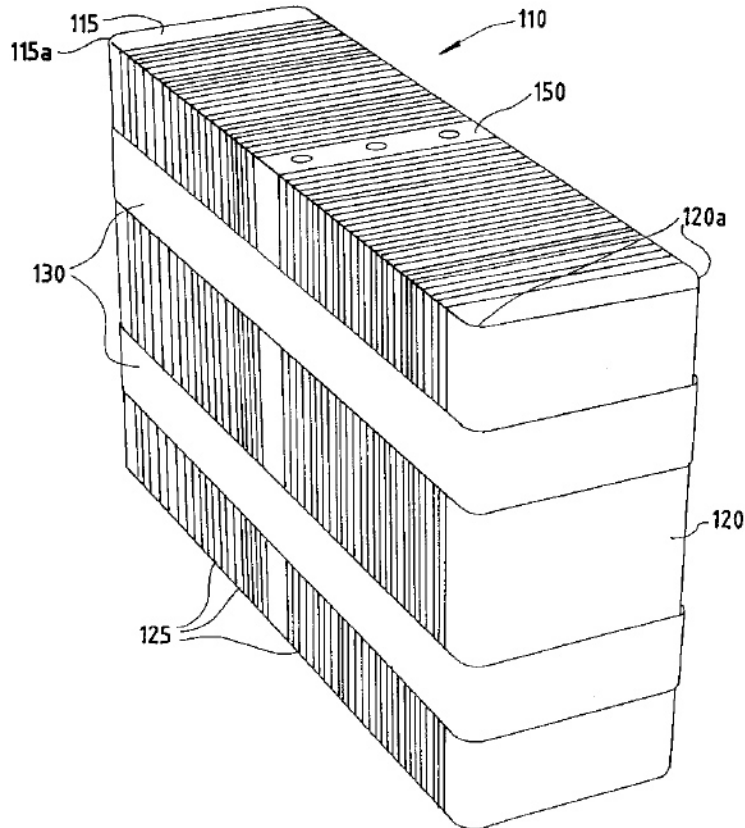
Figure 106. Stack compression bands concept (Figure courtesy of US patent 5,993,987)

8.1.15 Stack Assembly

Stack assembly costs were based on the amortized workstation costs and the estimated times to perform the required actions. Two methods of stack assembly were analyzed: manual and semi-automated.

At the lowest production rate of 1,000 systems per year, manual assembly was selected. Manual assembly consists of workers using their hands to individually acquire and place each element of the stack: end plate, insulator, current collector, bipolar plate, gasketed MEA, bipolar plate, and so on. An entire stack is assembled at a single workstation. The worker sequentially builds the stack (vertically) and then binds the cells with metallic compression bands. The finished stacks are removed from the workstation by conveyor belt.

At higher production levels, stack assembly is semi-automatic, requiring less time and labor and ensuring superior quality control. This is termed "semi-automatic" because the end components (end plates, current conductors, and initial cells) are assembled manually but the ~378 active cell repeat units are assembled via automated fixture. Figure 107 details the layout of the assembly workstations and Figure 108 and Figure 109 list additional processing parameters.

Station 1: Assembly of stack repeat cells

Robotic assembly of stack repeat parts
Index Time: 6 seconds
Each carousel produces a "core stack" of
372 repeat cells every 18.65 minutes
=> 2 carousels working in unison
produce a "core stack" every 9.32 minutes

Cathode Plate Load
Anode Plate Load
Work Carriers
MEA Load
Rotating Carousels
MEA Load
Work Carriers
Cathode Plate Load
Anode Plate Load

Assembly Station Tender/Operator

372 rotations of carousel produces "core stack" of 372 repeat cells

Current Collectors
End Plates
Assembly Station Tender/Operator
Compression Bands
Stack Compression Device
Manual Assembly Station
Assembled Stack Storage

Station 2: Final stack assembly

Manual final stack assembly
Assembly work adds components
to each end of the "core stacks"
and attaches compression bands
to complete stack assembly

Figure 107. Semi-automated stack assembly work flow diagram

Following assembly, each stack is transported to a leak-check station where the three sets of fluid channels (hydrogen, air, and coolant) are individually pressurized with gas and monitored for leaks. This test is very brief and meant only to verify gas and liquid sealing. Full performance testing of the stack will occur during stack conditioning.

As shown in Figure 110, stack assembly is quite inexpensive, ranging from $0.98/kW_{net} at the most to only $0.41/kW_{net}. The only material costs are those of the compressive metal bands.

Annual Production Rate	1,000	10,000	30,000	80,000	100,000	500,000
Equipment Lifetime (years)	5	15	15	15	15	15
Interest Rate	10%	10%	10%	10%	10%	10%
Corporate Income Tax Rate	40%	40%	40%	40%	40%	40%
Capital Recovery Factor	0.306	0.175	0.175	0.175	0.175	0.175
Equipment Installation Factor	1.4	1.4	1.4	1.4	1.4	1.4
Maintenance/Spare Parts (% of CC)	10%	10%	10%	10%	10%	10%
Miscellanous Expenses (% of CC)	7%	7%	7%	7%	7%	7%
Power Consumption (kW)	1	7	7	7	7	7

Figure 108. Stack assembly process parameters

114

Annual Production Rate	1,000	10,000	30,000	80,000	100,000	500,000
Assembly Method	Manual	Semi-Auto	Semi-Auto	Semi-Auto	Semi-Auto	Semi-Auto
Capital Cost ($/line)	$11,212	$821,339	$821,339	$821,339	$821,339	$821,339
Simultaneous Lines	1	2	4	9	11	52
Laborers per Line	1.00	0.25	0.25	0.25	0.25	0.25
Line Utilization	48.8%	51.7%	77.4%	91.8%	93.8%	99.3%
Effective Total Machine Rate ($/hr)	$48.98	$175.04	$120.79	$103.78	$101.74	$96.85
Index Time (min)	98	21	21	21	21	21

Figure 109. Machine rate parameters for stack assembly process

Annual Production Rate	1,000	10,000	30,000	80,000	100,000	500,000
Compression Bands ($/stack)	$0	$0	$0	$0	$0	$0
Assembly ($/stack)	$80	$61	$42	$36	$35	$34
Total Cost ($/stack)	$80	$61	$42	$36	$35	$34
Total Cost ($/kWnet)	$1.00	$0.76	$0.52	$0.45	$0.44	$0.42

Figure 110. Cost breakdown for stack assembly

8.1.16 Stack Housing

The stack insulation housing is a plastic housing that encases the stack. It is meant primarily for protection from physical damage caused by road debris and liquids, as well as for protection from electrical shorting contacts and a small amount of thermal insulation. It is modeled as vacuum-thermoformed polypropylene. It is 0.5 cm thick, and is separated from the stack by a 1 cm gap. At high production rate, the cycle time is seven seconds: three for insertion, and four for the vacuum thermoforming. Processing parameters are shown in Figure 111 and Figure 112. A cost breakdown of the stack housing production is shown below in Figure 113.

Annual Production Rate	1,000	10,000	30,000	80,000	100,000	500,000
Equipment Lifetime (years)	8	8	8	15	15	15
Interest Rate	10%	10%	10%	10%	10%	10%
Corporate Income Tax Rate	40%	40%	40%	40%	40%	40%
Capital Recovery Factor	0.229	0.229	0.229	0.175	0.175	0.175
Equipment Installation Factor	1.4	1.4	1.4	1.4	1.4	1.4
Maintenance/Spare Parts (% of CC)	5%	5%	5%	5%	5%	5%
Miscellanous Expenses (% of CC)	6%	6%	6%	6%	6%	6%
Power Consumption (kW)	30	30	30	35	35	40

Figure 111. Stack housing vacuum thermoforming process parameters

Annual Production Rate	1,000	10,000	30,000	80,000	100,000	500,000
Capital Cost ($/line)	$50,000	$50,000	$50,000	$250,000	$250,000	$655,717
Costs per Tooling Set ($)	$96,352	$96,352	$96,352	$96,352	$96,352	$96,352
Tooling Lifetime (years)	3	3	3	3	3	3
Cavities per platen	1	1	1	1	1	1
Total Cycle Times (s)	71	71	71	15	15	7
Simultaneous Lines	1	1	1	1	1	1
Laborers per Line	1.00	1.00	1.00	1.00	1.00	0.25
Line Utilization	0.6%	5.9%	17.7%	10.1%	12.6%	28.9%
Effective Total Machine Rate ($/hr)	$1,136.85	$156.88	$84.29	$310.80	$258.32	$253.68
Material Cost ($/kg)	$1.48	$1.48	$1.48	$1.48	$1.48	$1.48

Figure 112. Machine rate parameters for stack housing vacuum thermoforming process

Annual Production Rate	1,000	10,000	30,000	80,000	100,000	500,000
Material ($/stack)	$5	$5	$5	$5	$5	$5
Manufacturing ($/stack)	$22	$3	$2	$1	$1	$0
Tooling ($/stack)	$36	$4	$1	$0	$0	$0
Total Cost ($/stack)	$64	$12	$8	$7	$7	$6
Total Cost ($/kWnet)	$0.80	$0.15	$0.10	$0.09	$0.08	$0.07

Figure 113. Cost breakdown for stack housing

8.1.17 Stack Conditioning and Testing

PEM fuel cell stacks have been observed to perform better in polarization tests if they first undergo "stack conditioning." Consequently, a series of conditioning steps are modeled based on a regulation scheme discussed in GM Global Technology Operations LLC's (subsidiary of General Motors (GM)) US patent 9,099,703 B2.[77] The GM patent describes voltage variation (current cycling), a fuel/oxidant stoichiometry, and temperature for conditioning. The conditioning would occur immediately after stack assembly at the factory. Because the conditioning process finishes with a final performance verification, the conditioning process also serves a stack quality control purpose and no further system checkout is required.

Figure 114 details the stack conditioning steps. The GM patent states that while prior-art conditioning times were 1-15 hours, the GM accelerated break-in methodology is able to achieve 70% of the performance benefit in 1.5 hours (with expectation of achieving 100% performance after additional hours). Two hours of conditioning time is selected for cost modeling.

---

[77] US Patent 9,099,703 B2, Rapaport et. al., "Fast MEA Break-In and Voltage Recovery", August 4, 2015.

Step	Description	H$_2$ Stoic.	Air Stoic.	Temp(°C)	Voltage (V)	Current Density (A/cm^2)
1	Shorting check (prior to voltage cycling)					
2	Room temp voltage cycling: Once voltage stops increasing, move to step 3, otherwise repeat step 2.	1.5	1.1	22	0.1-0.4	0.1-0.2
3	35°C voltage cycling: Once voltage stops increasing, move to step 4, otherwise repeat step 3.	1.5	1.1	35	0.1-0.4	0.2-0.3
4	50°C voltage cycling: Once voltage stops increasing, move to step 5, otherwise repeat step 4.	1.5	1.1	50	0.1-0.4	0.3-0.4
5	65°C voltage cycling: Once voltage stops increasing, move to step 6, otherwise repeat step 5.	1.5	1.1	65	0.1-0.4	0.4-0.5
6	80°C voltage cycling: Once voltage stops increasing, move to step 7, otherwise repeat step 6.	1.5	1.1	80	0.1-0.4	0.5-0.7
7	95°C voltage cycling: Once voltage stops increasing, move to step 8, otherwise repeat step 7.	1.5	1.1	95	0.1-0.4	0.7-0.85
8	Performance verification: If performance level adequate, move to step 9, otherwise, repeat step 7 and 8.					
9	H2 Take-over test: confirm absence of cross-over leaks after voltage cycling					

Figure 114. Stack conditioning process based on US patent 9,099,703 B2 ("Fast MEA Break-In and Voltage Recovery")

Conditioning cost is based on proprietary capital cost quotation of a programmable load bank to run the stacks up and down the polarization curve according to the power-conditioning regimen. The fuel cells load banks are assumed to condition two stacks simultaneously (between 30k and 100k systems per year production) and eight stacks simultaneously at 500k systems per year. Since the stacks can be staggered in starting time, peak power can be considerably less than 2 or 8 times the individual stack rated power of ~88.2 kW$_{gross}$. It is estimated that simultaneous peak power would be approximately 270 kW at 500,000 fuel cell systems per year. Hydrogen usage is estimated based on 50% fuel cell efficiency and $3/kg hydrogen. SA's standard machine rate methodology yields machine rates as low as $0.28/min for each load bank. Process parameters are shown in Figure 115 and Figure 116. Total costs for stack conditioning are shown in Figure 117. Note that considerable power is generated, and rather than dumping the load to a resistor bank, it may be advantageous to sell the electricity back to the grid. This would require considerable electrical infrastructure and is expected to provide only a relatively small benefit; sale of electricity to the grid is not included in our cost estimates.

Annual Production Rate	1,000	10,000	30,000	80,000	100,000	500,000
Equipment Lifetime (years)	19	19	19	19	19	19
Interest Rate	10%	10%	10%	10%	10%	10%
Corporate Income Tax Rate	40%	40%	40%	40%	40%	40%
Capital Recovery Factor	0.159	0.159	0.159	0.159	0.159	0.159
Equipment Installation Factor	1.4	1.4	1.4	1.4	1.4	1.4
Maintenance/Spare Parts (% of CC)	10%	10%	10%	10%	10%	10%
Miscellanous Expenses (% of CC)	7%	7%	7%	7%	7%	7%
Power Consumption (kW)	2	2	2	2	2	9

Figure 115. Stack conditioning process parameters

Annual Production Rate	1,000	10,000	30,000	80,000	100,000	500,000
Capital Cost ($/line)			Proprietary			
Simultaneous Lines	1	2	6	14	18	22
Laborers per Line	0.1	0.1	0.1	0.1	0.1	0.1
Line Utilization	99.2%	86.8%	86.8%	99.2%	96.5%	98.6%
Effective Total Machine Rate ($/hr)	$30.21	$17.88	$17.74	$16.26	$16.52	$51.41
Test Duration (hrs)	2	2	2	2	2	2

Figure 116. Machine rate parameters for stack conditioning process

Annual Production Rate	1,000	10,000	30,000	80,000	100,000	500,000
Conditioning/Testing ($/stack)	$60	$18	$18	$16	$17	$13
Total Cost ($/stack)	$60	$18	$18	$16	$17	$13
Total Cost ($/kWnet)	$0.76	$0.22	$0.22	$0.20	$0.21	$0.16

Figure 117. Cost breakdown for stack conditioning

8.2 Balance of Plant (BOP)

While the stack is the heart of the fuel cell system, many other components are necessary to create a functioning system. In general, our cost analysis utilizes a DFMA[TM]-style analysis methodology for the stack but a less detailed methodology for the balance of plant (BOP) components. Each of the BOP components is discussed below along with its corresponding cost basis.

8.2.1 Air Loop

The air loop of the fuel cell power system consists of five elements:

- Air Compressor, Expander and Motor (CEM) Unit
- Air Mass Flow Sensor
- Air Filter and Housing
- Air Ducting

These components are described in the subsections below. The cost breakdown is show below in Figure 118.

118

Annual Production Rate	1,000	10,000	30,000	80,000	100,000	500,000
Filter and Housing ($/system)	$56	$56	$56	$56	$56	$56
Compressor, Expander & Motor ($/system)	$1,627	$1,223	$932	$799	$775	$753
Mass Flow Sensor ($/system)	$21	$19	$17	$13	$12	$10
Air Ducting ($/system)	$136	$132	$130	$124	$118	$112
Air Temperature Sensor ($/system)	$10	$9	$8	$6	$6	$5
Total Cost ($/system)	$1,850	$1,438	$1,143	$998	$966	$936
Total Cost ($/kW$_{net}$)	$23.13	$17.98	$14.29	$12.47	$12.08	$11.69

Figure 118. Cost breakdown for air loop

8.2.1.1   *Compressor-Expander-Motor Unit & Motor Controller*

The air compression system is envisioned as an integrated air compressor, exhaust gas expander, and permanent magnet motor. An electronic CEM controller is also included in the system. For the 2015 system analysis, the CEM is based on a Honeywell design for a high rpm, centrifugal compressor, radial inflow expander integrated unit.

In the 2008 and prior year system cost analyses, the fuel cell CEM unit was based on a multi-lobe compressor and expander from Opcon Autorotor of Sweden with cost based on a simplified DFMA^{TM} analysis in which the system was broken into seven cost elements: wheels/lobes, motor, controller, case, bearings, variable geometry, and assembly/test.

For the 2009 analysis, an all-new, extremely detailed CEM cost estimate was conducted in collaboration with Honeywell. It is a bottom-up cost analysis based directly on the blueprints from an existing Honeywell design, which pairs a centrifugal compressor and a radial-inflow expander, with a permanent-magnet motor running on air bearings at 100,000 rpm. After analyzing the base design, engineers from both SA and Honeywell simplified and improved the design to increase its performance and lower cost, to better-reflect a mass-production design. Ultimately, six different configurations were examined; three main configurations, plus a version of each without an expander.

The six different configurations examined are listed in Figure 119. "Design #1" is based on an existing Honeywell design, which runs at 100,000 rpm. Design #2 is an optimized version of Design #1 running at 165,000 rpm, in order to reduce its size. Design #3 is a further-optimized future system, based on Design #2 but with slightly more aggressive design assumptions. Designs #4, 5, and 6 are identical to Designs #1, 2, and 3 respectively, but with the expander removed.

	Baseline: 100k rpm	Current: 165k rpm	Future: 165k rpm
With Expander	Design 1	Design 2 (2015 cost estimate)	Design 3
Without Expander	Design 4	Design 5	Design 6

Figure 119. Matrix of CEM design configurations

The cost estimate utilizes a combination of DFMA^{TM} methodology and price quotes from established Honeywell vendors. Excluding repeat parts, the existing Honeywell turbocompressor design (Design #1) has 104 different components and assemblies. Each of these components is categorized into one of three different tiers. "Tier 1" consists of the 26 largest/most-significant components in need of the most careful cost analysis. "Tier 2" corresponds to the 42 mid-level components for which a vendor quote is sufficient. The "Tier 3" components are the minor components such as screws and adhesives that are insignificant enough that educated guesses are sufficient in lieu of vendor quotes. Honeywell engineers solicited price quotes from their existing supplier base for components in the top two tiers, as well as for some of the components in Tier 3, and supplied these values to SA for review and analysis.

In some cases, the high-volume quotes were judged to be inappropriate, as they were merely based on repeated use of low-production-rate manufacturing methods rather than low-cost, high-manufacturing-rate production and assembly methods. Consequently, these quotes were replaced with cost estimates based on a mix of DFMA^{TM} techniques and our best judgment.

After having completed the initial cost summation for Design #1, the unit costs seemed prohibitively high. Consequently, Honeywell engineers reviewed their design and created a list of potential improvements. SA augmented the list with some DFMA^{TM}-based suggestions, the list was vetted by both parties, and the design changes incorporated into the cost model. Changes deemed reasonable to describe as "current technology" were applied to Design #2, and the more aggressive improvements were used to define Design #3. The most important of these improvements is the switch from 100,000 to 165,000 rpm, which facilitates a reduction in the size of the CEM by roughly 35%, thereby saving greatly on material (and to a lesser extent, manufacturing) costs, while also providing the intrinsic benefits of reduced size. These improvements are listed in Figure 120, showing that Design #2 is used for the 2015 cost estimate.

Each of the six CEM designs was analyzed across the range of five production rates (1,000 to 500,000 systems per year): this yields 30 different cost estimates for each of the 100+ components. Summed together, they provide 30 different estimates for the CEM cost. The five Design #2 estimates provide the compressor costs across the range of production rates.

For the 2010 update, the CEM cost model was fully integrated into the fuel cell system cost model, and adjusted to scale dynamically based on the pressure and power requirements of the system. This was achieved via a complex system of multipliers that are applied differently for almost every different component, since there are a wide variety of combinations and permutations for costing methods across the range of components, and not everything scales at the same rate. For example, as the pressure ratio increases and the CEM increases in size, the diameter of the turbine wheel increases, and its volume increases at a rate proportional to the square of its diameter. The diameter of the compressor wheel scales at a different rate than that of the turbine (expander) wheel, and the shaft length and motor mass each scale at yet another rate. The geometric scaling factors were derived from data that Honeywell provided showing dimensions of key components across a range of performance parameters such as pressure ratio, mass flow rate, and shaft power.

	2015 Cost Estimate				
Design #	**1**	**2**	**3**	**4**	**5**	**6**
	With Expander			**Without Expander**		
	Baseline (100k rpm)	**Current (165k rpm)**	**Future (165k rpm)**	**Baseline (100k rpm)**	**Current (165k rpm)**	**Future (165k rpm)**
Removed Turbine (Expander)				x	x	x
Increased speed from 100,000 to 165,000 rpm		x	x		x	x
Improved turbine wheel design		x	x		x	x
Improved variable nozzle technology		x	x		x	x
Lower cost electrical connectors		x	x		x	x
Design change to integrate housing into single casting	[Baseline System Design]		x			x
Integrate/eliminate mounting bosses on main housing			x			x
compressor housing design change to re-route cooling air over motor			x			x
Improved foil bearing design			x			x
Back-to-back compressor wheel			x			x
Removed washers/face bolts			x			x
Improved bearing installation/design			x			x
Impreoved labryinth seal			x			x
Changed fasterns to more common, inexpensive design			x			x
Changed threaded inserts to more common, inexpensive design			x			x
Reduced testing of machine/cast parts			x			x
Aluminum turbine wheel			x			x

Figure 120. List of Improvements for the 6 compressor configurations

The materials cost of each component increases proportionately with the volume of material needed, and the manufacturing costs scale separately, at rates dependent on the manufacturing processes involved and the specifics of each process.

For components whose cost estimates are derived partially or completely from price quotes rather than full DFMA[TM] analysis (such as those in Tier 2 and Tier 3), assumptions were made about the fractional split between the component's material and manufacturing costs, so that each fraction can be scaled independently.

With this new scaling and integration into the main fuel cell system cost model, the size and cost of the CEM now scale dynamically based on the performance requirements of the system. So if a new electrical component is added to the BOP that increases the parasitic load (and thus increases the gross power required), the CEM will automatically scale to accommodate.

The SA/Honeywell CEM analysis also examined the motor controller, for which the same design was deemed applicable to control all six compressor designs. Unlike with the custom parts involved in the

compressor, the motor controller uses almost exclusively off-the-shelf parts that are already manufactured at high volume. As such, there is limited value in conducting a detailed DFMA^{TM} analysis, so the cost analysis is primarily based on vendor quotation. The original Honeywell controller design was a standalone unit with its own air or water cooling. However, in order to cut costs, it is now assumed that the CEM controller is integrated into the water-cooled electronics housing for the overall fuel cell system controller. Thirty percent of the controller base cost is assumed to correspond to logic functions, with the remaining 70% corresponding to power management. Accordingly, to scale the controller cost for different input powers (as is necessary when varying stack operating parameters to determine the lowest possible system cost), the 30% of the baseline controller cost (i.e. the portion for logic circuitry) is held at a constant cost, the remaining 70% of baseline cost (i.e. the portion for power management) is assumed to scale linearly with input power.

The CEM and motor controller costs for the various configurations are shown below in Figure 121 for the various 2015 system CEM options. Design 2 is selected for the 2015 cost analysis. Note that the costs at 10k and 30k systems per year are reported as identical values. This is a slight inaccuracy based on not scaling the 10k/year cost estimates.

8.2.1.2   Air Mass Flow Sensor
A high-performance (~2% signal error) automotive hot-wire mass flow sensor is used for measuring the air flow rate into the fuel cell system. Since these devices are already produced in very high quantities, little change in cost is expected between high and low production rates.

8.2.1.3   Air Ducting
The air ducting is modeled as conformal polymer tubes to guide the cathode air in and out of the stack.

8.2.1.4   Air Filter and Housing
Some fuel cell manufacturers filter inlet air both for particles and for volatile organic compounds. However, while particle filters are needed, it is not clear that VOC filters are necessary. Consequently, a standard automotive air particle filter and polymer filter housing are assumed.

Design	Sys/yr	2015 CEM Cost	Assy	Markup	2015 Motor Controller Cost	Assy	Markup	2015 Total Cost
Design #1 Baseline Tech. 100,000 RPM	1,000	$1,310.93	$23.00	15%	$484.72	$7.67	10%	$2,075.64
	10,000	$580.47			$403.15			$1,145.89
	30,000	$580.47			$403.15			$1,145.89
	80,000	$453.63			$389.91			$985.46
	100,000	$446.24			$372.48			$957.79
	500,000	$434.93			$359.63			$930.64
Design #2 Current Tech. 165,000 RPM	1,000	$921.12	$23.00	15%	$484.72	$7.67	10%	$1,627.36
	10,000	$394.61			$403.15			$932.15
	30,000	$394.61			$403.15			$932.15
	80,000	$291.80			$389.91			$799.35
	100,000	$287.02			$372.48			$774.69
	500,000	$280.05			$359.63			$752.54
Design #3 Future Tech. 100,000 RPM	1,000	$782.00	$23.00	15%	$484.72	$7.67	10%	$1,467.37
	10,000	$344.44			$403.15			$874.46
	30,000	$344.44			$403.15			$874.46
	80,000	$249.54			$389.91			$750.75
	100,000	$245.39			$372.48			$726.81
	500,000	$239.31			$359.63			$705.68
Design #4 Baseline Tech. 100,000 RPM No Expander	1,000	$950.59	$23.00	15%	$484.72	$7.67	10%	$1,661.25
	10,000	$385.81			$403.15			$922.03
	30,000	$385.81			$403.15			$922.03
	80,000	$270.28			$389.91			$774.61
	100,000	$266.45			$372.48			$751.03
	500,000	$261.14			$359.63			$730.79
Design #5 Current Tech. 165,000 RPM No Expander	1,000	$758.85	$23.00	15%	$484.72	$7.67	10%	$1,440.75
	10,000	$287.09			$403.15			$808.51
	30,000	$287.09			$403.15			$808.51
	80,000	$190.46			$389.91			$682.81
	100,000	$187.73			$372.48			$660.49
	500,000	$183.63			$359.63			$641.65
Design #6 Future Tech. 100,000 RPM No Expander	1,000	$633.40	$23.00	15%	$484.72	$7.67	10%	$1,296.49
	10,000	$249.15			$403.15			$764.87
	30,000	$249.15			$403.15			$764.87
	80,000	$160.08			$389.91			$647.88
	100,000	$157.90			$372.48			$626.19
	500,000	$154.58			$359.63			$608.24

Figure 121. CEM cost results

8.2.2   Humidifier & Water Recovery Loop

The humidifier and water recovery loop consists of three components:

- Air precooler
- Demister
- Humidifier

Total subsystem cost is shown in Figure 122. Further details of each subsystem component appear below.

Annual Production Rate	1,000	10,000	30,000	80,000	100,000	500,000
Air Precooler ($/system)	$35	$35	$35	$35	$35	$35
Demister ($/system)	$119	$22	$13	$9	$8	$6
Membrane Air Humidifier ($/system)	$1,055	$242	$133	$103	$94	$66
Total Cost ($/system)	$1,209	$298	$181	$147	$137	$107
Total Cost ($/kW$_{net}$)	$15.11	$3.72	$2.26	$1.83	$1.71	$1.33

Figure 122. Cost breakdown for humidifier & water recovery loop

8.2.2.1 Air Precooler

The air precooler sits between the air compressor and the membrane humidifier, where it cools the hot compressed air to the humidifier's optimal inlet temperature. The design is based on the ANL-supplied key parameters for a compact liquid/air cross-flow intercooler, and the dimensions are scaled based on the specific heat transfer requirements. The unit is 100% aluminum and uses an array of 0.4-mm-thick tubes with 0.08-mm-thick fins spaced at 24 fins per inch, which cool the air with a very minimal pressure drop (0.1 psi). Because the cost impact of the precooler is small, a full DFMA^{TM} analysis was not conducted. Instead, the mass and volume of the radiator core were determined by heat transfer calculations conducted at ANL, and the materials cost of the unit was estimated based on detailed geometry assumptions and the cost of aluminum ($6.82/kg). The materials cost was then simply doubled to account for the cost of manufacturing. As a result of this simplified costing methodology, air precooler cost does not vary with annual production rate. Air precooler cost is detailed in Figure 123.

Annual Production Rate	1,000	10,000	30,000	80,000	100,000	500,000
Material ($/system)	$17	$17	$17	$17	$17	$17
Manufacturing ($/system)	$17	$17	$17	$17	$17	$17
Total Cost ($/system)	$35	$35	$35	$35	$35	$35
Total Cost ($/kWnet)	$0.43	$0.43	$0.43	$0.43	$0.43	$0.43

Figure 123. Cost breakdown for air precooler

8.2.2.2 Demister

The demister removes liquid water droplets from the cathode exhaust stream and thereby prevents erosion of the turbine blades. Designed by SA, the demister's housing consists of two threaded, hollow 2-mm-thick polypropylene frustums that unscrew from one another to allow access to the filter inside. The filter is a nylon mesh Millipore product designed for water removal and cost $5.84 each at high volume (assuming 81 cm^2 per demister). The polypropylene adds only ~10 cents of material cost per part, and at high volume, the injection molding process is only 15 cents per part. Because the housing is so inexpensive, the filter dominates the total demister cost ($6.30/demister, or $0.08/kW$_{net}$ at 500,000 systems per year).

Figure 124 and Figure 125 show demister processing parameters. Figure 126 details demister cost results.

Annual Production Rate	1,000	10,000	30,000	80,000	100,000	500,000
Equipment Lifetime (years)	15	15	15	15	15	15
Interest Rate	10%	10%	10%	10%	10%	10%
Corporate Income Tax Rate	40%	40%	40%	40%	40%	40%
Capital Recovery Factor	0.175	0.175	0.175	0.175	0.175	0.175
Equipment Installation Factor	1.4	1.4	1.4	1.4	1.4	1.4
Maintenance/Spare Parts (% of CC)	5%	5%	5%	5%	5%	5%
Miscellanous Expenses (% of CC)	6%	6%	6%	6%	6%	6%
Power Consumption (kW)	21	21	21	21	21	21

Figure 124. Demister injection molding process parameters

Annual Production Rate	1,000	10,000	30,000	80,000	100,000	500,000
Capital Cost ($/line)	$288,522	$288,522	$288,522	$288,522	$288,522	$288,522
Costs per Tooling Set ($)	$16,193	$16,193	$16,193	$16,193	$16,193	$16,193
Tooling Lifetime (cycles)	1,000,000	1,000,000	1,000,000	1,000,000	1,000,000	1,000,000
Cavities per platen	1	1	1	1	1	1
Total Cycle Time (s)	6	6	6	6	6	6
Simultaneous Lines	1	1	1	1	1	1
Laborers per Line	0.50	0.50	0.50	0.50	0.50	0.50
Line Utilization	0.1%	0.6%	1.6%	4.3%	5.4%	26.5%
Effective Total Machine Rate ($/hr)	$27,124.97	$5,219.18	$1,895.87	$756.53	$616.26	$162.10
Material Cost ($/kg)	$1.33	$1.33	$1.33	$1.33	$1.33	$1.33

Figure 125. Machine rate parameters for demister injection molding process

Annual Production Rate	1,000	10,000	30,000	80,000	100,000	500,000
Material ($/system)	$12	$11	$10	$7	$7	$6
Manufacturing ($/system)	$102	$10	$3	$1	$1	$0
Tooling ($/system)	$4	$0	$0	$0	$0	$0
Total Cost ($/system)	$119	$22	$13	$9	$8	$6
Total Cost ($/kWnet)	$1.49	$0.27	$0.17	$0.11	$0.10	$0.08

Figure 126. Cost breakdown for demister

8.2.2.3 Membrane Humidifier

The 2012 and prior year cost analyses were based on a tubular membrane design from Perma Pure LLC (model FC200-780-7PP) as shown in Figure 127.
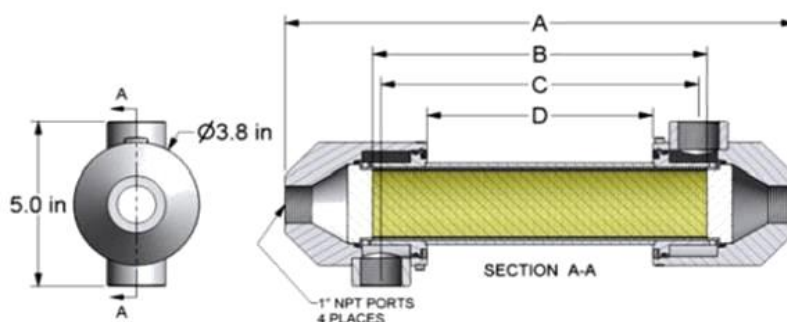
Figure 127. Perma Pure FC200-780-7PP humidifier

In 2013, the plate frame air humidifier was examined as a potentially lower cost and smaller volume alternative to the previously modeled tubular membrane humidifier. Compared to tubular membrane designs, the plate frame membrane humidifiers allow a thinner membrane (5 microns) to be used. Since membrane thickness correlates with required membrane area for a given amount of water transport, plate frame humidifiers are expected to be more compact and lower cost than tubular humidifiers.

The design and projected manufacturing methods for the 2013 plate frame humidifier are based on publicly available information from W.L Gore & Associates, Inc. and DPoint Technologies Inc.[78] Both companies were consulted and provided input during the cost analysis process but information transfer was entirely public domain and non-proprietary. The resulting design is thus a Strategic Analysis Inc. interpretation of the Gore/DPoint Technologies unit, and may differ in design and manufacturing process from the actual unit. However, it is expected that the key cost influencing aspects have been adequately captured in the cost analysis.

The modeled Gore plate frame humidifier design is composed of multiple stacked cell pouches made of a 4-layer composite membrane with stainless steel flow fields inside the pouch and stainless steel rib spacers between each pouch in the stack. The total process consists of eight steps:

1. Fabrication of Composite Membranes
2. Fabrication of Stainless Steel Flow Fields and Separators
3. Pouch Formation
4. Stainless Steel Rib Formation
5. Stack Formation
6. Formation of the Housing
7. Assembly of the Composite Membrane and Flow Fields into the Housing
8. System Testing

---

[78] Johnson, William B. "Materials and Modules for Low-Cost, High Performance Fuel Cell Humidifiers," W.L. Gore & Associates, Inc., presentation at the 2012 DOE Hydrogen and Fuel Cell Program Annual Merit Review, Washington, DC, 17 May 2012.

The cost for the membrane humidifier is estimated to be about $66 for a 58-cell pouch stack (sized for an 80-kWe automotive fuel cell system operating at 1.5 air stoichiometry) including housing, assembly, and testing at 500,000 systems per year. Over 50% of the total cost is attributed to materials, primarily the composite membrane.

2015 cost results are based on a humidifier containing 1.15 m^2 of membrane area (0.92m^2 x 1.25 oversizing for degradation) based on ANL modeling analysis for membrane water transport at the 2015 fuel cell operating conditions. Much discussion surrounded selection of this membrane area.

Past analysis has sought to reconcile various estimates of required humidifier membrane area. Separately funded experimental testing was conducted at Ford on the Gore/DPoint humidifier and showed very good correlation with ANL modeling predictions.[79] Both experimental and modeling results showed that ~2m^2 of humidifier membrane area was required for an 80kWe fuel cell system at the 2013 DOE specified operating conditions. However, when ANL applied their performance model at the 2013 SA/ANL specified system operating conditions, the required membrane area dropped to 0.5m^2. This significant membrane area reduction was due primary to higher pressure, lower air flow, and higher temperature conditions included in the model. Additionally, Gore raised a concern that membrane performance degradation was not factored into any of the modeled estimates. Consequently, in 2013 a value of 1.6m^2 humidifier membrane area was selected for SA cost modeling to reflect both a deliberate humidifier oversizing (to offset the expected but quantitatively unknown rate of degradation) and a conservative estimate. DPoint was consulted on this area selection and expressed acceptance. Gore continues to prefer the use of 2 m^2 membrane area (or even greater). In 2014, the automotive fuel cell air stoichiometric ratio increased from 1.5 to 2, therefore the amount of membrane area was linearly scaled from 1.6m^2 at air stoic of 1.5 to 2.13m^2 at air stoic 2. In 2015, the air stoic went back down to 1.5, although SA did not scale with stoic but rather used a calculated membrane area provided by ANL (0.92m^2). SA added a 1.25 oversizing factor to account for degradation over the life of the humidifier, yielding 1.15m^2 for the 2015 baseline total humidifier area.

For the automotive application, the modeled design is composed of 58 "cell pouches" where each cell pouch is a loop of membrane with a metal spacer within the loop. The dimension of each cell pouch is 10cm by 10cm, summing to a total humidifier membrane area of 1.15 m^2. The cell pouches allow dry primary inlet air to flow through the inside of the pouch and humid secondary outlet oxygen-depleted air from the cathode to flow cross-wise over the outside of the pouch (as seen in Figure 128). Stamped metal "ribs" are used to separate the pouches and thus enable gas flow between the pouches. The cell pouches are arranged in a simple aluminum cast-metal housing to direct the gas flows.

---

[79] Ahluwalia, R., K., Wang, X. , *Fuel Cells Systems Analysis*, Presentation to the Fuel Cell Tech Team, Southfield, MI, 14 August, 2013.
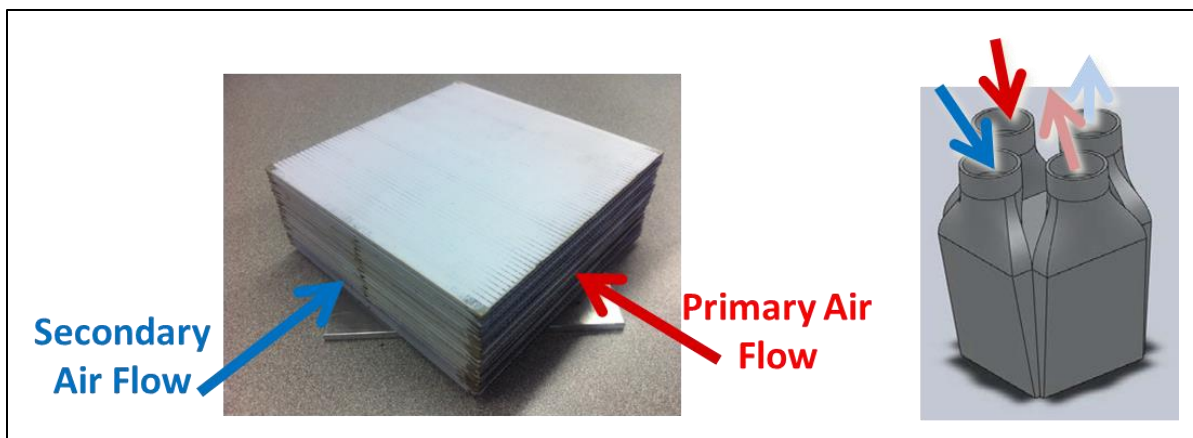
Figure 128. Images from W.L. Gore & Associates presentation[80] showing (Left) stack of cell pouches with primary flow (dry air) flowing through the cell pouches and secondary flow (wet air) flowing over/under and between pouches and (Right) humidifier housing with four ports: primary and secondary flow inlet and outlet ports.

8.2.2.3.1   Membrane Humidifier Manufacturing Process

The manufacturing process for the plate frame membrane humidifier is modeled as eight steps:

1. Fabrication of Composite Membranes
2. Fabrication of Etched Stainless Steel Flow Fields
3. Pouch Formation
4. Stainless Steel Rib Formation
5. Stack Formation
6. Formation of the Housing
7. Assembly of the Composite Membrane and Flow Fields into the Housing
8. Humidifier System Testing

Manufacturing details and cost components for each process are described in the following sections.

Fabrication of Composite Humidifier Membranes

The postulated process for manufacture of the composite humidifier membrane is based on a slot die coating roll-to-roll system.

a. A 10µm thick ePTFE layer is unrolled onto a Mylar backer.
b. A 5µm thick slot die coated layer of Nafion® ionomer is laid on top of the ePTFE.
c. A second layer of 10µm thick ePTFE is unrolled onto the ionomer layer.
d. The stacked layers are passed through a continuous curing oven.
e. In the final step, all three layers are hot laminated to a 180µm polyethylene terephthalate (PET) non-woven porous layer, also known as a gas diffusion layer (GDL).

---

[80] Johnson, William B. "Materials and Modules for Low-Cost, High Performance Fuel Cell Humidifiers," W.L. Gore & Associates, Inc., presentation at the 2012 DOE Hydrogen and Fuel Cell Program Annual Merit Review, Washington, DC, 17 May 2012.

The ePTFE layers bracket and mechanically support the very thin, and thus high water flux, ionomer layer and are arranged in a symmetrical orientation to minimize stresses during thermal cycling and thereby enhance lifetime. The much thicker PET layer provides additional mechanical support and abrasion resistance. Figure 129 shows a schematic of the postulated fabrication process inspired by a Ballard patent for composite membrane manufacturing[81] and a Gore patent for integral composite membranes.[82]
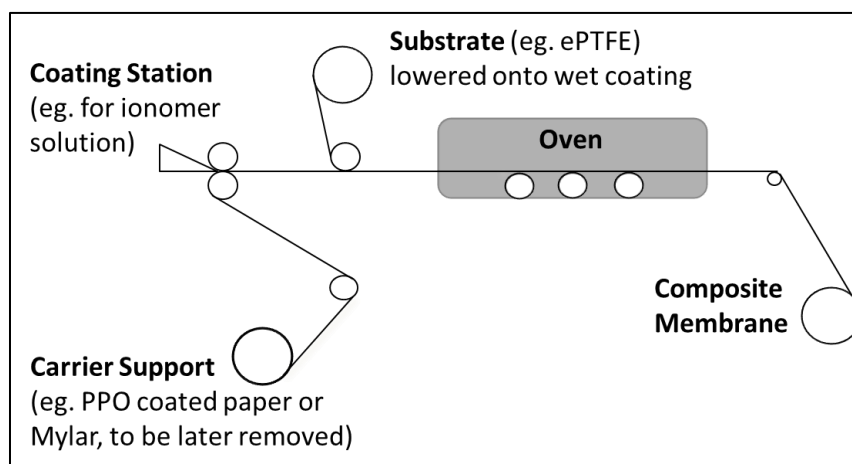
Figure 129. Design for ionomer addition to ePTFE, followed by oven drying to form a composite membrane from combination of Ballard Patent (U.S. Patent 6,689,501 B2) and Gore patent (U.S. Patent 5,599,614).

Key elements of composite membrane fabrication process include:
- Adding a porous substrate (eg. ePTFE) onto a wet impregnate solution (eg. ionomer) (shown in Figure 129).
- Coating ionomer directly onto a porous substrate (eg. Slot die coating onto the top of the ePTFE) (not shown in Figure 129).
- Adding a second porous substrate (eg. ePTFE) onto the top of a wet solution layer (eg. ionomer) (not shown in Figure 129).

The process is modeled using a 1m web width at a baseline speed of 10m/min (based on Dupont patent).[83] Curing oven residence time is a total of 9 minutes (3 minutes at 40°C, 3 minutes at 60°C and 3 minutes at 90°C), also based on the DuPont patent. The total capital cost of manufacturing equipment for the composite membrane is approximately $3M with the cost breakdown and cost basis listed in Figure 130. Figure 131 and Figure 132 show membrane processing parameters. Cost results are shown Figure 133 and reveal that (at 500,000 systems per year) material cost is the largest cost contributor, with ePTFE cost being the dominating cost element. Consequently, ePTFE cost was carefully assessed and found to vary substantially vendor to vendor, partly due to variations in ePTFE precursor

---

[81] Ballard Patent: U.S. Patent 6,689,501 B2
[82] Gore Patent: "Integral composite Membrane" U.S. Patent 5,599,614.
[83] DuPont Patent US 7,648,660 B2

materials and processing steps (together referred to as ePTFE "quality"). A discussion of the range of ePTFE costs used within the cost analysis appears in Section 8.1.2.2.

Component	Capital Cost	Basis
Web Casting Operation		
Base slot die coating system	$800k	Frontier Industrial Technology Inc. quote
Additional Pump Cart	$25k	Frontier Industrial Technology Inc. quote
ePTFE Unwind stands	2 x $60k	Machine Works Inc. quote
Customization Adder	2x	Conservatism for custom machinery
Total Web Casting Capital Cost	**$1.9M**	
Additional heating zones	$37k	Modified Wisconsin Ovens quote
Tensioner for laminator	$60k	Estimated based on similar machinery
Laminator	$864k	Modified Andritz Kuster quote
Clean Room	$166k	Industrial ROM estimate
Quality Control Equipment	$165k	Line Cameras to provide 100micron anomaly resolution after ionomer addition and 350 micron resolution of each ePTFE layer.
Total Capital (uninstalled)	**$3M**	

Figure 130. Capital cost of manufacturing equipment required for the composite membrane fabrication process.

Annual Production Rate	1,000	10,000	30,000	80,000	100,000	500,000
Equipment Lifetime (years)	16	15	15	15	15	15
Interest Rate	10%	10%	10%	10%	10%	10%
Corporate Income Tax Rate	40%	40%	40%	40%	40%	40%
Capital Recovery Factor	0.175	0.175	0.175	0.175	0.175	0.175
Equipment Installation Factor	1.4	1.4	1.4	1.4	1.4	1.4
Maintenance/Spare Parts (% of CC)	10%	10%	10%	10%	10%	10%
Miscellanous Expenses (% of CC)	7%	7%	7%	7%	7%	7%
Power Consumption (kW)	278	278	278	294	294	294

Figure 131. Fabrication of composite membranes process parameters

Annual Production Rate	1,000	10,000	30,000	80,000	100,000	500,000
Capital Cost ($/line)	$1,281,402	$1,251,191	$1,251,191	$2,836,683	$2,836,683	$3,019,397
Simultaneous Lines	1	1	1	1	1	1
Laborers per Line	0.67	0.67	0.67	0.67	0.67	0.67
Line Utilization	0.2%	3.3%	9.5%	9.2%	11.4%	37.6%
Casting Line Rate (m/s)	0.26	0.14	0.14	0.17	0.17	0.17
Effective Total Machine Rate ($/hr)	$70,034	$4,715	$1,675	$3,849	$3,116	$1,043
Backer Cost ($/m^2)	$0.96	$0.96	$0.96	$0.96	$0.96	$0.96

Figure 132. Machine rate parameters for fabrication of composite membranes

Annual Production Rate	1,000	10,000	30,000	80,000	100,000	500,000
Materials ($/stack)	$58	$39	$31	$27	$26	$16
Manufacturings ($/stack)	$111	$55	$19	$15	$12	$3
Toolings ($/stack)	$0	$0	$0	$0	$0	$0
Markups ($/stack)	$68	$33	$18	$13	$10	$5
Total Costs ($/stack)	$237	$127	$68	$55	$48	$23
Total Costs ($/kWnet)	$2.96	$1.59	$0.85	$0.69	$0.60	$0.29

Figure 133. Cost breakdown for fabrication of composite membranes

Fabrication of Etched Stainless Steel Flow Fields

The humidifier flow field plates serve to separate the sides of the cell pouch and open a channel through which the air may pass. The plates are fabricated by electrochemical etching of 0.6mm stainless steel 316L sheet. Etching is selected as it grants the design flexibility and dimensional tolerance critical to achieving low pressure drop and high membrane water transport performance. To reduce the cost of the etching process, multiple flow fields are etched from a single large panel of SS. The process includes the following stages:

- **Stage 1 (Add Photoresist)**: Photoresist is first laminated to both sides of a 0.6mm (24mils) SS316 metal coil and cut to 1m by 2m panel size (holding 180 parts).
- **Stage 2 (Illuminate with light):** Two SS/photoresist panels are manually loaded into a light chamber, covered with stencils (one stencil on each side of each panel), exposed to light simultaneously on each side of panel for 7.5 minutes to activate the photoresist not covered by the stencil, and then the panels are removed from the light chamber. The photoresist has now been selectively removed from the panel in the exact pattern desired for etching.
- **Stage 3 (Stripping):** Ten panels are loaded into a vertical fixture, simultaneously lowered into a stripping tank of alkaline solution (sodium carbonate), the exposed portions of photoresist are striped/dissolved by the alkaline solution over a 5 minutes submersion, the panel are then lifted from the tank.
- **Stage 4 (Etching):** The ten panels fixture is moved to an electrochemically etching bath, electrodes are connected to each panel, the panels are simultaneously lowered into the etching tank, an electric current is applied to electrochemically etch the exposed SS surface. The electrochemical etching rate is estimated at 6.7 μm per minute, taking a total of 45 minutes to etch 600 microns (300 microns from each side simultaneously). Perforations are also etched into the material to allow for easy flow field separation using a low force stamping machine. The average power consumption estimated is approximately 1.2kW per 100cm^2 part (2.16MW for 10 panels).
- **Stage 5 (Cleaning):** After the etching is complete, the panels are lowered into a wash tank of alkaline solution (sodium hydroxide) for 4 minutes to remove the remaining photoresist.

Additionally, the etched plates are anodized for corrosion resistance, separated by stamping into 10cm by 10cm pouch cell sizes, and packaged into magazines for robotic assembly. Anodizing cost is estimated at 1.6 cents per 50cm^2 of anodizing surface ($3 for a 100 cell stack) with the parts being anodized while in panel form before separated. Figure 134 and Figure 135 show flow field processing parameters. Cost results for the etching process are shown in Figure 136.

Annual Production Rate	1,000	10,000	30,000	80,000	100,000	500,000
Equipment Lifetime (years)	15	15	15	15	15	15
Interest Rate	10%	10%	10%	10%	10%	10%
Corporate Income Tax Rate	40%	40%	40%	40%	40%	40%
Capital Recovery Factor	0.175	0.175	0.175	0.175	0.175	0.175
Equipment Installation Factor	1.4	1.4	1.4	1.4	1.4	1.4
Maintenance/Spare Parts (% of CC)	13%	13%	13%	13%	13%	13%
Miscellanous Expenses (% of CC)	2%	2%	2%	2%	2%	2%
Power Consumption (kW)	2,226	2,226	2,226	2,226	2,226	2,226

Figure 134. Fabrication of etched stainless steel flow fields process parameters

Annual Production Rate	1,000	10,000	30,000	80,000	100,000	500,000
Capital Cost ($/line)	$1,018,602	$1,018,602	$1,018,602	$1,018,602	$1,018,602	$2,293,602
Stage 1 Simultaneous Lines	1	1	1	1	1	1
Stage 2 Simultaneous Lines	1	1	1	1	1	4
Stage 3 Simultaneous Lines	1	1	1	1	1	1
Stage 4 Simultaneous Lines	1	1	1	1	1	4
Stage 5 Simultaneous Lines	1	1	1	1	1	1
Stage 1 Line Utilization	0.0%	0.2%	0.5%	1.3%	1.6%	8.0%
Stage 2 Line Utilization	0.6%	6.4%	19.2%	51.1%	63.9%	79.9%
Stage 3 Line Utilization	0.1%	0.9%	2.6%	7.0%	8.8%	44.0%
Stage 4 Line Utilization	0.8%	7.4%	22.1%	58.8%	73.6%	91.9%
Stage 5 Line Utilization	0.1%	0.8%	2.4%	6.4%	8.0%	40.0%
Stage 1 Laborers per Line	1	1	1	1	1	1
Stage 2 Laborers per Line	2	2	2	2	2	2
Stage 3 Laborers per Line	1	1	1	1	1	1
Stage 4 Laborers per Line	0	0	0	0	0	0
Stage 5 Laborers per Line	1	1	1	1	1	1
Stage 1 Cycle Time (s)	6	6	6	6	6	6
Stage 2 Cycle Time (s)	480	480	480	480	480	480
Stage 3 Cycle Time (s)	330	330	330	330	330	330
Stage 4 Cycle Time (s)	2,761	2,761	2,761	2,761	2,761	2,761
Stage 5 Cycle Time (s)	300	300	300	300	300	300
Effective Total Machine Rate ($/hr)	$15,084.76	$1,752.35	$743.51	$427.36	$389.37	$305.96
Stainless Steel Cost ($/kg)	$3.93	$3.93	$3.93	$3.93	$3.93	$3.93

Figure 135. Machine rate parameters for fabrication of etched stainless steel flow fields

Annual Production Rate	1,000	10,000	30,000	80,000	100,000	500,000
Materials ($/stack)	$11	$11	$11	$11	$11	$11
Manufacturings ($/stack)	$408	$46	$20	$11	$10	$8
Total Costs ($/stack)	$419	$57	$31	$22	$21	$19
Total Costs ($/kWnet)	$5.24	$0.72	$0.38	$0.28	$0.27	$0.24

Figure 136. Cost breakdown for fabrication of etched stainless steel flow fields

Pouch Formation

The cell pouches are formed using custom machinery to wrap a flow field with composite membrane and apply adhesive to seal the ends of the membrane and form a membrane loop. An image of a complete single cell pouch is shown in Figure 137. The process order used to fabricate these cell pouches is as follows:

a. Composite humidifier membrane material is unrolled on to a cutting deck.
b. The custom machine cuts the composite membrane to a 20cm length.

132

c.   A flow field is placed in the center of the membrane.
d.   One end of the membrane is wrapped around the flow field.
e.   A bead of silicone adhesive is applied to the membrane end wrapped around the flow field.
f.   The other end of the membrane is wrapped around the flow field and onto the adhesive bead. The ends are held in place until bonded.
g.   A vision quality control system is used to verify alignment of the cell pouch.
h.   The cell pouch is removed and stacked in a magazine to be used in the next stack assembly process.

A schematic of the process steps is shown in Figure 138. (The schematic does not show the quality control system.) The complete system is estimated at $413,000 and able to simultaneously prepare 10 pouches with a 9 second cycle time (i.e. 9 seconds per 10 pouches).

Figure 137. Plate Frame Membrane Humidifier single cell pouch (Source: Johnson, William B. "Materials and Modules for Low-Cost, High Performance Fuel Cell Humidifiers," W.L. Gore & Associates, Inc., presentation at the 2012 DOE Hydrogen and Fuel Cell Program Annual Merit Review, Washington, DC, 17 May 2012.)
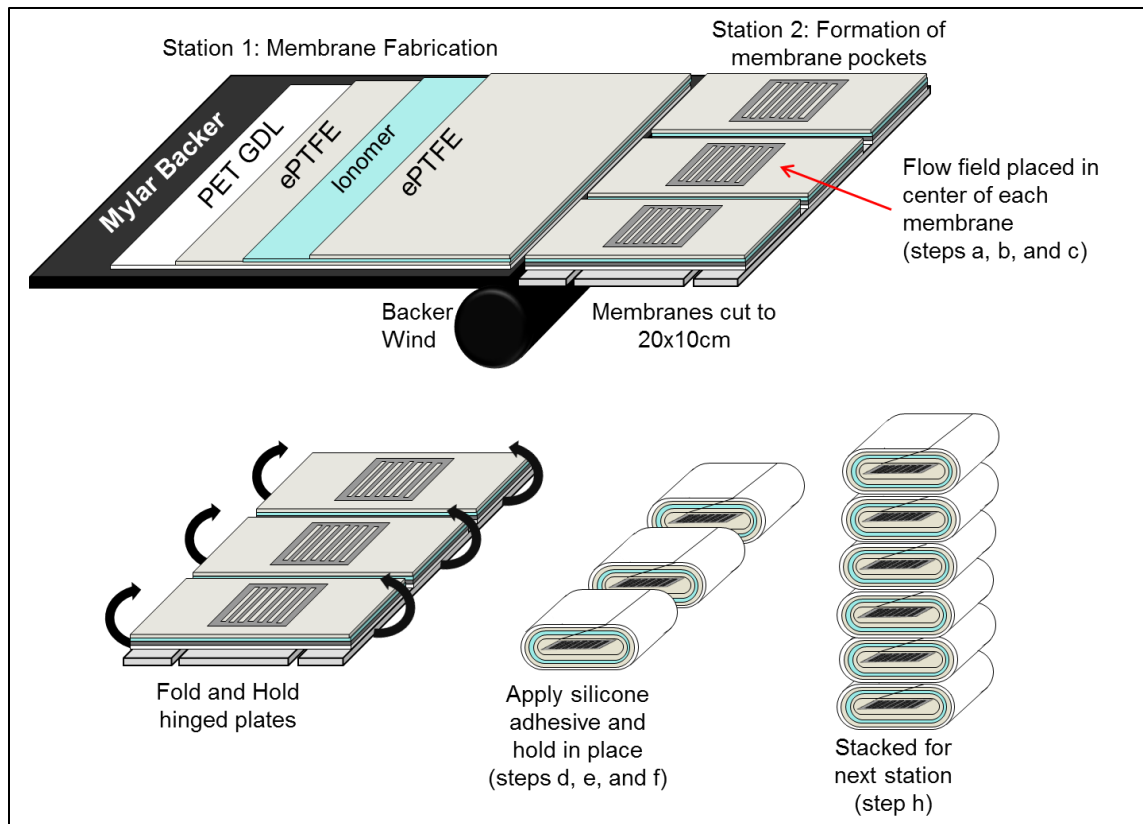
Figure 138. Process steps used in DFMA^{TM} analysis for humidifier cell pouch formation.

Figure 139 and Figure 140 show cell pouch formation processing parameters. Cost results for the cell pouch formation process are in Figure 141.

Annual Production Rate	1,000	10,000	30,000	80,000	100,000	500,000
Equipment Lifetime (years)	15	15	15	15	15	15
Interest Rate	10%	10%	10%	10%	10%	10%
Corporate Income Tax Rate	40%	40%	40%	40%	40%	40%
Capital Recovery Factor	0.175	0.175	0.175	0.175	0.175	0.175
Equipment Installation Factor	1.4	1.4	1.4	1.4	1.4	1.4
Maintenance/Spare Parts (% of CC)	10%	10%	10%	10%	10%	10%
Miscellanous Expenses (% of CC)	7%	7%	7%	7%	7%	7%
Power Consumption (kW)	27	27	27	27	27	27

Figure 139. Pouch formation process parameters

Annual Production Rate	1,000	10,000	30,000	80,000	100,000	500,000
Capital Cost ($/line)	$413,179	$413,179	$413,179	$413,179	$413,179	$413,179
Costs per Tooling Set ($)	$1,259	$1,259	$1,259	$779	$686	$274
Costs per Tooling Set 2 ($)	1,400	1,400	1,400	1,400	1,400	977
Tooling Lifetime (cycles)	2,000,000	2,000,000	2,000,000	2,000,000	2,000,000	2,000,000
Simultaneous Lines	1	1	1	1	1	3
Laborers per Line	0.25	0.25	0.25	0.25	0.25	0.25
Line Utilization	0.5%	4.6%	13.8%	34.9%	43.6%	71.9%
Cycle Time (s)	0.875	0.875	0.875	0.875	0.875	0.875
Effective Total Machine Rate ($/hr)	$11,076.25	$1,121.81	$383.39	$159.46	$130.29	$84.40
Silicon Adhesive Cost ($/kg)	$12.05	$12.05	$12.05	$12.05	$12.05	$12.05

Figure 140. Machine rate parameters for pouch formation

Annual Production Rate	1,000	10,000	30,000	80,000	100,000	500,000
Materials ($/stack)	$0	$0	$0	$0	$0	$0
Manufacturings ($/stack)	$171	$17	$6	$2	$2	$1
Toolings ($/stack)	$0	$0	$0	$0	$0	$0
Total Costs ($/stack)	$172	$18	$6	$3	$2	$2
Total Costs ($/kWnet)	$2.15	$0.22	$0.08	$0.03	$0.03	$0.02

Figure 141. Cost breakdown for pouch formation

Stainless Steel Rib Formation

Metal ribs are used to create air passageways between the cell pouches of the plate frame humidifier. The ribs are stamped from 0.6mm thick stainless steel 316L sheeting and formed into 10cm by 0.25cm by 0.6mm ribs. Plate handling robots are used to collect and stack the ribs into magazines to be used during stack assembly. The capital cost of the stamping press is $160,000 and the cycle time is approximately 0.67 seconds per rib (90 stamps per minute).

Figure 142 and Figure 143 show rib formation processing parameters. Cost results for rib formation are shown in Figure 144.

Annual Production Rate	1,000	10,000	30,000	80,000	100,000	500,000
Equipment Lifetime (years)	15	15	15	15	15	15
Interest Rate	10%	10%	10%	10%	10%	10%
Corporate Income Tax Rate	40%	40%	40%	40%	40%	40%
Capital Recovery Factor	0.175	0.175	0.175	0.175	0.175	0.175
Equipment Installation Factor	1.4	1.4	1.4	1.4	1.4	1.4
Maintenance/Spare Parts (% of CC)	13%	13%	13%	13%	13%	13%
Miscellanous Expenses (% of CC)	2%	2%	2%	2%	2%	2%
Power Consumption (kW)	18	18	18	18	18	18

Figure 142. Stainless steel rib formation process parameters

Annual Production Rate	1,000	10,000	30,000	80,000	100,000	500,000
Capital Cost ($/line)	$158,587	$158,460	$158,460	$158,460	$158,460	$158,460
Costs per Tooling Set ($)	$6,000	$6,000	$6,000	$6,000	$6,000	$6,000
Tooling Lifetime (cycles)	400,000	400,000	400,000	400,000	400,000	400,000
Simultaneous Lines	1	1	1	1	1	5
Laborers per Line	0.25	0.25	0.25	0.25	0.25	0.25
Line Utilization	1.0%	9.5%	28.6%	76.3%	95.3%	95.3%
Cycle Time (s)	0.66	0.66	0.66	0.66	0.66	0.66
Effective Total Machine Rate ($/hr)	$1,950.87	$1,422.02	$1,422.02	$1,422.02	$1,422.02	$1,422.02
Stainless Steel Rib Material Cost ($/kg)	$3.93	$3.93	$3.93	$3.93	$3.93	$3.93

Figure 143. Machine rate parameters for stainless steel rib formation

Annual Production Rate	1,000	10,000	30,000	80,000	100,000	500,000
Materials ($/stack)	$1	$1	$1	$1	$1	$1
Manufacturings ($/stack)	$63	$7	$2	$1	$1	$1
Toolings ($/stack)	$3	$3	$3	$3	$3	$3
Total Costs ($/stack)	$67	$10	$6	$5	$5	$5
Total Costs ($/kWnet)	$0.83	$0.13	$0.07	$0.06	$0.06	$0.06

Figure 144. Cost breakdown for stainless steel rib formation

Stack Formation

The plate frame membrane humidifier stack is assembled by "pick and place" robots. The following steps are used for assembly.

1. Repeated robotic steps for the number of pouches required in the stack (58 cell pouches for automotive system).
   a. Robot acquires and places pouch cell with flow field insert
   b. Apply silicone gasket/adhesive bead on three sealing lines
   c. Acquire and place three parallel SS rib spacers onto the sealing lines
   d. Apply additional silicone gasket/adhesive beads on three sealing lines on rib spacers

2. Compress stack in an assembly jig and hold for 24 hours in a humidified warm enclosure. (72 hours curing time would be required if left at room temperature.)
3. Use optical quality control system to detect membrane misalignment in stack.

The total capital cost of the pick and place robots and other equipment required for the system is $185,000. The cycle time is 9 seconds for each pouch (~9 min for an 80 cell pouch stack).

Figure 145 and Figure 146 show stack formation processing parameters. Cost results for stack formation process are in Figure 147.

Annual Production Rate	1,000	10,000	30,000	80,000	100,000	500,000
Equipment Lifetime (years)	15	15	15	15	15	15
Interest Rate	10%	10%	10%	10%	10%	10%
Corporate Income Tax Rate	40%	40%	40%	40%	40%	40%
Capital Recovery Factor	0.175	0.175	0.175	0.175	0.175	0.175
Equipment Installation Factor	1.4	1.4	1.4	1.4	1.4	1.4
Maintenance/Spare Parts (% of CC)	10%	10%	10%	10%	10%	10%
Miscellanous Expenses (% of CC)	7%	7%	7%	7%	7%	7%
Power Consumption (kW)	22	22	22	22	22	22

Figure 145. Stack formation process parameters

Annual Production Rate	1,000	10,000	30,000	80,000	100,000	500,000
Capital Cost ($/line)	$185,000	$185,000	$185,000	$185,000	$185,000	$185,000
Simultaneous Lines	1	1	2	4	5	22
Laborers per Line	0	0	0	0	0	0
Line Utilization	4%	43%	65%	86%	86%	98%
Cycle Time (s)	9	9	9	9	9	9
Effective Total Machine Rate ($/hr)	$542.05	$66.04	$48.41	$39.59	$39.59	$36.42
Silicon Adhesive Cost ($/kg)	$12.05	$12.05	$12.05	$12.05	$12.05	$12.05

Figure 146. Machine rate parameters for stack formation

Annual Production Rate	1,000	10,000	30,000	80,000	100,000	500,000
Materials ($/stack)	$3	$3	$3	$3	$3	$3
Manufacturings ($/stack)	$79	$10	$7	$6	$6	$5
Total Costs ($/stack)	$82	$13	$10	$9	$9	$8
Total Costs ($/kWnet)	$1.02	$0.16	$0.13	$0.11	$0.11	$0.11

Figure 147. Cost breakdown for stack formation

Formation of the Housing

The humidifier aluminum housing is formed using a 900 ton cold chamber die casting machine to form two separate parts (body and upper lid). Boothroyd Dewhurst Inc. (BDI) software was used for the cost estimate. The housing walls are 2.5mm thick and have approximate dimensions of 11cm tall by 11cm length and width. The volume is less than 5 liters and the mass of the housing about 0.65kg. Four bolts/nuts are used to connect the body to the lid with an elastomer O-ring for sealing. A CAD drawing of the complete housing is shown in Figure 148. Process steps used in DFMATM analysis for humidifier cell pouch formation along with the corresponding cost results are displayed in Figure 149.
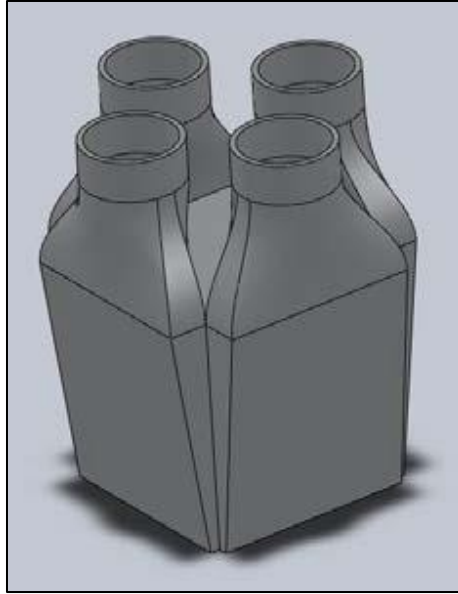
Figure 148. Process steps used in DFMA^{TM} analysis for humidifier cell pouch formation (Source: Johnson, William B. "Materials and Modules for Low-Cost, High Performance Fuel Cell Humidifiers," W.L. Gore & Associates, Inc., presentation at the 2012 DOE Hydrogen and Fuel Cell Program Annual Merit Review, Washington, DC, 17 May 2012.)

Annual Production Rate	1,000	10,000	30,000	80,000	100,000	500,000
Material ($/stack)	$5	$5	$5	$5	$5	$5
Manufacturing ($/stack)	$18	$4	$1	$1	$1	$1
Tooling ($/stack)	$31	$3	$2	$1	$1	$1
Total Cost ($/stack)	$53	$12	$9	$7	$7	$7
Total Cost ($/kWnet)	$0.66	$0.15	$0.11	$0.09	$0.09	$0.08

Figure 149. Cost breakdown for formation of the Housing

Assembly of the Composite Membrane and Flow Fields into the Housing

Complete manual assembly of the plate frame humidifier is performed at a custom work stand using the following sequence:

a. Acquire housing body and insert into fixture.
b. Acquire pouch stack and load stack into housing.
c. Acquire and insert gasket into housing body.
d. Acquire upper lid and place onto gasket/housing-body.
e. Acquire, insert and fasten 4 bolts/nuts.
f. Acquire finished housing and move to cart.
g. Weigh finished unit to detect missing/additional parts. (Quality control step.)

The cycle time is approximately 2 minutes per system. Figure 150 and Figure 151 show assembly process parameters. Cost results for assembly are shown in Figure 152.

Annual Production Rate	1,000	10,000	30,000	80,000	100,000	500,000
Equipment Lifetime (years)	10	10	10	10	10	10
Interest Rate	10%	10%	10%	10%	10%	10%
Corporate Income Tax Rate	40%	40%	40%	40%	40%	40%
Capital Recovery Factor	0.205	0.205	0.205	0.205	0.205	0.205
Equipment Installation Factor	1.4	1.4	1.4	1.4	1.4	1.4
Maintenance/Spare Parts (% of CC)	10%	10%	10%	10%	10%	10%
Miscellanous Expenses (% of CC)	7%	7%	7%	7%	7%	7%
Power Consumption (kW)	18	18	18	18	18	18

Figure 150. Assembly of the composite membrane and flow fields into the housing process parameters

Annual Production Rate	1,000	10,000	30,000	80,000	100,000	500,000
Assembly Method	Manual	Manual	Manual	Manual	Manual	Manual
Capital Cost ($/line)	$34,212	$34,212	$34,212	$34,212	$34,212	$34,212
Simultaneous Lines	1	1	1	1	1	5
Laborers per Line	1	1	1	1	1	1
Line Utilization	1.0%	9.9%	29.8%	79.4%	99.2%	99.2%
Index Time (min)	2	2	2	2	2	2
Effective Total Machine Rate ($/hr)	$429.56	$85.42	$59.83	$51.82	$50.86	$50.86

Figure 151. Machine rate parameters for assembly of the composite membrane and flow fields into the housing

Annual Production Rate	1,000	10,000	30,000	80,000	100,000	500,000
Manufacturings ($/stack)	$14	$3	$2	$2	$2	$2
Total Costs ($/stack)	$14	$3	$2	$2	$2	$2
Total Costs ($/kWnet)	$0.18	$0.04	$0.02	$0.02	$0.02	$0.00

Figure 152. Cost breakdown for assembly of the composite membrane and flow fields into the housing

Humidifier System Testing

A simple functionality test is completed for each completed humidifier system. It includes testing for air flow pressure drop and air leakage. These tests require an air compressor, gas manifolding, and a diagnostic measurement system. The steps considered in this testing process are:

a. Acquire unit and insert into fixture.
b. Connect 4 inlet and outlet air manifolds.
c. Sequentially flow gas (as appropriate) to test:
   - Pressure drop in primary flow (20 seconds)
   - Pressure drop in secondary flow (20 seconds)
   - Air leakage (primary to secondary) (20 seconds)
d. Disconnect inlet and outlet air manifolds.
e. Remove unit from fixture.

The estimated capital cost is:
- $30,000 for a 1-system test fixture (used at low production levels)
- $40,000 for a 3-system test fixture (used at high production levels)

The cycle time for testing is about 83 seconds per cycle.
- 83 seconds per system for a 1-system test fixture and 1 worker
- 23 seconds per system for a 3-system test fixture and 1 worker

Figure 153 and Figure 154 show humidifier system testing process parameters. Cost results are displayed in Figure 155.

Annual Production Rate	1,000	10,000	30,000	80,000	100,000	500,000
Equipment Lifetime (years)	15	15	15	15	15	15
Interest Rate	10%	10%	10%	10%	10%	10%
Corporate Income Tax Rate	40%	40%	40%	40%	40%	40%
Capital Recovery Factor	0.175	0.175	0.175	0.175	0.175	0.175
Equipment Installation Factor	1.4	1.4	1.4	1.4	1.4	1.4
Maintenance/Spare Parts (% of CC)	10%	10%	10%	10%	10%	10%
Miscellanous Expenses (% of CC)	7%	7%	7%	7%	7%	7%
Power Consumption (kW)	2	2	2	5	5	5

Figure 153. Humidifier system testing process parameters

Annual Production Rate	1,000	10,000	30,000	80,000	100,000	500,000
Capital Cost ($/line)	$30,000	$30,000	$30,000	$40,000	$40,000	$40,000
Simultaneous Lines	1	1	1	1	1	1
Laborers per Line	1	1	1	1	1	1
Line Utilization	0.7%	6.9%	20.6%	15.2%	19.0%	95.1%
Systems partially connected at any one time	1	1	1	3	3	3
Selected Effective Test time per System (min)	1.4	1.4	1.4	0.4	0.4	0.4
Effective Total Machine Rate ($/hr)	$492.07	$90.61	$60.75	$73.01	$67.62	$50.35

Figure 154. Machine rate parameters for humidifier system testing

Annual Production Rate	1,000	10,000	30,000	80,000	100,000	500,000
Manufacturings ($/stack)	$11	$2	$1	$0	$0	$0
Total Costs ($/stack)	$11	$2	$1	$0	$0	$0
Total Costs ($/kWnet)	$0.143	$0.026	$0.018	$0.006	$0.005	$0.004

Figure 155. Cost breakdown for humidifier system testing

8.2.2.3.2 Combined Cost Results for Plate Frame Membrane Humidifier

Cost results for the Gore plate frame membrane humidifier are summarized in Figure 156 at 500,000 systems per year and in Figure 157 for all manufacturing rates, with costs further subdivided into materials, manufacturing, tooling, markup, and total costs. The greatest cost drivers are the material costs, particularly for the membrane materials at ~$16/humidifier. Costs are strongly impacted by the quantity of membrane material needed for the humidifier. The largest processing cost for the humidifier is the flow field fabrication due to the innate details of the flow field design which are deemed to

require a (relatively) expensive etching process. Membrane and flow fields make up approximately 2/3^{rds} of the total cost and materials are about half the total humidifier cost (at 500,000 systems per year), as seen in Figure 158.

Component Costs per Humidifier System		All at 500k systems per year				
		Materials	Manuf.	Tools	Markup	Total
Station 1: Membrane Fabrication	$/stack	$15.81	$2.69	$0.11	$4.65	$23.27
Station 2: Humidifier Etching (Flow Field Plates)	$/stack	$10.94	$8.10	$0.00	$0.00	$19.04
Station 3: Pouch Forming	$/stack	$0.32	$1.22	$0.04	$0.00	$1.58
Station 4: Stamp SS ribs	$/stack	$0.86	$1.04	$2.61	$0.00	$4.51
Station 5: Stack Forming	$/stack	$3.19	$5.28	$0.00	$0.00	$8.47
Station 6: Stack Housing	$/stack	$5.05	$0.50	$1.21	$0.00	$6.76
Station 7: Assembly of Stack into Housing	$/stack	$0.00	$1.70	$0.00	$0.00	$1.70
Station 8: System Test	$/stack	$0.00	$0.32	$0.00	$0.00	$0.32
Totals =		**$36.17**	**$20.85**	**$3.97**	**$4.65**	**$65.64**

Figure 156. Membrane humidifier system cost results: ~$110 at 500k systems/year

Annual Production Rate	1,000	10,000	30,000	80,000	100,000	500,000
Materials ($/stack)	$78	$59	$52	$47	$46	$36
Manufacturings ($/stack)	$876	$143	$58	$39	$34	$21
Toolings ($/stack)	$34	$6	$5	$4	$4	$4
Markups ($/stack)	$68	$33	$18	$13	$10	$5
Total Costs ($/stack)	$1,055	$242	$133	$103	$94	$66
Total Costs ($/kWnet)	$13.19	$3.02	$1.66	$1.29	$1.18	$0.82

Figure 157. Combined cost results for all plate frame humidifier processes.

Markup is typically applied to the sum of materials, manufacturing, and tooling to capture the real business costs associated with overhead, general administrative (G&A), scrap, R&D, and profit. Per previous DOE directive, markup is only applied to lower-tier suppliers and is NOT applied to the system assembler. A high degree of vertical integration for the overall auto fuel cell power system is assumed. (As discussed in more detail in Section 2.3, a lower level of vertical integration is assumed for the bus fuel cell system, therefore markup is applied to the humidifier.) For the plate frame membrane humidifier, markup is not applied to the auto humidifier assembler. However, markup is included in the costs of the ePTFE, PET, and composite humidifier membrane as those components are assumed to be manufactured by lower tier suppliers. (Markup on the manufacturing process for the composite membrane appears in the markup column in Figure 156.)
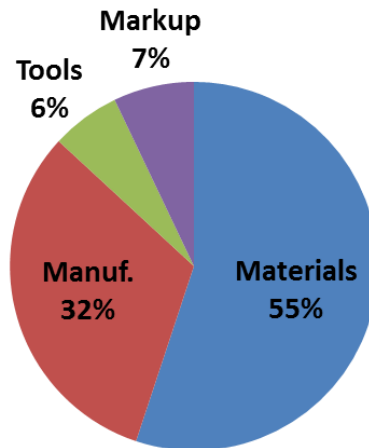
Figure 158. Humidifier membrane cost dominated by material cost at 500k systems/year

In cost analysis of fuel cell system components, it is beneficial to benchmark results with currently developed systems. Figure 159 compares SA's cost estimate to Gore's cost estimate and shows good agreement at medium and high production rates (for the same 2m^2 of membrane area). SA estimates are much higher than Gore's at low manufacturing rates due to poor utilization of expensive equipment (i.e. composite membrane fabrication). At low utilization of equipment, a business may decide to "job shop" or outsource the work to a company that has higher utilization of similar equipment. Such "job shopping" is not assumed for the humidifier in the 2015 analysis although as mentioned in Section 6.7.4, the production of membrane area is assumed to be five times more than what is used for 1,000 systems per year. This multiplier stems from the assumption that the membrane manufacturer would most likely supply to more than one customer and may have multiple industrial applications for this membrane.
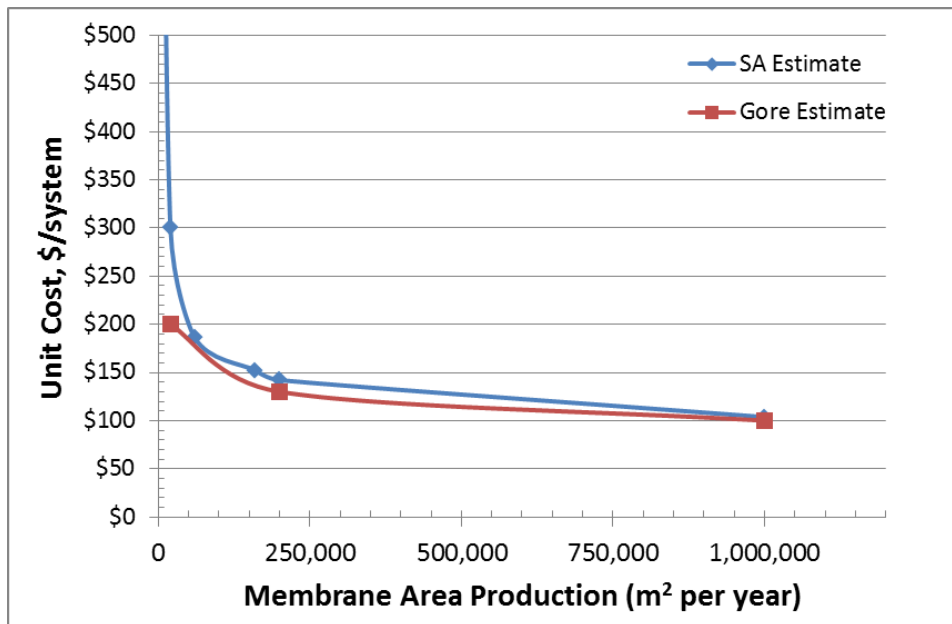
Figure 159. Comparison of Gore and SA cost estimates for the plate frame membrane humidifier (for 2m^2 membrane area).

In 2014, SA ran a sensitivity analysis of multiple parameters at 500,000 systems per year (can be seen in SA's 2014 Update report).[84] The most important cost driver for the humidifier is the quantity of membrane material required. This indicates that between $0.5m^2$ and $2.6m^2$ of membrane area the plate frame humidifier would cost between \$35/system and \$131/system. The second most important cost driver is the price of the ePTFE material used in the membrane. Both the fuel cell stack MEA and humidifier manufactured costs are quite sensitive to the cost of ePTFE. While plate frame humidifier uncertainty is high (-68%/+19%), the overall humidifier cost is low compared to the total auto fuel cell power system cost.

In comparison to the tubular membrane humidifier previously used in the 2012 analysis, the 2015 plate frame humidifier is projected to be higher cost. However, in retrospect, the 2012 tubular membrane humidifier is now viewed as undersized for the flow conditions (even at $3.8m^2$ of membrane area) and thus a direct comparison of the two systems is not valid. In general, plate frame humidifiers will require less membrane area than tubular designs since their membranes may be thinner, (by virtue of being supported on ePTFE). However, the cost of the ePTFE support is a significant fraction of the total plate frame humidifier cost, and manufacturing (particularly of the etched plates) also adds considerably to cost (see Figure 160).

As shown by the sensitivity analysis, membrane area is an extremely important parameter in determination of humidifier cost. Uncertainty exists related to the required membrane area. Consequently, an optimistic value of $0.5m^2$/system was included in the sensitivity analysis based on ANL modeling projections and a pessimistic value of $2.6m^2$ was included to reflect a large allowance for performance degradation. Further testing is required to confidently determine the membrane area requirement.

---

[84] "Mass Production Cost Estimation of Direct H2 PEM Fuel Cell Systems for Transportation Applications: 2014 Update" Brian D. James, Jennie M. Moton & Whitney G. Colella, Strategic Analysis, Inc., January 2015.
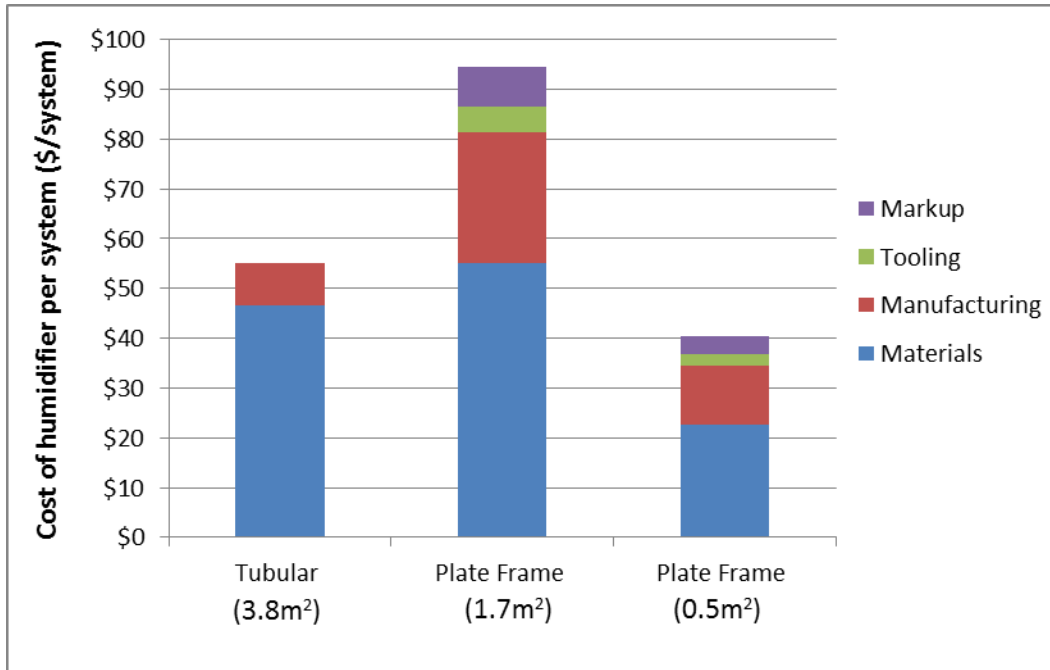
Figure 160. Graph showing the cost (at 500k sys/yr) comparison between a tubular membrane humidifier and two plate frame membrane humidifiers with different membrane area requirements.

8.2.3 Coolant Loops

The 2014 system has two coolant loops, a high-temperature loop to cool the fuel cell stacks and a low-temperature loop to cool electronic components. The low temperature loop is also used to cool the CEM motor and in the precooler (to cool the compressed intake air prior to going into the membrane humidifier).

8.2.3.1 High-Temperature Coolant Loop

Coolant Reservoir: The cost is based on a molded plastic water tank.

Coolant Pump: Small pumps to provide this flow are commercially available in large quantities at approximately $97 per pump at quantities of 1,000, dropping to $74 at high quantity.

Coolant DI Filter: The cost is based on a resin deionizer bed in a plastic housing.

Thermostat & Valve: The cost is based on standard automotive components.

Radiator: The heat dissipation requirements of the fuel cell system are similar to those of today's standard passenger cars. Consequently, costs for the high and low-temperature loop radiators are aligned with those of appropriately sized radiators used in contemporary automotive applications.

Radiator Fan: The cost is based on a standard automotive radiator fan and sized based on the cooling load.

Coolant Piping: Cost is based on 2" diameter rubber pipe from McMaster Carr and set at a constant $6.93/ft.

High-temperature coolant loop cost results are shown in Figure 161.

Annual Production Rate	1,000	10,000	30,000	80,000	100,000	500,000
Coolant Reservoir ($/system)	$13	$12	$11	$8	$8	$6
Coolant Pump ($/system)	$63	$63	$63	$63	$63	$63
Coolant DI Filter ($/system)	$81	$71	$65	$49	$45	$39
Thermostat & Valve ($/system)	$11	$9	$9	$6	$6	$5
Radiator ($/system)	$195	$185	$175	$166	$156	$146
Radiator Fan ($/system)	$89	$78	$68	$52	$50	$47
Coolant Piping ($/system)	$25	$24	$24	$23	$22	$20
Total Cost ($/system)	$476	$443	$414	$366	$349	$327
Total Cost ($/kW$_{net}$)	$5.95	$5.54	$5.17	$4.58	$4.37	$4.09

Figure 161. Cost breakdown for high-temperature coolant loop

8.2.3.2   *Low-Temperature Coolant Loop*

In the 2012 analysis, the low-temperature loop previously cooled components both within the fuel cell system (precooler, CEM motor) and the drive train system (main traction motor inverter (TIM) electronics). Consequently, the cost of the 2012 low-temperature coolant loop was apportioned between these systems and only the cost of the loop associated with the fuel cell system was tabulated in the fuel cell cost summary. Based on the expected duties of the components, 67% of the low-temperature coolant loop cost was attributable to the fuel cell system.

The low-temperature loop for the 2014 analysis is modeled as a dedicated fuel cell system cooling loop and thus only cools components within the fuel cell system (precooler, CEM motor). Drive train components have been removed from the cooling loop: thus 100% of the coolant loop cost is charged to the fuel cell system. This change was made in order to simplify the analysis and to be in closer alignment with Argonne National Laboratory modeling methodology.

Coolant Reservoir: The cost is based on a molded plastic water tank.

Coolant Pump: The low and high-temperature loops require similar flow rates, so the same type of pump is used in each.

Thermostat & Valve: The cost is based on standard automotive components.

Radiator: As with the radiator for the high-temperature coolant loop, the exhaust loop uses a radiator similar to those used in conventional automotive applications. It does not need to be as large as the one for the coolant loop however, so it is scaled down in cost.

Radiator Fan: It is assumed that the radiators for the high and low-temperature loops are installed together such that the air flow exiting the low-temperature radiator immediately enters the high-temperature radiator, and as such, there is a single fan for both radiators, which is accounted for in the high-temperature coolant loop (Reason why radiator fan cost is $0 in Figure 162).

Coolant Piping: Assumed 2" diameter rubber pipe from McMaster Carr, at $6.93/ft.

Low-temperature coolant loop cost results are shown in Figure 162.

Annual Production Rate	1,000	10,000	30,000	80,000	100,000	500,000
Coolant Reservoir ($/system)	$2	$130	$130	$130	$130	$130
Coolant Pump ($/system)	$17	$2	$2	$2	$2	$2
Thermostat & Valve ($/system)	$4	$2,164	$2,164	$2,164	$2,164	$2,164
Radiator ($/system)	$47	$78	$68	$52	$50	$47
Radiator Fan ($/system)	$0	$0	$0	$0	$0	$0
Coolant Piping ($/system)	$6	$480	$480	$480	$480	$480
Total Cost ($/system)	$76	$72	$70	$66	$63	$60
Total Cost ($/kW$_{net}$)	$0.95	$151.50	$145.35	$137.29	$131.34	$124.87

Figure 162. Cost breakdown for low-temperature coolant loop

8.2.4 Fuel Loop

Per DOE system analysis guidelines, the hydrogen tank, the hydrogen pressure-relief device & regulator, hydrogen fueling receptacle, proportional valve, and pressure transducer are not included in the fuel cell power system cost analysis as they are considered part of the hydrogen storage system.

Inline Filter for Gas Purity Excursions: This filter ensures that any contaminants that may have gotten into the fuel lines do not damage the stack.

Flow Diverter Valve: The flow diverter valve routes hydrogen to either the low-flow or the high-flow ejector, depending on the pressure.

Over-Pressure Cut-Off (OPCO) Valve: The over-pressure cut-off valve is included as a safety precaution to prevent inadvertent stack pressurization from the high pressure (>5000psi) in the hydrogen storage tank.

Low-Flow and High-Flow Ejectors: Dual static ejectors are employed to re-circulate hydrogen from the anode exhaust to the anode inlet to achieve target flow rates and hence high stack performance. The ejectors operate on the Bernoulli Principle wherein high-pressure hydrogen gas from the fuel tank (>250 psi) flows through a converging-diverging nozzle to entrain lower-pressure anode exhaust gas. Two ejectors (high-flow and low-flow) are operated in parallel to achieve a wide turn-down range. The design of the ejectors is based on concepts from Graham Manufacturing and the patent literature (US Patent 5,441,821). The fabrication of each ejector consists of stainless steel investment casting of a two-part assembly, followed by machining, welding, and polishing. Ejectors with variable geometry are a possible design improvement for future systems. While ANL modeling suggests that a hydrogen recirculation blower is needed during very low part-power system operation to ensure proper gas flow, only the ejector system is included in the analysis.

Check Valves: The check valves ensure that no hydrogen may flow backwards from the ejectors

Purge Valve: The purge valve allows for periodic purging of the hydrogen in the fuel loop.

Hydrogen Piping: The hydrogen flow lines are modeled as 1/2" SS316 schedule 10 pipe and are priced between $90 and $100/system based on estimate provided by Ford.

Fuel loop cost breakdown is shown in Figure 163.

Annual Production Rate	1,000	10,000	30,000	80,000	100,000	500,000
Inline Filter for GPE ($/system)	$15	$15	$15	$15	$15	$15
Flow Diverter Valve ($/system)	$16	$16	$16	$16	$16	$16
Over-Pressure Cut-Off Valve ($/system)	$25	$22	$20	$15	$14	$12
Hydrogen High-Flow Ejector ($/system)	$51	$38	$36	$33	$31	$31
Hydrogen Low-Flow Ejector ($/system)	$44	$31	$29	$26	$25	$24
Check Valves ($/system)	$10	$10	$10	$10	$10	$10
Purge Valves ($/system)	$80	$70	$64	$48	$45	$38
Hydrogen Piping ($/system)	$106	$104	$103	$99	$96	$92
Total Cost ($/system)	$346	$306	$291	$261	$251	$238
Total Cost ($/kW$_{net}$)	$4.32	$0.40	$0.38	$0.34	$0.33	$0.31

Figure 163. Cost breakdown for fuel loop

8.2.5 System Controller

Conventional electronic engine controllers (EEC's) are assumed to control the fuel cell power system. These programmable circuit boards are currently mass-produced for all conventional gasoline engines and are readily adaptable for fuel cell use. Prototype fuel cell vehicles may use four or more controllers out of convenience, so that each subsystem is able to have a separate controller. However, even at 1,000 vehicles per year, the system will be refined enough to minimize controller use on the rationale of simplicity of cost and design. A single EEC is judged adequate for control and sensor leads to the power plant.

Controller cost is assessed by a bottom-up analysis of the system controller which breaks the controller into 17 input and output circuits, as listed in Figure 164.

For each input or output circuit, it is estimated that approximately 50 cents in electronic components (referencing catalog prices) would be needed. The costs of input and output connectors, an embedded controller, and the housing are also estimated by catalog pricing. A price quote forms the basis for the assumed dual-layer 6.5" x 4.5"circuit board. Assembly of 50 parts is based on robotic pick-and-place methods. A 10% cost contingency is added to cover any unforeseen cost increases.

Name	Signal
Inputs	
Air Mass Flow Sensor	Analog
H2 pressure Sensor (upstream of ejector)	Analog
H2 Pressure Sensor (stack inlet manifold)	Analog
Air Pressure sensor (after compressor)	Analog
Stack Voltage (DC bus)	Analog
Throttle Request	Analog
Current Sensors (drawn from motor)	Analog
Current Sensors (output from stack)	Analog
Singnal for Coolant Temperature	Analog
H2 Leak Detector 1	Digital
H2 Leak Detector 2	Digital
Outputs	
Singnal to TIM	Analog
Singnal to CEM	Analog
Singnal to Ejector 1	PWM
Singnal to Ejector 2	PWM
High voltage System Relay	Digital
Signal to Coolant Pump	PWM
Signal to H2 Purge Valve	Digital
Total Analog	11
Total Digital	4
Total PWM	3
Total Inputs/Outputs	**18**

Figure 164. System controller input & output requirements

Figure 165 and Figure 166 detail estimated system controller costs.

Component	Description	Cost at 500k systems/year	Cost Basis
Main Circuit Board	2 layer punnchboard	$8.01	$5.34 for single layer of 6.5"x4.5" punchboard, Q=500, Assume 25% discount for Q=500k
Input Connector	Wire Connector for inputs	$0.18	$0.23 each in Q=10k, reduced ~20% for Q=500k
Output Connector	Wire Connector for outputs	$0.20	$0.23 each in Q=10k, reduced ~20% for Q=500k
Embedded Controller	25 MHz, 25 channel microprocessor board	$32.50	Digi-Key Part no. 336-1489-ND, $50 @Q=1, assumed 35% reduction for Q=500k
MOSFETs (18 total, 1 each per I/O)	P-channel, 2W, 49MOhm @5A, 10V	$3.93	Digi-Key Part No. 785-1047-2-ND, $0.2352 @Q=3k, $0.2184@Q=12k
Misc. Board Elements	Capacitor, resistors, etc.	$4.50	Estimate based on $0.25 component for each input/output
Housing	Shielded plastic housing, watertight	$5.00	Estimate based on comparable shielded, electronic enclosures. Includes fasteners.
Assembly	Assembly of boards/housing	$5.83	Robotic Assembly of approx. 50 parts at 3.5 sec each, $2/min assembly cost
Contingency	10% of all components	$6.02	Standard DFMA additional cost to capture un-enumerated elements/activities.
Markup	25% of all components	$16.54	Manufacturer's Markup
Total		**$82.72**	

Figure 165. System controller component costs

Annual Production Rate	1,000	10,000	30,000	80,000	100,000	500,000
System Controller	$172	$152	$138	$103	$97	$83
Total Cost ($/system)	$172	$152	$138	$103	$97	$83
Total Cost ($/kW$_{net}$)	$2.15	$1.90	$1.72	$1.29	$1.21	$1.03

Figure 166. Cost breakdown for system controller

8.2.6 Sensors

Aside from the air mass flow sensor (which is book-kept as part of the air loop), there are three types of sensors in the fuel cell system: current sensors, voltage sensors, and hydrogen sensors. The basic sensor descriptions and their costs are listed in Figure 167 and Figure 168.

Component	Description	Cost at 500k systems/year	Cost Basis
Current Sensor (for stack current)	~400A, Hall Effect transducer	$10	Based on LEM Automotive Current Transducer HAH1BV S/06, 400A
Current Sensor (for CEM motor current)	~400A, Hall Effect transducer	$10	Based on LEM Automotive Current Transducer HAH1BV S/06, 400A
Voltage Sensor	225-335 V	$8	Rough estimate based on a small Hall Effect sensor in series with a resistor
H$_2$ Sensor	Sensor unit for 0.25% to 4% H$_2$ concentrations in air in 5 seconds	$91.91	NTM Sensors
H$_2$ Sensor	Sensor unit for 0.25% to 4% H$_2$ concentrations in air in 5 seconds	$91.91	NTM Sensors
Total		$211.81	

Figure 167. Sensor details

Annual Production Rate	1,000	10,000	30,000	80,000	100,000	500,000
Current Sensors ($/system)	$20	$20	$20	$20	$20	$20
Voltage Sensors ($/system)	$8	$8	$8	$8	$8	$8
Hydrogen Sensors ($/system)	$409	$303	$263	$232	$225	$184
Total Cost ($/system)	$437	$331	$291	$260	$253	$212
Total Cost ($/kW$_{net}$)	$5.46	$4.14	$3.64	$3.25	$3.17	$2.65

Figure 168. Cost breakdown for sensors

8.2.6.1 Current Sensors

The current sensors are located on the stack, and allow the system controller to monitor the current being produced.

8.2.6.2 Voltage Sensors

The voltage sensors are located on the stack, and allow the system controller to monitor the voltage being produced.

8.2.6.3 Hydrogen Sensors

The vehicle will require a hydrogen sensing system to guard against hydrogen leakage accumulation and fire. It is postulated that a declining number of hydrogen sensors will be used within the fuel cell power

system as a function of time and as real-world safety data is accumulated. Consequently, it is estimated that two sensors would initially be used in the engine compartment, eventually dropping to zero. Additional sensors may be necessary for the passenger compartment and the fuel storage subsystem but these are not in the defined boundary of our fuel cell power system assessment.

The hydrogen sensor system specified is from NTM Sensors, based on the technology used in current fuel cell bus systems. According to a DOE funded report by Lawrence Livermore National Laboratory,[85] the detection threshold for vehicular uses of H_2 sensors is 1% (10,000 ppm) H_2 with a response time of less than 1 min. Each NTM sensor unit can detect between 0.25% and 4% H_2 in air in 5 seconds. The replacement schedule required for these sensors is 5 years; however an annual calibration test is needed. Similar to oil changes, this would be checked during routine annual maintenance.

Hydrogen sensors are currently quite expensive. 2010 discussion with Makel Engineering reveals that the specified hydrogen sensors are currently hand built and cost approximately $850 each. Jeffrey Stroh from Makel estimates that such units would cost approximately $100 each if mass-produced at 500,000 per year. With further technology and manufacturing improvements, including a move to integrated circuitry, he estimates that the unit cost could drop to only $20 per sensor. In recent discussions with NTM Sensors, the cost for a single sensor is $399, $299 for quantity 3, $199 for quantity 1,000, and $75 for quantity 1 million (projected cost target) Figure 169 lists the estimated hydrogen sensor costs that include additional connectors ($17-$24) needed to plug into the system power controller.

Annual Production Rate	1,000	10,000	30,000	80,000	100,000	500,000
Sensors per system	2	2	2	2	2	2
Sensor ($)	$204	$151	$131	$116	$113	$92
Total Cost ($/system)	$409	$303	$263	$232	$225	$184
Total Cost ($/kW_net)	$5.11	$3.79	$3.29	$2.90	$2.82	$2.30

Figure 169. Cost breakdown for hydrogen sensors

8.2.7   Miscellaneous BOP

The BOP components which do not fit into any of the other categories are listed here in the miscellaneous section.

Figure 170 shows the cost breakdown for these components.

Annual Production Rate	1,000	10,000	30,000	80,000	100,000	500,000
Belly Pan ($/system)	$63	$11	$7	$6	$6	$5
Mounting Frames ($/system)	$100	$64	$43	$33	$30	$30
Wiring ($/system)	$83	$75	$72	$70	$69	$67
Fasteners for Wiring & Piping ($/system)	$17	$15	$14	$14	$14	$13
Total Cost ($/system)	$263	$165	$136	$123	$119	$115
Total Cost ($/kW_net)	$3.28	$2.06	$1.70	$1.54	$1.48	$1.43

Figure 170. Cost breakdown for miscellaneous BOP components

---

[85] R.S. Glass, J. Milliken, K. Howden, R. Sullivan (Eds.), Sensor Needs and Requirements for Proton-Exchange Membrane Fuel Cell Systems and Direct-Injection Engines, 2000, pp. 7 – 15. DOE, UCRL-ID-137767.

8.2.7.1 Belly Pan

The belly pan is modeled as a 1 x 1.5 m shallow rectangular pan, bolted to the underside of the fuel cell system to protect it from weather and stone strikes.

The belly pan manufacturing process is modeled as a vacuum thermoforming process, in which thin polypropylene sheets are softened with heat and vacuum drawn onto the top of a one-sided mold. The capital cost of the vacuum thermoforming machine is approximately $300,000, and utilizes an optional automatic loading system, which costs another $200,000. If manual loading is selected, the process requires one laborer per line, instead of the 1/4 laborer facilitated by the automatic loading system. The analysis shows that the automatic system is only cost effective at the 500,000 systems per year production rate. Naturally, the loading option also changes the time per part; the vacuum time is 8 seconds per part, on top of which the insertion time adds another 11.2 seconds for the manual loading, or 2 seconds for the automatic method. The process parameters are shown in Figure 171, and the machine rate parameters are shown in Figure 172.

Annual Production Rate	1,000	10,000	30,000	80,000	100,000	500,000
Equipment Lifetime (years)	8	8	8	15	15	15
Interest Rate	10%	10%	10%	10%	10%	10%
Corporate Income Tax Rate	40%	40%	40%	40%	40%	40%
Capital Recovery Factor	0.229	0.229	0.229	0.175	0.175	0.175
Equipment Installation Factor	1.4	1.4	1.4	1.4	1.4	1.4
Maintenance/Spare Parts (% of CC)	5%	5%	5%	5%	5%	5%
Miscellanous Expenses (% of CC)	6%	6%	6%	6%	6%	6%
Power Consumption (kW)	30	30	30	35	35	40

Figure 171. Belly pan thermoforming process parameters

Annual Production Rate	1,000	10,000	30,000	80,000	100,000	500,000
Machine Selection	Vacuum Thermo-former #1	Vacuum Thermo-former #1	Vacuum Thermo-former #1	Vacuum Thermo-former #2	Vacuum Thermo-former #2	Vacuum Thermo-former #2
Assembly Type	Manual	Manual	Manual	Manual	Manual	Auto
Capital Cost ($/line)	$50,000	$50,000	$50,000	$250,000	$250,000	$655,717
Costs per Tooling Set ($)	$96,352	$96,352	$96,352	$96,352	$96,352	$96,352
Tooling Lifetime (years)	3	3	3	3	3	3
Cavities per platen	1	1	1	1	1	1
Total Cycle Time (s)	71.20	71.20	71.20	15.20	15.20	7.00
Simultaneous Lines	1	1	1	1	1	1
Laborers per Line	1	1	1	1	1	0.25
Line Utilization	0.6%	5.9%	17.7%	10.1%	12.6%	28.9%
Effective Total Machine Rate ($/hr)	$1,136.85	$156.88	$84.29	$310.80	$258.32	$253.68
Material Cost ($/kg)	$1.48	$1.48	$1.48	$1.48	$1.48	$1.48

Figure 172. Machine rate parameters for belly pan thermoforming process

Because of the extremely soft nature of the hot polypropylene and the low impact of the process, each mold (~$85,056) will easily last the entire lifetime of the thermoforming machine. However, belly pan designs are likely to change well before the forming machine wears out, so the mold's lifetime is set at three years. This means that the tooling costs are sufficiently low to ignore at all but the 1,000 systems per year level, where they account for almost 4% of the part cost. Figure 173 shows the cost breakdown.

Annual Production Rate	1,000	10,000	30,000	80,000	100,000	500,000
Material ($/system)	$4	$4	$4	$4	$4	$4
Manufacturing ($/system)	$22	$3	$2	$1	$1	$0
Tooling ($/system)	$36	$4	$1	$0	$0	$0
Total Cost ($/system)	$63	$11	$7	$6	$6	$5
Total Cost ($/kWnet)	$0.79	$0.14	$0.09	$0.08	$0.07	$0.06

Figure 173. Cost breakdown for belly pan

8.2.7.2 Mounting Frames

It is assumed that the fuel cell power system would be built as a subsystem, and then hoisted as an assembly into the automotive engine compartment. Consequently, the power system attaches to a mounting frame substructure to allow easy transport. These mounting frames are assumed to be contoured steel beams with various attachment points for power system components, facilitating attachment to the vehicle chassis. The cost is roughly estimated at $30 at 500,000 systems per year to $100 at 1,000 systems per year.

8.2.7.3 Wiring

Wiring costs include only wiring materials as wiring installation costs are covered under the system assembly calculations.

A conceptual fuel cell system wiring schematic (Figure 174) was created to determine where cables were needed and whether they were for transmission of data, power, or both. Cable types, detailed in Figure 175, are selected based on the maximum current required by each electrical component.

With the exception of the heavy-duty power cables attached to the current collectors, every cable is comprised of multiple wires. Each cable also requires a unique type of connector, of which two are needed for each cable.

It is assumed that the wires and connectors would be purchased rather than manufactured in-house, with high-volume pricing estimates obtained for the cable components from Waytek, Inc. Taking into account the required length of each cable, the number of wires per cable, and selecting the appropriate connectors, the component prices are applied to the wiring bill of materials and the total wiring cost is calculated for each system (seeFigure 176).
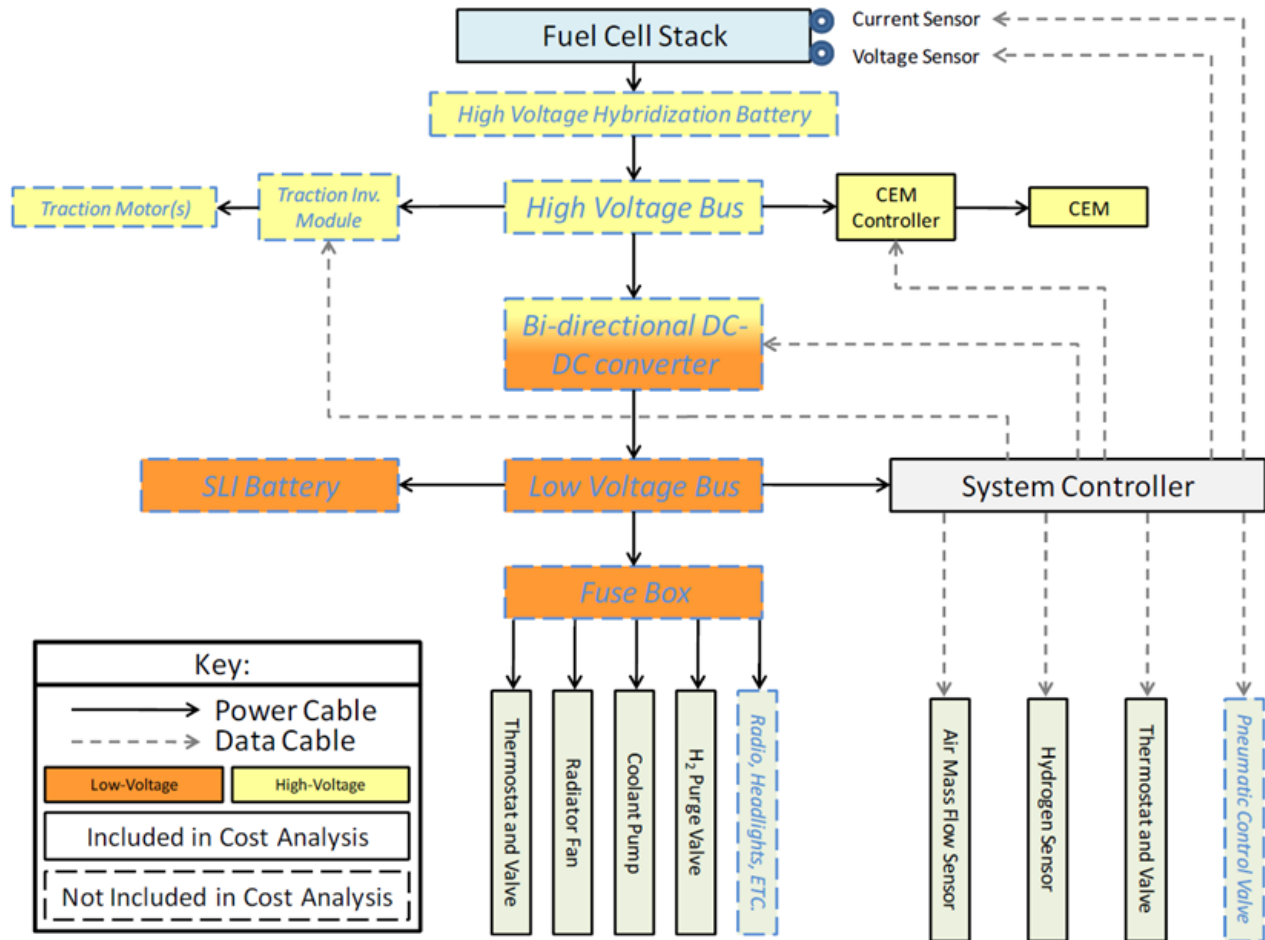
Figure 174. Fuel cell system wiring schematic

	Quantity	Length (m)
Cable Types		
Power Cable, OOOO Gauge	2	0.5
Power Cable, 6 Gauge	1	0.25
Power Cable, 7 Gauge	4	3.5
Power Cable, 12 Gauge	3	3
Power Cable, 16 Gauge	10	9
Totals	20	16.25

Figure 175. Wiring details

Annual Production Rate	1,000	10,000	30,000	80,000	100,000	500,000
Cables ($/system)	$29	$26	$25	$24	$24	$23
Connectors ($/System)	$54	$49	$46	$45	$45	$43
Total Cost ($/system)	$83	$75	$72	$70	$69	$67
Total Cost ($/kWnet)	$1.04	$0.94	$0.89	$0.87	$0.86	$0.83

Figure 176. Cost breakdown for wiring

153

8.2.7.4   Fasteners for Wiring & Piping

A detailed DFMA^{TM} analysis was not conducted for these components since the level of detailed required is well outside the bounds of this project. However, these components are necessary and, in aggregate, are of appreciable cost. Cost is estimated at 20% of the wiring and piping cost.

8.2.8   System Assembly

A detailed analysis of system assembly was not conducted since that would require detailed specification of all assembly steps including identification of all screws, clips, brackets, and a definition of specific component placement within the system. Such an analysis is beyond the scope of this project. Instead, an estimate of system assembly time is obtained by breaking the system down into five categories of assembly components (major, minor, piping, hoses, wiring), estimating the number of components within each category, and then postulating a time to assemble each of those components. Specific assumptions and total estimated assembly time for manual assembly are shown in Figure 177.

	Number of Components	Component Placement Time (seconds)	Component Fixation Time (seconds)	Component Totals (minutes)
Major Components (Stack, motors, pumps, vessels, etc.)	**19**	**45**	**60**	**33.3**
Minor Components (instruments, devices, etc.)	**22**	**30**	**45**	**27.5**
Piping				
# of pipe segments	5			
bends per segment	2			
time per bend	0			
pipe placement time	30			
# welds per pipe	2			
weld time	90			
# threaded ends per pipe	0			
threading time	0			
				17.5
Hoses	**21**	**30**	105	**47.3**
Wiring (manual)	**23**	**41.8**	66.7	**41.6**
System Basic Functionality Test				**10.0**
Total System Assembly Time				**177.1**

Figure 177. Single-station system assembly assumptions

Two types of system assembly methods are examined: single-station and assembly line. In single-station assembly approach, a single workstation is used to conduct assembly of the entire fuel cell power plant. Very little custom machinery is needed to assemble the system and components and subsystems are arrayed around the workstation for easy access. For 1,000 systems per year, only one such workstation is required. Assembly process parameters are listed in Figure 178.

Annual Production Rate	1,000	10,000	30,000	80,000	100,000	500,000
Assembly Method	Assembly	Assembly	Assembly	Assembly	Assembly	Assembly
Index Time (min)	104.55	83.64	83.64	83.64	83.64	83.64
Capital Cost ($/line)	$50,000	$100,000	$100,000	$100,000	$100,000	$100,000
Simultaneous Lines	1	1	2	5	6	27
Laborers per Line	10	10	10	10	10	10
Line Utilization	6.7%	53.2%	79.8%	85.1%	88.7%	98.5%
Effective Total Machine Rate ($/hr)	$663.94	$577.36	$567.74	$566.54	$565.82	$564.09
Cost per Stack ($)	$148	$103	$101	$101	$101	$101

Figure 178. System assembly process parameters

The assembly for all other annual production rates uses a ten-workstation assembly line configuration. Each fuel cell system flows through the assembly line sequentially. The line reduces the total cumulative time required for system assembly because workers at each workstation on the line have their tools and components closer at hand than they do under the single workstation approach, and because tool changes are minimized due to the higher repetitive nature of an assembly line. This method is approximately 20% faster than the single-workstation approach, with an assembly line index time[86] of only 14.2 minutes. The system assembly cost is detailed in Figure 179.

Annual Production Rate	1,000	10,000	30,000	80,000	100,000	500,000
System Assembly & Testing ($/System)	$148	$103	$101	$101	$101	$101
Total Cost ($/system)	$148	$103	$101	$101	$101	$101
Total Cost ($/kWnet)	$1.85	$1.29	$1.27	$1.27	$1.26	$1.26

Figure 179. Cost breakdown for system assembly & testing

8.2.9 System Testing

A ten-minute system functionality and performance test is included in the system assembly process. Each stack has separately undergone multiple hours of testing as part of stack conditioning and thus there is high confidence in the stack performance. System testing is only needed to ensure that the peripheral systems are functioning properly and adequately supporting the stack. Typically, the only testing of gasoline engines contained within automobiles is a simple engine startup as the vehicles are driven off the assembly line. Corresponding, the fuel cell "engines" are only minimally tested for functionality. Cost for this system testing is reported under system assembly.

8.2.10 Cost Contingency

It is common practice in the automotive industry to include a 10% cost contingency to cover the cost of procedures or materials not already explicitly included in the analysis. This serves as a guard against an underestimation of cost which can derail a cost estimator's career within the automotive industry. However, no such cost contingency has been included in this cost analysis upon the request of the DOE.

---

[86] Assembly line index time is defined as the time interval each system spends at a given workstation.

9   Bus Fuel Cell Power System

In addition to the annual automotive fuel cell power system cost update, a 40' transit bus fuel cell power system is also analyzed for the 2015 cost report. The bus fuel cell system was cost analyzed for the first time in 2012, thus the 2015 analysis represents an annual update to last year's bus study. Primary differences between the 2014 bus and the 2015 bus include all of the above listed changes between the 2014 and 2015 auto technology systems, updates to the catalyst material, increased polarization performance, and changes to operating conditions affecting gross power.

The 2015 automotive and bus power plants are very similar in operation but possess key differences in:

- power level, operating pressure, and catalyst loading,
- manufacturing rate, and
- level of vertical integration.

Section 9.1 below details the key differences between auto and bus power systems. If no difference is documented in this section, then details of material selection, manufacturing processes, and system design are assumed not to differ from that of the automotive system.

9.1   Bus Power System Overview

9.1.1   Comparison with Automotive Power System

Figure 180 below is a basic comparison summary of the 2015 auto and bus systems. As shown, most stack mechanical construction and system design features are identical between the bus and automotive power plants. Primary system differences include:

- Use of two ~90kW$_{gross}$ fuel cell stacks to achieve a net system power of 160kW$_{net}$ (instead of one ~90kW$_{net}$ stack for an 80kW$_{net}$ power level as used in the automotive system)
- Higher cell platinum loading (0.5mgPt/cm^2 instead of 0.142 mgPt/cm^2 as used in the automotive system)
- Differences in cell active area and number of active cells per stack
- Higher system voltage (reflecting two stacks electrically in series and the desire to keep current below 400 amps)
- Operation at 1.9 atm (instead of 2.5 atm as used in the automotive system)
- Use of a multi-lobe air compressor (based on an Eaton-style design) without an exhaust gas expander (instead of a centrifugal-compressor/radial-inflow-expander based on a Honeywell-style design as used in the automotive system)
- Reduced stack operating temperature (72°C instead of 95°C as used in the auto system)
- Increased size of balance of plant components to reflect higher system gross power

	2015 Auto Technology System	2015 Bus Technology System
Power Density (mW/cm^2)	746	739
Total Pt loading (mgPt/cm^2)	0.142	0.5
Net Power (kW$_{net}$)	80	160
Gross Power (kW$_{gross}$)	88.22	194.2
Cell Voltage (V)	0.661	0.659
Operating Pressure (atm)	2.5	1.9
Stack Temp. (Coolant Exit Temp) (°C)	94	72
Air Stoichiometry	1.5	1.8
Q/ΔT (kW/°C)	1.45	5.4
Active Cells	378	758
Membrane Material	Nafion on 25-micron ePTFE	Nafion on 25-micron ePTFE
Radiator/ Cooling System	Aluminum Radiator, Water/Glycol Coolant, DI Filter, Air Precooler	Aluminum Radiator, Water/Glycol Coolant, DI Filter, Air Precooler
Bipolar Plates	Stamped SS 316L with TreadStone Coating	Stamped SS 316L with TreadStone Litecell^{TM} Coating
Air Compression	Centrifugal Compressor, Radial-Inflow Expander	Eaton-Style Multi-Lobe Compressor, Without Expander
Gas Diffusion Layers	Carbon Paper Macroporous Layer with Microporous Layer (Ballard Cost)	Carbon Paper Macroporous Layer with Microporous Layer (Ballard Cost)
Catalyst & Application	Slot Die Coating of: Cath.: Dispersed 0.092 mgPt/cm^2 d-PtNi on C Anode: Dispersed 0.05mgPt/cm^2 Pt on C	Slot Die Coating of: Cath.: Dispersed 0.5 mgPt/cm^2 Pt on C Anode: Dispersed 0.1mgPt/cm^2 Pt on C
Air Humidification	Plate Frame Membrane Humidifier	Plate Frame Membrane Humidifier
Hydrogen Humidification	None	None
Exhaust Water Recovery	None	None
MEA Containment	Screen Printed Seal on MEA Sub-gaskets, GDL hot pressed to CCM	Screen Printed Seal on MEA Sub-gaskets, GDL hot pressed to CCM
Coolant & End Gaskets	Laser Welded(Cooling)/ Screen-Printed Adhesive Resin (End)	Laser Welded (Cooling), Screen-Printed Adhesive Resin (End)
Freeze Protection	Drain Water at Shutdown	Drain Water at Shutdown
Hydrogen Sensors	2 for FC System[87]	3 for FC System[88]
End Plates/ Compression System	Composite Molded End Plates with Compression Bands	Composite Molded End Plates with Compression Bands
Stack Conditioning (hours)	2	2

Figure 180: Comparison table between 2015 auto and 2015 bus technology systems

9.1.2   Changes to Bus System Analysis since the 2014 Report

This report represents the third annual update of the 2012 SA bus fuel cell system cost analysis and updates the previous work to incorporate advances made over the course of 2015. These advances may include new technologies, improvements and corrections made in the cost analysis, and alterations of how the systems are likely to develop. This 2015 analysis closely matches the methodology and results

---

[87] There are a total of 4 hydrogen sensors on-board the FC vehicle: 2 under the hood in the power system (within cost estimate), 1 in the passenger cabin (not in cost estimate), and 1 in the fuel system (not in cost estimate).

[88] Additional sensor added to bus system due to larger fuel cell compartment.

formatting of the 2014 analysis.[89]

Change	Reason	Change from previous value	Cost ($/kW) (@ 1,000 sys/yr)
2014 Final Cost Estimate		**NA**	**$278.62**
Operating Conditions	Voltage: 0.676 to 0.659V Power Density: 601 to 739mW/cm2 Pressure: 1.8 to 1.9atm, Temp: 74 to 72.2C Catalyst Loading: 0.4 to 0.5mg/cm2 (0.1 anode and 0.4 cathode) O2 stoic: 2.1 to 1.8 Air Humidifier Membrane Area: 5 to 3.9m2	**($4.83)**	**$273.80**
Catalyst and Application to Membrane	Switched from PtCoMn NSTF to dispersed Pt on carbon using slot die coating. Includes addition of XRF to quality control equipment.	**$1.07**	**$274.87**
Parasitic Loads	Re-evaluated parasitic loads.	**$5.02**	**$279.89**
Quality Control Systems	Membrane QC from XRF to ODS MEA Cutting and Slitting QC from XRF to ODS Membrane Humidifier Membrane Fabrication QC change with increased anomaly detection size to 100 microns.	**($4.83)**	**$275.06**
H2 Sensors	Updated H2 sensor costs with NTM Sensor quotation.	**($15.84)**	**$259.22**
Geometry	Changed active to total area ratio from 0.8 to 0.625.	**$8.00**	**$267.22**
Miscellaneous	Updated stack conditioning time based on GM patent from 5hrs to 2hrs. Includes change in load bank and testing equipment capital cost. Switch from subgasket with roll-to-roll process to robotic stacking process.	**($5.25)**	**$261.97**
2015 Value		**($16.66)**	**$261.97**

Figure 181 lists changes made on the bus system for the 2015 analysis with combined cost reduction of $16.66/kWnet at 1,000 systems per year. Changes to polarization and operating conditions were made in coordination with the 2015 change in catalyst from ternary PtCoMn NSTF to dispersed Pt on carbon using slot die coating. The parasitic power for the system was adjusted to align with ANL system performance modeling values. Several quality control changes similar to what were made to the automotive system (particularly at low volume) were also updated for the bus system. Hydrogen sensor quotations were also updated for the bus, resulting in an unexpectedly significant cost reduction compared to all other changes made in 2015. Changes to the active-to-total area ratio, stack conditioning, and sub-gasket processing were also ported over to the bus system.

---

[89] "Mass Production Cost Estimation of Direct H2 PEM Fuel Cell Systems for Transportation Applications: 2014 Update" Brian D. James, Jennie M. Moton & Whitney G. Colella, Strategic Analysis, Inc., January 2015.

Change	Reason	Change from previous value	Cost ($/kW) (@ 1,000 sys/yr)
2014 Final Cost Estimate		NA	$278.62
Operating Conditions	Voltage: 0.676 to 0.659V Power Density: 601 to 739mW/cm2 Pressure: 1.8 to 1.9atm, Temp: 74 to 72.2C Catalyst Loading: 0.4 to 0.5mg/cm2 (0.1 anode and 0.4 cathode) O2 stoic: 2.1 to 1.8 Air Humidifier Membrane Area: 5 to 3.9m2	($4.83)	$273.80
Catalyst and Application to Membrane	Switched from PtCoMn NSTF to dispersed Pt on carbon using slot die coating. Includes addition of XRF to quality control equipment.	$1.07	$274.87
Parasitic Loads	Re-evaluated parasitic loads.	$5.02	$279.89
Quality Control Systems	Membrane QC from XRF to ODS MEA Cutting and Slitting QC from XRF to ODS Membrane Humidifier Membrane Fabrication QC change with increased anomaly detection size to 100 microns.	($4.83)	$275.06
H2 Sensors	Updated H2 sensor costs with NTM Sensor quotation.	($15.84)	$259.22
Geometry	Changed active to total area ratio from 0.8 to 0.625.	$8.00	$267.22
Miscellaneous	Updated stack conditioning time based on GM patent from 5hrs to 2hrs. Includes change in load bank and testing equipment capital cost. Switch from subgasket with roll-to-roll process to robotic stacking process.	($5.25)	$261.97
2015 Value		($16.66)	$261.97

Figure 181. Table of changes made between the 2014 and 2015 bus system analysis

9.2   Bus System Performance Parameters

The bus and automotive power systems function in nearly identical fashion but have different power levels, flow rates, and pressure levels. The following sections describe the sizing methodology and values for key parameters of the bus power system.

9.2.1   Power Level

To provide sufficient power, two 80 kW$_{net}$ stacks are used, for a total net electrical power of 160 kW. This power level was chosen as an intermediate point in existing bus FC power systems, which nominally range from 140 kW$_{net}$ to 190 kW$_{net}$ electrical. Modeling a system which is an even multiple of 80 kW has the additional advantage of allowing a comparison between a dedicated bus system and a pair of automotive systems.

9.2.2   Polarization Performance Basis

Stack performance within the bus system is based on Argonne National Laboratory modeling of dispersed platinum on carbon catalyst membrane electrode assembly (MEA) performance data. The polarization curve model used for the bus stacks is different from the 2015 automotive system with modification for different operating conditions, catalyst material, and catalyst loading (as discussed below). As understood by the authors, the main bus fuel cell power plant supplier is Ballard Power Systems. They use the same stack construction and MEA composition within their bus power system stacks as they do for their light-duty vehicle stacks. From 2012 to 2014, SA assumed the stack

construction and MEA composition was the same in the auto as the bus. In 2015, the stack construction is the same, but the MEA composition is different with an alternative catalyst material (dispersed Pt on C for the bus vs. dispersed d-PtNi on C for the auto system).

Beginning-of-life (BOL) stack design conditions at peak power selected for the 2015 bus power system are shown in Figure 182 compared to the 2012, 2013, and 2014 analysis values. No changes were made to the operating conditions or performance curves for the bus between 2013 and 2014, but changed from 2014 to 2015.

	2012 Bus Analysis	2013 Bus Analysis	2014 Bus Analysis	2015 Bus Analysis
Cell Voltage (volts/cell)	0.676	0.676	0.676	0.659
Current Density (mA/cm^2)	1,060	889	889	1,121
Power Density (mW/cm^2)	716	601	601	739
Stack Pressure (atm)	1.8	1.8	1.8	1.9
Stack Temperature (outlet coolant temperature)	74°C	74°C	74°C	72°C
Air Stoichiometry	1.5	2.1	2.1	1.8
Total Catalyst Loading (mg/cm^2)	0.4	0.4	0.4	0.5
Cells per System	739	739	740	758

Figure 182: Bus fuel cell power system stack operating parameters from 2012 to 2015

Past discussions with Ballard[90] regarding their latest generation[91] (HD7) fuel cell stacks suggests an anticipated bus application design peak power operating point of ~0.69 volts/cell at ~1,100 mA/cm^2 yielding a power density of 759mW/cm^2 at a stack pressure of 1.8 atm and a ~0.4mgPt/cm^2 total catalyst loading. This operating point is very similar to the selected 2015 bus design point and is primarily a consequence of the 2015 polarization curve.

As seen in Figure 183, the selected power density is noted to be slightly lower than the design point chosen for the automotive systems (746 vs. 739mW/cm^2) and consequently results in a correspondingly larger bus fuel cell stack.

---

[90] Personal communication, Peter Bach, Ballard Power Systems, October 2012.
[91] Ballard FCvelocity® HD6 stacks are currently used in Ballard bus fleets. The HD7 stack is the next generation stack, has been extensively tested at Ballard, and is expected to be used in both automotive and bus vehicle power systems future years.
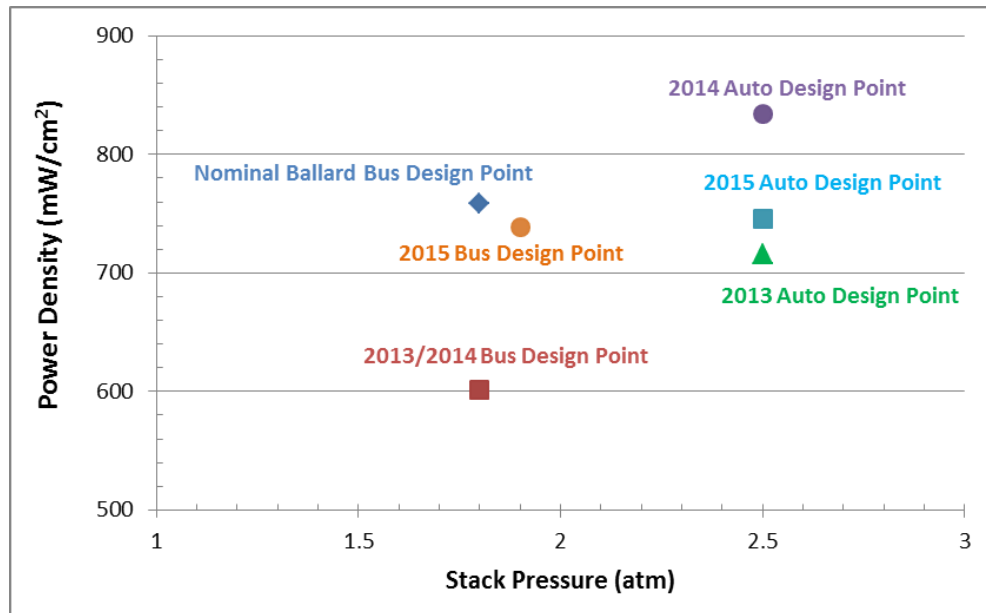
Figure 183: 2015 Bus peak power design point: Based on 2015 ANL Modeling data, 0.5mgPt/cm^2 total catalyst loading, 1.8 air stoic, 0.659V/cell

9.2.3 Catalyst Loading

Catalyst loading is a key driver of system cost and significant effort on the part of fuel cell suppliers has gone towards its reduction. In general, bus applications are less cost-sensitive and have longer lifetime requirements than automotive systems. Consequently, bus fuel cell stacks are more likely to have high catalyst loading since there is a general correlation between platinum loading and stack durability[92]. Whereas past examination of the 3M NSTF cell performance as represented by ANL modeling results and discussions with 3M researchers revealed that increases in catalyst cathode loading past ~0.2mgPt/cm^2 result in declining polarization performance due to a catalyst crowding[93] effect, such an effect is not expected for dispersed Pt on C catalyst systems. Consequently, for the bus application, catalyst loading is set at 0.5 mgPt/cm^2 total loading (nominally 0.4mgPt/cm^2 on the cathode and 0.1mgPt/cm^2 on the anode) to achieve a balance of performance, durability, and cost based on ANL system modeling. This level of catalyst loading is also approximately consistent with the levels used in Ballard fuel cell stacks.

---

[92] Many factors affect stack lifetime and degradation rate. But to the extent that degradation is caused by platinum catalyst poisoning, reduction in surface area, and/or reduced utilization, high catalyst loading tends to correlate with longer lifetime.

[93] The term "catalyst crowding" is meant to represent the situation where the catalyst layer on the substrate whiskers of the NSTF catalyst layer becomes so thick that it blocks gas flow or otherwise adversely affects performance.

9.2.4 Catalyst Ink

The catalyst layer is formed by applying a catalyst ink to the membrane as described in the next section. The catalyst ink is based on a slurry of platinum, Vulcan XC-72 carbon powder, and 5% wt ionomer solution, with an aqueous methanol solution for a solvent. The platinum is dispersed on the carbon powder via a chloroplatinic acid (CPA) precipitation method. The overall catalyst ink preparation process used in the DFMA^{TM} model is described in Figure 184. For a full description of CPA formulation, see Section 8.1.3.2.
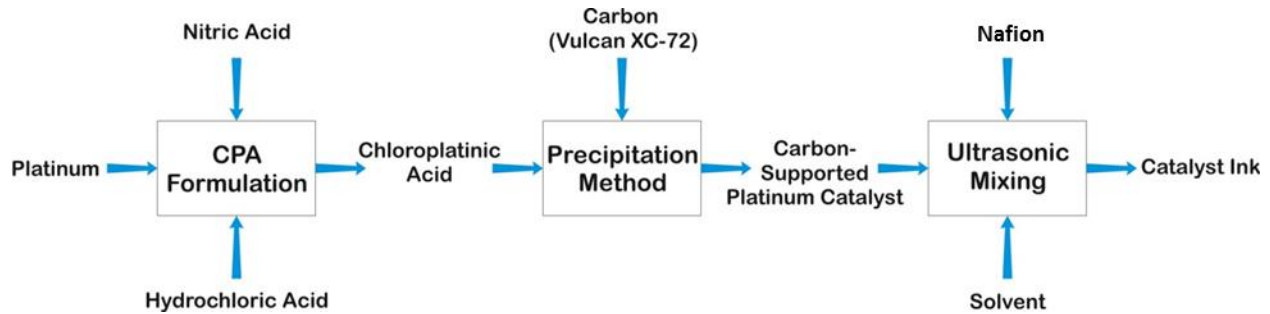
Figure 184. Catalyst ink preparation

9.2.5 Parasitic Load Requirements

As described previously in the auto system changes for 2015 (Section 6.3), the parasitic loads were also updated for the bus system to bring them in alignment with ANL modeling results. The most significant change to the parasitic loads is the electrical power for the high temperature coolant loop radiator fan which increased from 0.9kw to 8.26kW. The previous 0.9kW power estimate was based on the automotive system and scaled with system net power. For 2015, the radiator fan power is based on ANL's fan power of 4.3kW for an 83kWnet bus system and is scaled to the 160kWnet bus system. This significant radiator fan power difference between automotive and bus systems is thought to be due to the lower operating temperature of the bus, the diminished use of ram air for the bus fuel cell due to fuel cell placement near the rear of the vehicle, and higher pressure drop through the bus radiator system due to radiator placement and size. The same component efficiencies are used in the bus as in the automotive application: 45% fan efficiency, 90% fan motor efficiency, and 95% DC-DC converter efficiency. Other bus parasitic loads stayed approximately the same between 2014 and 2015 as seen in Figure 185.

Parasitic Load (kW)	2014 Value	2015 Value
Air Compressor Shaft Power	24.05	23.74
Air Compressor/Motor Input Required (gross)	25.31	24.99
High-Temperature Coolant Loop Pump	1.1	1.15
High-Temperature Coolant Loop Radiator Fan	0.9	8.26
Low-Temperature Coolant Loop Pump	0.12	0.11
Other (Controller, Instruments, etc.)	0.2	0.2
Total Parasitic Loads	**27.63**	**34.71**

Figure 185. Table of parasitic loads for the 2014 and 2015 systems.

9.2.6 Operating Pressure

As previously stated, the two main fuel cell bus power plant developers are Ballard Power Systems and UTC Power/US Hybrid.[94] Recent Ballard buses, using their FCvelocity® HD6 fuel cell stacks, typically operating at a stack pressure of ~1.8 atm (at rated power) and do not employ an exhaust gas expander. Recent UTC Power fuel cell bus power plants, using their porous carbon bipolar plates, typically operate near ambient pressure. The UTC Power porous carbon plates allow water management within the cell (both humidification and product water removal) and are a key element of their ability to achieve high polarization performance at low pressure. The porous carbon bipolar plate construction has not been cost-modeled under this effort and it would be inappropriate to postulate the combination of stamped metal bipolar plate construction with performance of platinum on carbon catalyst MEA at near ambient pressure.[95] Consequently, ambient pressure operation is not selected for bus application cost modeling at this time, although it could be considered in future analysis tasks.

A stack pressure of 1.9 atm is selected as the bus system baseline operating stack pressure at rated power to reflect ANL's 2015 optimized performance model. An exhaust gas expander is not used as there is a limited power available from the expansion of gas at this moderate pressure. This operating point of 1.9 atm without expander is in contrast to the optimized automotive system operating conditions of 2.5 atm with expander. A system level cost optimization (i.e. varying stack operating conditions to determine the combination of parameters leading to lowest system cost) was not conducted as polarization performance is not available at the higher catalyst loadings expected to be employed to ensure durability.

9.2.7 Stack Operating Temperature

In the 2012 bus analysis, design stack temperature[96] at rated (peak) power was determined by an ANL correlation with stack operating pressure and was set at 72°C to be consistent with 1.9 atm. This was a significant reduction from the 95°C temperature of the 2014/2015 automotive system at 2.5 atm. For the 2013/2014 analysis, ANL added temperature as an independent variable in their polarization model, thereby potentially allowing an optimization of operating temperature for lowest system cost. However, for a variety of non-polarization curve related reasons (as discussed below), bus fuel cell systems tend to operate at cooler temperatures. Thus rather than estimating stack performance on an optimal (high) temperature as determined by polarization data, it is more realistic to base performance on the temperature most likely to be experienced with the bus stacks. For this reason, a broader system level cost optimization is not conducted and the 72°C stack temperature is retained for the 2015 analysis. Future analysis is planned to more fully explore the impact of bus stack temperature on performance and cost.

---

[94] In January 2014, UTC announced the execution of a global technology and patent licensing agreement with US Hybrid Corporation for the commercialization of UTC's Proton Exchange Membrane (PEM) fuel cell technologies for the medium and heavy duty commercial vehicle sectors.
[95] This combination is theoretically possible but experimental data is not readily available nor, to the author's knowledge, have NSTF catalyst MEA parameters been optimized for ambient pressure operation.
[96] For modeling purposes, stack operating temperature is defined as the stack exit coolant temperature. Modeling suggests approximately a 10°C temperature difference between coolant inlet and outlet temperatures and the cathode exhaust temperature to be approximately 5°C higher than coolant exit temperature.

It is noted that Ballard reports their fuel cell bus stack temperatures at only 60°C. The reasons for this are several-fold. First, the system may not typically operate at rated power for long enough times for stack temperature to rise to its nominal value. This is particularly true for a bus power plant for which, depending on the bus route, maximum power may be demanded only a low fraction of the time. Second, various stack and membrane failure mode mechanisms are associated with high temperature. Thus it may be desirable to deliberately limit stack peak temperature as a means to achieving the stack lifetime goal of >12,000 hours (this is less of a concern for auto applications with lower lifetime requirements). Thirdly, higher stack temperature reduces the size of the heat rejection temperature since it increases the temperature difference with the ambient air. For an automobile, volume and frontal area are at a premium under the hood. Minimizing the size of the radiator is important for the auto application but is less important for the bus application where radiators may be placed on the roof. Thus, there are several good reasons—and fewer disadvantages—in selecting a low operating temperature for the bus compared to the auto application.

9.2.8   Q/DT Radiator Constraint

A Q/ΔT radiator constraint of <1.45 kW/°C was applied to the automotive system for the first time in 2013. However, such a radiator constraint is not applied to the bus fuel cell system because 1) buses are larger vehicles and have generally larger frontal areas to accommodate radiators, and 2) an appropriate numerical Q/ΔT constraint is not obvious.[97] Additional analysis to determine the appropriate Q/ΔT constraint is needed before it can be imposed.

9.2.9   Cell Active Area and System Voltage

Because the system consists of two stacks electrically in series, system voltage has been set to 500V at design conditions.[98] This bus voltage represents a doubling relative to the automotive system and is necessary to maintain the total electrical current below 400 amps. These values are broadly consistent with the Ballard fuel cell bus voltage range[99] of 465 to 730V. Specific cell and system parameters are detailed in Figure 186 for beginning-of-life (BOL) conditions.

Parameter	Value
Cell Voltage (BOL at rated power)	0.659 V/cell
System Voltage (BOL at rated power)	500 V
Number of Stacks	2
Active Cells per Stack	379
Total Cells per System	758
Active Area per Cell	348cm^2
Stack Gross Power at Rated Power Conditions (BOL)	194.7 kW

Figure 186: Bus stack parameters

---

[97] The automotive Q/ΔT constraint of <=1.45 kW/°C was set by DOE per suggestion of the Fuel Cell Technical Team (FCTT). Neither the DOE nor the FCTT has set a comparable constraint for the bus application.
[98] For purposed of the system cost analysis, design conditions correlate to rated maximum power at beginning of life.
[99] Ballard FCvelocity®-HD6 Spec Sheet. http://www.ballard.com/fuel-cell-products/fc-velocity-hd6.aspx
Accessed 9 October 2012.

9.3 Eaton-style Multi-Lobe Air Compressor-Motor (CM) Unit

9.3.1 Design and Operational Overview

An Eaton-style twin vortex, Roots-type air compressor such as that currently used in Ballard fuel cell buses is used for the 2015 bus cost analysis. A complete DFMA^{TM} analysis of the Eaton-style air compressor was conducted in 2013 and cost of the bus air compressor unit (including motor and motor controller) was updated for 2015. No additional changes were made in 2015. Cost is projected at $5,680 for a compressor unit at 1,000 units per year. The baseline compressor is SA's interpretation of a unit using Eaton technology and is modeled on Eaton's R340 supercharger (part of Eaton's Twin Vortices Series (TVS)) and Eaton's DOE program.[100]

The 2013 bus compressor-motor system efficiency was based on the DOE MYRD&D 2011 status values for an 80kW automotive compressor, motor, and motor controller, as seen in Figure 187. For the 2014 and 2015 baseline values, SA uses Eaton's 2014 projected minimum bus compressor efficiency and Eaton's motor/motor-controller combined efficiency. The change in efficiencies from 2013 to 2014/2015 is significant and results in a larger motor (due to lower compressor efficiency and motor scaling with shaft power). This increased the total cost of the bus fuel cell system by about $5/kW$_{net}$ at 1,000 systems per year. SA's 2013, 2014, and 2015 compressor unit does not include an exhaust gas expander as expanders are not typically utilized by deployed fuel cell buses. However Eaton projects a >=59% expander efficiency on a future, advanced design compressor/expander/motor integrated unit. Future SA analysis may consider the combined compressor/expander for the bus system, but for 2015, the baseline bus system does not include an expander.

Parameter	2013 Bus Values	2014 Bus Values	2015 Bus Values	2014 Eaton Projected Bus Values
Compression Ratio at Design Point	1.96	1.96	1.96	1.96
Air Flow Rate at Design Point	732 kg/hr (203 g/s)	750 kg/hr (208 g/s)	684 kg/hr (190g/s)	662 kg/hr (184 g/s)
Compression Efficiency[101] at Design Point	71%	58%	58%	>58%
Expander Efficiency[102] at Design Point	Not used	Not used	Not Used	>59%
Combined Motor and Motor Controller Efficiency[103]	80%	95%	95%	>95%

Figure 187: Details of the baseline bus roots (twin vortices) air compressor.

---

[100] Eaton/DOE Contract Number DE-EE0005665.
[101] Compression efficiency is defined as adiabatic efficiency.
[102] Expander efficiency is defined as adiabatic efficiency.
[103] Combined efficiency is defined as the product of motor efficiency and motor controller efficiency.

9.3.2 Compressor Manufacturing Process

The compressor-motor unit modeled as part of the bus DFMA[TM] analysis consists of several components including the motor, motor controller, compressor rotors, drive shafts, couplings, bearings, housing, and other components. A schematic of the SA conceptual design used for the cost analysis (derived from Eaton R340 supercharger design) is shown in Figure 188. The motor shaft is attached to a torsional coupling that fits onto one of the compressor drive shafts with multiple dowels for alignment. Two timing gears drive the second compressor shaft at the same rotation speed as the electric motor. Each shaft has a key slot where the rotor slides on and attaches. Each rotor-shaft assembly has both ball bearings and needle bearings that hold it in place against a bearing plate and the compressor housing. Shaft seals are required so as to isolate any oil within the gear housing and to maintain pressure within the compressor. A complete list of the compressor-motor unit components is shown in Figure 189 along with selected material, type of manufacturing process used in the analysis, dimensions, quantity, and mass.

Within the DFMA[TM] model, compressor-motor system parameters are adjusted to match requirements from the fuel cell system. Thus as stack efficiency and gross power change, the compressor-motor system is resized to the altered air flow requirement, dimensions (rotors, compressor wheel, motor size), and power level (of motor and controller). Compressor-motor system cost is correspondingly updated.

Cost of the compressor-motor system components were estimated by use of Boothroyd Dewhurst Inc. (BDI) software (housings), vendor cost quotes (electric motor and most small purchased items such as bearings, seals, nuts, etc.), or by DFMA[TM] analysis (compressor rotors and timing drive gears).
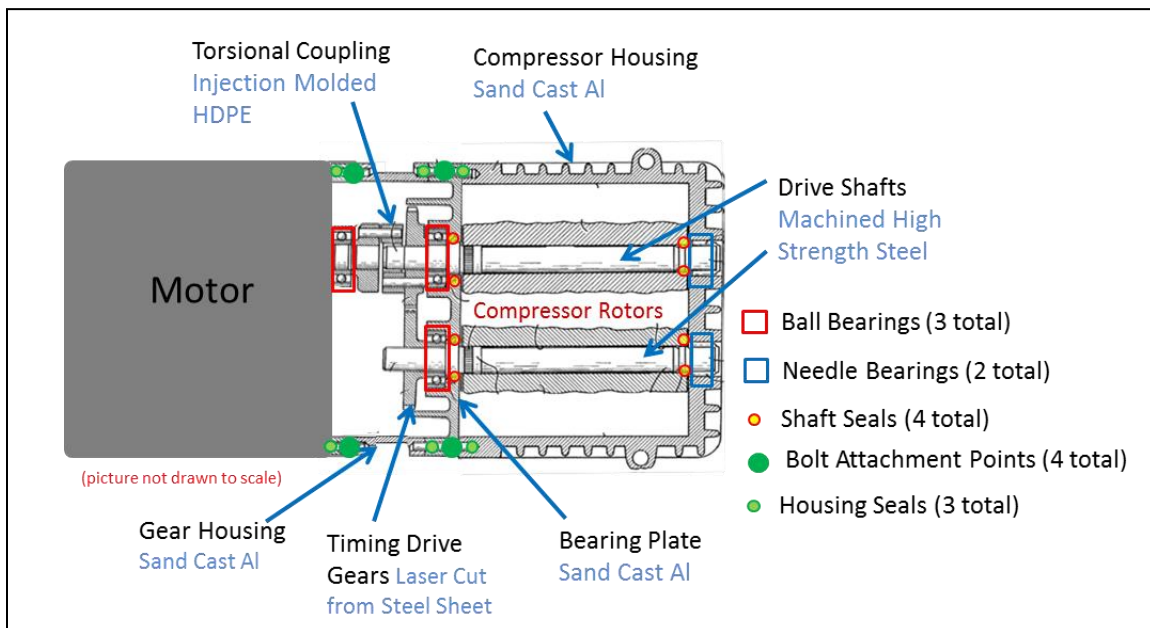
Figure 188. Schematic of cross-section of compressor-motor unit used in the DFMA[TM] cost analysis (Source: Drawing derivation from US patent 4,828,467: Richard J. Brown, Marshall, Mich. "Supercharger and Rotor and Shaft Arrangement Therefor", Eaton Corporation, Cleveland, Ohio, May 9, 1989)

The compressor rotors were modeled as hot extrusions of aluminum 6061-T1. Aluminum billets are assumed to be fed to an aluminum extrusion machine, such as that shown in Figure 190, using a custom stainless steel die to add twist to the extruded rotor billet. Extrusion rates are estimated at approximately 3 cm/sec[104] plus 30 seconds setup time (total 0.62min/rotor). At this extrusion rate and for only 1,000 systems per year, the machinery is highly underutilized. Consequently, the rotors are assumed to be fabricated by a vendor who can pool orders to more highly utilize machinery and thereby lower fabrication cost. A 30% markup is added to the projected vendor costs to reflect G&A, scrap, R&D, and profit and thereby translate the vendor cost into a sales price to the compressor manufacturer/assembler. Cost for extra precision machinery and quality control using a conjugate pair measuring machine[105] is included in the cost.

---

[104] Khalifa, N. B., Tekkaya, A.E., "Newest Developments on the Manufacture of Helical Profiles by Hot Extrusion", Journal of Manufacturing Science and Engineering, ASME, December 2011, Vol 133, 061010-1 to 8.

[105] "Inspection of Screw Compressor Rotors for the Prediction of Performance, Reliability, and Noise" International Compressor Engineering Conference at Purdue University, School of Mechanical Engineering, July 12-15,2004. http://docs.lib.purdue.edu/cgi/viewcontent.cgi?article=2691&context=icec

Summary of Components for SA Compressor/Motor Unit for Bus (Based on Eaton Design)						Annual Production Rate (systems/year)	
						200	1,000
	Material	Manufacturing Method	Qty/sys	Dimensions	kg/part	kg/sys	$/system	

	Material	Manufacturing Method	Qty/sys	Dimensions	kg/part	kg/sys	200	1,000
Compressor Components								
Compressor Rotor	6061-T1 Aluminum	Extrusion w/twist	2	21cm x 15cm Max OD	4.68	9.36	$143.77	$134.20
Compressor Housing	6061 Aluminum	Permanent Mold	1	26cm x 17cm x 22cm x 1cm (aver. Thickness)	2.33	2.33	$997.72	$223.79
Compressor Bearing Plate	6061-T1 Aluminum	Permanent Mold	1	17cm (width) x 22cm (height) x 1cm (aver. Thickness)	0.43	0.43	$329.84	$69.48
Compressor Shaft Seals	O-ring seal, polymer	Purchased	4	1.9cm (ID), 5cm (OD)	0.005	0.02	$11.17	$10.92
Timing Drive Gears (compressor: steel)	Stainless Steel	Laser cut from sheet	2	8.76 cm max OD, 1cm thick	0.435	0.869	$33.65	$32.91
Total						**13.00**	**$1,516.14**	**$471.32**
Other Components								
Housing/Motor Seals	O-ring seal, PET	Injection molded	3	17cm x 22cm x 0.2cm (diameter round X-section)	0.07	0.21	$93.51	$20.38
Housing Screws	SS 316	Purchased	4		0.005	0.02	$2.23	$2.18
Front Bearing	steel ball bearings, self lubricated	Purchased	3	5cm (diameter), 1.9cm (ID)	0.322	0.966	$9.05	$8.85
Rear Bearing	steel needle bearings, self lubricated	Purchased	2	5cm (diameter), 1.9cm (ID)	0.322	0.644	$8.71	$8.52
Rotor Drive Shafts	High carbon Steel Alloy	Rod, machined	2	1.9cm (diameter) x 23cm (length)	0.769	1.538	$20.24	$18.99
Torsionally Flexed Coupling	Fiberglass filled HDPE	Injection molded	1	3cm max OD, 1cm thick	0.004	0.004	$37.02	$9.24
Coupling Dowels	Steel	Rod, machined	3	0.25cm diameter, 3cm length	0.001	0.003	$1.73	$1.70
Gear Housing/Motor End Plates	6061-T1 Aluminum	Sand casting	1	17cm x 22cm (height) x 7cm (length) x 1cm (aver. Thickness)	1.08	1.08	$59.09	$24.10
Contingency (5% of total cost to account of any missing parts or erros in cost assumptions)							$396.28	$270.50
Assembly							$11.55	$11.16
Total						**4.47**	**$639.42**	**$375.62**
Motor Components								
Motor		Purchased	1		est 30	est 30	$4,094.85	$2,949.94
Motor Shaft Seal	formed seal	Purchased	1		0.01	0.01	$3.49	$3.41
Total						**30.01**	**$4,098.34**	**$2,953.36**
Subtotal Without Motor Controller								**$3,800.30**
Motor Controller Components								
Controller		Purchased	1		2.00	2.00	$2,067.94	$1,880.20
Total						**2.00**	**$2,067.94**	**$1,880.20**
Total Cost for 160kW Bus Fuel Cell System (including assembly and markup*)						**> 50**	**$8,321.83**	**$5,680.50**

*Each cost per system includes either a manufacturer markup (25% @ 1ksys/yr and 29% at 200sys/yr) or a pass-through markup (18%@1ksys/yr and 20%@200 sys/yr)

Figure 189. List of components for compressor, motor, and motor controller unit for the bus DFMA^{TM} analysis.

The timing drive gears are laser cut from a stainless steel sheet 1cm thick. The assumed laser cutting speed is approximately 0.6 cm per second (generously slower to account for intricate details in the driving gear geometry). The drive shafts for the compressor are made of a high carbon steel material and machined with a precision surface finish.

Figure 190. Medium hot extrusion press (HEP-112/72)[106]

The motor used in the analysis is considered to be a purchased component. Estimates obtained by Eaton through their DOE program suggest the cost of the motor for an automotive system to be ~$340 at 10,000 systems per year, $190 at 200,000 systems per year, and $160 at 500,000 systems per year. Cost of the compressor-motor drive motor for the bus system was scaled with air compressor motor shaft power and adjusted for lower manufacturing rates. The projected cost for the motor is shown in Figure 191 and is the most expensive component in the system other than the motor controller. The motor controller is about 40% the cost of the compressor-motor bus unit. The DFMA^{TM} analysis of the motor controller was completed in the previous 2012 bus analysis and re-used for the 2013 to 2015 analyses, after scaling for controller input power. The motor controller was also adjusted for lower manufacturing rates. Motor controller costs can also be viewed in Figure 191.

---

[106] Image from http://www.hydrononline.com/machines/hep-medium.htm

2015 Bus Compressor/Motor System Cost					
Annual Production Rate	*systems/year*	**200**	**400**	**800**	**1,000**
Compressor/Motor Components					
Compressor Rotor	$/sys	$143.77	$138.00	$135.15	$134.20
Compressor Housing	$/sys	$997.72	$512.57	$271.74	$223.79
Compressor Bearing Plate	$/sys	$329.84	$166.61	$85.59	$69.48
Compressor Shaft Seals	$/sys	$11.17	$11.06	$10.96	$10.92
Compressor Timing Drive Gears	$/sys	$33.65	$33.33	$33.02	$32.91
Housing/Motor Seals	$/sys	$93.51	$47.66	$24.19	$20.38
Housing Screws	$/sys	$2.23	$2.21	$2.19	$2.18
Front Bearing	$/sys	$9.05	$8.96	$8.87	$8.85
Rear Bearing	$/sys	$8.71	$8.63	$8.55	$8.52
Rotor Drive Shaft	$/sys	$20.24	$19.53	$19.09	$18.99
Torsionally Flexed Coupling	$/sys	$37.02	$19.62	$10.97	$9.24
Coupling Dowels	$/sys	$1.73	$1.72	$1.70	$1.70
Gear Housing/Motor end plates	$/sys	$59.09	$38.06	$26.41	$24.10
Contingency (5% of total)	$/sys	$396.28	$328.23	$282.30	$270.50
Assembly	$/sys	$11.55	$11.38	$11.21	$11.16
Motor	$/sys	$4,094.85	$3,555.70	$3,087.26	$2,949.94
Motor Shaft Seals	$/sys	$3.49	$3.46	$3.42	$3.41
Controller	$/sys	$2,067.94	$1,986.09	$1,905.75	$1,880.20
Total Eaton CEM Cost With Markup	**$/sys**	**$8,321.83**	**$6,892.82**	**$5,928.39**	**$5,680.50**
Total CEM Cost (Net)	**$/kWnet**	**$52.01**	**$43.08**	**$37.05**	**$35.50**
Total CEM Cost (Gross)	**$/kWgross**	**$42.74**	**$35.40**	**$30.45**	**$29.17**

Figure 191. Cost breakdown for bus compressor-motor unit

Figure 192 compares the cost of the Honeywell-style centrifugal compressor with that of the 2015 bus analysis Eaton-style compressor system. The Eaton-style system is observed to be appreciably more expensive, owing primarily to an increased motor cost. While real differences in type of motor exist (Honeywell uses a high rpm permanent magnet motor whereas Eaton uses a much lower rpm permanent magnet motor), the motor cost difference may be significantly influenced by differences in costing methodology between the two estimates: quote based vs. DFMA[TM] analysis. The Eaton-style motor cost was based on quotations for automotive size motors at high manufacturing rates (10,000 to 500,000 sys/yr), with a curve fit extrapolation used to predict cost of the automotive size motors at lower manufacturing rates (200-1,000 sys/yr). This projected cost was then scaled with power to reflect the cost of a bus size unit. In contrast, the Honeywell-style motor cost was based on a detailed DFMA[TM] analysis. The same markup percentages were applied to both the Honeywell and Eaton-style compressor systems for the bus so as to allow a fair comparison. However, the authors feel that the resulting motor cost may not accurately represent a motor used in the Eaton-style compressor-motor system and that using a curve fit extrapolation at such low production volumes (200-800 systems per year) does not accurately represent the cost. SA planned to re-evaluate more cost effective manufacturing processes at low volumes, particularly for the motor and motor controller in 2015. Instead SA focused on fuel cell stack-related manufacturing processes for low volume, but intends to follow through with balance of plant components next year. For 2015, motor controller cost was held constant for the Honeywell-style and Eaton-style systems, which may not be a valid assumption given the disparate compressor speeds

(165,000 rpm for the Honeywell-style unit vs. 24,000 rpm for the Eaton-style unit). There were no changes between the 2014 and 2015 bus CEM analyses.
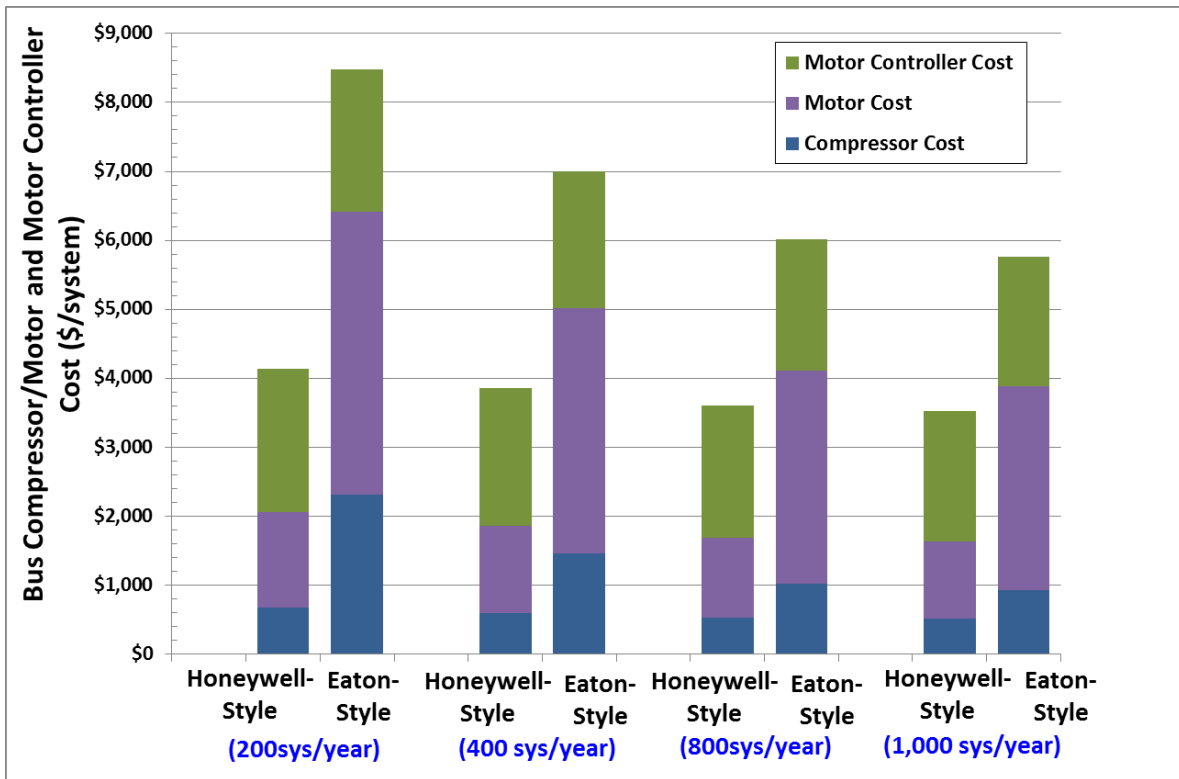
Figure 192. Comparison of cost for Honeywell-style design and the Eaton-style Compressor-Motor for a bus

9.4 Bus System Balance of Plant Components

To accommodate the increased flows and power level of a two-stack 160 kW$_{net}$ system, many balance of plant (BOP) components had to be revised. In some cases, the previous automotive DFMA^{TM}-style analysis of the balance of plant component automatically adjusted in response to the system design change. In other cases, new quotes were obtained, part scaling was included, or individual parts were increased in number (e.g. some parts are used on each of the two stacks). The changes to BOP components to reflect a bus system are summarized in Figure 193.

Balance of Plant Item	Bus System Change
CEM & Motor Controller	DFMA^{TM} analysis scaled to new flow and pressure ratio parameters, but switched to design without Expander
Air Mass Flow Sensor	New quote obtained for higher mass flow of bus system
Air Temperature Sensor	No change
Air Filter & Housing	New quote obtained for higher mass flow of bus system
Air Ducting	Piping and tubing diameters increased by a factor of 1.5 to adjust for higher mass flow of bus system
Air Precooler	DFMA^{TM} analysis scaled to new mass flow and temperature parameters.
Demister	Area size scaled by ratio of bus to automotive air flows
Membrane Air Humidifier	DFMA^{TM} analysis scaled to new gas mass flow and temperature parameters
HTL Coolant Reservoir	New quote obtained for larger expected coolant liquid volume of bus system
HTL Coolant Pump	New quote obtained for larger expected coolant flow of bus system
HTL Coolant DI Filter	Size scaled by factor of 2 to correspond to higher expected coolant flow rates of bus system
HTL Thermostat & Valve	New quote obtained for larger flow rate and pipe diameter of bus system
HTL Radiator	DFMA^{TM} analysis scaled to new heat rejection and temperature parameters of bus system
HTL Radiator Fan	New quote obtained corresponding to larger fan diameter and air flow rate parameters of bus system
HTL Coolant piping	Piping and tubing diameters increased by a factor of 1.5 to adjust for higher coolant flow of bus system
LTL Coolant Reservoir	New quote obtained for larger expected coolant liquid volume of bus system
LTL Coolant Pump	New quote obtained for larger expected coolant flow of bus system
LTL Thermostat & Valve	New quote obtained for larger flow rate and pipe diameter of bus system
LTL Radiator	DFMA^{TM} analysis scaled to new heat rejection and temperature parameters of bus system
LTL Radiator Fan	New quote obtained corresponding to larger fan diameter and air flow rate parameters of bus system
LTL Coolant Piping	Piping and tubing diameters increased by a factor of 1.5 to adjust for higher coolant flow of bus system
Inline Filter for Gas Purity Excursions	Size scaled by factor of 2 to correlate to increased hydrogen flow rate of bus system
Flow Diverter Valve	Quantity doubled to reflect use of two stacks in bus system
Over-Pressure Cut-Off Valve	Quantity doubled to reflect use of two stacks in bus system
Hydrogen High-Flow Ejector	Quantity doubled to reflect use of two stacks in bus system
Hydrogen Low-Flow Ejector	Quantity doubled to reflect use of two stacks in bus system
Check Valves	Quantity doubled to reflect use of two stacks in bus system
Hydrogen Purge Valve	Quantity doubled to reflect use of two stacks in bus system
Hydrogen Piping	Piping and tubing diameters increased by a factor of 1.5 to adjust

	for higher hydrogen flow of bus system
System Controller	Quantity doubled to reflect increased control/sensors data channels in bus system
Current Sensors	Quantity doubled to reflect use of two stacks in bus system
Voltage Sensors	Quantity doubled to reflect use of two stacks in bus system
Hydrogen Sensors	One additional sensor added to fuel cell compartment to reflect much larger volume of bus fuel cell system
Belly Pan	Excluded from bus system since a dedicated, enclosed engine compartment is expected to be used
Mounting Frames	Size increased to reflect use of two stacks and larger BOP component in bus system
Wiring	Cost doubled to reflect use of two stacks in bus system
Wiring Fasteners	Cost doubled to reflect use of two stacks in bus system

Figure 193: Explanation of BOP component scaling for bus power plant

10 Capital Equipment Cost

Figure 194 and Figure 195 display the tabulation of manufacturing/assembly processing steps along with the capital cost of each corresponding process train.[107] Multiple process trains are usually required to achieve very high manufacturing rates. The total capital cost (process train capital cost multiplied by the number of process trains) is also tabulated and shows that bipolar plate coatings is the highest capital cost process of the stack. This tabulation is meant to give an approximate cost of the uninstalled capital required for automotive stack and BOP production at 500,000 vehicles per year. Some steps are not included in the tabulation as they modeled as purchased components and thus their equipment cost is not estimated. Furthermore, the capital equipment estimates do not include installation, buildings, or support infrastructure and thus should not be used as an estimate of total capital needed for power plant fabrication. None the less, some insight may be obtained from this partial tabulation.

---

[107] A process train is a grouping of related manufacturing or assembly equipment, typically connected by the continuous flow of parts on a conveyor belt. For instance, the bipolar plate stamping process train consists of a sheet metal uncoiling unit, a tensioner, a 4-stage progressive stamping die, and a re-coil unit.

Stack Manufacturing Machinery Capital Costs at 500,000 sys/yr			
Step	**Capital Cost per Process Train**	**Number of Process Trains**	**Total Capital Cost**
Bipolar Plate Stamping	$530,446	59	$31,296,301
BPP Coating Step 1	*$1,764,868*	34	$60,005,500.45
BPP Coating Step 2	*$1,267,865*	*26*	$32,964,482.16
BPP Coating Step 3	*$249,563*	*16*	$3,993,007.43
BPP Coating	$3,282,295	25	$96,962,990
Membrane Production	$35,000,000	1	$35,000,000
NSTF Coating	$2,002,728	16	$32,043,651
Microporous GDL Creation	Purchased Comp.		Not Incl.
MEA Gasketing-Subgaskets	$2,958,600	3	$8,875,800
MEA Cutting and Slitting	$469,136	2	$938,272
MEA Gasketing - Screen Printed Coo	$1,458,755	17	$24,798,842
Coolant Gaskets (Laser Welding)	$856,433	34	$29,118,736
End Gaskets (Screen Printing)	$392,735	1	$392,735
End Plates	$541,337	3	$1,624,010
Current Collectors	$166,573	1	$166,573
Stack Assembly	$821,339	52	$42,709,638
Stack Housing	$655,717	1	$655,717
Stack Conditioning	$673,202	22	$14,810,447
Stack Total			**$319,393,711**

* Bipolar plate coating is based on a vendor-proprietary manufacturing method that consists of multiple sub-process trains. The process train quantity listed is an average of the constituent sub-trains.

Figure 194. Automotive stack manufacturing machinery capital costs at 500,000 systems per year

Balance of Plant Manufacturing Machinery Capital Costs at 500,000 sys/yr			
Step	Capital Cost per Process Train	Number of Process Trains	Total Capital Cost
Membrane Air Humidifier	6,143,850	5	$11,625,896
Belly Pan	655,717	1	$655,717
Ejectors	[Not Calculated]	N/A	[Not Calculated]
Stack Insulation Housing	655,717	1	$655,717
Air Precooler	[Not Calculated]	N/A	[Not Calculated]
Demister	288,522	1	$288,522
CEM	[Not Calculated]	N/A	[Not Calculated]
(Partial) BOP Total	Does not include processes with un-calculated capital costs ⟶		$13,225,852

* The membrane air humidifier involves an aluminum casting step which is not included in the capital equipment tabulation.

Figure 195. Automotive balance of plant manufacturing machinery capital costs at 500,000 systems per year

11 Automotive Simplified Cost Model Function

A simplified cost model to estimate the total automotive power system cost at 500,000 systems/year production rate is shown in Figure 196. The simplified model splits the total system cost into five subcategories (stack cost, thermal management cost, humidification management cost, air management cost, fuel management cost, and balance of plant cost) and generates a scaling equation for each one. The scaling equations for individual cost components are based on key system parameters for that component that are likely to be known to analysts conducting a general study. The curves are generated by regression analysis of data generated by successive runs of the full DFMA^{TM}-style cost model over many variations of the chosen parameters. The simplified model allows a quick and convenient method to estimate system cost at off-baseline conditions.

C_system = Total System Cost = C_stack + C_thermal + C_Humid + C_air + C_Fuel + C_BOP

C_{stack} = **Total Fuel Cell Stack Cost**

100 Volt, Cstack = $8.8345 \times 10^{-5} \times ((0.37932 \times A + 1{,}698.25) \times L \times PC) + (0.00787 \times A) + 203.17$

150 Volt, Cstack = $8.8345 \times 10^{-5} \times ((0.37932 \times A + 1{,}698.25) \times L \times PC) + (0.00707 \times A) + 287.70$

200 Volt, Cstack = $8.8345 \times 10^{-5} \times ((0.37932 \times A + 1{,}698.25) \times L \times PC) + (0.00710 \times A) + 304.55$

250 Volt, Cstack = $8.8345 \times 10^{-5} \times ((0.37932 \times A + 1{,}698.25) \times L \times PC) + (0.00695 \times A) + 349.63$

300 Volt, Cstack = $8.8345 \times 10^{-5} \times ((0.37932 \times A + 1{,}698.25) \times L \times PC) + (0.00684 \times A) + 398.96$

Where: A = Total active area of the stack (cm^2)

L = Pt Loading (mg/cm^2) **Baseline Stack Cost: $2,051**

PC = Platinum cost ($/troy ounce)

$C_{thermal}$ = **Thermal Management System Cost**

$= [\, 100.11447 \times (Q_{HT} / \Delta T_{HT}) + 180.82\,]$

$+ [\, 1.01412 \times (Q_{LT} / \Delta T_{LT})^2 + 108.53612 \times (Q_{LT} / \Delta T_{LT}) - 2.51664 \times P^2 + 23.62612 \times P - 2.75845 \times P \times (Q_{LT} / \Delta T_{LT}) - 19.09\,]$

Where: Q_{HT} = Radiator Duty ($kW_{thermal}$) of High Temperature Loop

Q_{LT} = Radiator Duty ($kW_{thermal}$) of Low Temperature Loop

ΔT_{HT} = Difference between coolant outlet temperature from fuel cell stack and ambient temperature (°C)

ΔT_{LT} = Difference between coolant outlet temperature from air precooler and ambient temperature (°C)

P = Stack Operating Pressure (atm)

*High Temperature Loop includes: coolant reservoir, coolant pump, coolant DI filter, coolant piping, thermostat & valve, radiator fan, and radiator.

*Low Temperature Loop includes: coolant reservoir, coolant pump, coolant piping, thermostat & valve, and radiator.

Baseline Thermal Management System Cost: $387

C_{Humid} = **Humidification Management System Cost**

$= (0.586199 \times A^2 + 43.76653 \times A + 14.74) + (496.93495 \times (Q / \Delta T) - 1.86)$

Where: A = Humidifier Membrane Area (m^2)

Q = Heat Duty for Precooler (kW)

ΔT = Delta Temp. (compr. exit air minus coolant temperature into air precooler)(°C)

*Includes Air Precooler and Membrane Humidifier.

Baseline Humidification Management System Cost: $107

C_{air} = **Air Management System Cost**

$= 479.42 + (19.80524 \times P) + (0.59662 \times P \times MF)$

Where: P = Air Peak Pressure (atm)

MF = Max Air Mass Flow Out of Compressor (kg/hr)

*Includes demister, compressor, expander, motor, motor controller, air mass flow sensor, air/stack inlet manifold, air temperature sensor, air filter and housing, and air ducting.

Baseline Air Management System Cost: $936

C_{Fuel} = **Fuel Management System Cost**

$= (3801.97 \times BP^3 - 2967.73 \times BP^2 + 1573.1 \times BP - 87.81) + 237.59$

Where: BP = blower power (kW)

*Includes valves, ejectors, hydrogen inlet and outlet of stack manifolds, piping, and recirculation blower. Baseline system does not include blower, therefore the Fuel Management System is a constant $238.

Baseline Fuel Management System Cost: $238

C_{BOP} = **Additional Balance of Plant Cost**

Where: C_{BOP} = $509.53

*Includes system controllers, sensors, and miscellaneous components.

Baseline Additional BOP Cost: $509

Figure 196: Simplified automotive cost model at 500,000 systems per year production rate

Because the simplified cost model equations are based upon regression analysis, there is an input parameter range outside of which the resulting cost estimates are not guaranteed to be accurate. The ranges for each parameter in each sub-equation are given in Figure 197 below.

Validity Range for Stack Cost				
Parameter	Min Value	Baseline Value	Max Value	Units
System Power	60	80	120	kW_{net}
Stack Voltage	100	250	300	V
L	0.1	0.142	0.8	mg/cm^2
A	88,987	118,253	177,086	cm^2
PC	800	1,500	2,000	$/troy ounce
Validity Range for Thermal Management System				
Parameter	Min Value	Baseline Value	Max Value	Units
ΔT_{HT}	38	54	70	°C
ΔT_{LT}	25	25	70	°C
Q_{HT}	57	79	120	kW
Q_{LT}	1.8	9	18	kW
P	1.5	2.5	3.0	atm
Validity Range for Humidification Management System				
Parameter	Min Value	Baseline Value	Max Value	Units
A	0.3	1.15	4	m^2
Q	2	7.3	15	kW
ΔT	22	99	132	°C
Validity Range for Air Management System				
Parameter	Min Value	Baseline Value	Max Value	Units
P	1.65	2.57	3.15	atm
MF	258	263	544	kg/hr
Validity Range for Fuel Management System				
Parameter	Min Value	Baseline Value	Max Value	Units
BP	0.2	0	0.3	kW

Figure 197: Range of validity for simplified cost model parameters

As a check on the accuracy of the simplified regression model, the results of the full DFMA[TM] model are compared to the calculations from the simplified model for the parameter of system net power. These results are displayed in Figure 198 indicating very good agreement between the two models within the range of validity.
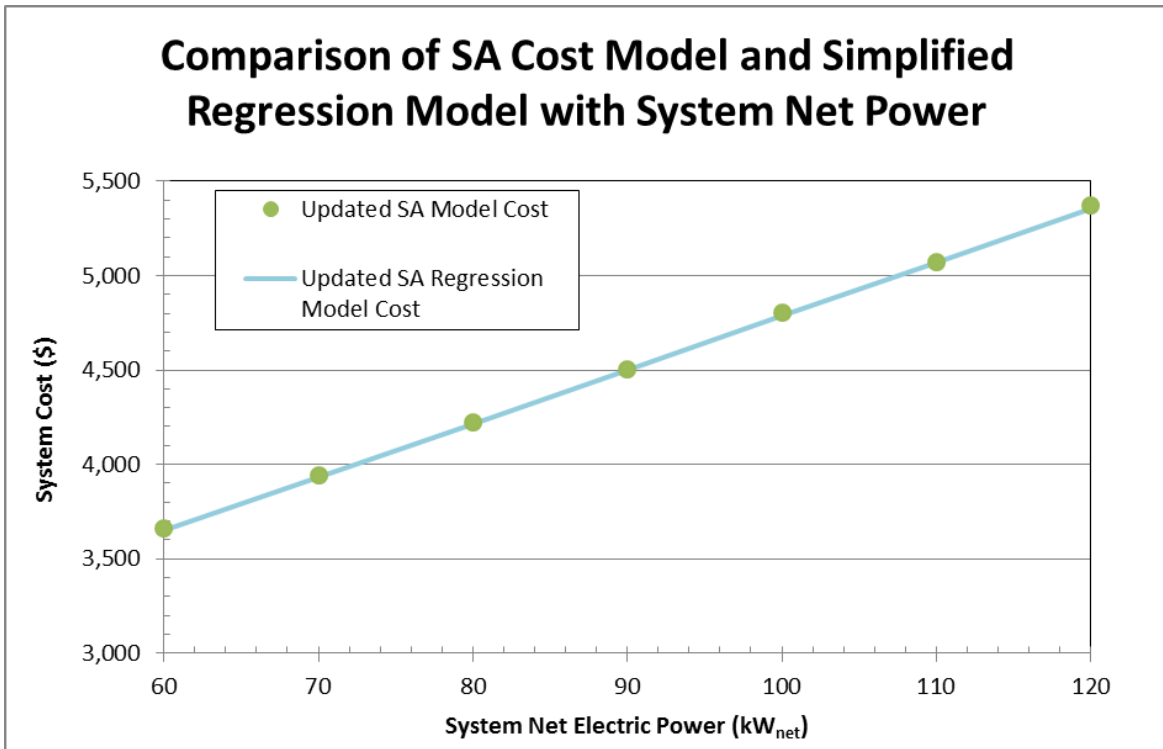
Figure 198: Comparison of SA cost model with simplified cost model at 500,000 systems per year.

12 Life Cycle Analysis (LCA)

Up-front cost per kW, while a useful metric and the primary focus of this report, is not the sole determining factor in market worthiness of a power system. Total life cycle cost is an equally important consideration that takes into account the initial purchase price, cost of fuel used over the lifetime of the system, system decommissioning costs and recycle credits, and operating and maintenance expenses, all discounted to the present value using a discounted cash flow methodology. By comparing life cycle costs, it is possible to determine whether an inexpensive but inefficient system (low initial capital cost but high operating and fuel expenses) or an expensive but efficient system (high initial capital cost but low operating and fuel expenses) is a better financial value to the customer over the entire system lifetime.

12.1 Platinum Recycling Cost

Since cost of the catalyst platinum within the fuel cell stacks represents a significant fraction of total system cost, particular attention is paid to recovering the Pt at the end of stack life. Two basic approaches are possible for allocating Pt cost:

- An ownership paradigm wherein the consumer buys the Pt contained within the stacks of the fuel cell vehicle, and thus the Pt has a value to the vehicle owner at the end of stack life. (This is the paradigm used in the baseline cost analysis and in the LCA.)
- A renting paradigm, wherein a precious metal dealer (such as Johnson-Matthey or the vehicle manufacturer) owns the Pt in the stacks, the Pt purchase price is not charged to the vehicle owner at the time of purchase, and the value of the Pt at the end of stack life accrues to the precious metal dealer (not to the vehicle owner). (This paradigm is not used in the baseline analysis or LCA but may be considered in future years.)

The ownership paradigm will now be more fully explored.

The life cycle cost analysis under the ownership paradigm is based upon adapting existing vehicular catalytic converter recycling parameters to expectations for a fuel cell system.[108,109] Based on analysis of platinum recycling conducted by Mike Ulsh at the National Renewable Energy Laboratory, total platinum loss during operation and recovery is estimated at:

- a 1% loss during operational life,
- 5% loss during recycling handing, and
- 2%-9% loss during the recycling process itself.[110,111]

---

[108] "The impact of widespread deployment of fuel cell vehicles on platinum demand and price," Yongling Sun, et. al. International Journal of Hydrogen Energy 36 (2011).

[109] "Evaluation of a platinum leasing program for fuel cell vehicles," Matthew A. Kromer et. al., International Journal of Hydrogen Energy 34 (2009).

[110] L. Shore, "Platinum Group Metal Recycling Technology Development," BASF Catalysts LLC final project report to DOE under subcontract number DE-FC36-03GO13104, 2009.

[111] "The impact of widespread deployment of fuel cell vehicles on platinum demand and price," Yongling Sun, et. al. International Journal of Hydrogen Energy 36 (2011).

Ten percent (10%) is chosen as the Pt loss baseline value while the low (8%) and high (15%) end are represented in the sensitivity analysis below. The cost of recycling[112] is expected to range between $75 and $90 per troy ounce of recovered platinum. However this is only the cost incurred by running the actual recycle process. In addition, there are supply chain costs as the capturer or salvager collecting the unit desires to be paid. Based on current catalyst converter practice, the salvager expects to be paid by the recycler about 70%-75% of the total value of recycled platinum[113] with the remaining Pt value going to the recycle as payment for the recycle process. Whether this comparatively high fraction of Pt value would continue to accrue to the supply chain salvager for fuel cell stack platinum is unclear. If it does, the owner of the fuel cell automobile effectively gets no value from the recycled Pt, just as, in general, a person selling an internal combustion vehicle for scrap does not separately receive payment for the catalytic converter. However, as the value of Pt in the fuel cell may be greater than that of a catalytic converter, the paradigm may be different in the future. Consequently, as a baseline for the LCC analysis, the salvager is estimated to receive 35% (half the value received for catalytic converters) of the value of the recovered Pt less recycling cost. A sensitivity analysis is conducted for cases where the salvager captures only 10% and 75% of the recovered value. Finally, due to platinum market price volatility, it is unlikely that Pt price will be exactly the same at system purchase as it is 10 years later at time of recycle. Consequently, for purposes of the baseline LCC analysis, the price of platinum is held constant at the purchase price used for the catalyst within a new vehicle ($1,500 / tr. oz.), and sensitivity analysis is conducted for a future[114] higher Pt price ($2100/tr. oz. at end of life).

To further explore these assumptions, additional conversations with precious metal suppliers were initiated in 2014. Those talks were not sufficiently completed to be incorporated into the 2014 or 2015 analyses but a few comments may be shared. In the opinion of at least one precious metal supplier, a rental paradigm rather than a Pt ownership paradigm is considered most likely for future FCV sales. Additionally, the current methodology for recovery Pt was described as consisting of the following steps:

1) Agreement between refiner and supplier of the expected total Pt in the sample
2) Assay of contaminates within the sample
3) Assessment of a "deleterious elements" charge
4) Imposition of a Retention charge (typically 2-3%)
5) Imposition of a Refining charge (typically 1-2%)

This would appear to place the recycling charge within the 2-9% range as projected above, thereby broadly confirming the analysis assumptions. However, further clarification of terms and values is needed and will be pursued in future analyses.

---

[112] Ibid.

[113] Ibid.

[114] Platinum price is considered more likely to increase in the future rather than decrease. Consequently, the future price of Pt is based on the current Pt market price (~$1500/tr. oz) plus a $60/tr. oz. per year increase, resulting in a $2100/tr. oz. price after 10 years.

12.2 Life Cycle Analysis Assumptions and Results

The life cycle analysis (LCA) of life cycle cost analysis (LCCA[115]) for this report assumes a set of driving conditions and platinum recycling costs to compute the total present value cost of ownership for the lifetime of the vehicle. These assumptions are summarized in the figure below.

Life Cycle Cost Assumption	Value
Sales markup	25% of calculated system cost
Discount rate	10%
System lifetime	10 years
Distance driven annually	12,000 miles
System efficiency at rated power	48% (calculated by model)
Fuel economy	61.4 mpgge[116]
Hydrogen to gasoline lower heating value ratio	1.011 kgH$_2$/gal gasoline
Fuel cost	$5 / kg H$_2$
Total Pt loss during system lifetime and the Pt recovery process	10%
Market Pt price at end of system lifetime	$1,500 / tr. oz.
Cost of Pt recovery	$80 / tr. oz.
% of final salvaged Pt value charged by salvager	35%

Figure 199. Life cycle cost assumptions

Under these assumptions, a basic set of cost results is calculated and displayed in Figure 200. Note that these results are only computed for the automotive system and not for the bus system; bus drive cycle and use patterns are vastly different from the average personal vehicle. Additional modeling and research is required to develop a representative equation governing the fuel economy of transit buses.

	2015 Auto System Life Cycle Costs					
Annual Production Rate	**1,000**	**10,000**	**30,000**	**80,000**	**130,000**	**500,000**
System Cost	$16,336	$7,357	$5,749	$4,920	$4,742	$4,228
System Price (After Markup)	$20,420	$9,196	$7,186	$6,150	$5,927	$5,284
Annual Fuel Cost	$965	$965	$965	$965	$965	$965
Lifecycle Fuel Cost	$5,930	$5,930	$5,930	$5,930	$5,930	$5,930
Net Present Value of Recoverable Pt in System at End of System Lifetime	$266	$266	$266	$266	$266	$266
Final Pt Net Present Value Recovered	$173	$173	$173	$173	$173	$173
Total Lifecycle Cost	$26,177	$14,953	$12,943	$11,907	$11,684	$11,041
Total Lifecycle Cost ($/mile)	**$0.218**	**$0.125**	**$0.108**	**$0.099**	**$0.097**	**$0.092**

Figure 200: Auto LCC results for the baseline assumptions

The variation of life cycle cost with system efficiency was studied in order to examine the trade-offs between low efficiency (higher operating costs but lower initial capital costs) and high efficiency (lower

---

[115] The abbreviations LCA and LCCA are both used within the analysis community.
[116] Calculated from system efficiency at rated power based on formula derived from ANL modeling results: Fuel economy = 0.0028x^3 - 0.3272X^2+12.993X - 116.45, where x = system efficiency at rated power.

operating costs but higher initial capital costs) systems. Figure 201 shows the polarization curve with system efficiency at rated power.
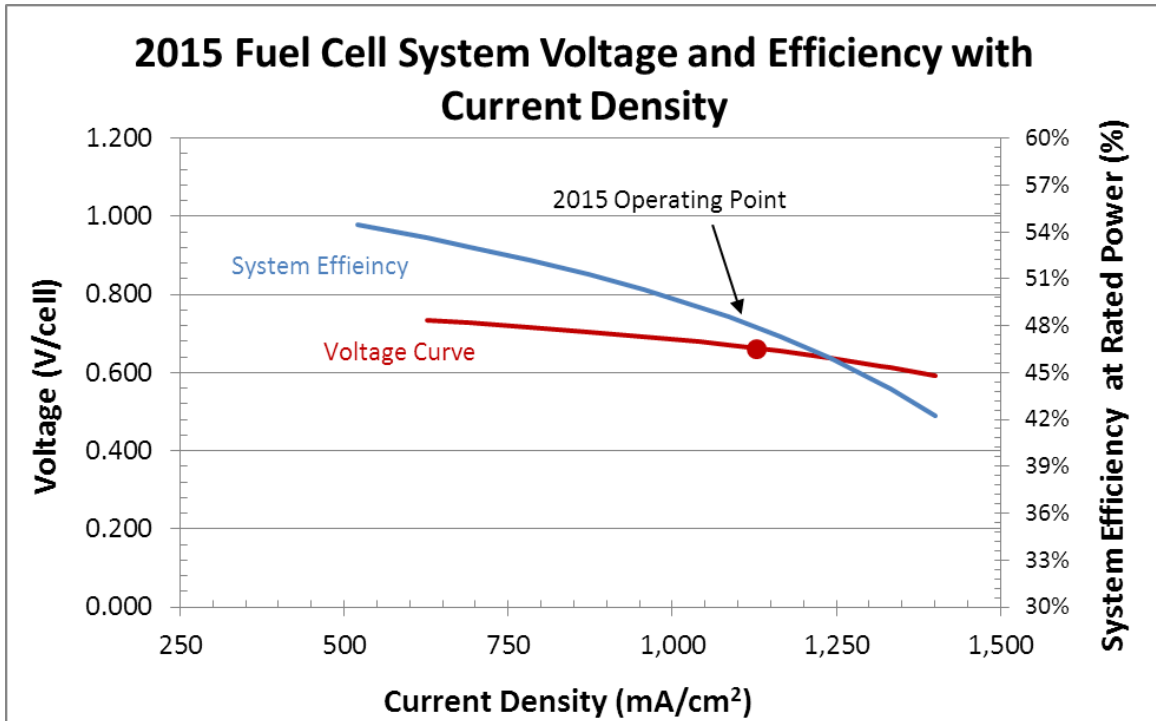
Figure 201: Polarization curves for efficiency sensitivity analysis

With this relationship, it is possible to calculate the variation in life cycle cost contributors over a range of efficiencies. These results are shown below. Figure 202 displays the results for the total life cycle cost as well as its component costs on an absolute scale. Note that the total life cycle cost (i.e. the present value of the 10 year expenses of the power system) is expressed as a $/mile value for easy comparison with internal combustion engine vehicle life cycle analyses. Figure 203 shows a zoomed-in look at the total cost, indicating a minimum total life cycle cost at the baseline system value of 48% system efficiency (corresponding to 53% fuel cell stack efficiency and cell voltage of 0.661 V/cell). However, the range of LCC cost variation over the range of system efficiencies examined is quite small, indicating that LCC is generally insensitive to system efficiency.
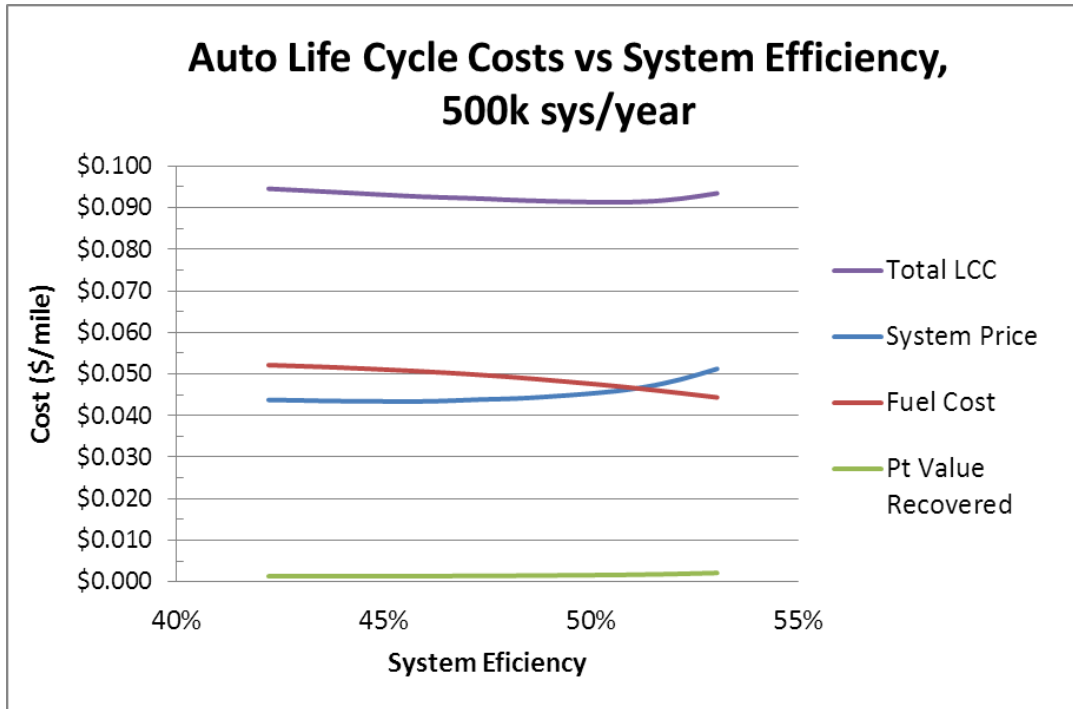
Figure 202: Life cycle cost components vs. fuel cell efficiency for 500k automobile systems/ year
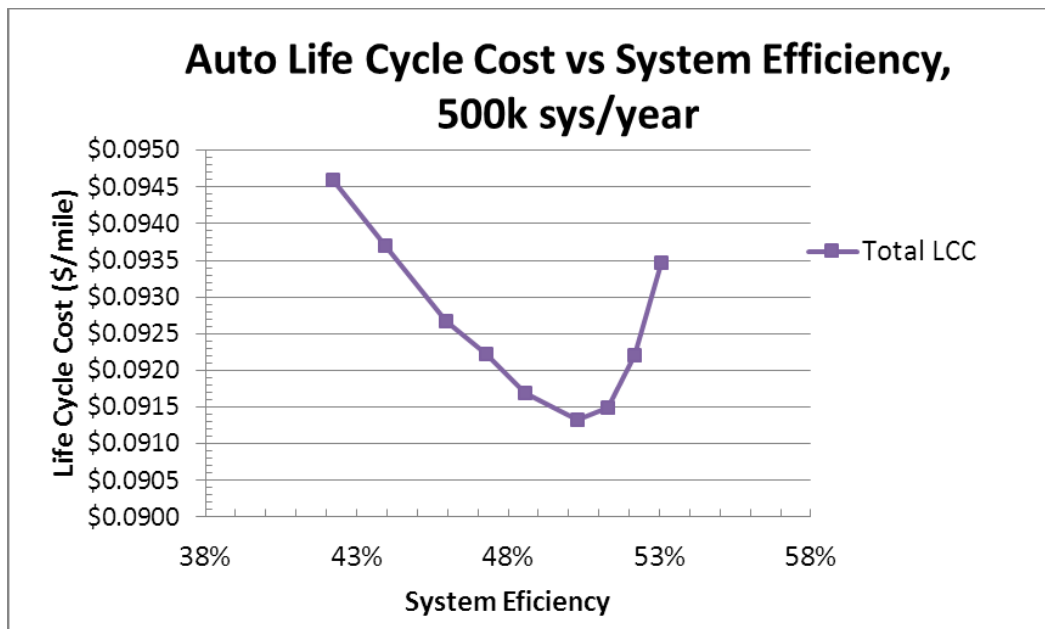
Figure 203: Life cycle cost vs. fuel cell efficiency for 500k automobile systems/year

In addition to the efficiency analysis, a simple sensitivity study was conducted on the parameters governing the platinum recycle, to determine the magnitude of the effect platinum recycling has on the life cycle cost. Figure 204 below displays the total life cycle cost in $ per mile as a function of platinum price during the year of the recycle for three scenarios: the baseline case where the salvager captures 35% of the value of recovered platinum and two sensitivity cases where the salvager captures 10% of the value at the low end and 75% of the value at the high end.

185
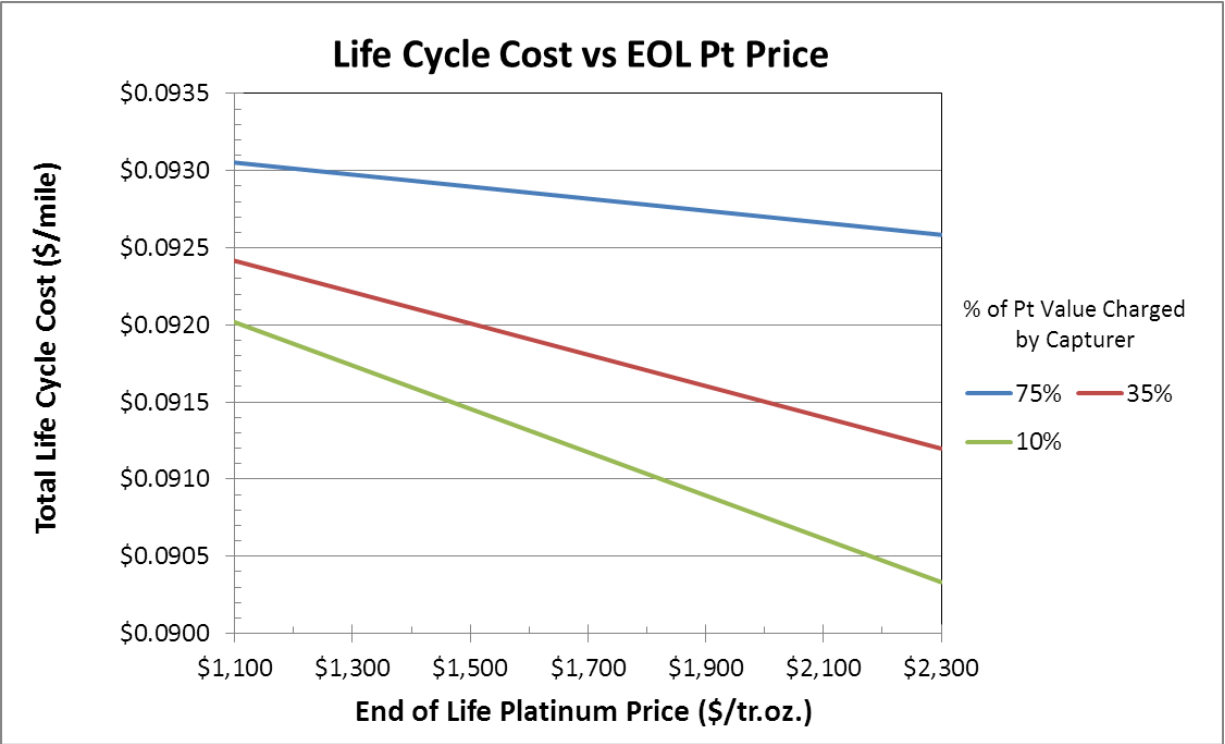
Figure 204: Life cycle cost vs. end of life platinum price (at 500k system/year)

Additional parameters were explored and are displayed as a tornado chart in Figure 205 and Figure 206. These results indicate that platinum recycle parameters do not have a large effect on the overall life cycle cost (~1%).

Life Cycle Cost ($/mile), 500,000 systems/year				
Parameter	Units	Low Value of Variable	Base Value	High Value of Variable
Salvage Value Charged	%	10%	35%	75%
Pt Price at Recovery	$/tr.oz.	$1,100	$1,500	$2,100
Total Pt Loss	%	8%	10%	15%
Cost of Recovery	$	$70	$80	$90
2015 Auto System LLC ($/mile)			**$0.09201**	

Figure 205: Life cycle cost tornado chart parameters
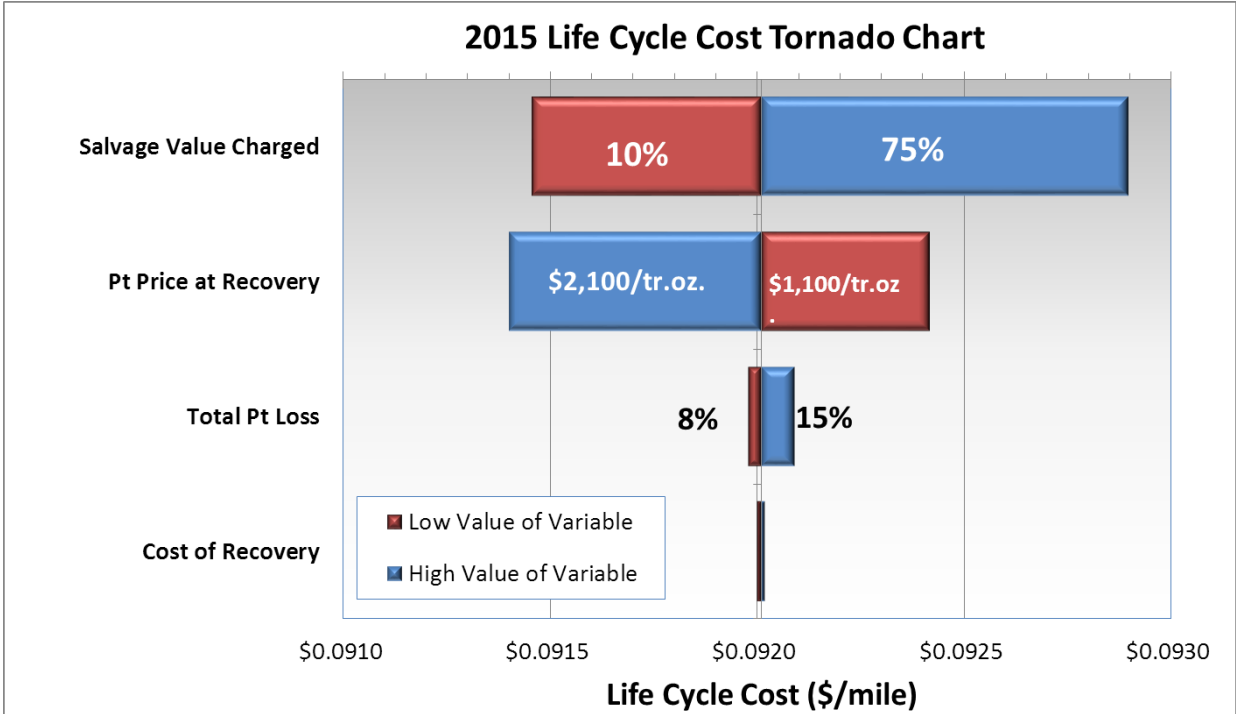
Figure 206: Life cycle cost tornado chart (at 500k systems/year)

13 Sensitivity Studies

A series of tornado and Monte Carlo sensitivity analyses were conducted to determine key parameters and assess avenues to further reduce cost.

13.1 Single Variable Analysis

13.1.1 Single Variable Automotive Analysis

A single variable analysis was performed to evaluate which parameters have the largest effect on system cost. Figure 207 shows the parameter ranges used to develop the tornado chart, while Figure 208 displays the results of the analysis.

2015 Auto Sensitivity Ranges (500,000 sys/year)				
Parameter	Units	Min Param. Value	Base Value	Max Param. Value
Pt Loading	mgPt/cm^2	0.125	0.142	0.300
Power Density	mW/cm^2	634	746	1119
Air Loop Cost (including CEM)	$/system	$555	$936	$1,231
Bipolar Plate Cost	$/kW$_{net}$	$3.00	$6.98	$10.00
Air Stoichiometry		1.5	1.5	2.0
Hydrogen Recirculation System Cost	$/system	$158.48	$237.59	$356.39
Active to Total Area Ratio		0.55	0.625	0.80
Bipolar Plate Welding Speed	m/min	2.5	15.0	15.0
Q/DT Constraint	kW/°C	1.35	1.45	1.55
EPTFE Cost	$/m2	$3.00	$6.00	$10.20
Ionomer Cost	$/kg	$49.22	$82.04	$164.08
GDL Cost	$/m2	$2.98	$4.08	$5.30
Membrane Humidifier Cost	$/system	$49.23	$65.64	$98.47
2015 Auto System Cost ($/kWnet)			$52.84	

Figure 207: 2015 automotive results tornado chart parameter values

As shown in Figure 208, variations in operating condition parameters power density and platinum loading have the most capacity to affect system cost. For the case of power density, this affects the size and performance of the entire system, trickling down into cost changes in many components. Platinum loading's large effect is attributable to the very high price of platinum relative to the quantities used in the system. Active to total area ratio and Q/ΔT are newly added variables for the 2015 Tornado sensitivity analysis. Air loop cost range takes into account the air compressor cost range,[117] efficiencies

---

[117] CEM cost multiplier: Low end is 33% reduction of calculated cost to get a min value of $500/system from DOE targets. High end is 20% increase of calculated cost.

for the air compressor, expander, and motor controller,[118] and balance of air compressor cost range.[119] Note that while resizing of the compressor and stack to reflect a different air flow rate (range in stoichiometric rates) is included in the system cost impact, the impact on power density is not.
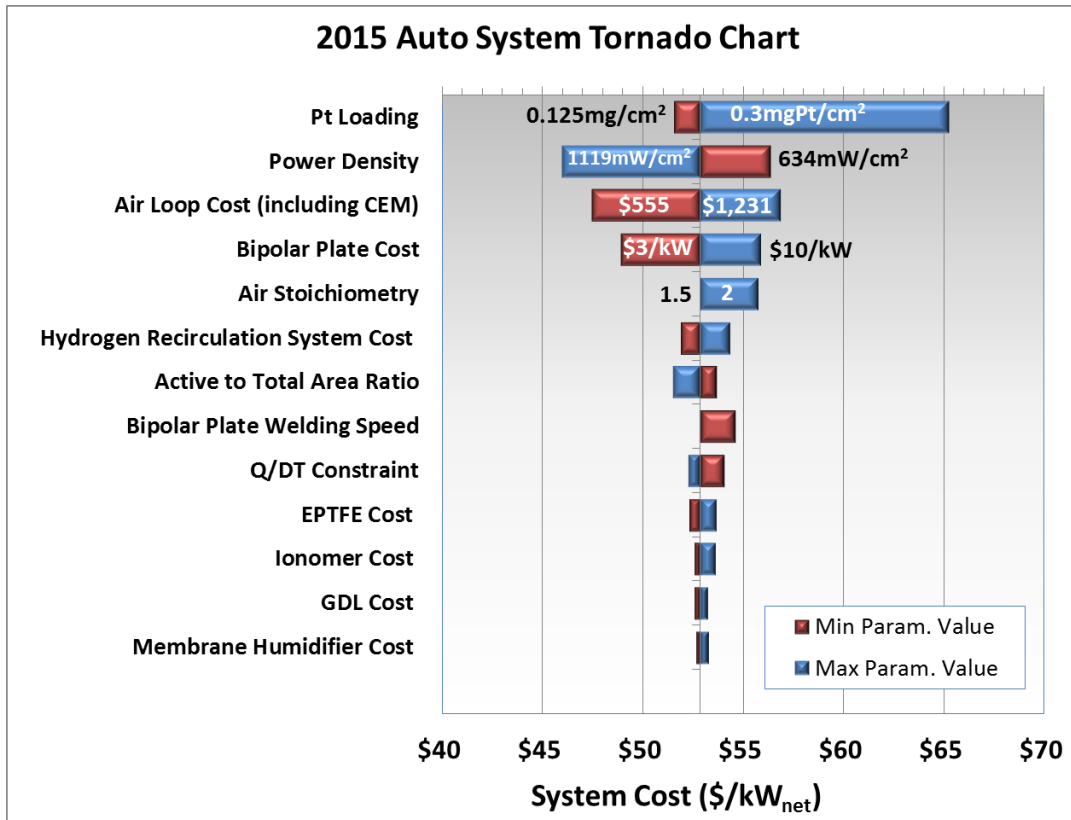
Figure 208: 2015 Auto results tornado chart

13.1.2 Automotive Analysis at a Pt price of $1100/troy ounce

To aid in comparisons to other previous cost studies, the automotive system was also evaluated with a platinum price of $1,100/troy ounce (instead of the baseline value of $1,500/troy ounce). All other parameters remain the same. Results are shown in Figure 209.

---

[118] Efficiencies: 0.97 factor on efficiency for min values and max value is DOE target: Compressor Effic.: 69% min (71% baseline) to 75% max; Expander Effic.: 71% min (73% baseline) to 80% max; Motor/Controller Effic.: 78% min (80% baseline) to 90% max.
[119] Balance of Air Compressor Cost: 2/3 of value at min, 1.5 factor at max.

Annual Production Rate	systems/year	2015 Automotive System					
		1,000	10,000	30,000	80,000	100,000	500,000
System Net Electric Power (Output)	kWnet	80	80	80	80	80	80
System Gross Electric Power (Output)	kWgross	88	88	88	88	88	88
Component Cost/System							
Fuel Cell Stacks	$/system	$11,117	$3,810	$2,748	$2,260	$2,171	$1,818
Balance of Plant	$/system	$4,828	$3,204	$2,662	$2,323	$2,234	$2,075
System Assembly & Testing	$/system	$148	$103	$101	$101	$101	$101
Total System Cost	$/system	$16,093	$7,118	$5,511	$4,684	$4,506	$3,994
Total System Cost	$/kWnet	$201.17	$88.97	$68.89	$58.55	$56.33	$49.92
Cost/kWgross	$/kWgross	$182.42	$80.68	$62.47	$53.10	$51.08	$45.27

Figure 209: Detailed system cost for the 2015 automotive technology system with a Pt price of $1,100/troy ounce

13.1.3 Single Variable Bus Analysis

A single variable Tornado Chart analysis of the bus system was also conducted. Assumptions are shown in Figure 210 and results in Figure 211.

As with the automotive system, power density and platinum loading have the largest potential to vary system cost. Unlike the automotive system, however, there is also a large cost variation potential to be found in GDL cost variations. This is because at lower manufacturing rate, the cost of manufactured component items is high and subject to large changes in cost relative to components manufactured at high volume, as in the automotive case.

2015 Bus System Cost ($/kWnet), 1,000 sys/year				
Parameter	Units	Low Value	Base Value	High Value
Power Density	mW/cm^2	517	**739**	1012
Pt Loading	mgPt/cm^2	0.25	**0.5**	1
GDL Cost	$/m^2	$85.40	**$116.98**	$152.07
Air Stoichiometry		1.5	**1.8**	2.1
Air Compressor Cost Factor		0.8	**1**	1.2
Compressor / Motor & Motor Controller Efficiencies	%	56%/92%	**58%/95%**	75%/95%
Bipolar Plate & Coating Cost Factor		1	**1**	2
EPTFE Cost Multiplier		0.667	**1.00**	2.20
Ionomer Cost	$/kg	$46.16	**$209.83**	$514.08
Hydrogen Recirculation System Cost	$/system	$594.20	**$891.26**	$1,782.52
Membrane Humidifier Cost	$/system	$324.64	**$649.28**	$1,298.56
Active to Total Area Ratio		0.55	**0.625**	0.8
Balance of Air Compressor Cost	$/system	$341.88	**$512.79**	$1,025.57
Membrane Thickness	μm	15	**25.4**	25.4
2015 Bus System Cost			**$261.97**	

Figure 210: 2015 Bus results tornado chart parameter values
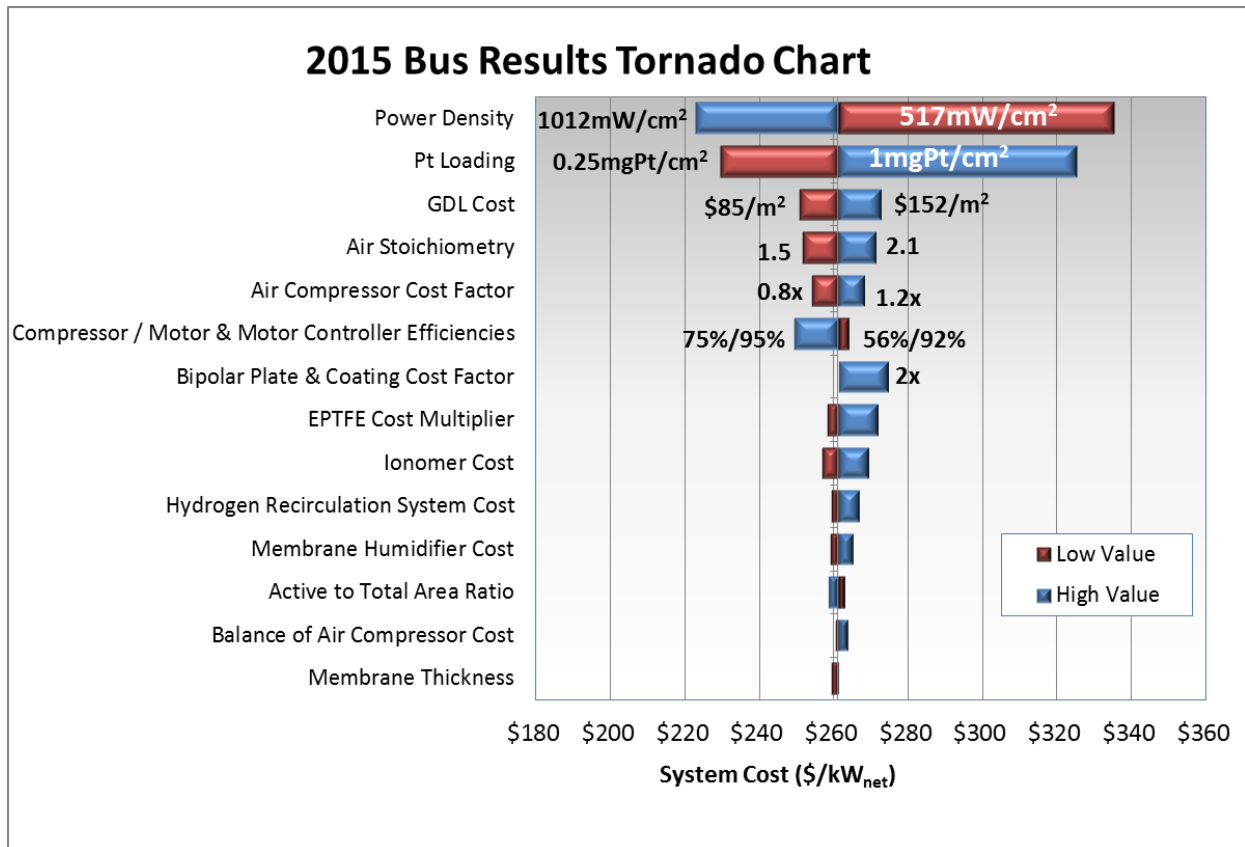
Figure 211: 2015 Bus results tornado chart

13.2 Monte Carlo Analysis

In order to evaluate the bounds for the likely variation in final results, a Monte Carlo analysis was conducted for both the automotive and bus results. With these results, it is possible to examine the probability of various model outcomes based upon assumed probability distribution functions (PDFs) for selected inputs. For all inputs, triangular distributions were chosen with a minimum, maximum, and most likely value. The most likely value is the result used in the baseline cost analysis, while the maximum and minimum were chosen with the input of the Fuel Cell Tech Team to reflect likely real-world bounds for 2015. The 2015 limits are quite similar to those from 2014, with no major deviations.

13.2.1 Monte Carlo Automotive Analysis

Assumptions and results for the Monte Carlo analysis of the automotive system are shown in Figure 212. In previous years, the Monte Carlo analysis was conducted solely for 500,000 systems per year. In 2014 the Monte Carlo analysis was expanded to all manufacturing rates. The lower and upper limits for the Monte Carlo analysis are presented as multipliers (or percentages) on each parameter's most likely value (eg. lower bound = 50% of the likeliest value, upper bound = 150% of the likeliest value). While these limits were initially conceived solely for application at 500,000 systems per year, upon consideration they were judged to be reasonably applied to all manufacturing rates.

The numerical bounds for the Monte Carlo Results for manufacturing rate of 500,000 systems per year are shown in Figure 213. Results are shown graphically in Figure 214. Further results of automotive stack, BOP, and total system cost are shown in Section 0.

Monte Carlo analysis indicates that the middle 90% probability range of cost is between $47.81/kW$_{net}$ and $62.27/kW$_{net}$ for the automotive system at 500,000 systems per year.

2015 Auto Technology Monte Carlo Analysis				
Parameter	Unit	Minimum Value	Likeliest Value	Maximum Value
Power Density	mW/cm2	634	**746**	1119
Pt Loading	mgPt/cm2	0.125	**0.142**	0.3
Ionomer Cost Multiplier		0.6	**1**	2
GDL Cost Multiplier		0.73	**1**	1.30
Bipolar Plate Welding Speed	m/min	2.5	**15**	15
Air Stoichiometry		1.5	**1.5**	2
Membrane Humidifier Cost Multiplier		0.75	**1**	1.5
Compressor Effic. Multiplier		0.97	**1**	1.06
Expander Effic. Multiplier		0.97	**1**	1.10
Motor/Controller Effic.Multiplier		0.97	**1**	1.125
Air Compressor Cost Multiplier		0.664	**1**	1.2
Balance of Air Compressor Cost Multiplier		0.667	**1**	1.5
Hydrogen Recirculation System Cost Multiplier		0.667	**1**	1.5
EPTFE Cost Multiplier		0.5	**1**	1.7
JM Catalyst Processing Cost multiplier		0.75	1	2
Active to Total Area Ratio		0.55	**0.625**	0.8
Bipolar Plate Cost Multiplier		0.43	1	1.433

Figure 212. Parameter values used in Monte Carlo analysis for all manufacturing rates.

2015 Auto Technology Monte Carlo Analysis, 500k sys/year				
Parameter	Unit	Minimum Value	Likeliest Value	Maximum Value
Power Density	mW/cm^2	634	**746**	1119
Pt Loading	mgPt/cm^2	0.125	**0.142**	0.3
Ionomer Cost	$/kg	$49.22	**$82.04**	$164.08
GDL Cost	$/m^2 of GDL	$2.98	**$4.08**	$5.30
Bipolar Plate Welding Speed	m/min	2.5	**15**	15
Air Stoichiometry		1.5	**1.5**	2
Membrane Humidifier Cost	$/system	$49.23	**$65.64**	$98.47
Compressor Effic.	%	69%	**71%**	75%
Expander Effic.	%	71%	**73%**	80%
Motor/Controller Effic.	%	78%	**80%**	90%
Air Compressor Cost		$500	**$753**	$903
Balance of Air Compressor Cost	$/system	$122.06	**$183.00**	$274.49
Hydrogen Recirculation System Cost	$/system	$158.48	**$237.59**	$356.39
EPTFE Cost	$/m^2 of EPTFE	$3.00	**$6.00**	$10.20
JM Catalyst Processing Cost	$/system	$3.01	**$4.01**	$8.02
Active to Total Area Ratio		0.55	**0.625**	0.8
Bipolar Plate Cost	$/kWnet	$3.00	**$6.98**	$10.00

Figure 213: 2015 automotive Monte Carlo analysis bounds at 500,000 systems per year
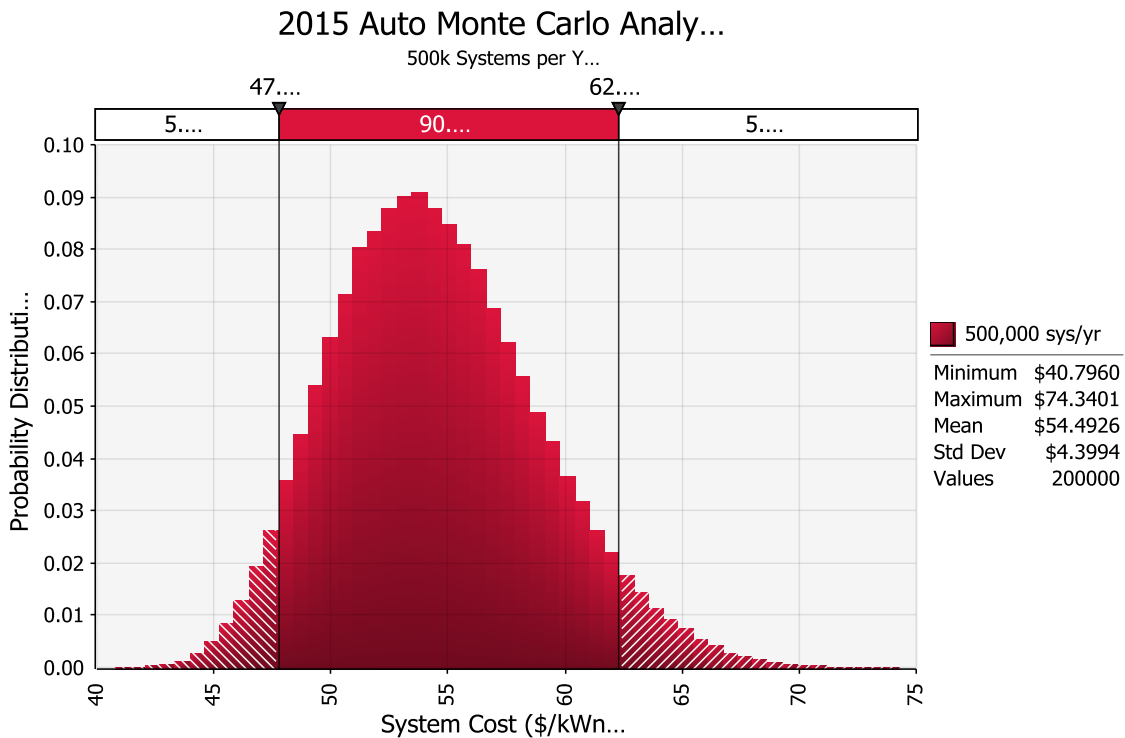
Figure 214: 2015 automotive Monte Carlo analysis results at 500k systems per year

194

13.2.2 Monte Carlo Bus Analysis

Similar to the auto sensitivity analysis, Monte Carlo analysis was also conducted for all manufacturing rates of the bus cost study (200, 400, 800, and 1,000 systems per year). The same multiplication factors for the parameters were used at all manufacturing rates. The range in cost for the bus stack, BOP, and total system cost are detailed in Section 0. Assumptions and results for the Monte Carlo analysis of the bus system are shown in Figure 215 and the graph at a manufacturing rate of 1,000 systems per year appears in Figure 216.

Monte Carlo analysis indicates that the middle 90% probability range of cost is between $228.84/kW$_{net}$ and $328.16/kW$_{net}$ for the bus system at 1,000 systems per year.

2015 Bus Technology Monte Carlo Sensitivity Analysis				
Parameter	Unit	Minimum Value	Likeliest Value	Maximum Value
Power Density	mW/cm2	517	**739**	1012
Pt Loading	mgPt/cm2	0.25	**0.5**	1
Ionomer Cost Multiplier		0.22	**1.00**	2.45
Ionomer Cost (@ 1ksys/yr)	$/kg	$46.16	$209.83	$514.08
GDL Cost Multiplier		0.73	**1.00**	1.30
GDL Cost (@ 1ksys/yr)	$/m2	85.40	$116.98	152.07
Bipolar Plate & Coating Cost Multiplier		1	**1**	2
Membrane Humidifier Cost Multiplier		0.5	**1.00**	2
Membrane Humidifier Cost (@ 1ksys/yr)	$/system	$324.64	$649.28	$1,298.56
Compressor Effic. Multiplier		0.97	**1.00**	1.29
Compressor Effic	%	56%	58%	75%
Motor/Controller Effic.Multiplier		0.97	**1.00**	1.00
Motor/Controller Effic	%	92%	95%	95%
Air Compressor Cost Multiplier		0.8	**1.00**	1.2
Air compressor Cost	$/system	$4,544	**$5,680**	$6,817
Balance of Air Compressor Cost Multiplier		0.6667	**1.00**	2
Balance of Air Compressor Cost (@ 1ksys/yr)	$/system	$341.88	$512.79	$1,025.57
Hydrogen Recirculation System Cost Multiplier		0.6667	**1.00**	2
Hydrogen Recirculation System Cost (@ 1ksys/yr)	$/system	$594.20	$891.26	$1,782.52
EPTFE Cost Multiplier		0.667	**1.00**	2.20
EPTFE Cost (@ 1ksys/yr)	$/m2	$9.71	$14.56	$32.04
Membrane Thickness	μm	15	**25.4**	25.4
Active to Total Area Ratio		0.55	0.625	0.80

Figure 215: 2015 bus Monte Carlo analysis bounds. Cost multipliers listed were applied to all manufacturing rates. Most of the individual costs are specified for the 1,000 systems per year manufacturing rate.
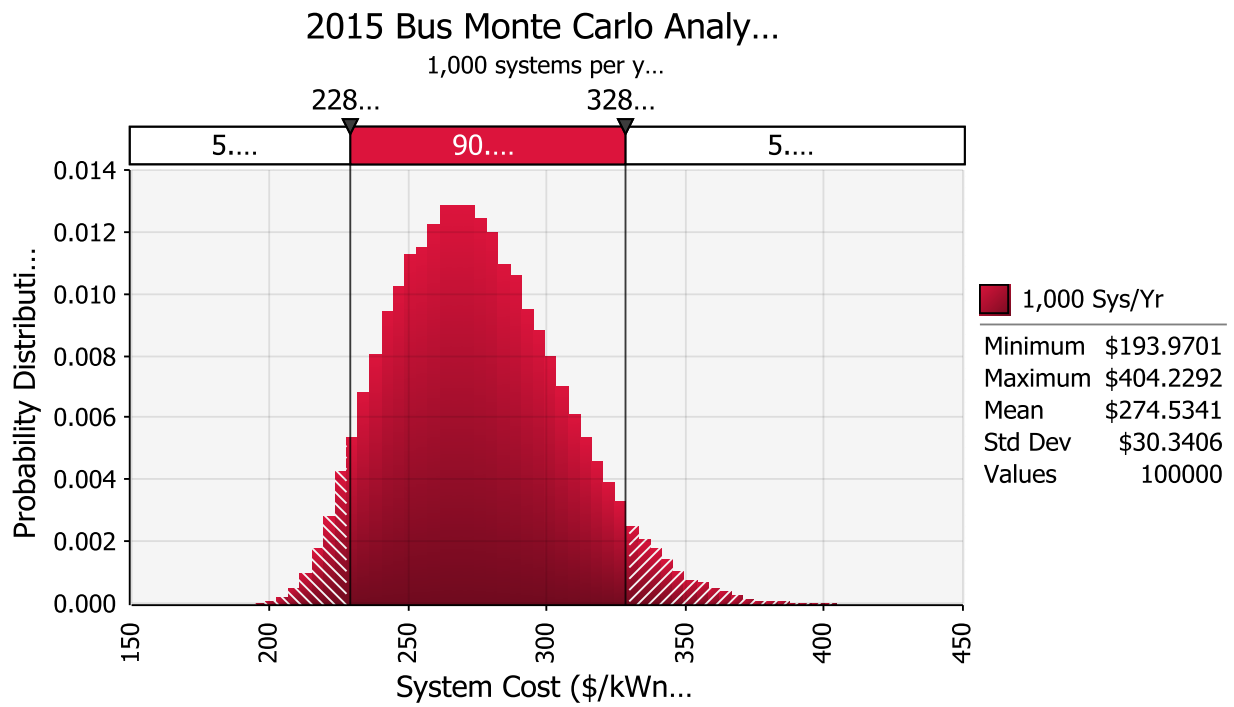
Figure 216: 2015 bus Monte Carlo analysis results

13.2.3 Extension of Monte Carlo Sensitivity

Monte Carlo multi-variable sensitivity analyses are updated each analysis year, however prior to 2014 the analysis has always focused on highlighting results for the highest manufacturing volumes (500,000 systems per year for the auto system and 1,000 systems per year for the bus system).

The 2014 analysis extended the Monte Carlo sensitivities to all manufacturing rates so that cost results may be shown as both a nominal value and a range of most likely values. Figure 217 graphs the range in cost for the 2015 automotive system at all manufacturing rates based on Monte Carlo analysis. The range in cost for the automotive system generally decreases as manufacturing volume increases. Additionally, Monte Carlo results are reported for the stack and total BOP cost categories. These results are shown in Section 0. As in previous years, the range of cost correlates with the middle 90% of results from the Monte Carlo analysis. The summation of the stack and BOP low value costs do not exactly numerically equal the low value for total system cost. Similarly, the summation of the stack and BOP high value costs do not equal the high value for total system cost.
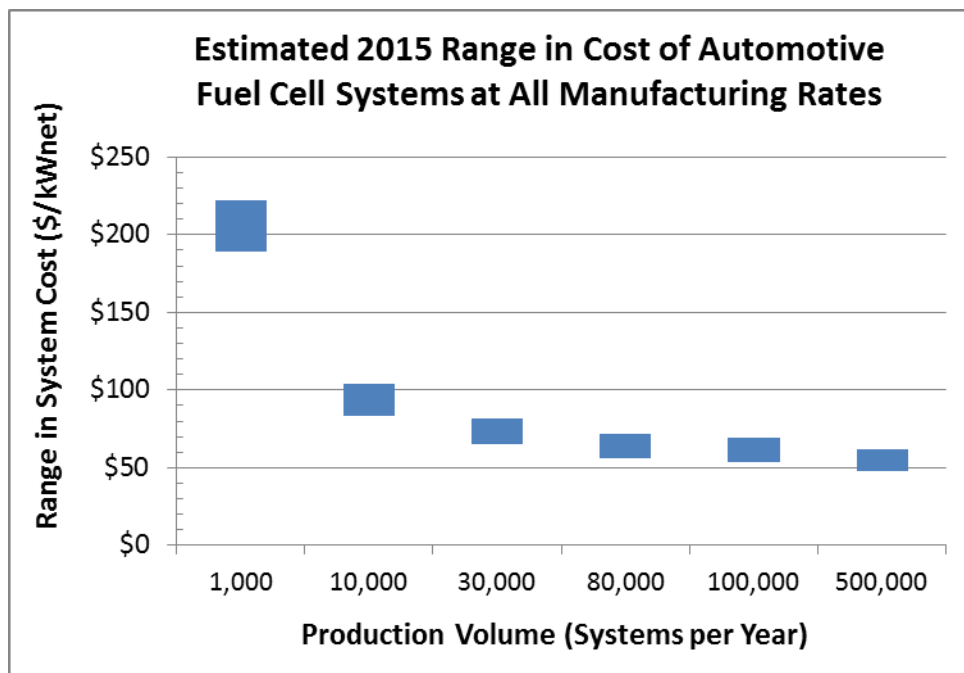
Figure 217. Middle 90% range is 2015 automotive fuel cell cost based on Monte Carlo results at all production rates.

14 Future System Cost Projection to $40/kW_{net}

In a previous SA study in 2006, automotive fuel cell system costs were projected for 2010 and 2015 technology. In 2015, an alternate approach is used to project a potential pathway to lower automotive fuel cell system cost: target values are applied to significant cost-driving components/parameters and the resulting system cost assessed. In an example pathway to $40/kW_{net}$ (at 500,000 systems per year) is shown in a waterfall chart, each step corresponding to a system cost parameter improvement. At the left end of the waterfall chart is the 80kW_{net} 2015 baseline system cost ($53/kW_{net}$). By varying the input values in the DFMA^{TM} model for power density, Pt content, air CEM cost, and bipolar plate (BPP) cost, the combined improvements result in a projected cost of $40/kW_{net}$, the DOE 2020 cost target. The target values used in this waterfall chart are taken from the Fuel Cell Technical Team US Drive 2013 Roadmap.[120] The most significant steps in reducing cost are the system power density (delta $5/kW_{net}$, based on an increase from 746 to 1,000 mW/cm^2) and the air CEM unit cost (delta $3/kW_{net}$, based on a decrease from $752 to $500 for the CEM unit). Additional performance or component cost parameters will need to be improved to meet or beat the ultimate DOE system cost target of $30/kWnet.
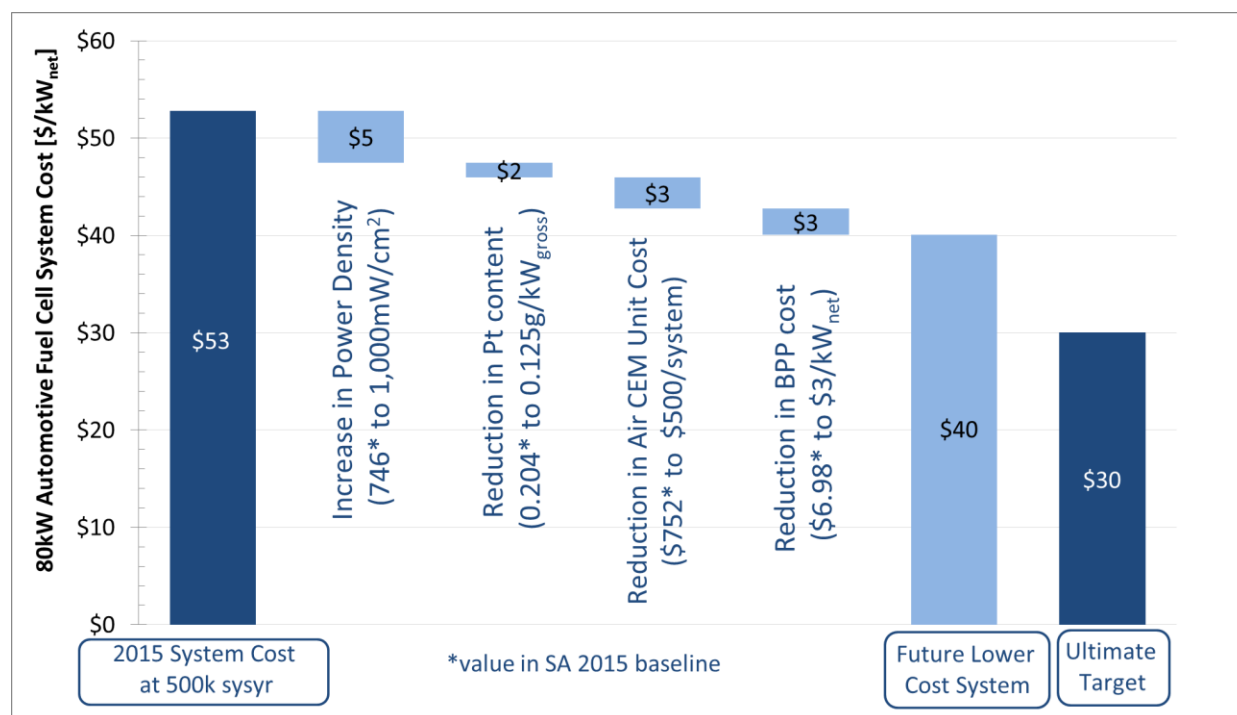
Figure 218. Waterfall chart for projection of automotive fuel cell system cost down to DOE 2020 target $40/kW_{net}, and DOE ultimate target $30/kW_{net}

[120] http://energy.gov/sites/prod/files/2014/02/f8/fctt_roadmap_june2013.pdf

15 Key Progress in the 2015 Automotive and Bus Analyses

This section summarizes key progress for both the automotive and bus power systems analyses.

80 kW$_{e\ net}$ light-duty automotive fuel cell power systems:

- The 2014 DFMA^{TM}-style cost analysis was updated to reflect changes/improvements achieved in 2015.
- Performance is based on updated 2015 stack polarization projections provided by ANL (based on single cell test data for Johnson-Matthey dispersed binary dealloyed PtNi on carbon catalyst).
- The 2015 system is optimized for low cost, and the resulting design point (at rated power) is shown in Figure 219. These optimized operating conditions differ from the 2013 and 2014 optimization conditions.

	2013 Design Point	2014 Design Point	2015 Design Point
Cell voltage	0.695 volts/cell	0.672 volts/cell	0.661 volts/cell
Power density	692 mW/cm^2	834 mW/cm^2	746 mW/cm^2
Pressure	2.5 atm	2.5 atm	2.5 atm
Total catalyst loading	0.153 mgPt/cm^2	0.153 mgPt/cm^2	0.142 mgPt/cm^2
Stack Temp. (Coolant Exit Temp)	92.3°C	95°C	95°C
Cathode Air Stoichiometry	1.5	2	1.5

Figure 219. Design point comparison between 2013, 2014, and 2015.

- Other significant changes for 2015 include:
  - adjustment of active to total area from 0.8 to 0.625,
  - change to sub-gasket processing assumption for processing web width,
  - updated hydrogen sensor pricing based on quotation from NTM Sensors,
  - Re-sizing of the air humidifier membrane area based on ANL modeling for design operating conditions,
  - low production volume investigations:
    - Catalyst application methods (NSTF Vs. Slot Die Coating)
    - Robotic stacking of sub-gasket instead of roll-to-roll process
    - Job shop logic showed considerable cost reduction for non-repeat components (end gaskets, end plates, and current collectors)
    - Reconsideration of annual air humidifier membrane area production to reflect external vendor sales to multiple humidifier manufacturers
  - and, re-evaluation of the quality control procedures and equipment.
- Several analyses were performed to explore alternate manufacturing procedures or types of system components (but were not incorporated into the baseline cost analysis):
  - Giner dimensionally stable membrane (DSM^{TM}) substrates compared to ePTFE substrates (Section 7.1)
  - Dealloyed PtNi NSTF catalyst application with interlayer on cathode GDL (Section 7.2)

- o Non-Platinum polyaniline (PANI)-Fe-C catalyst synthesis (Section 7.3)
  - o Additional low production volume side analyses:
    - ▪ stamped titanium bipolar plates instead of stamped stainless steel plates: Ti plates shown to be higher cost
    - ▪ progressive stamping vs. sequential stamping vs. hydroforming: progressive die stamping was shown to be lower cost than the other options at system production rates >130 systems per year. (Sections 7.4.1 and 7.4.2).
- The estimated fuel cell system cost for automobiles is $52.84/kW$_{net}$ at 500,000 systems per year and represents the "2015 Update" to previous annual estimates. (This value does not include the cost of hydrogen storage or the electric drive train.)
- A Monte Carlo analysis indicates that the fuel cell system cost is likely to be between $47.81/kW$_{net}$ and $62.27/kW$_{net}$ for the automotive system, with 90% probability.
- The 2015 automotive system balance of plant components represent approximately 49% of the overall system cost at a production rate of 500,000 systems per year.

160 kW$_{net}$ bus fuel cell power systems:

- Primary differences between the bus and automotive power systems include:
  - o system power (160kW$_{net}$ vs. 80kW$_{net}$),
  - o number of stacks (two vs. one),
  - o operating pressure (1.9 atm vs. 2.5 atm),
  - o catalyst loading (0.5 mgPt/cm^2 vs. 0.142 mgPt/cm^2),
  - o use of an exhaust gas expander (no expander vs. expander), and
  - o type of air compressor (twin vortex vs. centrifugal).
- Stack performance is based on a 2015 stack polarization model provided by Argonne National Laboratory with the total Pt loading raised from 0.4 mgPt/cm^2 to 0.5 mgPt/cm^2 based on dispersed Pt on carbon instead of ternary PtCoMn NSTF within the MEAs.
- Power density, voltage, pressure, and catalyst loading of the selected system design point are roughly consistent with the actual operating conditions of Ballard fuel cell buses currently in service.

	Approximate Ballard Bus Design Point	2013 Bus Design Point	2014 Bus Design Point	2015 Bus Design Point
Cell voltage	~0.69 volts/cell	0.676 volts/cell	0.676 volts/cell	0.659 volts/cell
Power density	~759 mW/cm^2	601 mW/cm^2	601 mW/cm^2	739 mW/cm^2
Pressure	~1.8 atm	1.8 atm	1.8 atm	1.9 atm
Total catalyst loading	~0.4 mgPt/cm^2	0.4 mgPt/cm^2	0.4 mgPt/cm^2	0.5 mgPt/cm^2
Stack Temperature	~60°C	74°C	74°C	72°C
Cathode Air Stoichiometry	1.5-2.0	1.5	1.5	1.8

Figure 220. Design Point Comparison for FC Bus between Ballard Bus, 2013, 2014, and 2015 analysis

- Additional changes between 2014 and 2015 bus analyses include:

- o all of 2015 automotive updates (adjustment to polarization performance, operating conditions, geometry of active to total area ratio from 0.8 to 0.625, QC systems, and hydrogen sensor quotations),
- The system schematics and stack construction are nearly identical between the bus and automobile systems.
- The final 2015 bus cost is $261.97/kW$_{net}$ at 1,000 systems per year.
- A Monte Carlo analysis indicates that the bus fuel cell system cost is likely to be between $228.84/kW$_{net}$ and $328.16/kW$_{net}$, with 90% probability.
- The 2015 bus system balance of plant represented only 30% of the overall system cost at a production rate of 1,000 systems per year.
- Because bus systems are expected to be produced in much lower rates than auto systems (1,000/year vs. 500,000/year), bus system costs are much more sensitive to component cost variations (eg. GDL, bipolar plate manufacturing, coating costs). Reducing the uncertainty in component costs will improve the accuracy of the bus system cost.

16 Appendix A: 2015 Transit Bus Cost Results

16.1 Fuel Cell Stack Materials, Manufacturing, and Assembly Cost Results

16.1.1 Bipolar Plates

Annual Production Rate	200	400	800	1,000
Manufacture or Job Shop	Job Shop	Job Shop	Job Shop	Job Shop
Job Shop Line Utilization (%)	42%	47%	57%	62%
Job Shop Total Machine Rate ($/min)	$3.67	$3.32	$2.79	$2.60
Manufactured Line Utilization (%)	5%	10%	20%	25%
Manufactured Total Machine Rate ($/min)	$22.24	$11.24	$5.74	$4.64
Line Utilization Used (%)	42%	47%	57%	62%
Total Machine Rate Used ($/min)	$3.67	$3.32	$2.79	$2.60

Annual Production Rate	200	400	800	1,000
Material ($/stack)	$308	$308	$308	$308
Manufacturing ($/stack)	$91	$83	$69	$65
Tooling ($/stack)	$114	$114	$104	$99
Secondary Operations: Coating ($/stack)	$358	$343	$317	$306
Markup ($/stack)	$352	$333	$305	$295
Total Cost ($/stack)	$1,222	$1,180	$1,104	$1,072
Total Cost ($/kWnet)	$15.28	$14.75	$13.80	$13.40

16.1.1.1 Alloy Selection and Corrosion Concerns

Annual Production Rate	200	400	800	1,000
Material ($/stack)	$80	$80	$80	$80
Manufacturing ($/stack)	$278	$263	$237	$226
Total Cost ($/stack)	$358	$343	$317	$306
Total Cost ($/kWnet)	$4.48	$4.28	$3.96	$3.83

16.1.2 Membrane

Annual Production Rate	200	400	800	1,000
Material ($/m^2)	$51	$46	$39	$38
Manufacturing ($/m^2)	$291	$187	$108	$94
Markup ($/m^2)	$138	$92	$56	$50
Total Cost ($/m^2 (total))	$481	$324	$203	$181
Total Cost ($/stack)	$8,806.61	$5,942.00	$4,519.01	$4,029.25
Total Cost ($/kWnet)	$110.08	$74.27	$56.49	$50.37

16.1.3 Pt on Carbon Catalyst

16.1.3.1 Catalyst Synthesis Cost

Annual Production Rate	200	400	800	1,000
Manufacture or Job Shop	Job Shop	Job Shop	Job Shop	Job Shop
Job Shop Line Utilization (%)	55%	73%	70%	86%
Job Shop Total Machine Rate ($/min)	$1.08	$0.94	$0.96	$0.87
Manufactured Line Utilization (%)	18%	36%	70%	86%
Manufactured Total Machine Rate ($/min)	$1.70	$1.06	$0.74	$0.67
Line Utilization Used (%)	55%	73%	70%	86%
Total Machine Rate Used ($/min)	$1.08	$0.94	$0.96	$0.87

Annual Production Rate	200	400	800	1,000
Pt cost ($/system)	$7,162	$7,133	$7,105	$7,096
Material (exluding Pt) ($/system)	$135	$93	$58	$50
Total Material ($/system)	$7,297	$7,226	$7,163	$7,146
Manufacturing ($/system)	$227	$183	$175	$157
Markup ($/system)	$3,433	$3,198	$3,036	$2,969
Total Cost ($/system)	$10,957	$10,608	$10,375	$10,273
Total Cost ($/kWnet)	$68	$66	$65	$64
Total Cost/kgCatalyst(net)	$23,304	$22,562	$22,066	$21,848

16.1.3.2 Catalyst Application: Slot Die Coating

Annual Production Rate	200	400	800	1,000
Manufacture or Job Shop	Job Shop	Manufactured	Job Shop	Job Shop
Job Shop Line Utilization (%)	39%	0%	41%	42%
Job Shop Total Machine Rate ($/min)	$8.56	$3.89	$10.95	$10.73
Manufactured Line Utilization (%)	39%	74%	4%	5%
Manufactured Total Machine Rate ($/min)	$6.59	$3.89	$80.58	$65.17
Line Utilization Used (%)	39%	74%	41%	42%
Total Machine Rate Used ($/min)	$8.56	$3.89	$10.95	$10.73

Annual Production Rate	200	400	800	1,000
Materials ($/stack)	$25	$22	$19	$18
Manufacturing ($/stack)	$2,988	$1,261	$92	$89
Markup ($/stack)	$1,216	$948	$42	$40
Total Cost ($/stack)	$4,229	$2,231	$152	$147
Total Cost ($/kWnet)	$52.86	$27.88	$1.91	$1.83

16.1.4 Gas Diffusion Layer

Annual Production Rate	200	400	800	1,000
GDL Cost ($/stack)	$4,272	$2,970	$2,065	$1,837
Markup ($/stack)	$3,374	$2,196	$1,430	$1,246
Total Cost ($/stack)	$7,646	$5,166	$3,495	$3,082
Total Cost ($/kWnet)	$95.57	$64.57	$43.68	$38.53

16.1.5 MEA Sub-Gaskets Total

Annual Production Rate	200	400	800	1,000
Material ($/stack)	$84	$84	$84	$84
Manufacturing ($/stack)	$275	$240	$191	$168
Tooling (Kapton Web) ($/stack)	$101	$53	$45	$38
Cost/Stack	$185	$148	$161	$142
Total Cost ($/stack)	$645	$524	$481	$432
Total Cost ($/kWnet)	$4.03	$3.28	$3.01	$2.70

16.1.5.1 Sub-Gasket Formation

Annual Production Rate	200	400	800	1,000
Manufacture or Job Shop	Job Shop	Job Shop	Job Shop	Job Shop
Job Shop Line Utilization (%)	40%	43%	45%	47%
Job Shop Total Machine Rate ($/min)	$7.89	$7.49	$7.36	$7.14
Manufactured Line Utilization (%)	3%	6%	8%	10%
Manufactured Total Machine Rate ($/min)	$56.65	$29.98	$23.26	$19.08
Line Utilization Used (%)	40%	43%	45%	47%
Total Machine Rate Used ($/min)	$7.89	$7.49	$7.36	$7.14

Annual Production Rate	200	400	800	1,000
Material ($/stack)	$70	$70	$70	$70
Manufacturing ($/stack)	$129	$118	$78	$75
Tooling (Kapton Web) ($/stack)	$101	$53	$45	$38
Markup ($/stack)	$121	$95	$74	$69
Total Cost ($/stack)	$421	$337	$268	$252
Total Cost ($/kWnet)	$5.26	$4.21	$3.35	$3.16

16.1.5.2 Sub-Gasket Adhesive Application (screen-printing)

Annual Production Rate	200	400	800	1,000
Manufacture or Job Shop	Job Shop	Job Shop	Manufactured	Manufactured
Job Shop Line Utilization (%)	49%	62%	49%	61%
Job Shop Total Machine Rate ($/min)	$2.36	$1.96	$2.36	$1.96
Manufactured Line Utilization (%)	12%	25%	49%	61%
Manufactured Total Machine Rate ($/min)	$6.46	$3.37	$1.82	$1.51
Line Utilization Used (%)	49%	62%	49%	61%
Total Machine Rate Used ($/min)	$2.36	$1.96	$1.82	$1.51

Annual Production Rate	200	400	800	1,000
Material ($/stack)	$13	$13	$13	$13
Manufacturing ($/stack)	$146	$121	$113	$93
Markup ($/stack)	$64	$53	$87	$73
Total Cost ($/stack)	$224	$188	$213	$179
Total Cost ($/kWnet)	$2.80	$2.35	$2.67	$2.24

16.1.6 Hot Pressing GDL to Catalyst Coated Membrane

Annual Production Rate	200	400	800	1,000
Capital Cost ($/Line)	$1,125,644	$1,125,644	$1,501,443	$1,501,443
Simultaneous Lines	1	1	1	1
Laborers per Line	0.25	0.25	0.25	0.25
Line Utilization (%)	13%	27%	40%	50%
Total Cycle Time (seconds)	95	95	95	95
Manufacture or Job Shop	Job Shop	Job Shop	Manufactured	Manufactured
Job Shop Line Utilization (%)	50%	64%	40%	50%
Job Shop Total Machine Rate ($/min)	$1.22	$1.02	$1.46	$1.22
Manufactured Line Utilization (%)	13%	27%	40%	50%
Manufactured Total Machine Rate ($/min)	$2.94	$1.58	$1.12	$0.94
Line Utilization Used (%)	50%	64%	40%	50%
Total Machine Rate Used ($/min)	$1.22	$1.02	$1.12	$0.94

Annual Production Rate	200	400	800	1,000
Manufacturing ($/stack)	$83	$69	$57	$48
Tooling ($/stack)	$1.87	$0.94	$0.47	$0.37
Markup ($/stack)	$67	$52	$40	$33
Total Cost ($/stack)	$152	$122	$97	$81
Total Cost ($/kWnet)	$1.90	$1.53	$1.22	$1.01

16.1.7 Cutting, and Slitting

Annual Production Rate	200	400	800	1,000
Manufacture or Job Shop	Job Shop	Job Shop	Job Shop	Job Shop
Job Shop Line Utilization (%)	37%	38%	38%	39%
Job Shop Total Machine Rate ($/min)	$2.37	$2.35	$2.47	$2.45
Manufactured Line Utilization (%)	0.5%	0.9%	1.3%	1.6%
Manufactured Total Machine Rate ($/min)	$130.69	$67.98	$50.64	$40.81
Line Utilization Used (%)	37%	38%	38%	39%
Total Machine Rate Used ($/min)	$2.37	$2.35	$2.47	$2.45

Annual Production Rate	200	400	800	1,000
Manufacturing ($/stack)	$6	$5	$4	$4
Tooling ($/stack)	$12	$11	$6	$6
Markup ($/stack)	$7	$7	$4	$4
Total Cost ($/stack)	$24	$23	$13	$13
Total Cost ($/kWnet)	$0.30	$0.29	$0.17	$0.17

16.1.8 End Plates

Annual Production Rate	200	400	800	1,000
Manufacture or Job Shop	Job Shop	Job Shop	Job Shop	Job Shop
Job Shop Line Utilization (%)	38%	39%	41%	42%
Job Shop Total Machine Rate ($/min)	$2.41	$2.36	$2.27	$2.23
Manufactured Line Utilization (%)	1%	2%	4%	5%
Manufactured Total Machine Rate ($/min)	$53.14	$26.78	$13.60	$10.97
Line Utilization Used (%)	38%	39%	41%	42%
Total Machine Rate Used ($/min)	$2.41	$2.36	$2.27	$2.23

Annual Production Rate	200	400	800	1,000
Material ($/stack)	$103	$97	$92	$91
Manufacturing ($/stack)	$13	$12	$12	$12
Tooling ($/stack)	$4	$2	$1	$1
Markup ($/stack)	$48	$44	$40	$39
Total Cost ($/stack)	$168	$156	$146	$143
Total Cost ($/kWnet)	$2.10	$1.95	$1.82	$1.78

16.1.9   Current Collectors

Annual Production Rate	200	400	800	1,000
Manufacture or Job Shop	Job Shop	Job Shop	Job Shop	Job Shop
Job Shop Line Utilization (%)	37%	37%	37%	37%
Job Shop Total Machine Rate ($/min)	$2.18	$2.18	$2.18	$2.18
Manufactured Line Utilization (%)	0%	0%	0%	0%
Manufactured Total Machine Rate ($/min)	$1,199.35	$694.70	$347.74	$287.40
Line Utilization Used (%)	37%	37%	37%	37%
Total Machine Rate Used ($/min)	$2.18	$2.18	$2.18	$2.18

Annual Production Rate	200	400	800	1,000
Material ($/stack)	$8	$8	$8	$8
Manufacturing ($/stack)	$0	$0	$0	$0
Tooling ($/stack)	$0	$0	$0	$0
Secondary Operation ($/stack)	$1	$1	$1	$1
Markup ($/stack)	$4	$4	$3	$3
Total Cost ($/stack)	$13	$13	$12	$12
Total Cost ($/kWnet)	$0.16	$0.16	$0.15	$0.15

16.1.10   Coolant Gaskets/Laser-welding

Annual Production Rate	200	400	800	1,000
Manufacture or Job Shop	Job Shop	Job Shop	Job Shop	Manufactured
Job Shop Line Utilization (%)	46%	54%	71%	43%
Job Shop Total Machine Rate ($/min)	$3.28	$2.81	$2.21	$3.48
Manufactured Line Utilization (%)	9%	17%	34%	43%
Manufactured Total Machine Rate ($/min)	$12.45	$6.34	$3.29	$2.68
Line Utilization Used (%)	46%	54%	71%	43%
Total Machine Rate Used ($/min)	$3.28	$2.81	$2.21	$2.68

Annual Production Rate	200	400	800	1,000
Material ($/stack)	$0	$0	$0	$0
Manufacturing ($/stack)	$141	$120	$95	$115
Tooling ($/stack)	$0	$0	$0	$0
Markup ($/stack)	$57	$47	$36	$78
Total Cost ($/stack)	$197	$168	$131	$193
Total Cost ($/kWnet)	$2.47	$2.10	$1.64	$2.41

16.1.11   End Gaskets

Annual Production Rate	200	400	800	1,000
Manufacture or Job Shop	Job Shop	Job Shop	Job Shop	Job Shop
Job Shop Line Utilization (%)	37%	37%	37%	37%
Job Shop Total Machine Rate ($/min)	$3.02	$3.02	$3.01	$3.00
Manufactured Line Utilization (%)	0.1%	0.1%	0.3%	0.3%
Manufactured Total Machine Rate ($/min)	$1,176.68	$588.53	$294.40	$235.57
Line Utilization Used (%)	37%	37%	37%	37%
Total Machine Rate Used ($/min)	$3.02	$3.02	$3.01	$3.00

Annual Production Rate	200	400	800	1,000
Material ($/stack)	$0	$0	$0	$0
Manufacturing ($/stack)	$1	$1	$1	$1
Markup ($/stack)	$0	$0	$0	$0
Total Cost ($/stack)	$2	$1	$1	$1
Total Cost ($/kWnet)	$0.02	$0.02	$0.02	$0.02

16.1.12   Stack Assembly

Annual Production Rate	200	400	800	1,000
Manufacture or Job Shop	Manufactured	Manufactured	Manufactured	Manufactured
Job Shop Line Utilization (%)	57%	39%	78%	98%
Job Shop Total Machine Rate ($/min)	$1.30	$1.22	$1.05	$1.03
Manufactured Line Utilization (%)	20%	39%	78%	98%
Manufactured Total Machine Rate ($/min)	$0.90	$0.83	$0.80	$0.79
Line Utilization Used (%)	20%	39%	78%	98%
Total Machine Rate Used ($/min)	$0.90	$0.83	$0.80	$0.79

Annual Production Rate	200	400	800	1,000
Compression Bands ($/stack)	$0	$0	$0	$0
Assembly ($/stack)	$88	$82	$78	$78
Markup ($/stack)	$70	$60	$54	$53
Total Cost ($/stack)	$158	$142	$132	$130
Total Cost ($/kWnet)	$1.97	$1.77	$1.66	$1.63

16.1.13 Stack Housing

Annual Production Rate	200	400	800	1,000
Manufacture or Job Shop	Job Shop	Job Shop	Job Shop	Job Shop
Job Shop Line Utilization (%)	37%	37%	38%	38%
Job Shop Total Machine Rate ($/min)	$1.41	$1.41	$1.41	$1.41
Manufactured Line Utilization (%)	0%	0%	1%	1%
Manufactured Total Machine Rate ($/min)	$46.17	$23.49	$12.14	$9.87
Line Utilization Used (%)	37%	37%	38%	38%
Total Machine Rate Used ($/min)	$1.41	$1.41	$1.41	$1.41

Annual Production Rate	200	400	800	1,000
Material ($/stack)	$12	$12	$12	$12
Manufacturing ($/stack)	$3	$3	$3	$3
Tooling ($/stack)	$181	$91	$45	$36
Markup ($/stack)	$79	$42	$23	$20
Total Cost ($/stack)	$276	$148	$84	$71
Total Cost ($/kWnet)	$1.72	$0.92	$0.52	$0.44

16.1.14 Stack Conditioning and Testing

Annual Production Rate	200	400	800	1,000
Capital Cost ($/line)	Proprietary			
Simultaneous Lines	1	1	2	2
Laborers per Line	0.1	0.1	0.1	0.1
Test Duration (hrs/stack)	2	2	2	2
Line Utilization Used (%)	14%	28%	28%	35%
Total Machine Rate Used ($/min)	$1.35	$0.72	$0.72	$0.60

Annual Production Rate	200	400	800	1,000
Conditioning/Testing ($/stack)	$162	$87	$87	$71
Markup ($/stack)	$128	$64	$60	$48
Total Cost ($/stack)	$290	$151	$146	$120
Total Cost ($/kWnet)	$3.62	$1.88	$1.83	$1.50

16.2 2015 Transit Bus Balance of Plant (BOP) Cost Results

16.2.1 Air Loop

Annual Production Rate	200	400	800	1,000
Filter and Housing ($/system)	$75	$75	$74	$74
Compressor, Expander & Motor ($/system)	$8,322	$6,893	$5,928	$5,681
Mass Flow Sensor ($/system)	$102	$101	$100	$100
Air Ducting ($/system)	$197	$194	$190	$189
Air Temperature Sensor ($/system)	$11	$10	$10	$10
Markup on Purchased Components ($/system)	$156	$149	$143	$141
Total Cost ($/system)	$8,863	$7,421	$6,445	$6,193
Total Cost ($/kW$_{net}$)	$55.39	$46.38	$40.28	$38.71

16.2.2 Humidifier & Water Recovery Loop

Annual Production Rate	200	400	800	1,000
Air Precooler ($/system)	$162	$157	$153	$152
Demister ($/system)	$101	$75	$61	$58
Membrane Air Humidifier ($/system)	$1,016	$810	$682	$649
Total Cost ($/system)	$1,278	$1,043	$896	$859
Total Cost ($/kW$_{net}$)	$7.99	$6.52	$5.60	$5.37

16.2.2.1 Air Precooler

Annual Production Rate	200	400	800	1,000
Material ($/system)	$45	$45	$45	$45
Manufacturing ($/system)	$45	$45	$45	$45
Markup ($/system)	$71	$67	$63	$61
Total Cost ($/system)	$162	$157	$153	$152
Total Cost ($/kWnet)	$1.01	$0.98	$0.96	$0.95

16.2.2.2 Demister

Annual Production Rate	200	400	800	1,000
Manufacture or Job Shop	Job Shop	Job Shop	Job Shop	Job Shop
Job Shop Line Utilization (%)	37%	37%	37%	37%
Job Shop Total Machine Rate ($/min)	$3.09	$3.09	$3.09	$3.09
Manufactured Line Utilization (%)	0.07%	0.08%	0.11%	0.12%
Manufactured Total Machine Rate ($/min)	$819.46	$705.18	$551.46	$497.28
Line Utilization Used (%)	37%	37%	37%	37%
Total Machine Rate Used ($/min)	$3.09	$3.09	$3.09	$3.09

Annual Production Rate	200	400	800	1,000
Material ($/system)	$40	$38	$36	$35
Manufacturing ($/system)	$2	$1	$1	$1
Tooling ($/system)	$29	$15	$7	$6
Markup ($/system)	$29	$21	$17	$16
Total Cost ($/system)	$101	$75	$61	$58
Total Cost ($/kWnet)	$0.63	$0.47	$0.38	$0.36

16.2.2.3 Membrane Humidifier

16.2.2.3.1 Membrane Humidifier Manufacturing Process
Station 1: Fabrication of Composite Humidifier Membranes

Annual Production Rate	200	400	800	1,000
Manufacture or Job Shop	Job Shop	Job Shop	Job Shop	Job Shop
Job Shop Line Utilization (%)	37%	37%	37%	37%
Job Shop Total Machine Rate ($/min)	$22.96	$22.65	$22.30	$22.17
Manufactured Line Utilization (%)	0.1%	0.1%	0.3%	0.3%
Manufactured Total Machine Rate ($/min)	$7,675.15	$3,939.86	$2,022.63	$1,631.97
Line Utilization Used (%)	37.1%	37.1%	37.3%	37.3%
Total Machine Rate Used ($/min)	$22.96	$22.65	$22.30	$22.17

Annual Production Rate	200	400	800	1,000
Material ($/stack)	$255	$232	$210	$203
Manufacturing ($/stack)	$122	$69	$42	$36
Tooling ($/stack)	$0	$0	$0	$0
Markup ($/stack)	$149	$115	$93	$88
Total Cost ($/stack)	$526	$416	$346	$328
Total Cost ($/kWnet)	$3.29	$2.60	$2.16	$2.05

Station 2: Fabrication of Etched Stainless Steel Flow Fields

Annual Production Rate	200	400	800	1,000
Manufacture or Job Shop	Job Shop	Job Shop	Job Shop	Job Shop
Job Shop Line Utilization (%)	38%	38%	39%	39%
Job Shop Total Machine Rate ($/min)	$11.69	$11.60	$11.43	$11.35
Manufactured Line Utilization (%)	1%	1%	2%	2%
Manufactured Total Machine Rate ($/min)	$374.95	$189.45	$96.71	$78.80
Line Utilization Used (%)	38%	38%	39%	39%
Total Machine Rate Used ($/min)	$11.69	$11.60	$11.43	$11.35

Annual Production Rate	200	400	800	1,000
Material ($/stack)	$37	$37	$37	$37
Manufacturing ($/stack)	$63	$63	$62	$61
Markup ($/stack)	$40	$38	$37	$36
Total Cost ($/stack)	$140	$138	$135	$134
Total Cost ($/kWnet)	$0.88	$0.86	$0.85	$0.84

Station 3: Pouch Formation

Annual Production Rate	200	400	800	1,000
Manufacture or Job Shop	Job Shop	Job Shop	Job Shop	Job Shop
Job Shop Line Utilization (%)	37%	38%	38%	38%
Job Shop Total Machine Rate ($/min)	$3.25	$3.23	$3.19	$3.16
Manufactured Line Utilization (%)	0%	1%	1%	1%
Manufactured Total Machine Rate ($/min)	$289.15	$144.77	$72.54	$58.09
Line Utilization Used (%)	37%	38%	38%	38%
Total Machine Rate Used ($/min)	$3.25	$3.23	$3.19	$3.16

Annual Production Rate	200	400	800	1,000
Material ($/stack)	$1	$1	$1	$1
Manufacturing ($/stack)	$10	$10	$9	$9
Tooling ($/stack)	$0	$0	$0	$0
Markup ($/stack)	$4	$4	$4	$4
Total Cost ($/stack)	$15	$15	$15	$15
Total Cost ($/kWnet)	$0.10	$0.09	$0.09	$0.09

Station 4: Stainless Steel Rib Formation

Annual Production Rate	200	400	800	1,000
Manufacture or Job Shop	Job Shop	Job Shop	Job Shop	Job Shop
Job Shop Line Utilization (%)	38%	38%	40%	40%
Job Shop Total Machine Rate ($/min)	$1.35	$1.33	$1.30	$1.28
Manufactured Line Utilization (%)	1%	1%	3%	3%
Manufactured Total Machine Rate ($/min)	$47.87	$24.18	$12.23	$9.84
Line Utilization Used (%)	38%	38%	40%	40%
Total Machine Rate Used ($/min)	$1.35	$1.33	$1.30	$1.28

Annual Production Rate	200	400	800	1,000
Material ($/stack)	$3	$3	$3	$3
Manufacturing ($/stack)	$9	$9	$8	$8
Tooling ($/stack)	$10	$9	$9	$9
Markup ($/system)	$9	$8	$8	$7
Total Cost ($/stack)	$30	$28	$28	$28
Total Cost ($/kWnet)	$0.19	$0.18	$0.17	$0.17

Station 5: Stack Formation

Annual Production Rate	200	400	800	1,000
Manufacture or Job Shop	Job Shop	Job Shop	Job Shop	Job Shop
Job Shop Line Utilization (%)	40%	43%	49%	52%
Job Shop Total Machine Rate ($/min)	$1.52	$1.44	$1.30	$1.24
Manufactured Line Utilization (%)	3%	6%	12%	15%
Manufactured Total Machine Rate ($/min)	$13.26	$6.74	$3.48	$2.83
Line Utilization Used (%)	40%	43%	49%	52%
Total Machine Rate Used ($/min)	$1.52	$1.44	$1.30	$1.24

Annual Production Rate	200	400	800	1,000
Material ($/stack)	$11	$11	$11	$11
Manufacturing ($/stack)	$45	$42	$38	$37
Markup ($/system)	$22	$20	$18	$17
Total Cost ($/stack)	$77	$73	$67	$64
Total Cost ($/kWnet)	$0.48	$0.46	$0.42	$0.40

Station 6: Formation of the Housing

Annual Production Rate	200	400	800	1,000
Material ($/stack)	$13	$13	$13	$13
Manufacturing ($/stack)	$48	$28	$17	$15
Tooling ($/stack)	$97	$56	$33	$27
Markup ($/system)	$63	$37	$23	$20
Total Cost ($/stack)	$220	$133	$86	$75
Total Cost ($/kWnet)	$1.38	$0.83	$0.53	$0.47

Station 7: Assembly of the Composite Membrane and Flow Fields into the Housing

Annual Production Rate	200	400	800	1,000
Manufacture or Job Shop	Job Shop	Job Shop	Job Shop	Job Shop
Job Shop Line Utilization (%)	37%	37%	38%	38%
Job Shop Total Machine Rate ($/min)	$1.24	$1.24	$1.24	$1.24
Manufactured Line Utilization (%)	0%	0%	1%	1%
Manufactured Total Machine Rate ($/min)	$32.68	$16.73	$8.76	$7.16
Line Utilization Used (%)	37%	37%	38%	38%
Total Machine Rate Used ($/min)	$1.24	$1.24	$1.24	$1.24

Annual Production Rate	200	400	800	1,000
Manufacturing ($/stack)	$2	$2	$2	$2
Markup ($/system)	$1	$1	$1	$1
Total Cost ($/stack)	$3	$3	$3	$3
Total Cost ($/kWnet)	$0.02	$0.02	$0.02	$0.02

Station 8: Humidifier System Testing

Annual Production Rate	200	400	800	1,000
Manufacture or Job Shop	Job Shop	Job Shop	Job Shop	Job Shop
Job Shop Line Utilization (%)	37%	38%	38%	38%
Job Shop Total Machine Rate ($/min)	$1.17	$1.17	$1.17	$1.17
Manufactured Line Utilization (%)	0%	1%	1%	1%
Manufactured Total Machine Rate ($/min)	$19.36	$10.06	$5.41	$4.48
Line Utilization Used (%)	37%	38%	38%	38%
Total Machine Rate Used ($/min)	$1.17	$1.17	$1.17	$1.17

Annual Production Rate	200	400	800	1,000
Manufacturing ($/stack)	$2	$2	$2	$2
Markup ($/system)	$1	$1	$1	$1
Total Cost ($/stack)	$2	$2	$2	$2
Total Cost ($/kWnet)	$0.03	$0.03	$0.03	$0.03

16.2.2.3.2 Combined Cost Results for Plate Frame Membrane Humidifier

Annual Production Rate	200	400	800	1,000
Material ($/stack)	$319	$296	$274	$268
Manufacturings ($/stack)	$301	$224	$181	$171
Tooling ($/stack)	$108	$66	$42	$37
Markup ($/stack)	$288	$224	$184	$174
Total Cost ($/stack)	$1,016	$810	$682	$649
Total Cost ($/kWnet)	$12.70	$10.13	$8.52	$8.12

16.2.3 Coolant Loops

16.2.3.1 High-Temperature Coolant Loop

Annual Production Rate	200	400	800	1,000
Coolant Reservoir ($/system)	$16	$16	$16	$16
Coolant Pump ($/system)	$141	$139	$136	$136
Coolant DI Filter ($/system)	$174	$167	$161	$158
Thermostat & Valve ($/system)	$20	$20	$20	$20
Radiator ($/system)	$785	$764	$744	$737
Radiator Fan ($/system)	$134	$132	$130	$129
Coolant Piping ($/system)	$109	$107	$105	$104
Markup ($/system)	$557	$528	$502	$493
Total Cost ($/system)	$1,935	$1,873	$1,813	$1,794
Total Cost ($/kW$_{net}$)	$12.10	$11.71	$11.33	$11.21

16.2.3.2 Low-Temperature Coolant Loop

Annual Production Rate	200	400	800	1,000
Coolant Reservoir ($/system)	$2	$2	$2	$2
Coolant Pump ($/system)	$35	$34	$34	$34
Thermostat & Valve ($/system)	$8	$8	$8	$8
Radiator ($/system)	$99	$97	$94	$93
Radiator Fan ($/system)	$0	$0	$0	$0
Coolant Piping ($/system)	$14	$14	$13	$13
Markup ($/system)	$64	$61	$58	$57
Total Cost ($/system)	$222	$216	$209	$207
Total Cost ($/kW$_{net}$)	$1.39	$1.35	$1.31	$1.30

16.2.4 Fuel Loop

Annual Production Rate	200	400	800	1,000
Inline Filter for GPE ($/system)	$27	$26	$25	$25
Flow Diverter Valve ($/system)	$31	$31	$31	$31
Over-Pressure Cut-Off Valve ($/system)	$54	$52	$50	$49
Hydrogen High-Flow Ejector ($/system)	$118	$110	$103	$101
Hydrogen Low-Flow Ejector ($/system)	$103	$96	$88	$86
Check Valves ($/system)	$20	$20	$20	$20
Purge Valves ($/system)	$171	$164	$157	$155
Hydrogen Piping ($/system)	$186	$183	$180	$179
Markup ($/system)	$287	$268	$250	$245
Total Cost ($/system)	$997	$950	$905	$891
Total Cost ($/kW$_{net}$)	$6.23	$5.94	$5.66	$5.57

16.2.5 System Controller

Annual Production Rate	200	400	800	1,000
System Controller	$416	$383	$353	$343
Markup ($/system)	$168	$150	$135	$130
Total Cost ($/system)	$584	$533	$488	$474
Total Cost ($/kW$_{net}$)	$3.65	$3.33	$3.05	$2.96

16.2.6 Sensors

Annual Production Rate	200	400	800	1,000
Current Sensors ($/system)	$40	$40	$40	$40
Voltage Sensors ($/system)	$16	$16	$16	$16
Hydrogen Sensors ($/system)	$743	$747	$751	$753
Markup ($/system)	$323	$316	$309	$307
Total Cost ($/system)	$1,121	$1,119	$1,116	$1,115
Total Cost ($/kW$_{net}$)	$7.01	$6.99	$6.97	$6.97

16.2.6.1 Hydrogen Sensors

Annual Production Rate	200	400	800	1,000
Sensors per system	3	3	3	3
Sensor ($)	$248	$249	$250	$251
Total Cost ($/system)	$743	$747	$751	$753
Total Cost ($/kW$_{net}$)	$4.64	$4.67	$4.70	$4.70

16.2.7 Miscellaneous BOP

Annual Production Rate	200	400	800	1,000
Belly Pan ($/system)	$263	$135	$71	$58
Mounting Frames ($/system)	$249	$239	$230	$227
Wiring ($/system)	$237	$232	$227	$225
Fasteners for Wiring & Piping ($/system)	$47	$46	$45	$45
Markup ($/system)	$322	$256	$219	$211
Total Cost ($/system)	$1,118	$909	$792	$766
Total Cost ($/kW$_{net}$)	$6.99	$5.68	$4.95	$4.79

16.2.7.1 Belly Pan

Annual Production Rate	200	400	800	1,000
Manufacture or Job Shop	Job Shop	Job Shop	Job Shop	Job Shop
Job Shop Line Utilization (%)	37%	37%	37%	38%
Job Shop Total Machine Rate ($/min)	$1.42	$1.41	$1.41	$1.41
Manufactured Line Utilization (%)	0.1%	0.2%	0.5%	0.6%
Manufactured Total Machine Rate ($/min)	$91.54	$46.17	$23.49	$18.95
Line Utilization Used (%)	37.1%	37.2%	37.5%	37.6%
Total Machine Rate Used ($/min)	$1.42	$1.41	$1.41	$1.41

Annual Production Rate	30,000	80,000	100,000	500,000
Material ($/system)	$4	$4	$4	$4
Manufacturing ($/system)	$2	$2	$2	$2
Tooling ($/system)	$181	$91	$45	$36
Markup ($/system)	$76	$38	$20	$16
Total Cost ($/system)	$263	$135	$71	$58
Total Cost ($/kWnet)	$1.64	$0.84	$0.44	$0.36

16.2.7.2 Wiring

Annual Production Rate	200	400	800	1,000
Cables ($/system)	$79	$77	$75	$75
Connectors ($/System)	$159	$155	$152	$151
Total Cost ($/system)	$237	$232	$227	$225
Total Cost ($/kWnet)	$1.48	$1.45	$1.42	$1.41

16.2.8 System Assembly

Annual Production Rate	200	400	800	1,000
Assembly Method	Assembly Line	Assembly Line	Assembly Line	Assembly Line
Index Time (min)	111	111	111	111
Capital Cost ($/line)	$50,000	$50,000	$50,000	$50,000
Simultaneous Lines	1	1	1	1
Laborers per Line	12	12	12	12
Cost per Stack ($)	$231.90	$169.28	$137.44	$130.86
Line Utilization Used (%)	1%	3%	6%	7%
Total Machine Rate Used ($/min)	$18.23	$13.69	$11.42	$10.97

Annual Production Rate	200	400	800	1,000
System Assembly & Testing ($/System)	$259	$195	$162	$156
Markup ($/system)	$205	$144	$112	$106
Total Cost ($/system)	$464	$339	$275	$262
Total Cost ($/kWnet)	$2.90	$2.12	$1.72	$1.64